U.PORTO

DOUTORAMENTO
MEDICINA

The Contribution of Contrast-Enhanced Ultrasound and MRI in the evaluation of Juvenile Idiopathic Arthritis of the Knee

Sílvia Cristina Pereira Costa Dias Tenreiro

D

2026

Dissertação de candidatura ao grau de Doutor apresentada à Faculdade de Medicina da Universidade do Porto no âmbito do Programa Doutoral em Medicina

This PhD thesis has been submitted in fulfilment of the requirements for the PhD degree in Medicina at the Faculdade de Medicina da Universidade do Porto

SUPERVISOR

Iva Brito, MD PhD

Departamento de Medicina, Faculdade de Medicina da Universidade do Porto, Portugal

Unidade de Reumatologia Pediátrica e do Jovem Adulto, Centro Hospitalar Universitário São João, Porto, Portugal

CO-SUPERVISORS

Isabel Ramos, MD PhD

Departamento de Medicina, Faculdade de Medicina da Universidade do Porto, Portugal

Karen Rosendahl, MD PhD

Department of Clinical Medicine, Faculty of Health Sciences, UiT the Arctic University of Norway, Tromsø, Norway

Section of Paediatric Radiology, University Hospital of North Norway, Tromsø, Norway



“We are all apprentices in a craft where no one ever becomes a master”

Ernest Hemingway

ACKNOWLEDGMENTS

"Aimer, c'est admirer avec le cœur; admirer, c'est aimer avec l'esprit."
Théophile Gautier

This thesis is rooted in years of learning, perseverance, and the generosity of many who walked alongside me.

To those I admire, and came to love with my mind

To Professor Iva, for the vision that shaped this work, for your unconditional support throughout every stage of this journey, and for the remarkable gift of turning every difficulty into possibility. Your positivity and constant encouragement gave me the strength to overcome obstacles I once thought impossible.

To Professor Isabel, it has been a true honour to have had you as my leader. You were the first to believe in me and to encourage me to pursue this path. I am profoundly grateful.

To Professor Karen, a compass and an inspiration. Your scientific brilliance and your immeasurable generosity in teaching and guidance have shaped me in ways I could not have anticipated. I have also had the rare privilege of witnessing, as a paediatric radiologist, your devotion to children and families, a care without equal. I can only be grateful for the fortune of having been close to such an example.

To Professor Damjana, an extraordinary person in every sense: in kindness, in academic excellence, and in constant availability as a friend. Your presence has been a gift throughout this journey.

To Professor Sarmento, my mentor in a broader and deeper dimension, including the spiritual one. A friend of infinite availability, whose wisdom and companionship have meant more than words can express.

To Professor Altamiro Costa Pereira, my sincere gratitude for your trust and counsel. Your resilience and clarity of vision have been a powerful inspiration.

To Professor Ana Filipa, a pillar of rare academic depth, generosity, and empathy. You were my lighthouse, always with a light burning on the darkest days, and my sunshine on the brightest ones. I am deeply fortunate.

I have been blessed with many teachers whose wisdom contributed to my growth in ways both seen and unseen: Professor Bastos Leite, Professor João Fonseca, Professor Estevão Costa, Professor Patrício Costa, Professor Camila Dias and Professor Tiago Gil Oliveira.

A very special acknowledgement to Vasco Mendes, my father in Radiology. And to all who watched me grow in that small, warm, and irreplaceable department in Braga: Dra. Carolina, Dr. Jaime, and Dr. Pedro, and others, thank you for being part of who I became.

I also wish to express my gratitude to the department directors, especially Dra. Ana Catarina Silva for the unconditional support. I am equally thankful to others, such as the hospital boards who believed in my work and projects over the years, highlighting Professor Tiago Guimarães, Dra. Elisabete Barbosa and Professor Maria João Baptista.

A heartfelt thank you to my friends Manuel Melo and Bernardo Almada-Lobo for their unwavering support across these years.

To my working group and dear friends: Miguel, Catarina, Diogo, Mariana, Francisca, Professor Vítor, and Enf. Joana, your companionship made this road far less solitary. To my dearest colleagues Daniela and Conceição, thank you for your warmth every single day. To D. Margarete, D. Helena, D. Ana, and D. Dores, for your kindness and availability, you are extremely missed.

To those I love, with all my heart

To my fellow doctoral colleague Lídia, a companion in this shared adventure, and to all my friends who sustained me with their unconditional presence: André, Margarida, João Nuno, Sara, Luísa, Sarinha, Ana Prima, Mariana, Joana, Catarina, Alexandra, Sophie, Derk, Laura, Hanne, Vânia, Maria da Luz and all the others whose names fill my heart even when space does not permit.

A very special tenderness for Mariana, Lúcia and Anabela, friends without equal, whose generosity and love have been without limit.

To my parents-in-law, who have been parents to me in every sense that matters, and to my sister-in-law Ana, thank you for being family.

To my parents, my greatest examples, teaching me the true meaning of unconditional love. To my brothers and sisters (my godmothers, who always guided me through life), brothers-in-law, sister-in-law, nieces and nephews, for sharing that same love. And to my grandmother, whose candles burned for me throughout this journey.

To my family, Rui, Catarina, and Manuel, for always considering my projects as our projects, and for the lightness and happiness with which we face life together, even in moments where that was never expected. Joy is always the main feeling. In you, I find my greatest reason.

Finally, to all the children and families I have had the privilege of caring for, you are the true purpose of this work. This thesis belongs to you.

ABBREVIATIONS AND ACRONYMS

bDMARDs: biologic disease-modifying antirheumatic drugs

BMO: Bone Marrow Oedema

CEMRI: Contrast-enhanced MRI

CEUS: Contrast-enhanced Ultrasound

csDMARDs: Conventional synthetic disease-modifying antirheumatic drugs

DCEMRI: Dynamic Contrast-enhanced MRI

DIR: Double inversion recovery

DWI - Diffusion weighted imaging

EMA: European medicines agency

FLAIR-FS - Fluid attenuated inversion recovery with fat suppression

GBCAs: Gadolinium-based contrast agents

GD: Gadolinium

iAUC: initial Area Under the Curve

ICC: Intraclass Correlation Coefficient

IL-1: Interleukin-1

IL-6: Interleukin-6

ILAR: International League of Associations for Rheumatology

JAMRIS: Juvenile Arthritis MRI Scoring

JIA: Juvenile Idiopathic Arthritis

LoA: Limits of Agreement

MD: Microvascular Doppler

MRI: Magnetic resonance imaging

MS: milliseconds

MSUS: Multiparametric musculoskeletal ultrasound

NSAIDs: Non-steroidal anti-inflammatory drugs

PD-FS: Proton Density with fat saturation

PDUS: Power Doppler Ultrasound

PE: Peak Enhancement

PEI: Peak Enhancement Intensity

qDESS: Quantitative Double Echo Steady State

RA: Rheumatoid Arthritis

ROC: Receiver Operating Characteristic

ROI: Region of Interest

SMI: Superb Microvascular Imaging

SPACE: Sampling Perfection with Application-optimised Contrasts using different flip angle Evolution

TE: Echo time

TI: Inversion time

TNF: tumour necrosis factor

TTP: Time to Peak

UCAs: Ultrasound contrast agents

US: Ultrasound

WiAUC: Wash-in Area Under the Curve

THESIS OUTPUTS

THESIS OUTPUTS

RESEARCH LINE I

PAPER 1 - Dias SC, Carvalho DC, Castro M, Dias CC, Ramos I, Brito I, Rosendahl K. **Knee-ultrasound: reference values for the amount of joint fluid and synovial appearances in healthy children and adolescents**. *Pediatr Radiol* **55**, 1127–1137 (2025). https://doi.org/10.1007/s00247-025-06243-0

PAPER 2 - Costa Dias S, Habre C, Di Paolo PL, d'Angelo P, Augdal TA, Angenete OW, Kljucevsek D, Inarejos Clemente EJ, Tanturri de Horatio L, Rosendahl K. **ESR Essentials: juvenile idiopathic arthritis; what every radiologist needs to know-practice recommendations by the European Society of Paediatric Radiology**. *Eur Radiol* **36**, 1261–1271 (2026). https://doi.org/10.1007/s00330-025-11891-9

RESEARCH LINE II

PAPER 3 –Dias SC, Ferreira CC, Santos I, Castro M, Rodrigues M, Aguiar F, Dias CC, Nguyen B, Silva V, Ramos I, Ključevšek D, Brito I, Rosendahl K. **Reliability of CEUS and MRI for grading knee-joint inflammation in juvenile idiopathic arthritis.** *Eur Radiol* **36**, 7379–7390 (2026). https://doi.org/10.1007/s00330-026-12627-z

PAPER 4 – Costa Dias S, Ferreira CC, Santos I, Castro M, Rodrigues M, Aguiar F, Dias CC, Silva V, Ramos I, Ključevšek D, Rosendahl K, Brito I. **Can CEUS or FLAIR-FS MRI replace Contrast-enhanced MRI for the detection and grading of synovitis in juvenile idiopathic arthritis of the knee? A diagnostic accuracy study.**

Submitted, Arthritis Research & Therapy

RESEARCH LINE III

PAPER 5 - Costa Dias S, Ferreira CC, Santos I, Castro M, Rodrigues M, Aguiar F, Dias CC, Ramos I, Ključevšek D, Brito I, Rosendahl K. **Knee Ultrasound in Juvenile Idiopathic Arthritis: A Comparative Study with Normative Reference Values.** Submitted, Pediatric Rheumatology.

CONTENTS

SUMMARY 12

RESUMO 15

INTRODUCTION 18

AIMS 31

METHODS 34

THESIS OUTPUTS 44

A. Research Line I 45

Paper 1 - Knee-ultrasound: reference values for the amount of joint fluid and synovial appearances in healthy children and adolescents 46

Paper 2 - ESR Essentials: juvenile idiopathic arthritis; what every radiologist needs to know-practice recommendations by the European Society of Paediatric Radiology ... 47

B. Research Line II 48

Paper 3 - Reliability of CEUS and MRI for grading knee-joint inflammation in juvenile idiopathic arthritis 49

Paper 4 - Can CEUS or FLAIR-FS MRI replace Contrast-enhanced MRI for the detection and grading of synovitis in juvenile idiopathic arthritis of the knee? A diagnostic accuracy study 50

C. Research Line III 51

Paper 5 - Knee Ultrasound in Juvenile Idiopathic Arthritis: A Comparative Study with Normative Reference Values 52

DISCUSSION 53

A. Research Line I 56

B. Research Line II 60

C. Research Line III 71

D. The Pinnacle of Subclinical Synovitis 75

E. A Proposed Stratified Imaging Algorithm for the Suspicion of JIA in the Knee. 78

F. Strengths and Limitations of Our Work 80

FUTURE DIRECTIONS/PERSPECTIVES & CONCLUSIONS 82

REFERENCES 87

SUMMARY

SUMMARY

Background

Juvenile idiopathic arthritis (JIA) is the most common chronic inflammatory arthropathy of childhood, with knee synovitis representing the leading source of morbidity in polyarticular and oligoarticular subtypes. Although contrast-enhanced magnetic resonance imaging (CEMRI) is the accepted imaging reference standard, its reliance on intravenous gadolinium poses significant concerns in children requiring long-term monitoring. This thesis evaluates gadolinium-free advanced imaging modalities against CEMRI, with the clinical rationale of optimising the imaging pathway to reduce gadolinium exposure, without compromising diagnostic accuracy.

Main Aim

To evaluate the diagnostic accuracy of contrast-enhanced ultrasound (CEUS) and fluid-attenuated inversion recovery with fat suppression (FLAIR-FS) in detecting and grading knee synovial inflammation, compared against the current reference standard used in routine clinical practice, CEMRI.

Methods

Studies were conducted at a school and a single tertiary paediatric centre, encompassing ultrasound with Doppler modalities including Microvascular/Micro Doppler Imaging (MD), CEUS, unenhanced FLAIR-FS MRI, and CEMRI, alongside subjective 0–3 synovial grading scales and quantitative perfusion analysis. Healthy volunteer cohorts served as normative comparators. Intra- and interobserver reliability for 0-3 grading scales was determined using linear weighted kappa coefficients. Interobserver reproducibility was assessed using intraclass correlation coefficients and Bland-Altman limits of agreement in continuous measurements, and diagnostic accuracy was evaluated using receiver operating characteristic (ROC) curve analysis.

Results

CEUS demonstrated the highest sensitivity among all the evaluated modalities and techniques for grading active knee synovitis. Unenhanced FLAIR-FS achieved near-

perfect agreement with CEMRI. Both modalities independently detected subclinical synovitis in clinically inactive joints, highlighting the limited discriminative performance of clinical assessment at the lower end of the inflammation spectrum. Normative ultrasound data further revealed significant synovial thickening in clinically unaffected knees of oligoarticular JIA patients compared to healthy group. Subjective 0–3 grading scales proved highly reliable and reproducible for routine clinical use, whilst conventional Doppler demonstrated high specificity but significant sensitivity loss in low-grade inflammation. Quantitative perfusion analysis yielded high intraclass correlation coefficients; however, Bland-Altman analysis revealed substantial absolute interobserver variance.

Discussion/Conclusions

CEUS and unenhanced FLAIR-FS emerge as the most clinically promising modalities for gadolinium-sparing assessment of paediatric JIA synovitis. CEUS offers a sedation-free approach and FLAIR-FS demonstrates a robust agreement with CEMRI, both with demonstrated capacity to detect subclinical disease beyond clinical evaluation alone. The sensitivity limitations of conventional Doppler in detecting low-grade synovial inflammation provide the rationale for more advanced techniques such as microvascular Doppler imaging; however, even microvascular Doppler falls short compared with CEUS, which despite being a more complex procedure, demonstrated superior sensitivity for knee synovitis. While quantitative perfusion analysis shows potential, current interobserver variance indicates that perfusion metrics do not yet achieve the precision required for reliable longitudinal therapeutic monitoring. Robust grading frameworks and rigorous reliability methodology are essential for safe long-term follow-up, and the transition toward high-sensitivity, gadolinium-free imaging pipelines represents a meaningful advancement in the management of children with chronic inflammatory arthritis.

Keywords: juvenile idiopathic arthritis, synovitis, contrast-enhanced ultrasound, FLAIR-FS, magnetic resonance imaging, contrast-enhanced magnetic resonance imaging, gadolinium, paediatric imaging, diagnostic accuracy, interobserver reliability

RESUMO

RESUMO

Introdução

A artrite idiopática juvenil (AIJ) é a artropatia inflamatória crónica mais comum em idade pediátrica, sendo a sinovite do joelho a principal fonte de morbilidade nas formas poliarticular e oligoarticular. Embora a ressonância magnética com contraste (CEMRI) seja o padrão de referência aceite, a necessidade de gadolínio intravenoso levanta preocupações significativas em crianças sujeitas a monitorização a longo prazo. Esta tese avalia modalidades imagiológicas avançadas sem gadolínio comparativamente à CEMRI, com o racional clínico de otimizar a abordagem imagiológica para reduzir a exposição ao gadolínio, sem comprometer a acuidade diagnóstica.

Objetivo Principal

Avaliar a acuidade diagnóstica da ecografia com contraste (CEUS) e da sequência sem contraste *fluid attenuated inversion recovery* com supressão de gordura (FLAIR-FS) na deteção e classificação da inflamação sinovial do joelho, comparativamente ao padrão de referência utilizado na prática clínica corrente, a CEMRI.

Métodos

Os estudos foram realizados numa escola e num centro pediátrico terciário de referência, englobando ecografia com Doppler incluindo Doppler Microvascular/Micro (MD), CEUS, sequência sem contraste FLAIR-FS e CEMRI, bem como escalas subjetivas de gradação sinovial de 0 a 3 e análise quantitativa de perfusão. Coortes de voluntários saudáveis serviram como comparadores normativos. A fiabilidade intra- e interobservador das escalas de gradação de 0-3 foi determinada através de coeficientes kappa ponderados linearmente. A reprodutibilidade interobservador foi avaliada através de coeficientes de correlação intraclasse e limites de concordância de Bland-Altman, e a acuidade diagnóstica mediante análise de curvas ROC (receiver operating characteristic).

Resultados

A CEUS demonstrou a maior sensibilidade entre todas as modalidades e técnicas avaliadas na gradação da sinovite ativa do joelho. A sequência sem contraste FLAIR-FS

atingiu uma concordância quase perfeita com a CEMRI. Ambas as modalidades detetaram de forma independente sinovite subclínica em articulações clinicamente inativas, evidenciando o desempenho discriminativo limitado da avaliação clínica isolada nos estadios mais ligeiros do espectro inflamatório. Os dados normativos de ecografia revelaram ainda um espessamento sinovial significativo nos joelhos clinicamente não afetados de doentes com AIJ oligoarticular comparativamente aos saudáveis. As escalas de gradação subjetiva de 0 a 3 revelaram-se altamente fiáveis e reprodutíveis para uso clínico de rotina, enquanto o Doppler convencional demonstrou elevada especificidade, mas uma perda de sensibilidade significativa na inflamação de baixo grau. A análise quantitativa de perfusão obteve coeficientes de correlação intraclasse elevados; contudo, a análise de Bland-Altman revelou uma variância interobservador absoluta substancial.

Discussão/Conclusões

A CEUS e a sequência sem contraste FLAIR-FS emergem como as modalidades clinicamente mais promissoras para a avaliação poupadora de gadolínio na sinovite pediátrica na AIJ. A CEUS oferece uma abordagem sem sedação e a sequência FLAIR-FS demonstra uma concordância robusta com a CEMRI. Ambas as modalidades demonstraram capacidade para detetar doença subclínica, para além do alcance da avaliação clínica isolada. As limitações de sensibilidade do Doppler convencional na deteção de inflamação sinovial de baixo grau fundamentam o recurso a técnicas mais avançadas, como o Doppler microvascular. No entanto, mesmo o Doppler microvascular fica aquém quando comparado com a CEUS, que apesar de ser um procedimento mais complexo, demonstrou uma sensibilidade superior na deteção de sinovite do joelho. Embora a análise quantitativa de perfusão demonstre potencial, a variância interobservador atual indica que as métricas de perfusão não atingem ainda a precisão necessária para uma monitorização terapêutica longitudinal fiável. Modelos de classificação robustos e uma metodologia de fiabilidade rigorosa são essenciais para um seguimento longitudinal seguro, sendo a transição para protocolos imagiológicos de alta sensibilidade sem gadolínio um avanço significativo no seguimento de crianças com artrite inflamatória crónica.

Palavras-chave: artrite idiopática juvenil, sinovite, ecografia com contraste, FLAIR-FS, ressonância magnética, ressonância magnética com contraste, gadolínio, imagiologia pediátrica, acuidade diagnóstica, reprodutibilidade interobservador

INTRODUCTION

INTRODUCTION

Juvenile idiopathic arthritis (JIA) is a heterogeneous group of diseases encompassing all forms of chronic arthritis of unknown origin with an onset before 16 years of age, lasting for at least six weeks [1]. The reported prevalence ranges from 16 to 150 per 100,000 children, with a pooled global estimate of 20.5 per 100,000, and an overall female-to-male predominance of roughly 3:1, although this ratio varies significantly across the distinct clinical International League of Associations for Rheumatology (ILAR) subtypes [2, 3]. The disease is characterised by chronic synovial inflammation, which carries a substantial risk of developing progressive joint destruction, cartilage loss, and long-term disability [2, 4]. Although modern therapeutic strategies have drastically reduced overall morbidity, many affected children still face debilitating periods of active disease, chronic pain, and reduced mobility, which frequently persist into adulthood [2, 3, 5].

A. Pathology, Diagnosis, and Treatment

The underlying pathology of JIA is driven by immune-mediated proliferation of the synovium. This chronic synovitis is characterised by hypervascularity, infiltration of inflammatory cells (such as T-lymphocytes, B-cells, and macrophages), and the formation of a thickened, destructive pannus [3, 4]. Left untreated, this inflamed synovial tissue invades neighbouring articular cartilage and subchondral bone. In paediatric populations, this inflammatory process also directly alters skeletal maturation, potentially causing accelerated epiphyseal growth, premature growth plate closure, and limb-length discrepancies.

Diagnosing JIA remains fundamentally clinical, requiring the careful exclusion of other causes of paediatric arthritis, such as infectious, traumatic, neoplastic, or reactive aetiologies. The clinical diagnosis relies on identifying objective signs of joint inflammation, including swelling, restricted range of motion, warmth, and pain. However, detecting low-grade or subclinical synovitis through physical examination alone is difficult, particularly in deep-seated joints like the hip or behind thick paediatric joint capsules and physiological fat pads.

Over the past two decades, the treatment paradigm for JIA has shifted from purely symptomatic management to an aggressive, "treat-to-target" approach aimed at achieving prompt, complete clinical remission [2, 5]. Management typically begins with non-steroidal anti-inflammatory drugs (NSAIDs) and intra-articular corticosteroid injections for localised disease. For progressive or polyarticular involvement, conventional synthetic disease-modifying antirheumatic drugs (csDMARDs), primarily methotrexate, are widely utilised [6]. The prognosis has been further improved by biologic DMARDs (bDMARDs), such as tumour necrosis factor (TNF) inhibitors, interleukin-1 (IL-1), and interleukin-6 (IL-6) antagonists [4-6]. These targeted therapies successfully halt structural joint damage in a large proportion of patients, but their effective use depends entirely on early detection, accurate grading of active inflammation, and rigorous longitudinal monitoring [3, 5, 7].

B. Imaging in JIA

Traditionally, conventional radiographs have been the cornerstone for the diagnosis and follow-up of JIA. However, this modality is inherently limited by its inability to visualise soft tissue structures directly. Radiographs only capture the late, irreversible structural consequences of chronic inflammation, such as joint space narrowing, subchondral erosions, and growth disturbances, while remaining blind to early, active synovitis. Given that the therapeutic window for preventing permanent joint damage occurs long before radiographic changes manifest, cross-sectional imaging modalities have become indispensable in modern paediatric rheumatology.

B.1. Ultrasound in JIA

Ultrasound (US) has emerged as a first-line imaging modality in the routine management of JIA [8]. In paediatric radiology, US offers several unique practical advantages over magnetic resonance imaging (MRI): it is widely accessible, cost-effective, allows for real-time dynamic examination, and eliminates the need for patient sedation in younger children [9, 10]. Furthermore, US enables simultaneous screening of multiple joints during a single clinical encounter, which is highly valuable given the oligoarticular or polyarticular nature of JIA [11]. In the assessment of paediatric joints, high-resolution

grey-scale (B-mode) ultrasound is sensitive for detecting morphological changes such as joint effusion, synovial hypertrophy, and tenosynovitis [10, 11]. However, for the detection and grading of active inflammation, additional Doppler examination is required [11, 12]. Although conventional colour Doppler (CD) and Power Doppler (PD) provide high specificity when a signal is present [13], they often lack the sensitivity required to detect the low-velocity microvascular blood flow in mild synovitis. [14]. This limitation is particularly pronounced in children, where conventional Doppler often struggles to detect the slow, low-velocity microvascular blood flow characteristic of early or mild subclinical synovitis [15, 16]. Consequently, optimizing non-invasive vascular imaging remains a critical clinical priority.

B.2. Magnetic Resonance Imaging in JIA

MRI is widely established as the gold standard imaging modality for evaluating joint inflammation in JIA [9, 17, 18]. Unlike conventional radiography, MRI provides exquisite soft tissue contrast and multiplanar imaging capabilities, allowing for the direct visualisation and objective quantification of both early, reversible inflammatory changes and late, structural joint damage [9, 18]. The hallmark features of active JIA, specifically synovial hypertrophy, joint effusion, and bone marrow oedema (BMO), can be detected on MRI long before they manifest on conventional radiographs or physical examination [9, 19]. In standard clinical protocols, a comprehensive evaluation of the paediatric joint relies on a combination of unenhanced (non-contrast) and contrast-enhanced sequences [18, 20]. Fluid-sensitive sequences with fat suppression, such as T2-weighted or Short Tau Inversion Recovery (STIR) images, are highly sensitive for detecting joint effusions and hyperintense BMO [18, 21]. However, on these standard unenhanced sequences, distinguishing between active, inflamed synovial tissue and simple, non-inflammatory joint fluid remains a diagnostic challenge, as both structures appear hyperintense [9, 21, 22].

To overcome this limitation, conventional protocols mandate the use of contrast-enhanced MRI (CEMRI) using intravenous gadolinium-based contrast agents (GBCAs) [18, 23]. Active, hypervascularised synovium demonstrates rapid, intense contrast enhancement, allowing radiologists to clearly differentiate the thickened synovial lining from the non-enhancing adjacent joint fluid [9, 24]. Consequently, CEMRI has long been

considered the standard for diagnosing synovitis, determining disease activity, and monitoring therapeutic response in JIA [18, 19]. Despite its diagnostic superiority, however, the routine reliance on intravenous contrast administration faces growing challenges in modern paediatric radiology [25].

There is clear clinical imperative to reduce the use of GBCAs in children. This concern has intensified following substantial evidence of gadolinium deposition within the brain and other tissues after repeated CEMRI, supported by histological findings in rodent models and necropsy studies in both adults and children [26]. Consequently, contemporary literature emphasises the distinct physiological characteristics of paediatric patients and underscores the need for highly restrictive GBCA administration. A systematic review and meta-analysis by Yu et al. [27] confirmed a significant increase in dentate nucleus T1 signal intensity correlated with cumulative GBCA exposure in children. The clinical significance of this deposition remains uncertain, but Radiologists should carefully assess the necessity of using GBCAs to enhance diagnostic accuracy and prioritise the use of more stable macrocyclic ionic GBCAs [26, 28]. The European Medicines Agency (EMA) [29] has advocated for minimizing GBCA exposure in children requiring serial imaging, directly driving clinical and research interest toward non-contrast alternatives such as diffusion-weighted imaging (DWI), fluid attenuated inversion recovery with fat suppression (FLAIR-FS), double inversion recovery (DIR), and quantitative double echo steady state (qDESS).

B2.1. The implementation and limitations of Musculoskeletal DWI.

Early paediatric investigations into contrast-free synovial imaging with DWI were initiated by Neubauer et al. [30], reporting promising results with restricted diffusion identified in 12 out of 15 patients presenting with active synovitis. Subsequent studies built upon this groundwork. Barendregt et al. [31] demonstrated the utility of DWI in differentiating hyperplastic synovium from effusion, while Sauer et al. [32] highlighted the persistent difficulty in reliably differentiating non-inflamed knee joints from mild synovial inflammation using unenhanced diffusion metrics.

Further supporting the quantitative validity of the sequence, Barendregt et al. [33] showed that DWI-derived apparent diffusion coefficient (ADC) values had comparable performance to dynamic contrast-enhanced MRI (DCEMRI) in significantly differentiating MRI-active JIA patients from those with inactive disease. Later, in 2020, Barendregt et al. [23] analysed a cohort of 45 JIA patients, reporting that DWI achieved a sensitivity of 92% and a specificity of 78% for detecting knee synovial inflammation when compared directly against standard CEMRI.

Despite these strong diagnostic metrics, DWI possesses major inherent limitations in clinical practice. First, it suffers from a significantly higher inter-reader variability compared to post-contrast T1-weighted sequences [34]. Second, its most critical disadvantage is an intrinsic deficit in spatial resolution and anatomical detail. Because DWI operates fundamentally as a functional sequence rather than a structural one, it struggles to delineate the fine, millimetre scale margins of the synovium. This lack of anatomical fidelity represents a severe drawback in the musculoskeletal field, where isolating subtle synovial tissue boundaries from surrounding fat and fluid is paramount. To overcome these morphological limitations, high-resolution, unenhanced structural sequences have been actively developed over time.

B2.2. Evolution of High-Resolution Non-Contrast Sequences

Methodologically, FLAIR-FS addresses these spatial resolution limits by nulling freely mobile joint fluid through inversion recovery preparation while concurrently suppressing fat spectrally, rendering inflamed synovium highly conspicuous without exogenous contrast [35]. Performance is highly optimised at 3 Tesla using parameters modified from classic neuroimaging protocols [36], utilizing a lower echo time (our protocol echo time (TE) = 87 milliseconds (ms)), an inversion time (TI) of 2200 ms [35, 36], and a reduced flip angle (our protocol 150°).

The exploration of these high-resolution unenhanced protocols was introduced in adults by Jahng et al. in 2011 [37] who identified the utility of DIR sequence. Subsequently, Yoo et al. in 2017 [35] conducted a retrospective adult study on 33 patients evaluating peripatellar synovitis across five anatomical sites. They reported a high overall diagnostic accuracy for FLAIR-FS (92.1%–93.9% at the site level; 90.9% at the patient level), though sensitivity for Hoffa synovitis remained moderate (78.9%–87.5%) and specificity

was low (47.1%–64.3%). Notably, reader agreement on FLAIR-FS mirrored contrast-enhanced T1-weighted imaging, achieving a weighted kappa of 0.72–0.79 for synovitis assessment and an intraclass correlation coefficient (ICC) of 0.95. More recently, Feuerriegel et al. [38] evaluated 55 adults with suspected knee synovitis using a deep learning-accelerated FLAIR sequence, demonstrating no statistically significant difference in synovitis scores compared to post-contrast T1 turbo spin-echo FS images (10.69 ± 8.83 vs. 10.74 ± 10.32, respectively; $p = 0.521$).

In paediatric cohorts, comparative structural data remain scarce. Milks et al. [39] reported a sensitivity between 79-84% and a specificity of 83-94% for FLAIR-FS compared to CEMRI in 39 paediatric patients, though their sample was highly heterogeneous. In a study of 35 patients with JIA under 21 years of age, Handa et al. [40] evaluated unenhanced sagittal/axial T2-weighted fat-saturated and proton density-weighted Sampling Perfection with Application-optimised Contrasts using different flip angle Evolution (SPACE) sequences using the Juvenile Arthritis MRI Scoring (JAMRIS) system. While intra-observer reliability was moderate-to-high, the global inter-observer reliability for these unenhanced sequences was low, contrasting with the moderate reliability achieved on post-contrast images.

Alternative non-contrast structural sequences include DIR and qDESS. Verkuil et al. [41] published the first paediatric JIA study utilizing DIR in 26 patients (50% with active knee arthritis). While the median visual analogue scale confidence score to depict the synovium was lower for DIR than for CEMRI (88 vs. 100 out of 100), maximal synovial thickness on DIR was significantly greater in children with active knee arthritis (2.4 mm [IQR 2.1–3.1]) than in those without (1.4 mm [IQR: 1.0–1.6]) ($p < 0.001$). The inter-reader ICC was 0.87 for DIR and 0.90 for CEMRI. This Amsterdam-based research group represents the dominant international cohort publishing on DWI, DIR, and related unenhanced JIA techniques. Conversely, qDESS has not yet been validated in paediatric populations. In adult knee osteoarthritis (n=31), de Vries et al. [42] demonstrated that qDESS systematically underestimated synovitis severity, yielding lower mean sum scores than CEMRI (5.16 ± 3.75 vs. 7.13 ± 4.66), with an absolute agreement ICC of 0.84. The wider adoption of qDESS is restricted by its technical sophistication; hybrid image reconstruction via diffusion-gradient weighting is non-standard across vendor platforms, and the resulting image contrast is unfamiliar to most clinical radiologists. Furthermore,

its theoretical advantage of simultaneous T2 mapping of cartilage remains logistically difficult to implement in routine practice.

Synthesizing these modalities, a landmark adult review by Thoenen et al. in 2022 [43] compared DIR, FLAIR-FS, and qDESS against CEMRI, demonstrating strong to very strong correlations for all three sequences, with FLAIR-FS providing the highest intra-rater agreement. However, they summarised an important systematic bias: DIR tends to overestimate synovitis, whereas FLAIR-FS and qDESS tend to underestimate it. Guided by these technical capabilities and hardware compatibility across our institutional scanners, we selected FLAIR-FS as the primary non-contrast sequence for our protocol.

C. The Clinical Imperative and Rationale for Paediatric CEUS

Concurrently, there is a strong international trend expanding the indications for CEUS in paediatrics [44-46]. However, historical reluctance has persisted within the JIA musculoskeletal field, particularly due to the sensitivity reported for microvascular Doppler technologies. While Ntoulia et al. [47] reviewed musculoskeletal CEUS in children, confirming its clinical feasibility and superior sensitivity over conventional Doppler for capturing synovial hyperaemia, the question of why it has not been widely integrated into routine JIA synovitis monitoring remained unanswered. Indeed, only a single, early-generation paediatric study from 2001 [48] exists, which evaluated contrast-enhanced colour Doppler in 22 JIA patients and 5 controls with promising initial results.

To find a robust biological rationale for CEUS, we must look to the adult rheumatoid arthritis (RA) literature. Klauser et al. [49] established that CEUS significantly improves the differentiation of active synovitis from inactive intra-articular thickening. While conventional US and Power Doppler (PDUS) could differentiate active from inactive thickening in only 60.1% (68/113) of joints, CEUS enabled definitive differentiation in 97.3% (110/113) of joints ($p < 0.0001$), while significantly improving the thickness measurement of active synovitis ($p = 0.008$). Furthermore, a recent systematic review of 23 adult studies [50] encompassing 1,117 joints concluded that CEUS detects significantly more microvascularisation than standard PDUS in active RA, yielding a relative detection ratio of 1.49. Similarly, Song et al. in 2008 [51] compared knee osteoarthritis patients against six healthy adult controls, concluding that CEUS was more sensitive for detecting superior recess synovitis (95%) than either CEMRI (82%) or

Power Doppler (63%). However, neither of these high-sensitivity adult studies evaluated inter-observer reliability. While these adult data provide a powerful biological rationale for extrapolating CEUS to paediatrics, JIA subtype-specific validation and reliability testing remained a critical missing prerequisite.

Any proposal to introduce CEUS as an alternative or complementary imaging method in clinical practice must be accompanied by a real assessment of its safety profile. This is particularly relevant in the paediatric setting, where the justification for administering any exogenous contrast agent, whether iodinated, gadolinium-based, or microbubble-based, must be grounded in a clear understanding of the associated risks and benefits, and must be weighed against the risks of the imaging modality it seeks to replace or supplement.

In this context, it is important to recognise that no contrast agent is entirely without risk. Intravenous contrast administration, regardless of the agent used, carries a probability of adverse reactions, ranging from mild and self-limiting to, in rare cases, severe and life-threatening. The relevant clinical and ethical question is therefore not whether CEUS is risk-free, but whether its risk profile is acceptable relative to the diagnostic benefit it provides and, critically, relative to the alternatives. In paediatric imaging, the comparators typically include contrast-enhanced CT, which exposes children to ionising radiation and carries a higher rate of hypersensitivity reactions, with acute allergic-like reactions to low-osmolality nonionic iodinated contrast material documented in 0.18% of paediatric administrations, of which 15% were severe [52]. CEMRI often requires general anaesthesia or sedation in younger children, involves gadolinium retention concerns, and is associated with its own, though low, rate of adverse events. Compared to other contrast agents that are routinely used in paediatric radiology, such as iodinated contrast agents or gadolinium, second-generation ultrasound contrast agents (UCAs) have a very low incidence of adverse events, particularly serious adverse events [53].

Against this background, the available evidence consistently positions CEUS with SonoVue® (sulfur hexafluoride microbubbles, Bracco, Milan) as the safest of the available contrast-enhanced imaging options. Definity® and Optison® are two ultrasound contrast agents approved by the FDA in the United States, different from SonoVue® which is the agent used in Europe, approved by the European Medicines Agency (EMA). The ACR Manual on Contrast Media 2026 [54] affirms that ultrasound contrast agents carry an adverse event rate similar to or less than modern CT and MRI

contrast agents. A large retrospective study of over 78,000 doses of Definity® and Optison® found a severe reaction rate of only 0.01% with no deaths [55], while a study of SonoVue® across 23,188 subjects documented only two serious adverse events. Even in high-risk populations, adverse reactions remain exceptionally rare: among 1,513 hospitalised patients with pulmonary hypertension, the reaction rate to Definity® was just 0.002% [56]. The ACR further notes that a review by the Society for Pediatric Radiology and the International Contrast Ultrasound Society concluded that non-cardiac CEUS applications in children, both intravenous and intravesical, are safe, with side effects uncommon and typically minor.

The European Society of Paediatric Radiology (ESPR) abdominal imaging task force has confirmed that CEUS is radiation-free, safe, and easily repeatable in children, emphasising that ultrasound contrast agents are not nephrotoxic or hepatotoxic, that the gas is exhaled rather than excreted, and that no specific patient preparation, sedation, or preliminary laboratory screening is required prior to contrast administration [45]. CEUS is particularly indicated in children for whom sedation or general anaesthesia is considered, especially for those with serious renal impairment who cannot receive intravenous gadolinium-based contrast agents, and for patients requiring frequent repeat imaging (as parents can remain present in the room during the examination) [57]. The same authors report that hypersensitivity reactions to ultrasound contrast agents have been reported but with a low incidence of 0.002%, which is less than that observed with CT iodinated contrast agents, a figure originally reported by Chung and Kim [58]. SonoVue® is non-nephrotoxic, non-hepatotoxic, and eliminated via pulmonary exhalation within minutes, with no radiation exposure, making it particularly well-suited for use in children.

Real-world paediatric safety data from the European Federation of Societies for Ultrasound in Medicine and Biology (EFSUMB) Paediatric Registry, a prospective multicentre database spanning 19 European centres and 1,676 children, further corroborate this favourable profile [59]. No side effects were reported in 1,657 of 1,676 children (98.9%). Of the 15 confirmed post-injection hypersensitivity reactions, 6 were mild (0.4%), 5 were moderate (0.3%), and 4 were severe (0.2%), with full recovery in all cases and no fatalities recorded. A comprehensive systematic review by Ntoulia et al. [53], covering 4,518 children across 57 studies, confirmed an overall serious adverse

event rate of only 0.22%, with the large majority of reactions being non-serious. A summary of important properties of both contrast agents is provided in Table 1.

Nevertheless, the possibility of hypersensitivity reactions, including rare but severe anaphylactic responses, must be acknowledged, planned for, and communicated to patients and families prior to any contrast administration. The examination should therefore only be performed in a dedicated hospital-based setting where resuscitation equipment and appropriately trained personnel are immediately available.

Parameter	Gadolinium-Based Contrast Agents (GBCAs)	SonoVue® (SF_6 Microbubbles)
Composition & Pharmacology		
Composition	Gadolinium chelate (heavy metal + organic ligand); classified as linear or macrocyclic. (A+P) [60, 61]	SF_6 gas enclosed in phospholipid shell; microbubbles ~2.5 µm diameter; isotonic aqueous suspension. (A+P) [62]
Distribution	Extracellular; crosses into brain, bone, skin; tissue retention documented even in normal renal function. (A+P) [60, 61, 63, 64]	Strictly intravascular; confined to blood pool. (A+P) [62, 65]
Elimination	Renal excretion (glomerular filtration); impaired in renal insufficiency; residual Gd retained long-term in tissues. (A+P) [60, 66]	SF_6 exhaled via lungs within minutes; phospholipid shell metabolised physiologically (hepatic); no renal clearance required. (A+P) [62, 67]
Safety Profile		
Adverse Effects rate (overall)	Moderate. (A) 0.07%–2.4% acute reactions. [54] (P) Physiologic AE 0.25%; allergic-like 0.13%; pooled incidence of moderate allergic-like reactions 0.02%; delayed 0.04% (112,760 exams).[27] Physiologic reactions significantly higher in older children (12–17 y: 0.25% vs 2–12 y: 0.03%; p<0.001); no reactions in children <2 years. [68]	Low. (A) 0.020%–0.024%; no fatalities (30,222–83,778 exams). [65, 69] (A) SonoVue® n=23,188: 2 serious AEs (0.0086%); no fatalities. [70] (P) Non-serious 1.1%; serious 0.2% of all CEUS examinations; all resolved (57 studies, n=4,518). [53]
Severe / anaphylactic reactions	Uncommon. (A) Severe hypersensitivity ~0.001%–0.01%. [54] pooled severe allergic-like 0.52 per 10,000 administrations. [71] (P) Severe allergic-like 0.0003% (112,760 exams). [27] No severe reactions in cohort of 16,237 injections. [68]	Rare. (A) Anaphylactoid shock 2/30,222 (0.007%); all recovered. [69] Serious AE rate 0.0086%; anaphylactic-type reactions 0.013% (23,188 investigations); lower than ionic (0.09%–0.25%) and non-ionic iodinated CT contrast agents (0.02%–0.10%). [70] (P) Serious AEs 10 /4,518 children (0.22%); all resolved; no fatalities [53]
Gadolinium retention	Confirmed for all GBCAs; greater with linear agents (globus pallidus, dentate nucleus, bone, skin). (A+P) [60, 61, 72] (P) Brain deposition confirmed in paediatric autopsy and prospective MRI studies. [26, 63]	None. SF_6 biologically inert; no tissue accumulation; no long-term retention. (A+P). [62, 65]
Nephrotoxicity / NSF	(A) NSF linked to linear GBCAs (eGFR <30). Contraindicated in severe renal impairment. [66] (P) Special concern in neonates. 10 biopsy-confirmed cases (Yale Registry, all pre-guidelines); no new paediatric NSF cases reported post-2007, after guideline implementation. [54, 64]	None. No renal toxicity; usable at any eGFR including neonates; no renal screening required. (A+P) [62, 73]
Paediatric-Specific Considerations		
Sedation / GA	Frequently required. MRI demands immobility; children <5 years routinely require sedation or GA; risk of anaesthetic neurotoxicity. (P) [74-76]	Not required. CEUS performed awake; patient need not remain still; parents may remain in room. (P) [77-79]
Regulatory approval (paediatric)	Licensed macrocyclic agents (all ages, on-label). EMA 2017: multipurpose linear GBCAs suspended in Europe; macrocyclic agents and liver-specific linear agents retained. (P) [29, 54]	FDA (USA): approved for paediatric liver lesions. [73, 80] EMA (Europe): IV imaging off-label; use based on clinical indication - EFSUMB/WFUMB guidelines. (P) [62, 81]
Paediatric safety data	Extensive (adult-derived). Brain deposition confirmed in paediatric autopsy and prospective MRI studies. (A+P) [26, 27]	Systematic review: 57 studies, n=4,518 children; non-serious 1.10%, serious 0.2%, all resolved. [53] EFSUMB Registry: n=1,676, 19 centres; 98.9% no side effects; 19 children adverse reactions: 4 unlikely attributable to the UCAs; 15 reactions (6 mild, 5 moderate, 4 severe); all recovered. [59] Prospective study n=312: 6 cases (1.92%); 3 transient rash and 3 hypotension; all recovered [78]
Contraindications & risk factors	**Absolute:** Severe renal impairment (eGFR <30); avoid linear agents in children (EMA 2017). [29, 54, 66] **Relative:** Pregnancy; neonates <4 weeks; severe asthma; prior severe GBCA hypersensitivity; multi-allergic atopy; cumulative linear GBCA exposure. [54, 66]	**Absolute:** Hypersensitivity to SF_6/phospholipids/PEG; right-to-left shunt; severe PHT; uncontrolled systemic HTN; ARDS; combination with dobutamine. [62, 73] **Relative/Risk:** Mastocytosis [82]; Hereditary α-tryptasemia (HαT) [83]; recent Acute coronary syndrome; severe arrhythmia; acute systemic inflammation/infection/sepsis. [62] Resuscitation equipment mandatory. [62]
Practical & Logistical Aspects		
Imaging modality	MRI (1.5T minimum, preferably 3T); dedicated scanner; MR-incompatible device screening required. (A+P) [54]	Ultrasound; portable; bedside-capable. (A+P) [77, 79, 84]
Exam time & throughput	Prolonged (30–60 min); scheduling constraints; high resource demand. (A+P) [74, 76]	Brief (15–30 min); real-time dynamic imaging; may replace downstream CT or MRI in selected cases. (A+P) [77, 78, 81]

Table 1. Comparative Table of Gadolinium-Based Contrast Agents (GBCAs) and SonoVue® Population labels: (A) Adults (P) Paediatric (A+P) Adults & Paediatric. (AE) Adverse Effects

D. Identifying the Knowledge Gap and Defining the Thesis Scope

A critical review of the existing literature reveals a profound methodological gap: no prior studies evaluating non-contrast sequences (such as FLAIR-FS, in either adults or children) have included a healthy volunteer group. Consequently, no existing data could confirm whether these advanced sequences remain appropriately negative in truly healthy paediatric knees, leaving a substantial risk for false-positive overdiagnosis.

To resolve this ambiguity, we designed a prospective, age- and sex-matched group framework. For the MRI arm, we organised a cohort of 51 healthy volunteers to undergo a short, contrast-free protocol utilizing our optimised FLAIR-FS parameters. For the ultrasound arm, Paper 1 established our baseline normative values in 127 healthy children.

Furthermore, the existing reliability literature for the reference standard itself (CEMRI in JIA) is surprisingly scarce, often limited to small cohorts. For instance, Hemke et al. [19] published their foundational JAMRIS reliability with only 25 patients, noting higher ICCs for synovial assessment than for bone marrow changes, cartilage lesions, or erosions.

To provide the rigorous validation required to safely transition clinical paradigms, our project was executed as a prospective, single-centre diagnostic reliability and accuracy study during 2023–2024 at the University Hospital Centre of São João in Porto, Portugal.

AIMS

AIMS

This thesis addresses imaging of the knee joint in children and adolescents with juvenile idiopathic arthritis (JIA).

Primary objective:

1. To evaluate the diagnostic accuracy of contrast-enhanced ultrasound (CEUS) and fluid-attenuated inversion recovery with fat suppression (FLAIR-FS) in detecting and grading knee synovial inflammation, compared against the current reference standard used in routine clinical practice, contrast-enhanced MRI (CEMRI).

Secondary objectives:

1. To provide reference standards of knee ultrasound, including the amount of joint fluid and synovial thickness (Paper 1).
2. To provide practice recommendations on the appropriate use of imaging modalities for diagnosis and monitoring of JIA (Paper 2).
3. To analyse the reliability of CEUS and CEMRI for detecting and grading synovitis, both subjectively (0–3 scale) and quantitatively (Paper 3).
4. To evaluate the value of dynamic acquisitions for establishing optimal diagnostic cut-off thresholds in both CEUS and CEMRI (Paper 3).
5. To examine the reliability of the inflammatory components of the Juvenile Arthritis MRI Scoring (JAMRIS) system in assessing synovitis and bone marrow oedema (Paper 3).
6. To analyse the reliability of FLAIR-FS in grading synovitis, subjectively (0–3 scale), in the JIA and in the healthy volunteers cohorts (Paper 4).
7. To examine the agreement between CEUS, FLAIR-FS and CEMRI (Paper 4).
8. To determine the agreement between Clinical Grading and CEMRI (Paper 4).
9. To evaluate the accuracy of Colour Doppler, Power Doppler and Micro Doppler in detecting knee inflammation (Paper 4).
10. To examine the accuracy of Clinical Grading in detecting knee inflammation (Paper 4).

11. To compare US findings of a healthy population with the US findings of our JIA patients (Paper 5).
12. To establish, using ultrasound findings in volunteers and patients, a model for predicting the probability of disease (Paper 5).

We hypothesise that CEUS and FLAIR-FS offer high diagnostic accuracy for detecting and grading knee synovial inflammation in JIA, compared against the current reference standard, CEMRI.

METHODS

METHODS

This thesis is based on three distinct cohorts: first, one cohort of 127 healthy volunteers enrolled to establish normative reference values for knee ultrasound; second, a clinical cohort of 52 children diagnosed with JIA to evaluate the reliability and diagnostic accuracy of different imaging methods; and finally, one cohort of 51 healthy volunteers, matched to our clinical one, to establish reference standards for non-contrast FLAIR-FS MRI.

A. The healthy US-cohort

Single-centre, prospective, cross-sectional study, including volunteers from a private school in Porto, Portugal. The study was approved by the Institutional Ethics Committee (IEC) (registration number CE 191/22) and by the school board. Written, informed consent was obtained from all the participants and caretaker(s). Children and adolescents were invited to participate via invitations sent to parents' representatives. Exclusion criteria were (a) chronic medicated disease that might affect the skeletal system or (b) having experienced a knee trauma within the last 2 months.

A.1. Ultrasound examination

The examinations were performed during October 17th and 21st 2022, by two radiologists, using a Logiq E10 machine (Version R3, General Electric) with a linear 6-15 MHz transducer and defined pre-sets. With the participant supine, both knees were examined in 30° flexion, using a longitudinal standard view (Fig. 1) and thereafter a transverse view through the lateral and medial parapatellar recesses. Colour Doppler signals were scored. The presence of hyperechoic, small dots within the joint fluid was noted for each of the recesses (speckles). Further, the infrapatellar recess was assessed. The suprapatellar recess was also examined with knees extended and under provocation.

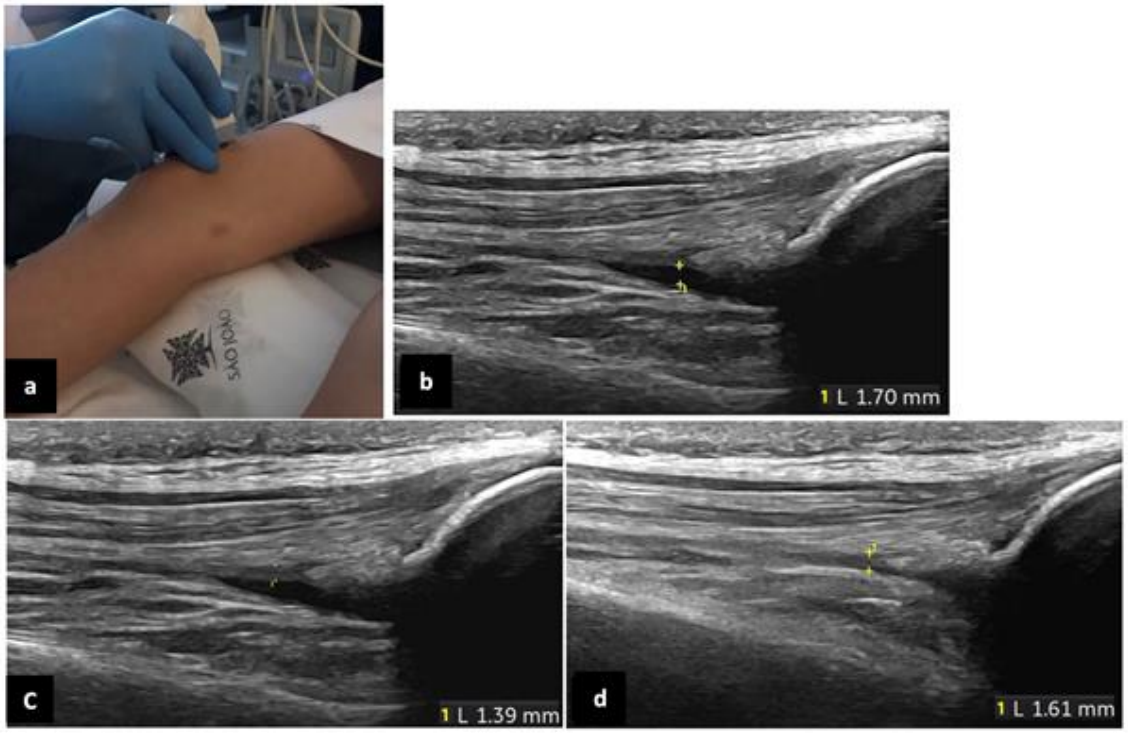


Fig. 1. With knee 30° flexed. **a** Suprapatellar recess was assessed using a central longitudinal view ("standard"); **b** Anteroposterior (AP) measurements of fluid (*arrowhead*); **c** single synovial layer (*arrowhead*); **d** double synovial layer (during light transducer compression to squeeze fluid away) (*arrowhead*).

B. The JIA cohort

Prospective study of children and adolescents with JIA, during 2023-2024. The study was approved by the Regional Ethics Committee (number 282-20), and written informed consent was obtained from each participant and/or their caregiver, according to national guidelines.

Participants were consecutively recruited from the Paediatric and Young Adult Rheumatology Unit at the São João University Hospital, Porto (CHUSJ). Pediatric patients meeting the ILAR criteria [1] for JIA, with current or previous knee involvement, were included. Excluded were children with a history of intra-articular steroid injection or a trauma to the knee within the last two months or with known contraindications to MRI and/or the contrast media used.

B.1. Ultrasound examination

All patients had US (the same protocol as school volunteers), US-Doppler (Colour, Power and Micro-Doppler), CEUS and CEMRI of the affected or most affected knee, clinical examination, clinical data collection and laboratory on the same day. The clinical examination was performed by one of three paediatric rheumatologists, classifying the knee joint, using a global clinical grade, into inactive (grade 0), equivocal (grade 1), or active arthritis (grade 2).

The US, US-Doppler and CEUS were performed by one radiologist. The Doppler evaluation consisted of colour Doppler, Power Doppler and Micro Doppler, graded according to the OMERACT Ultrasound Group consensus [85]. To choose the place for the 2 minutes CEUS acquisition (with Sulfur Hexafluoride - Sonovue® contrast) sagittal scans of three different locations (supra-, para- and infrapatellar) were used, and the location showing most pathology (thickened, hyperemic synovium) was chosen for the CEUS.

Two observers independently scored the CEUS-video-clip for inflammation (0-3 scale) (Fig. 2), with a second reading after 6 weeks, blinded to the clinical data (intra and inter-observer agreement). Using VueBox®, quantitative parameters were also measured by two observers, separately (inter-observer agreement): Peak Enhancement (PE), Wash-in Area Under the Curve (WiAUC) and Time to Peak (TTP).

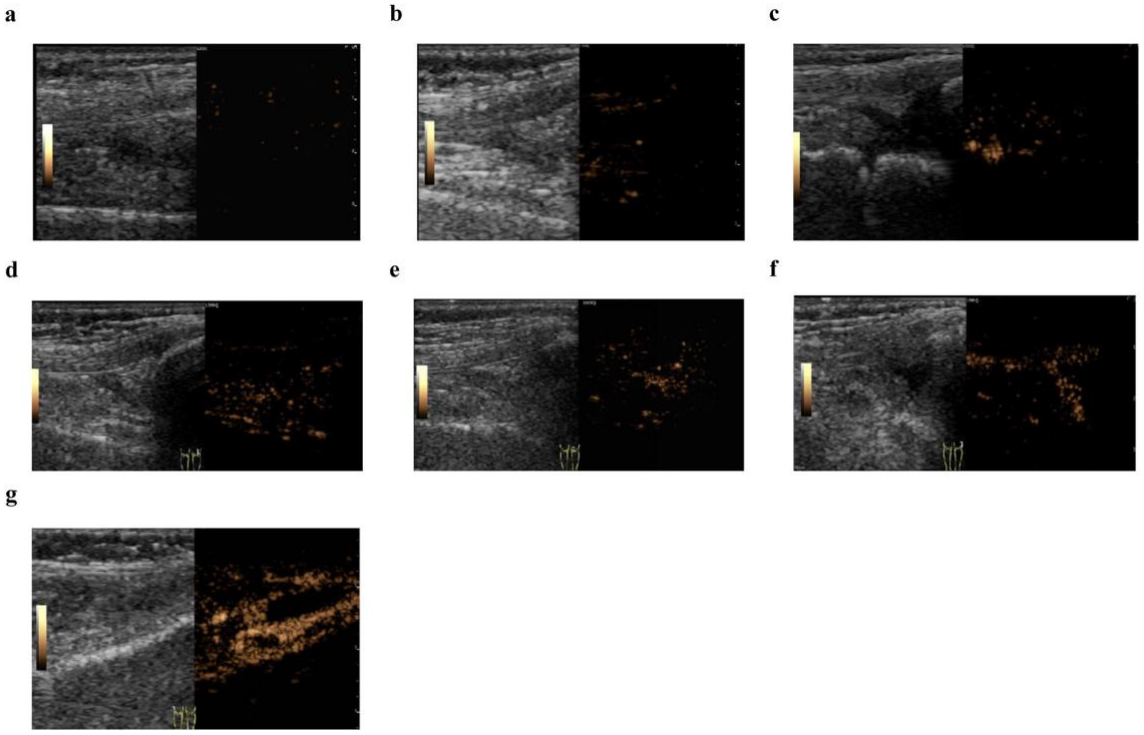


Fig. 2. CEUS atlas, with examples of the suprapatellar recess of the knee, longitudinal view. Software of VueBox® with Dual-screen mode with simultaneous display of grey-scale image (left) and contrast-only image (right) in the same view: **a**, **b** Grade 0 (few bubbles allowed); **c**, **d** Grade 1 (mild); **e**, **f** Grade 2 (moderate); **g** Grade 3 (severe). (Published in Paper 3 [86])

B.2. MRI examination

The CEMRI protocol included T1-weighted, T1 weighted fat-suppressed pre- and post-intravenous gadolinium (GD) contrast administration, Proton Density-weighted with fat suppression (PD-FS), DWI, FLAIR-FS, and a dynamic T1-weighted sequence (for the full MRI protocol please see Supplemental Material Paper 4).

The CEMRI (Fig. 3), CEMRI+PD-FS and the FLAIR-FS (Fig. 4) were scored for inflammation (0-3 scale), by two observers, twice (6 weeks apart), independently, blinded to the clinical data (intra and inter-observer agreement). With the application tissue 4D in Syngo.via®, CEMRI quantitative measures were also taken by two observers (inter-observer agreement), in same place as CEUS and also in the sagittal plane: Peak Enhancement Intensity (PEI), initial Area Under the Curve (iAUC) and TTP.



Fig. 3 CEMRI atlas with sagittal postcontrast examples of the knee: **a** Grade 0 (none/subtle synovial enhancement CEMRI); **b**, **c** Grade 1 (mild synovial enhancement/thickening CEMRI); **d** Grade 2 (moderate synovial enhancement/thickening CEMRI); **e** Grade 3 (severe synovial enhancement/thickening CEMRI) (Adapted from Paper 3 [86])

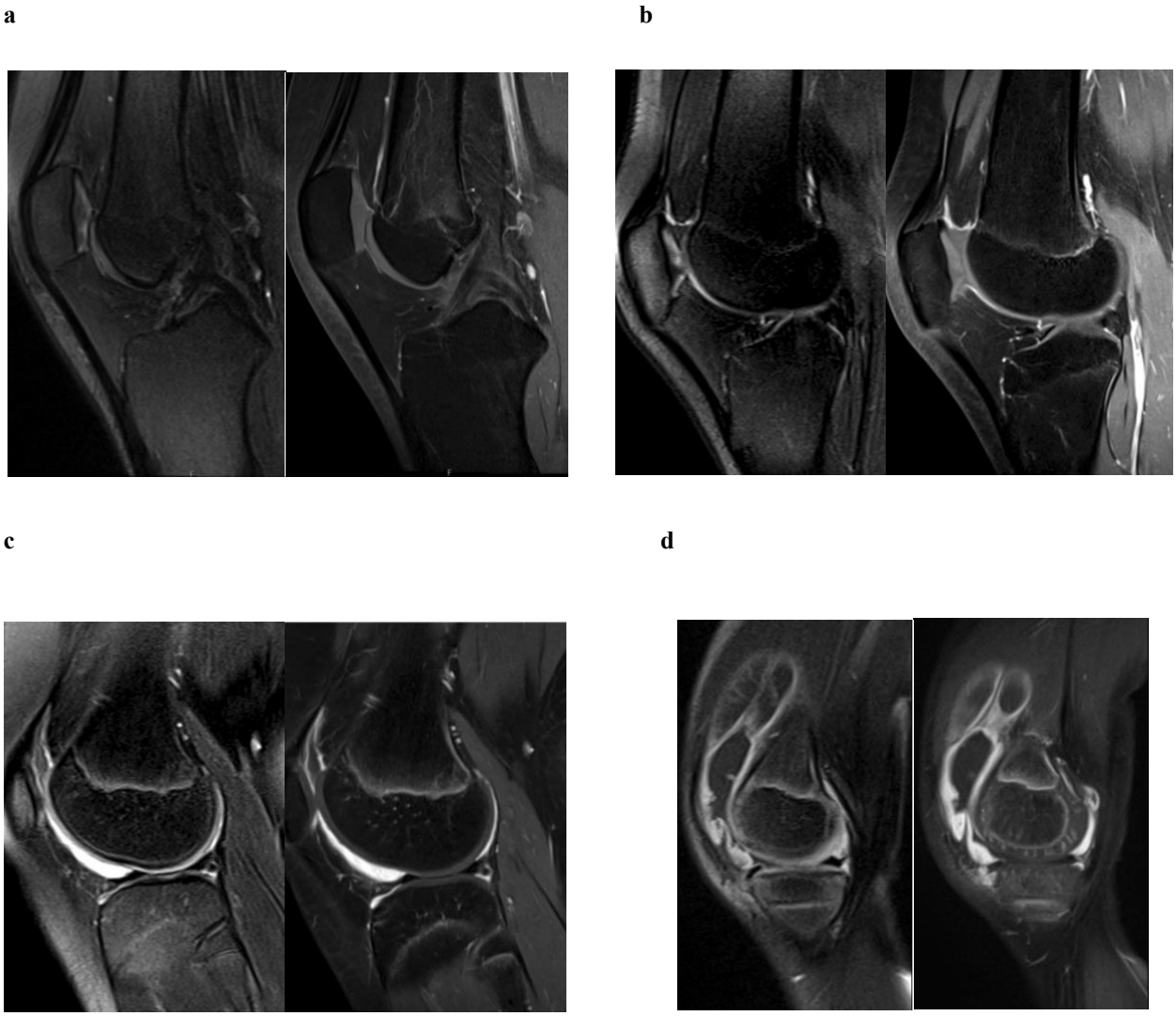


Fig. 4 FLAIR-FS/CEMRI atlas with paired examples of the knee: **a** Grade 0 (none/subtle synovial enhancement CEMRI); **b** Grade 1 (mild synovial enhancement/thickening CEMRI); **c** Grade 2 (moderate synovial enhancement/thickening CEMRI); **d** Grade 3 (severe synovial enhancement/thickening CEMRI) (Under Submission Paper 4)

C. The healthy FLAIR-FS MRI cohort

To establish normal appearances of the knee joint on a FLAIR-FS sequence, healthy and asymptomatic paediatric volunteers residing in the same area as the JIA cohort were invited to undergo an MRI without intravenous contrast, including a FLAIR-FS sequence (for the MRI protocol please see Supplemental Material Paper 4).

The study was approved by the Regional Ethics Committee (number 282-20), and written informed consent was obtained from each participant and/or their caregiver, according to national guidelines.

Recruitment was conducted via e-mail and direct invitations, with volunteers selected to frequency-match the age and sex distribution of the JIA cohort. Excluded were individuals with chronic diseases or undergoing treatments that could potentially affect the skeletal system, incapacity to perform the exam without sedation and knee trauma within the previous two months.

C.1. MRI examination

The FLAIR-FS sequence of the healthy volunteers was scored for inflammation (0-3 scale), by two observers (inter-observer agreement), independently, blinded to the demographic data.

D. Statistical analysis

D.1. Descriptive Statistics and Group Comparisons

Data normality was assessed across all cohorts. Except for age and height in the healthy school volunteer cohort, continuous variables consistently deviated from a normal distribution. Consequently, non-parametric analyses were applied, with continuous variables expressed as medians with corresponding percentiles (PCTL) or interquartile ranges (IQR). Baseline reference intervals for the US healthy volunteer cohort were defined using the 2.5th and 97.5th percentiles.

Differences between independent groups were evaluated using the Mann-Whitney U test or the Kruskal-Wallis test, as appropriate. For paired samples, including bilateral intra-subject or multi-modal comparisons, the Wilcoxon signed-rank test was utilised. Categorical variables were cross-tabulated and analysed using the Chi-Square test of

independence or Fisher's exact test. Spearman's rank correlation coefficient was employed to assess the strength and direction of associations between quantitative imaging metrics.

D.2. Reliability

Intra- and inter-observer reliability for categorical and semi-quantitative grading scales was determined using simple Cohen's kappa (κ) or linear weighted kappa coefficients with corresponding 95% confidence intervals (CI), supplemented by the proportion of absolute agreement.

For continuous and quantitative metrics, relative reproducibility was quantified using the ICC (two-way mixed-effects, consistency type) with 95% CIs. Absolute agreement and potential observer bias were visualised and quantified using Bland-Altman mean-difference plots with 95% limits of agreement (LoA). Inter-observer reproducibility for the ultrasound protocol was validated on a subset of 27 right knees.

D.3. Diagnostic Performance and Discriminative Ability

The diagnostic performance of CEUS and non-contrast FLAIR-FS was evaluated against the reference standard (CEMRI). Sensitivity, specificity, and overall diagnostic accuracy were calculated with their corresponding 95% CIs.

Binary Receiver Operating Characteristic (ROC) curve analysis was employed to evaluate the discriminative capability of the alternative imaging techniques relative to the reference standard. The Area Under the ROC Curve (AUC) and its 95% CIs were calculated, and optimal diagnostic cut-off thresholds were selected based on the clinical context.

D.4. Multivariable logistic regression model to predict JIA disease in the knee

A multivariable logistic regression model with backward stepwise selection identified independent predictors of the outcome probability. The model predictive performance was evaluated via receiver operating characteristic (ROC) curve analysis. The optimal

diagnostic cut-off was determined using Youden's Index, prioritizing a clinically relevant sensitivity threshold (≥ 80%).

D.5. Significance Threshold and Software

For all analyses, the threshold for statistical significance was set *a priori* at 5% ($p < 0.05$), and all reported *p*-values are two-tailed. Statistical computations were performed using IBM® SPSS® Statistics (versions 27.0 and 30.0; IBM Corp., Armonk, NY, USA) and Jamovi (versions 2.3 and 2.6.26; Jamovi Project, Sydney, Australia).

THESIS OUTPUTS

A. Research Line I

Paper 1 - Knee-ultrasound: reference values for the amount of joint fluid and synovial appearances in healthy children and adolescents

Dias SC, Carvalho DC, Castro M, Dias CC, Ramos I, Brito I, Rosendahl K.
Pediatr Radiol 55, 1127–1137 (2025). https://doi.org/10.1007/s00247-025-06243-0

Pediatric Radiology
https://doi.org/10.1007/s00247-025-06243-0

RESEARCH

Knee-ultrasound: reference values for the amount of joint fluid and synovial appearances in healthy children and adolescents

Sílvia Costa Dias[1,2] · Diogo Costa Carvalho[2] · Miguel Castro[2] · Cláudia Camila Dias[3,4] · Isabel Ramos[1] · Iva Brito[1,5] · Karen Rosendahl[6,7]

Received: 28 October 2024 / Revised: 2 April 2025 / Accepted: 7 April 2025
© The Author(s) 2025

Abstract

Background With increasing ultrasound use, data for the normal amount of joint fluid and synovial appearances are needed.

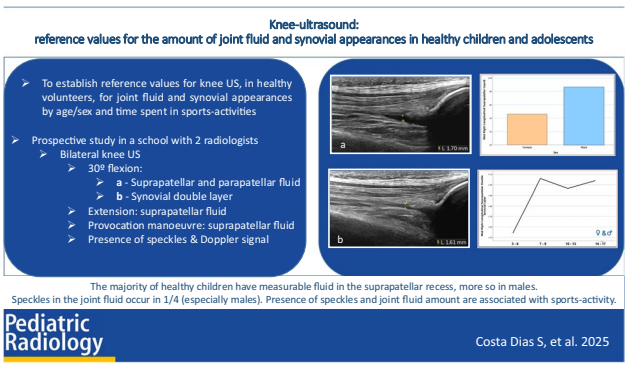
Objective To establish reference values for knee-ultrasound in healthy volunteers by age. To examine the association of joint fluid and synovial appearances with age, sex, and time spent in sports activities.

Materials and methods Prospective, cross-sectional, including 3–17-year-old volunteers. Examinations were performed by one of two experienced radiologists after meticulous standardisation of the technique. Knees were examined in 30° flexion, in extension and during provocation.

Results One hundred twenty-seven volunteers (67 females), median age 10.9 years (percentile 2.5th-97.5th: 3.4–17.2), were included. With 30° knee flexion, the median amount of suprapatellar recess joint fluid (sagittal view) was 0.5 mm for females and 0.9 mm for males ($P=0.014$), increasing to 1.9 mm and 2.4 mm ($P=0.031$), respectively, during provocation. The amount of fluid during provocation increased with age for both sexes ($P=0.007$ females; $P=0.012$ males) and by time spent in sport-activities ($P=0.003$). Further, there was a positive association between the presence of joint fluid speckles and sport-activities ($P=0.039$). Median double-layered synovium was 1.5 mm in 3–6-year-olds, increasing to 2.1 mm in 7–9-year-olds and 2.0 mm in 10–17-year-olds ($P=0.024$). No synovial Doppler signal was seen. Observers' agreement was excellent, with ICC values ≥ 0.9.

Conclusion The majority of healthy children have measurable knee joint fluid, more so when examined with a flexed knee and under provocation. Speckles within the joint fluid are seen in one-fourth, especially in males, and the presence of speckles and joint fluid amount are associated with sports-activity.

Graphical Abstract



Keywords Knee · Musculoskeletal ultrasound · Suprapatellar recess · Synovial fluid · Synovial membrane

Extended author information available on the last page of the article

Published online: 02 May 2025

Background

Recent advancements in ultrasound imaging technology have provided exquisite high-resolution images allowing for detailed differentiation between synovium and joint fluid, with the potential to improve diagnosis and follow-up of juvenile idiopathic arthritis (JIA). JIA is characterised by chronic synovial inflammation, e.g. thickened, hyperaemic synovium and effusion, with a potential risk of developing progressive joint destruction and serious functional disability [1, 2]. Recent research has shown that adult disease is seen in up to 70% of those having suffered JIA, underscoring the importance of close monitoring of disease activity to guide therapy during childhood [3]. Normally, joints contain a small amount of joint fluid; however, current literature on reference values is sparse, with a few studies addressing the wrist, elbow, or hip joints [4–6]. For knees, there are two main studies, one including 60 children aged 2–16 years (2007) [7] and one including 257 children aged 1–18 years (2016) [8]. Both studies have published reference values for the depth of the suprapatellar recess, of which one by age and sex [8]. However, none of the studies has distinguished between synovium and joint fluid, or addressed potential differences in appearances by knee positioning and provocation. Moreover, no studies have mentioned the presence of small echogenic dots, or speckles within normal joint fluid that might be seen in some children.

The purpose of our study is to provide ultrasound-data on the presence, amount, and appearances of joint fluid and the appearances of synovium of the knee joint in healthy children and adolescents, by sex, age, and sport-activities.

Materials and methods

Study design

This was a single-centre, prospective, cross-sectional study including volunteers from a private school in Porto/Portugal. The study was approved by the Institutional Ethics Committee (IEC) (registration number CE 191/22) and by the school board. Written, informed consent was obtained from all the participants and caretaker(s). Children aged 3–17 years were invited to participate via invitations sent to parents' representatives. Exclusion criteria were (a) chronic medicated disease that might affect the skeletal system or (b) having experienced a knee trauma within the last 2 months.

Questionnaire on diseases and knee pain: leg-length assessment

All participants/caretakers filled in a questionnaire on diseases, medication, knee pain/symptoms, and sport-habits (number of sports and hours per week). Knee pain/symptoms were scored as 0 = never, 1 = sporadic, 2 = sometimes, or 3 = frequent. In addition, leg length discrepancy was assessed subjectively at 0.5-cm intervals, by levelling the iliac crests with the child in an upright position.

Ultrasound examination of the knees

The ultrasound examinations were performed between October 17 and 21, 2022, by one of two examiners (paediatric and musculoskeletal radiologists with 10/12 years of experience, respectively), following meticulous discussions and standardisation of the ultrasound protocol [7–10]. All examinations were performed on a Logiq E10 machine—Version R3 (V.3.2), General Electric (GE Healthcare, Milwaukee, WI), with a linear 6–15-MHz transducer and defined pre-sets. To compare colour and power Doppler, both techniques were performed in the first 23 participants, whilst the remainder were examined with colour Doppler alone. We used low flow settings (adjusted from Ting et al. [9]), including a pulse repetition frequency < 1.0 (0.6), low wall filter (51 Hz), and frequency adjusted to obtain maximum sensitivity, as well as gain (set just below artefact levels). Signal was only considered if located within the synovial area, and scored as 0 (no signal); 1 (1 to 3 signals); 2 (> 3 signals or confluent signals in < 50% of area of synovium); or 3 (confluent signals in > 50% of area of synovium), according to Ting et al. [9].

With the participant supine, both knees were examined in 30° flexion, using a longitudinal (standard) view (Fig. 1) and thereafter a transverse view through the lateral and medial parapatellar recesses (Fig. 2). Doppler signals were scored. The presence of hyperechoic, small dots/speckles within the joint fluid was noted for each of the recesses, also including lateral and medial sections, and below the parapatellar view (Fig. 2). Further, the infrapatellar recess was assessed, with fluid measurements underneath the lower pole of the patella and in the deep infrapatellar bursa (Fig. 2). The suprapatellar recess was also examined with knees extended (Fig. 3) and under provocation (Fig. 4).

For inter-observer reproducibility, a second observer, blinded to the first results, examined the right knees in 27 participants within minutes of the first observer.

Statistical analysis

Except for age and height, continuous variables were not normally distributed; thus, non-parametric tests (Mann–Whitney or Kruskal–Wallis) were applied, using median (Mdn) and percentiles. Age-related values with Mdn 2.5^{th} and 97.5^{th} percentiles were calculated for four age groups (3–6, 7–9, 10–13, and 14–17 years). The Wilcoxon test was used for paired samples. To test the independence of categorical variables, the independent chi-square or the Fisher exact test was applied. The reproducibility between

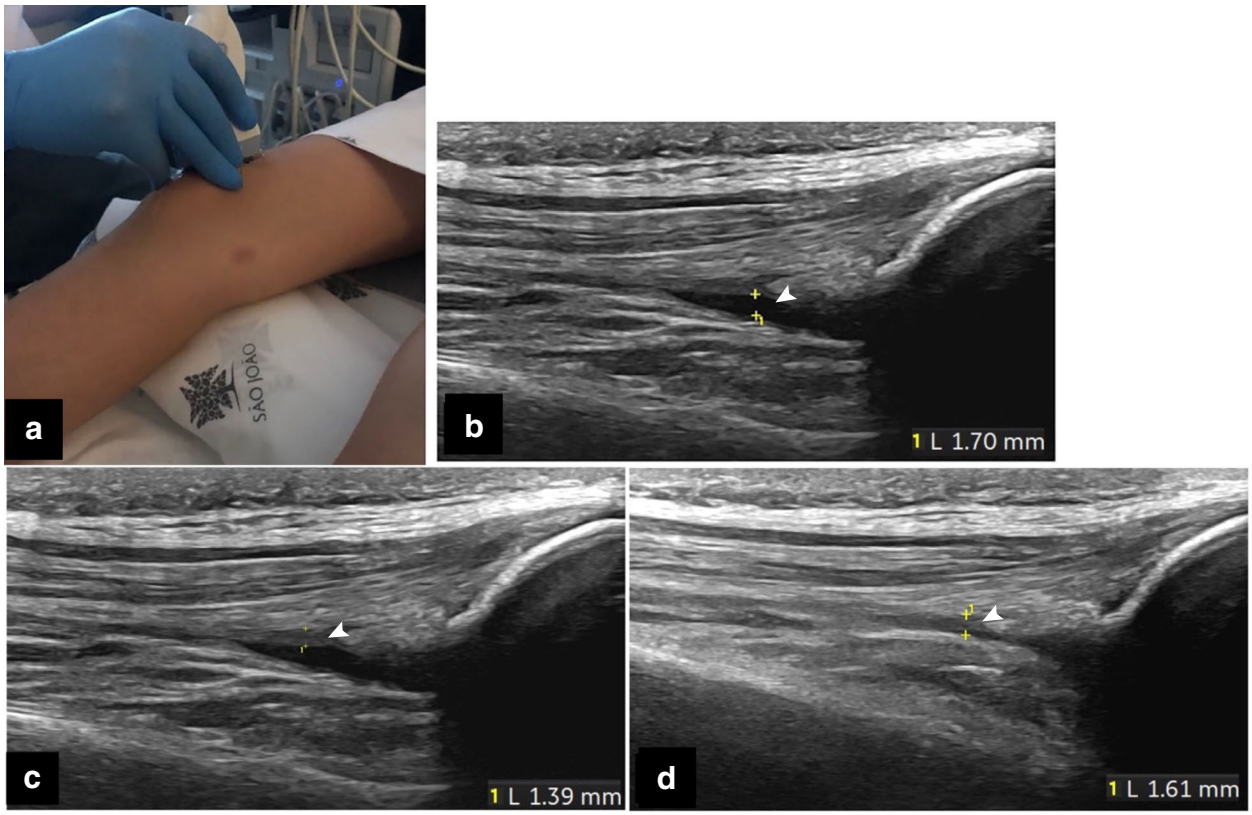


Fig. 1 **a** Knee 30° flexed, in a 10-year-old healthy boy, accessing the suprapatellar recess—central longitudinal view ("standard"). **b**-**d** A 13-year-old healthy boy, with 30° knee flexion, central longitudinal standard view. **b** Anteroposterior measurements of fluid (*arrowhead*). **c** Single synovial layer (*arrowhead*). **d** Double synovial layer (during light transducer compression to squeeze fluid away) (*arrowhead*)

two readers was analysed for 27 right knees, using intra-class correlation coefficient (ICC) with 95% confidence intervals (0–0.39 = poor; 0.40–0.59 = fair, 0.60–0.74 = good, and 0.75–1.00 = excellent agreement) [11] and Bland–Altman mean-difference plots. The mean difference and standard deviation of the differences are reported as measures of bias and variability within or between observers. Twice this standard deviation is defined by the British Standards Institution as a "repeatability coefficient". For categorical variables, simple Cohen kappa with 95% confidence intervals was used. A P-value < 0.05 was considered a priori statistically significant. The reported P-values are two tailed. The statistical analysis was performed in Statistical Package for the Social Sciences (SPSS®) v.27.0 and Jamovi (Version 2.3) (computer software).

Results

A total of 127 participants (67 female) were included. Median age was 10.9 years (PCTL 2.5 th- 97.5th 3.4–17.2 years). Demographic and clinical characteristics of the participants by sex are listed in Table 1.

Joint fluid

From the 127 participants, 96 (75.6%) had visible joint fluid in at least one of the suprapatellar recesses, knee 30° flexed, whilst 62 (48.8%) had bilateral fluid. Apart from the lateral parapatellar recess (right > left, $P = 0.004$), the amount of joint fluid did not differ according to side; thus, the main results are given for the right side only.

The Mdn amount of suprapatellar fluid for females was 0.5 mm with the knee 30° flexed, vs. 0.9 mm for males ($P = 0.014$), rising to 1.9 mm and 2.4 mm, respectively, under provocation ($P = 0.031$). No such difference was seen in either of the parapatellar views (Table 2). In extension, the Mdn amount of fluid was 0.0 mm for both sexes, and thus significantly lower as compared to 30° flexion ($P < 0.001$).

Females

In total, 36/67 (53.7%) had visible fluid in the suprapatellar recess (range 0.5–2.7 mm) whilst this was true for 29 (43.2%) of the medial parapatellar (range 0.3–1.4 mm), and 25 (37.3%) of the lateral parapatellar recesses (range 0.4–1.8 mm). The amount of fluid in the lateral and medial

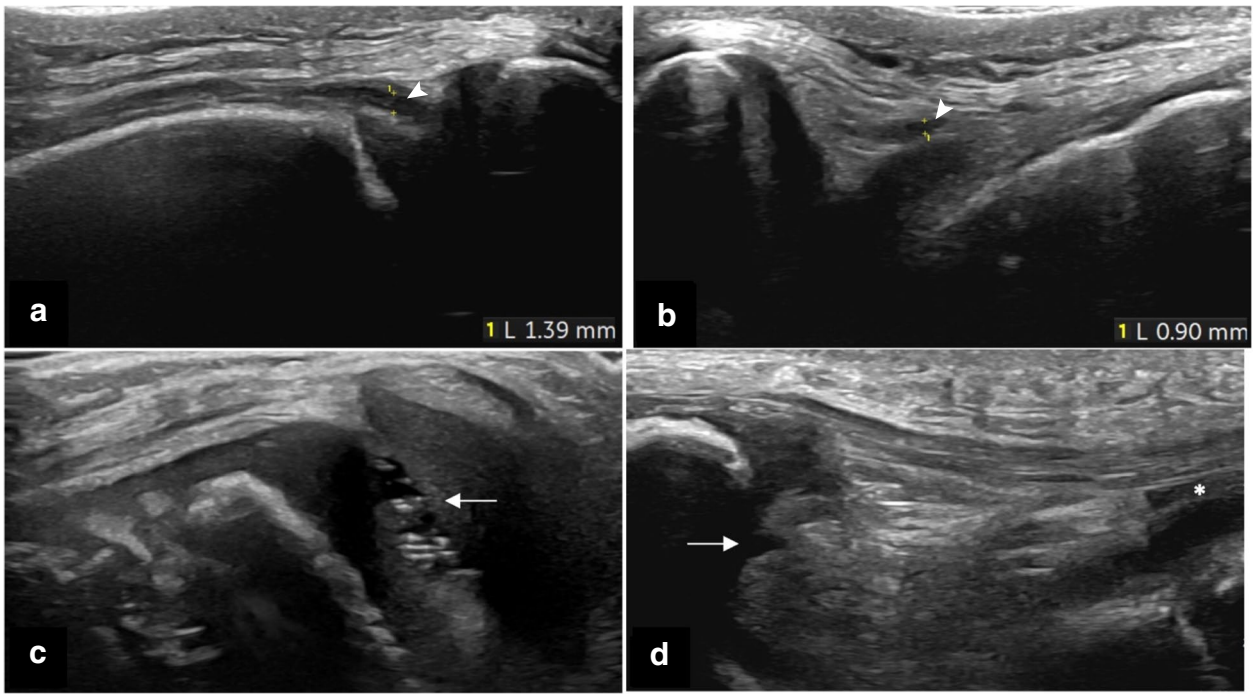


Fig. 2 Knee 30° flexed in healthy children. **a**, **b** Transverse views, with measurement of fluid (*arrowheads*) in lateral (**a**) and medial (**b**) parapatellar recesses in a 13-year-old boy. **c** Speckles in the lateral joint space (*arrow*) in a 7-year-old girl. **d** Infrapatellar recess in a 4-year-old girl: fluid is seen underneath the lower pole of the patella (*arrow*) and in the deep infrapatellar bursa (*asterisk*)

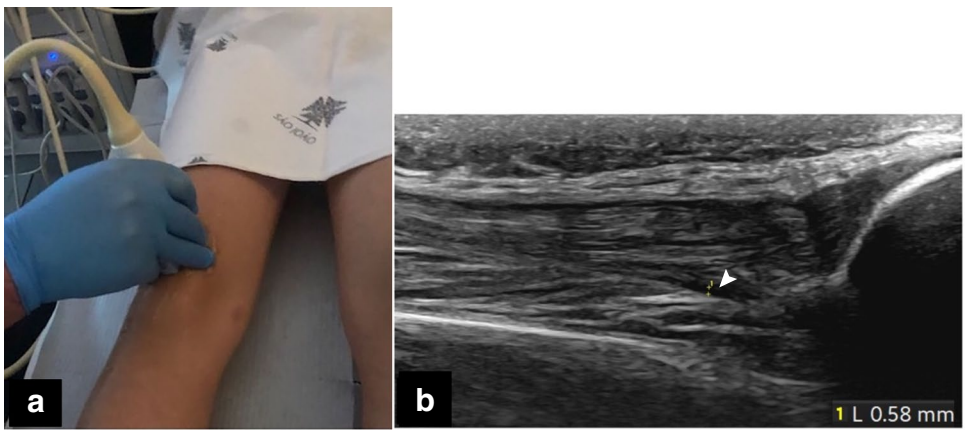


Fig. 3 Knee extended in healthy children. **a** Same participant as Fig. 1a, a 10-year-old boy, using the standard longitudinal view. **b** Same participant as Fig. 1b-d, a 13-year-old boy, anteroposterior measurement, showing less fluid in the recess (*arrowhead*)

parapatellar recess, as well as the amount of fluid on provocation, increased significantly across age groups (Table 3).

Males

In total, 44/60 (73.3%) had fluid in the suprapatellar recess (range 0.6–3.0 mm), whilst this was true for 23 (38.3%) in the medial (range 0.5–1.8 mm), and 27 (45.0%) in the lateral parapatellar recesses (range 0.5–2.4 mm). The amount of fluid in the lateral parapatellar recess, as well as the amount of fluid on provocation, increased significantly by age (Table 4).

Speckles within the joint fluid

Speckles in at least one recess were seen in 26 right knees (20.5%), in 18 (14.2%) of the suprapatellar recess, in 9 (7.1%) of the lateral and in 4 (3.1%) of the medial parapatellar recesses. In 56 (44.1%) right knees, there were speckles along the lateral joint space, whilst speckles along the medial joint space were seen in 30 (23.6%).

The number of recesses containing at least one speckle was lower for females, with at least one positive recess in 6 of the females (9.0%) versus 20 of the males (33.3%) ($P < 0.001$). Considering just the suprapatellar recess, the figures

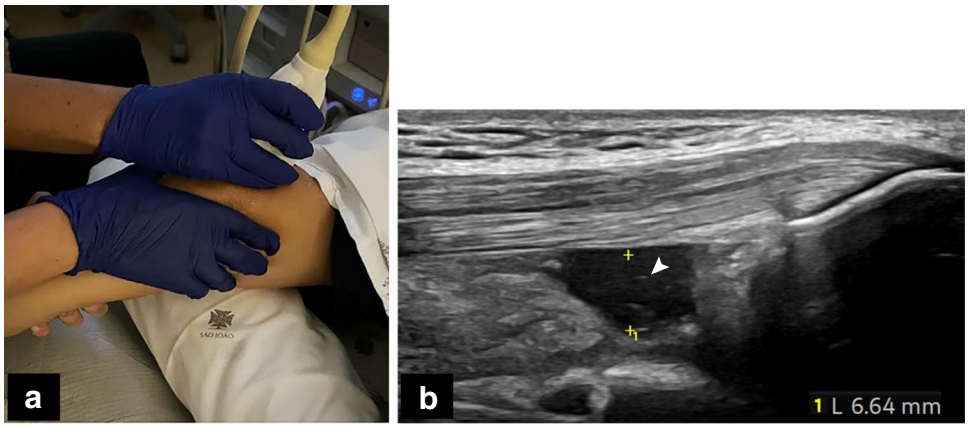


Fig. 4 Provocation manoeuvre, knee 30° flexed in healthy children. **a** With one hand squeezing from side to side, whilst performing an upward movement (same participant in Fig. 1a, a 10-year-old boy). **b** Fluid measurement (longitudinal standard view) (*callipers*) in a 16-year-old boy. Note speckles in the fluid (*arrowhead*)

Table 1 Descriptive statistic: study population

Participants	Total	Females	Males	*P*–value[a,b]
n (%)	127 (100%)	67 (52.8%)	60 (47.2%)	
Age years, Mdn (percentile 2.5th–97.5th)	10.9 (3.4–17.2)	10.9 (3.3–16.8)	10.9 (3.3–17.3)	0.723[a]
Height cm, Mdn (percentile2.5th–97.5th)	143.3 (97.6–182.9)	143.0 (95.1–170.0	143.5 (98.1–186.1)	0.467[a]
Weight kg, Mdn (percentile 2.5th–97.5th)	37.4 (15.4–72.8)	38.1 (15.6–69.8)	34.9 (14.8–74.3)	0.961[a]
BMI Mdn (percentile 2.5th–97.5th)	25.5 (15.5–41.6)	26.4 (16.3–43.3)	24.2 (15.0–41.6)	0.927[a]
Race – Caucasian, *n* (%)	123 (96.9)	64 (95.5)	59 (98.3)	0.621[b]
Past medical history, *n* (%)	18 (14.2)	7 (10.4)	11 (18.3)	0.203[b]
Medication[c], *n* (%)	4 (3.2)	1 (1.5)	3 (5.0)	0.343[b]
Trauma last 2–6 months, *n* (%)	2 (1.6)	2 (3.0)	0 (0.0)	0.498[b]
Previous history OSD (knees) *n*/individuals	5/4	2/2	3/2	
Knee symptoms (mainly mild pain)				
Sporadic or sometimes, *n* (%)	18 (14.2)	13 (10.2)	5 (8.3)	0.074[b]
Sport-activities, *n* (%)				
Number sports, Mdn (percentile 2.5th–97.5th)	1.0 (0.0–3.0)	1.0 (0.0–3.3)	1.0 (0.0–3.0)	0.932[a]
Total hours/week, Mdn (percentile 2.5th–97.5th)	3.0 (0.0–10.0)	2.0 (0.0–12.1)	3.0 (0.0–10.0)	0.080[a]
Limb discrepancy, *n* (%)	16 (12.8)	8 (11.9)	8 (13.3)	0.813[b]
Left limb shorter, *n*	10	4	6	0.608[b]

BMI body mass index, *Mdn* median, *OSD* Osgood-Schlatter disease

[a]Mann-Whitney

[b]Chi-square test

[c]Other than chronic anti-inflammatory or immunosuppressant drugs

were positive in 3 females (4.5%) versus 15 males (25.0%) ($P < 0.001$).

Associations between joint fluid, speckles, and additional features

The amount of joint fluid in the right suprapatellar recess increased significantly by the total hours of weekly sport-activity, both when based on the 30° flexed view ($P = 0.028$) and on provocation ($P = 0.003$), and in the lateral parapatellar recess ($P = 0.029$) (Fig. 5). Similarly, there was a significant association between total hours of sports-activity and the presence of speckles in the joint fluid ($P = 0.039$), with higher Mdn of hours for children with speckles (3.5 h vs. 2.0 h per week for children without speckles). No statistically significant associations were found between the amount of joint fluid and the presence of speckles, with past medical history, symptoms, medication, trauma, or lower limb length discrepancy.

Fluid in other locations

Fluid underneath the inferior pole of the right patella was identified in 3 (15.0%) children aged 3–6 years and in 2

Table 2 Amount of fluid in the recesses in millimetres, median with 2.5th–97.5th percentiles for 127 children, the right knee, by location and sex

Location	Female ($n = 67$)	Male ($n = 60$)	P–value[a]
Longitudinal suprapatellar			
30° flexion, Mdn (Percentile 2.5th–97.5th)	**0.5 (0.0–2.4)**	**0.9 (0.0–2.6)**	**0.014**
Extension, Mdn (Percentile 2.5th–97.5th)	0.0 (0.0–0.9)	0.0 (0.0–1.3)	0.239
Provocation, Mdn (Percentile 2.5th–97.5th)	**1.9 (0.4–4.5)**	**2.4 (0.8–5.8)**	**0.031**
Transverse parapatellar			
Lateral, Mdn (Percentile 2.5th–97.5th)	0.0 (0.0–1.8)	0.0 (0.0–2.3)	0.162
Medial, Mdn (Percentile 2.5th–97.5th)	0.0 (0.0–1.4)	0.0 (0.0–1.7)	0.843

Mdn median

[a]Mann-Whitney test

(6.9%) children aged 7–9 years, but not in the older age groups ($P = 0.017$). Of the 127 participants, 12 (9.4%) had some fluid in the right deep infrapatellar bursa, with no differences according to age ($P = 0.537$). For both findings, there were no differences according to sex ($P = 0.542$ and 0.823) or symptoms ($P = 0.735$ and 0.754).

Synovial thickness and Doppler signal

For the suprapatellar recess, no significant differences in thickness of the double-layered synovium were seen according to side ($P = 0.714$) or sex ($P = 0.627$). However, significant differences were found according to age groups. Thus, synovial thickness of the double-layered synovium is given for the right knee by age group (Table 5). A simple linear regression based on the right measures showed an equation, in which synovial double-layer thickness is predicted in millimetres based on age, with $P < 0.001$ (Table 5). No significant associations were found between synovial thickness and past medical history, medication, trauma, or leg length discrepancy.

No colour Doppler signal was seen within the synovium in either of the ultrasound views performed. In the first 23 children, an additional power Doppler examination was performed. No Doppler signal was seen on either of the two techniques; thus, for the remainder 104 participants, only colour Doppler was obtained.

Inter-observer agreement

Inter-observer agreement on the assessment of fluid and synovial thickness was excellent, with ICC values ≥ 0.9. One-sample *t*-tests showed that the corresponding mean difference (bias) was not significantly different from zero for fluid measurements or synovial thickness ($P > 0.999$ and $P = 0.899$, respectively). Ninety-five per cent limits of agreement were relatively wide for fluid (± 65% of the sample mean) and fair for synovial thickness (± 35% of the sample mean) (Supplementary Material 1). The agreement for identification of speckles and scoring of Doppler signals was excellent, with kappa values between 0.9–1.0 for speckles and 1.0 for Doppler.

Table 3 Amount of fluid in the recesses in millimetres, median with 2.5th–97.5th percentiles for 67 females, the right knee, by location and age group

Location	Age category, years				P–value[a]
	3–6 ($n = 10$)	7–9 ($n = 16$)	10–13 ($n = 29$)	14–17 ($n = 12$)	
Longitudinal suprapatellar					
30° flexion, Mdn (Percentile 2.5th–97.5th)	0.5 (0.0–1.3)	0.0 (0.0–2.4)	0.6 (0.0–2.2)	0.3 (0.0–2.0)	0.796
Extension, Mdn (Percentile 2.5th–97.5th)	0.0 (0.0–1.0)	0.0 (0.0–0.8)	0.0 (0.0–0.8)	0.0 (0.0–0.0)	0.367
Provocation, Mdn (Percentile 2.5th–97.5th)	**1.1 (0.2–2.3)**	**1.9 (0.3–3.3)**	**2.2 (0.9–4.4)**	**1.8 (1.0–4.6)**	**0.007**
Transverse parapatellar					
Lateral, Mdn (Percentile 2.5th–97.5th)	**0.0 (0.0–0.0)**	**0.0 (0.0–0.7)**	**0.0 (0.0–1.8)**	**1.0 (0.0–1.4)**	**< 0.001**
Medial, Mdn (Percentile 2.5th–97.5th)	**0.0 (0.0–0.2)**	**0.0 (0.0–1.1)**	**0.6 (0.0–1.1)**	**0.6 (0.0–1.4)**	**0.027**

Mdn median

[a]Kruskal-Wallis test

Table 4 Amount of fluid in the recesses in millimetres, median with 2.5th–97.5th percentiles for 60 males, the right knee, by location and age group

Location	Age category, years				*P*–value[a]
	3–6 ($n = 10$)	7–9 ($n = 13$)	10–13 ($n = 25$)	14–17 ($n = 12$)	
Longitudinal suprapatellar					
30° flexion, Mdn (Percentile 2.5th–97.5th)	0.8 (0.0–2.4)	0.8 (0.0–1.6)	1.0 (0.0–2.5)	0.8 (0.0–2.7)	0.841
Extension, Mdn (Percentile 2.5th–97.5th)	0.0 (0.0–0.5)	0.0 (0.0–0.7)	0.0 (0.0–1.0)	0.0 (0.0–1.6)	0.628
Provocation, Mdn (Percentile 2.5th–97.5th)	**1.9 (1.0–3.6)**	**1.7 (0.7–3.2)**	**2.8 (0.9–5.2)**	**3.1 (1.5–6.3)**	**0.012**
Transverse parapatellar					
Lateral Mdn (Percentile 2.5th–97.5th)	**0.0 (0.0–0.4)**	**0.0 (0.0–1.2)**	**0.0 (0.0–2.2)**	**1.1 (0.0–2.4)**	**0.001**
Medial Mdn (Percentile 2.5th–97.5th)	0.0 (0.0–0.0)	0.0 (0.0–1.1)	0.0 (0.0–1.8)	0.6 (0.0–1.3)	0.053

Mdn median

[a]Kruskal-Wallis test

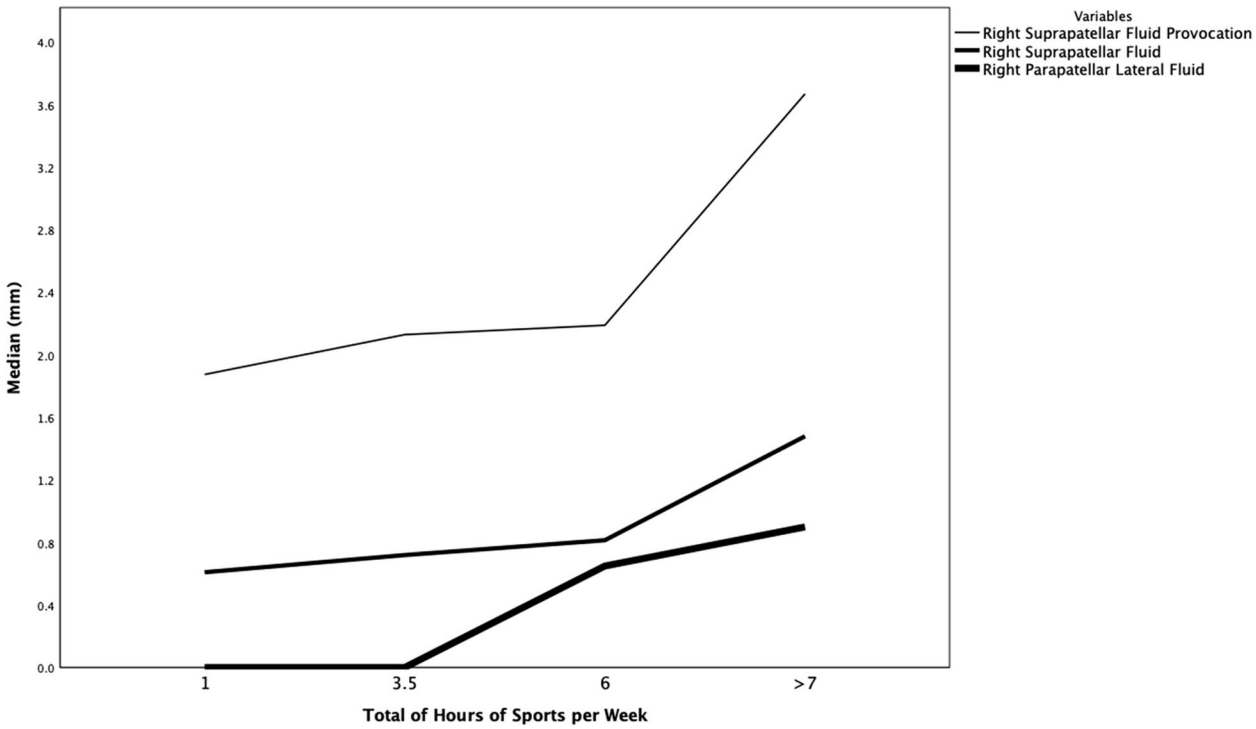


Fig. 5 Median amount of joint fluid millimetres in the right suprapatellar recess, with/without provocation, and in the lateral parapatellar recess through total hours of sports activities per week

Discussion

We have presented reference values for the amount of joint fluid and synovial thickness of the knee in healthy children and adolescents, examined for research purposes only. To the best of our knowledge, this is the first study to assess joint fluid and synovium separately, and to describe speckles within the joint fluid. More than 75% of the 127 volunteers had visible joint fluid in at least one of the suprapatellar recesses with the knee 30° flexed, whilst nearly half had bilateral fluid. Of note is that the amount of fluid was higher with the knee 30° flexed as compared to extended, that males had more fluid than females, and that the amount increased with age and on provocation. Moreover, that speckles were seen in at least one of the recesses

Table 5 Synovial thickness in millimetres, median with 2.5th–97.5th percentiles in 127 children (60 males), the right knee, by age group. Equation to predict synovial thickness in millimetres based on age in years

Location	Age category, years				*P*–value[a]
	3–6 (*n* = 20)	7–9 (*n* = 29)	10–13 (*n* = 54)	14–17 (*n* = 24)	
Longitudinal suprapatellar					
30° flexion, Mdn (Percentile 2.5th–97.5th)	**1.5 (1.1–2.5)**	**2.1 (1.2–2.9)**	**2.0 (1.3–3.9)**	**2.0 (1.4–3.3)**	**0.024**
Synovial thickness (mm) = 1.493 + 0.05 × age in years					

Mdn median, *mm* millimetres

[a]Kruskal-Wallis test

in one-fourth of the participants, more so in males, and that both the presence of speckles and the amount of joint fluid were associated with sports-activity.

Our results compare in part with those of others, although the examination techniques differ slightly. In a study of 60 healthy children aged 2–16 years-old, Collado et al. [7] found fluid in 60% of the suprapatellar recesses with knees in 30° flexion, as compared to 75% in our cohort. However, they applied pressure with the ultrasound probe whilst assessing the suprapatellar recess, leading to a fluid reduction. Furthermore, they reported fluid in 58% of the medial and 33% of the parapatellar recesses with the knees extended, which potentially also reduces the fluid. Thus, these technical issues may explain part of the differences.

Similarly, in a multicentre study of 435 children aged 1–18 years old, Windschall et al. [8] found that over 64% of the children had visible fluid in the suprapatellar recess, varying from 18% amongst 1–3-year-olds to 80% of 4–6-year-olds. The results were presented by age categories and sex; however, potential statistically significant differences between sexes were not analysed for these features. Their reported reference values for the suprapatellar recess were generally higher than ours, most likely reflecting differences in examination techniques. Whilst we measured fluid and synovial thickness separately in 30° flexion, followed by an extended knee position, their measurements were taken with the knees in a neutral position, measuring both a double-layered synovium and potential fluid. Our results showed that the amount of fluid in the suprapatellar recess differed significantly according to the position of the knee joint, with more fluid seen in 30° flexion compared to extension, highlighting the importance of a standardised examination technique. We could argue that assessing joint fluid and synovial thickness separately might prove more helpful, particularly when dealing with equivocal cases.

In our study, males had more fluid in the suprapatellar recess, both with the knee slightly flexed and during provocation, as compared to females. No such difference was seen for the parapatellar recesses. Further, no differences were seen according to age in either sex, except for most parapatellar recesses, showing an increase of fluid with age, particularly in the oldest age group and during provocation. The latter is interesting, as it might reflect differences in fluid localisation by age, similar to what has been reported for neonates with septic coxitis [12].

Not unexpectedly, the amount of joint fluid doubled or even tripled during the provocation manoeuvre, underscoring the importance of a standardised technique when monitoring patients with arthritis. We believe that the manoeuvre, mirroring the clinical "patella dip" test, helps understand the bigger picture as compared to one standard view alone. Moreover, the synovium was easier to assess with fluid in the recess.

Interestingly, we found a positive correlation between the amount of joint fluid and hours spent on sport-activities, indicating that mechanical stress might play a role. To our knowledge, this is a novel observation in children. Similarly, knee-MRI after exercise in adults has shown an increase of joint fluid [13, 14].

Fluid underneath the inferior pole of the patella was identified in almost 4% of the children, all under the age of 9. An explanation might be that a less ossified patella provides a better acoustic window. Another interesting finding was that 10% of children had some fluid within the deep infrapatellar bursa, with no differences according to age. Both features should be acknowledged as normal variations and not be mistaken for pathology.

We have previously noted that some children have numerous hyperechoic dots in otherwise anechoic joint fluid, not representing intra-articular gas. We have termed these findings "speckles". Interestingly, 25% of all the participants had such speckles in at least one recess, more so in males and on the lateral side of the joint space. Moreover, there was an association between the presence of speckles and hours spent on sport-activities. Their clinical significance is unclear, but we speculate that they might be related to joint fluid viscosity or with some fluid components. A study in adult patients with knee osteoarthritis reported a significant increase in joint fluid viscosity and molecular weight of hyaluronan after 12 weeks of exercise [15]; however, there was no ultrasound fluid assessment.

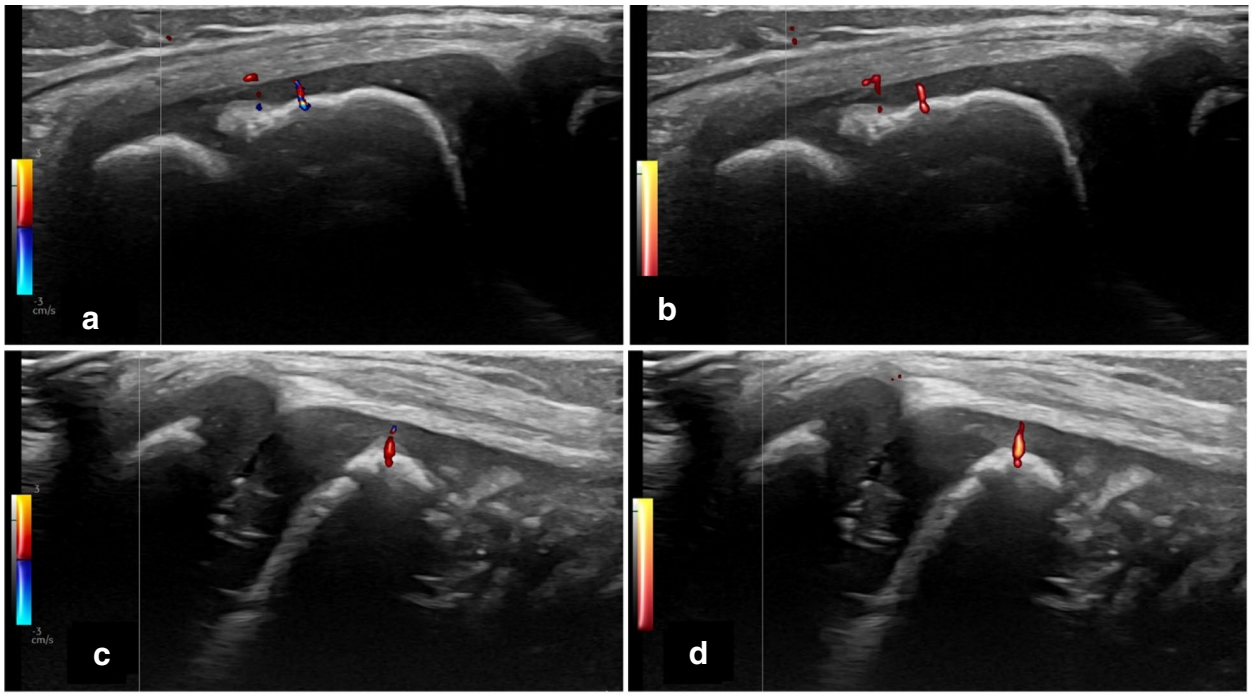


Fig. 6 Transverse knee-ultrasound images in two 7-year-old healthy girls, at the level of the lateral parapatellar recess (**a**, **b**) and at the level of the lateral joint space (**c**, **d**). The colour Doppler (**a**, **c**) and power Doppler (**b**, **d**) images show identical findings of normal vessels in cartilage

Traditionally, synovial hypertrophy in children has been graded subjectively (mild/moderate/marked). Direct measurements are less commonly used, in part due to challenges with the precision of small measurements. Roth J. et al. [16] stated that synovitis can be detected using B-mode alone, as an abnormal, intra-articular, anechoic, non-displaceable material. In our study, when the double-layered synovium was measured in the suprapatellar recess, exerting a mild pressure to remove fluid, we found a median thickness of around 2 mm, increasing with age. This is intriguing, as the Juvenile Arthritis MRI Scoring (JAMRIS) system [17] has defined synovial hypertrophy as enhancing synovium thicker than 2 mm. Their cut-off between normality and pathology is supported by an MRI-study of healthy children reporting that the normal, enhancing synovium does not exceed 1.8 mm in thickness [18]. Direct comparison between ultrasound and MRI is difficult due to different image technologies; however, ultrasound images have better spatial resolution as compared to MRI.

Measurements of single synovial layer revealed non-significant results. This might be due to difficulties in measuring a single layer, especially in the absence of joint fluid. Of note is that on MRI, measuring synovial thickness in locations without fluid will correspond to our double-layer measurement.

According to Roth et al. [16], both colour and power Doppler perform well in the assessment of hyperaemia. We found no Doppler signal in either of the synovial recesses, suggesting that when present, it indicates pathology. Our findings compare well with others. In a paper by Miotto e Silva et al. [19], the authors found no power Doppler signal in the synovium of 1,224 joints examined, except for one wrist joint in one of the controls. Similarly, Collado et al. [7] found no positive Doppler signal in his study of the knee joints in 60 healthy children.

Our small pilot, comparing the two Doppler techniques, yielded no differences; however, the comparison was hampered by lack of positive cases. Some physiological Doppler signals were seen, like vessels, for example across cartilage (Fig. 6) and in Hoffa's fat pad.

The strengths of our study are the prospective design, including healthy children examined for research purposes only, and second, the meticulous and extensive ultrasound examinations, using state-of-the art ultrasound equipment. We acknowledge, however, several limitations to our study. First, all participants were recruited from the same school, most being Caucasians, potentially limiting the generalizability. Second, the number of examinations per age group by sex varied, with smaller sample sizes for some of the analysis. Third, although there was an excellent agreement on measuring fluid and synovial thickness based on the ICCs, the reproducibility as assessed by the Bland–Altman approach was only fair, a finding also reported by others [20].

Conclusion

We have presented novel, ultrasound-based references by age for synovial thickness and fluid in the knee joint, the latter for males and females separately.

Supplementary Information The online version contains supplementary material available at https://doi.org/10.1007/s00247-025-06243-0.

Acknowledgements We thank the children, parents, and the school community for the participation in this study.

Author contribution Conceptualization: S.C.D.; I.R.; I.B. and K.R. Methodology: S.C.D.; C.C.D. and K.R. Formal analysis: S.C.D.; C.C.D. and K.R. Investigation: S.C.D.; D.C.C.; M.C. Resources: S.C.D.; D.C.C.; M.C.; I.R. e I.B. Writing—Original Draft: S.C.D. and K.R. Writing—Review & Editing: S.C.D.; D.C.C.; M.C.; C.C.D.;I.R.; I.B. e K.R. Project administration: S.C.D.

Funding Open access funding provided by FCT|FCCN (b-on).

Data availability No datasets were generated or analysed during the current study.

Declarations

Conflicts of interest The authors declare no competing interests.

Open Access This article is licensed under a Creative Commons Attribution 4.0 International License, which permits use, sharing, adaptation, distribution and reproduction in any medium or format, as long as you give appropriate credit to the original author(s) and the source, provide a link to the Creative Commons licence, and indicate if changes were made. The images or other third party material in this article are included in the article's Creative Commons licence, unless indicated otherwise in a credit line to the material. If material is not included in the article's Creative Commons licence and your intended use is not permitted by statutory regulation or exceeds the permitted use, you will need to obtain permission directly from the copyright holder. To view a copy of this licence, visit http://creativecommons.org/licenses/by/4.0/.

References

1. Ravelli A, Martini A (2007) Juvenile idiopathic arthritis. Lancet 369:767–778
2. Ruperto N, Lovell DJ, Cuttica R et al (2010) Long-term efficacy and safety of infliximab plus methotrexate for the treatment of polyarticular-course juvenile rheumatoid arthritis: findings from an open-label treatment extension. Ann Rheum Dis 69:718-22
3. Arvidsson LZ, Smith HJ, Flato B, Larheim TA (2010) Temporomandibular joint findings in adults with long-standing juvenile idiopathic arthritis: CT and MR imaging assessment. Radiology 256:191–200
4. Rosendahl K, Bruserud IS, Oehme N et al (2018) Normative ultrasound references for the paediatric wrist; dorsal soft tissues. RMD Open 4:e000642
5. Trauzeddel R, Lehman H, Trauzeddel RF et al (2019) Age dependent ultrasound B-mode findings of the elbow joint in healthy children and adolescents. Rheumatol Int 39:1007–1018
6. Rohrschneider WK, Fuchs G, Troger J (1996) Ultrasonographic evaluation of the anterior recess in the normal hip: a prospective study on 166 asymptomatic children. Pediatr Radiol 26:629–634
7. Collado P, Naredo E, Calvo C, Crespo M (2007) Assessment of the joint recesses and tendon sheaths in healthy children by high-resolution B-mode and power Doppler sonography. Clin Exp Rheumatol 25:915–921
8. Windschall D, Trauzeddel R, Haller M et al (2016) Imaging Working Group of the German Society of Rheumatology in C, Adolescense (2016) Pediatric musculoskeletal ultrasound: age- and sex-related normal B-mode findings of the knee. Rheumatol Int 36:1569–1577
9. Ting TV, Vega-Fernandez P, Oberle EJ et al (2019) Novel ultrasound image acquisition protocol and scoring system for the pediatric knee. Arthritis Care Res (Hoboken) 71:977-85
10. Collado P, Vojinovic J, Nieto JC et al (2016) Toward standardized musculoskeletal ultrasound in pediatric rheumatology: normal age-related ultrasound findings. Arthritis Care Res (Hoboken) 68:348–356
11. Hallgren KA (2012) Computing inter-rater reliability for observational data: an overview and tutorial. Tutor Quant Methods Psychol 8:23–34
12. Sreenivas T, Nataraj AR, Kumar A, Menon J (2016) Neonatal septic arthritis in a tertiary care hospital: a descriptive study. Eur J Orthop Surg Traumatol 26:477–481
13. Lohman M, Kivisaari A, Vehmas T et al (2001) MRI abnormalities of foot and ankle in asymptomatic, physically active individuals. Skeletal Radiol 30:61–66
14. Kursunoglu-Brahme S, Schwaighofer B, Gundry C et al (1990) Jogging causes acute changes in the knee joint: an MR study in normal volunteers. AJR Am J Roentgenol 154:1233–1235
15. Miyaguchi M, Kobayashi A, Kadoya Y et al (2003) Biochemical change in joint fluid after isometric quadriceps exercise for patients with osteoarthritis of the knee. Osteoarthritis Cartilage 11:252–259
16. Roth J, Ravagnani V, Backhaus M et al (2017) Preliminary definitions for the sonographic features of synovitis in children. Arthritis Care Res (Hoboken) 69:1217-23
17. Hemke R, van Rossum MA, van Veenendaal M et al (2013) Reliability and responsiveness of the Juvenile Arthritis MRI Scoring (JAMRIS) system for the knee. Eur Radiol 23:1075–1083
18. Hemke R, van den Berg JM, Nusman CM et al (2018) Contrast-enhanced MRI findings of the knee in healthy children; establishing normal values. Eur Radiol 28:1167–1174
19. Bugni Miotto e Silva V, de Freitas Tavares da Silva C, de Aguiar Vilela Mitraud S et al (2014) Do patients with juvenile idiopathic arthritis in remission exhibit active synovitis on joint ultrasound? Rheumatol Int 34:937-45
20. Bland JM, Altman DG (1999) Measuring agreement in method comparison studies. Stat Methods Med Res 8:135–160

Publisher's Note Springer Nature remains neutral with regard to jurisdictional claims in published maps and institutional affiliations.

Authors and Affiliations

Sílvia Costa Dias[1,2] · Diogo Costa Carvalho[2] · Miguel Castro[2] · Cláudia Camila Dias[3,4] · Isabel Ramos[1] · Iva Brito[1,5] · Karen Rosendahl[6,7]

✉ Sílvia Costa Dias
silvia.dias@ulssjoao.min-saude.pt

Diogo Costa Carvalho
diogofcostacarvalho@gmail.com

Miguel Castro
miguelhcastro@gmail.com

Cláudia Camila Dias
camila@med.up.pt

Isabel Ramos
radiologia.hsj@gmail.com

Iva Brito
ivaobrito@hotmail.com

Karen Rosendahl
karen.rosendahl@unn.no

[1] Faculty of Medicine of the University of Porto, Rua Pedro Hispano nº 190, 2º Dto, Porto 4100-393, Portugal

[2] Radiology Department, University Hospital Center of São João Porto, Porto, Portugal

[3] Knowledge Management Unit, Faculty of Medicine of the University of Porto, Porto, Portugal

[4] CINTESIS@RISE, Department of Community Medicine, Information and Health Decision Sciences (MEDCIDS), Faculty of Medicine of the University of Porto, Porto, Portugal

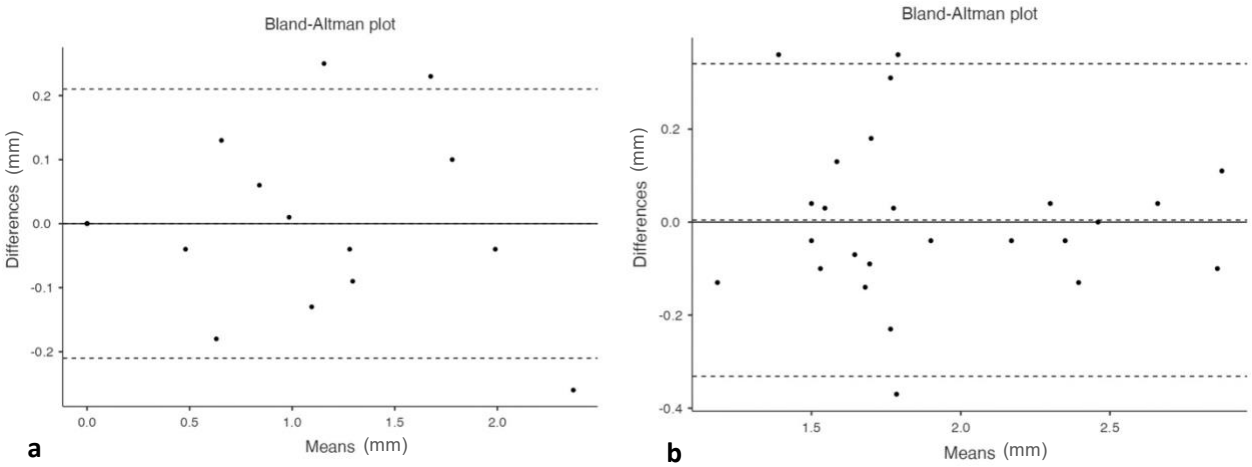
[5] Paediatric and Young Adult Rheumatology Unit, University Hospital Center of São João, Porto, Portugal

[6] Department of Clinical Medicine, Faculty of Health Sciences, UiT the Arctic University of Norway, Tromsø, Norway

[7] Section of Paediatric Radiology, University Hospital of North Norway, Tromsø, Norway

Supplementary Material 1

Bland-Altman mean-difference plots in millimetres **a** Showing relative wide 95% limitis of agreement for both the suprapatellar fluid (including repeted values represented by the same dot) and **b** The thickness of the double layered synovium between observers (based on the longitudinal standard view)



Paper 2 - ESR Essentials: juvenile idiopathic arthritis; what every radiologist needs to know-practice recommendations by the European Society of Paediatric Radiology

Costa Dias S, Habre C, Di Paolo PL, d'Angelo P, Augdal TA, Angenete OW, Kljucevsek D, Inarejos Clemente EJ, Tanturri de Horatio L, Rosendahl K.

Eur Radiol 36, 1261–1271 (2026). https://doi.org/10.1007/s00330-025-11891-9

Costa Dias et al. European Radiology (2026) 36:1261–1271
https://doi.org/10.1007/s00330-025-11891-9

EUROPEAN SOCIETY OF RADIOLOGY
European Radiology

INVITED REVIEW Open Access

ESR Essentials: juvenile idiopathic arthritis; what every radiologist needs to know—practice recommendations by the European Society of Paediatric Radiology

Sílvia Costa Dias[1,2], Celine Habre[3], Pier Luigi Di Paolo[4], Paola d'Angelo[4], Thomas A. Augdal[5,6], Oskar W. Angenete[7,8], Damjana Kljucevsek[9], Emilio J. Inarejos Clemente[10], Laura Tanturri de Horatio[4] and Karen Rosendahl[5,6]*

Abstract

Juvenile Idiopathic Arthritis (JIA) is a major contributor to chronic diseases, affecting around 1–2 in 1000 children under the age of 16. With modern treatments, the morbidity has been reduced; however, there is increasing evidence that many, if not most, children with JIA will have a chronic disease with ongoing activity into adulthood. Many studies discuss the possibility of an early window of opportunity in which patients have the best chance of responding to therapy, thereby underscoring the importance of timely and appropriate imaging. Children typically present at 4–5 years of age with one or more stiff and painful joints. If JIA is suspected, the child should undergo an ultrasound of the involved joint(s), performed by a radiologist with experience in paediatric imaging. If this is normal, with no abnormal laboratory tests and low clinical suspicion of JIA, no further imaging is required. If there is inconsistency between ultrasound and clinical findings, then they should proceed to MRI, including intravenous contrast, of the involved joint. Additional radiographs, or low-dose CT for the axial joints to examine for potential destructive change, deformation, or growth abnormalities, should be considered. In children presenting with monoarthritis, bacterial infection must be ruled out.

Key Points

- *Ultrasound is the initial modality in the diagnosis of JIA, and if there is inconsistency between ultrasound and clinical findings, MRI should be performed.*
- *Radiography for the assessment of destructive change, deformity, and malalignment should be considered, alternatively, low-dose CT for the temporomandibular and sacroiliac joints and the cervical spine.*
- *Knowledge of normal imaging features in children is mandatory.*

Keywords Child, Arthritis, (Juvenile), Diagnostic imaging, Ultrasonography, Magnetic resonance imaging

This article belongs to the ESR Essentials series, guest edited by Marc Dewey (Berlin/Germany).

*Correspondence:
Karen Rosendahl
karen.rosendahl@unn.no
Full list of author information is available at the end of the article

Springer

© The Author(s) 2025. **Open Access** This article is licensed under a Creative Commons Attribution 4.0 International License, which permits use, sharing, adaptation, distribution and reproduction in any medium or format, as long as you give appropriate credit to the original author(s) and the source, provide a link to the Creative Commons licence, and indicate if changes were made. The images or other third party material in this article are included in the article's Creative Commons licence, unless indicated otherwise in a credit line to the material. If material is not included in the article's Creative Commons licence and your intended use is not permitted by statutory regulation or exceeds the permitted use, you will need to obtain permission directly from the copyright holder. To view a copy of this licence, visit http://creativecommons.org/licenses/by/4.0/.

Key recommendations

- In the clinical setting of suspected JIA, the appropriate initial imaging protocol is a high-resolution ultrasound examination of the involved joint(s) and tendons, including Doppler. In case of monoarthritis, bacterial arthritis should be excluded. If ultrasound is inconclusive, an additional MRI with contrast should be performed. If a diagnosis of JIA is reached, an MRI of the temporomandibular joints (TMJ) should be contemplated, as involvement of these joints is asymptomatic in a high proportion of patients (level of evidence: moderate).
- For assessment of destructive change, deformation or growth abnormalities, radiography, or low-dose CT for the axial joints and the TMJs, is recommended (level of evidence: moderate).
- Knowledge on normal references for the amount of joint fluid and synovial thickness on ultrasound and MRI, as well as on bone marrow findings on MRI, is crucial to reduce misdiagnosis (level of evidence: moderate).

Introduction

Juvenile idiopathic arthritis (JIA) is a major contributor to chronic disease in childhood, affecting around 1–2 in 1000 children (f:m 3:1) under the age of 16 [1]. It is characterised by chronic synovial inflammation, with a potential risk of developing progressive joint destruction and serious functional disability. The aetiology is unknown [2]. Historically, the disease was characterised by high morbidity, such as physical disability and loss of mobility due to joint contractures and destruction from long-standing inflammation, pain, and fatigue. In addition, drugs like glucocorticoids add to morbidity by side effects such as growth and metabolic disturbances (osteoporosis). With modern treatment such as Methotrexate, introduced during the 80s and the biologics, introduced in the late 90s, the morbidity has been reduced, but still children are faced with periods of active disease with pain and reduced mobility, and the observed side effects of the new drugs are concerning [3, 4]. Moreover, there is increasing evidence that many, if not most, children with JIA will have a chronic disease with ongoing activity into adulthood [5, 6], thus underscoring the importance of early diagnosis and instigation of appropriate treatment.

Diagnosis and the role of imaging

JIA is a heterogeneous disease, classified into seven distinct categories: oligoarthritis, polyarthritis, systemic arthritis, psoriatic arthritis, enthesitis-related arthritis, and undifferentiated arthritis, of which oligoarthritis is the most common [7]. Although the diagnostic criteria are based on history and clinical and laboratory findings, imaging has become an important tool both in narrowing the differential diagnosis and monitoring disease activity, development, and potential complications to treatment. While evaluation of disease activity is performed with ultrasound and/or magnetic resonance imaging (MRI), joint damage and secondary growth disturbances are still performed radiographically [8]. However, there is a lack of comprehensive imaging guidelines across specialities.

Imaging techniques

Ultrasound with Doppler

Ultrasound is a valuable tool for evaluating inflammatory change, such as joint effusion, thickened, hyperaemic synovium, tenosynovitis (Fig. 1), and enthesitis, and guiding joint injections, whilst assessment of chronic change is less reliable [9]. To differentiate between normality and pathology, knowledge of age, gender, and joint-related reference standards for the amount of joint fluid and the appearances/thickness of the synovium are required. An update on adequately sized, population-based studies reporting on ultrasound-based references is provided in Table 1. Of note is the wide variation in the amount of joint fluid seen in otherwise healthy children by age and the ultrasound technique used. Obviously, borderline findings combined with equivocal clinical findings might lead to both over and underdiagnosis of arthritis.

Several examination techniques and protocols for the assessment of joints in children with JIA have been proposed [10, 11]. The ESPR (European Society of Paediatric Radiology) has endorsed the recommendations, including a detailed description of transducers and main parameter settings, given by the ESPR musculoskeletal task force group (https://www.espr.org/app/uploads/2022-US-Joints-in-children.pdf).

As for grading of inflammatory change, several US-based scoring systems have been suggested; however, no international consensus across specialities has been reached [10]. For example, in a recent paper from the PreS (Paediatric Rheumatology European Society) Imaging Working Party, a combination of five views through the knee joint were identified as being the most sensitive for synovitis [12]. The degree of synovitis was scored in accordance with the Paediatric Outcome Measures in Rheumatology group [13], a consensus-driven, international group, defining normality as the absence of effusion without providing cut-offs between normality and pathology. Obviously, this might introduce significant overdiagnosis.

Ultrasound has a number of limitations. Firstly, the reported sensitivity for detection of both acute and chronic changes varies widely, reflecting its operator dependency and limited visualisation of the entire joint. In

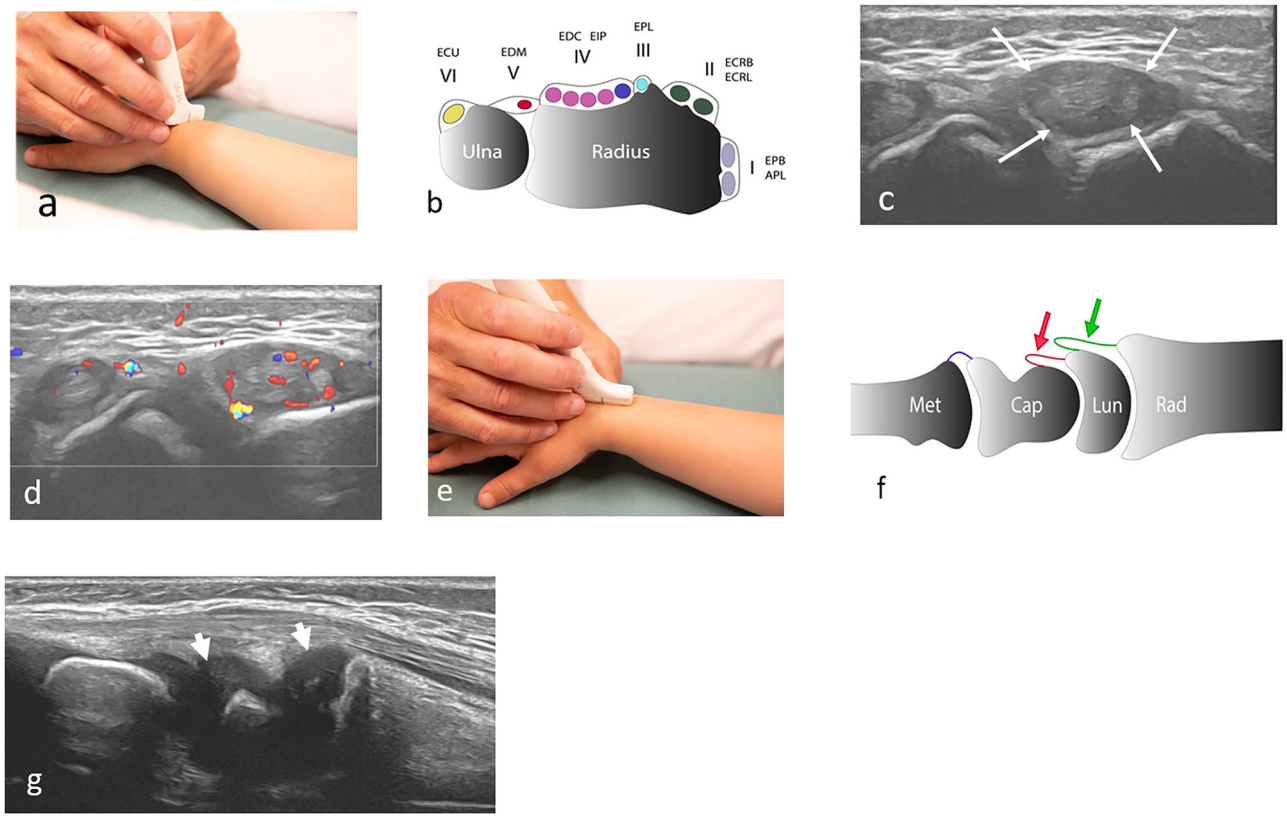


Fig. 1 Ultrasound of the wrist in a two-year-old boy with polyarticular JIA. **a** Axial view, dorsal wrist, visualising (**b**) the extensor tendons, showing (**c**) a thickened (long arrows) and (**d**) hyperaemic synovium consistent with tenosynovitis of compartments VI and IV. **e** shows a longitudinal view through the wrist, with **f** illustrating the radiocarpal (green arrow) and midcarpal (red arrow) recesses. **g** Note the appearances of the dark cartilage, which can easily be mistaken for fluid (arrow heads). To differentiate between the two, gain might be adjusted to visualise the typical "speckles" within cartilage, as compared to the dark/black fluid

particular, assessment and grading of chronic change appear to be imprecise [9]. Moreover, ultrasound findings have low prognostic value in patients in remission [14], and the accuracy for detecting enthesitis has yet to be standardised and further evaluated [15].

MRI

MRI plays an important role in assessing disease activity, as well as damage to cartilage and bone in children with JIA. However, the normal, growing skeleton often exhibits MR findings such as bone marrow oedema-like change, bony depressions, and irregular ossification; features that easily can be mistaken for true marrow oedema or erosions. For example, a study from 2008 indicated that MRI might detect erosive change of the carpals with greater sensitivity than radiography, particularly in early disease [9]. However, during normal maturation, the carpals can become quite irregular, thus mimicking pathology [16]. Moreover, bone marrow oedema might be a precursor of erosive change/joint damage progression [17, 18]. But again, since bone marrow oedema-like change, including «kissing lesions» of the carpals is a frequent finding in children, this feature must be interpreted with caution. The same goes for joint fluid, as it is difficult to differentiate when an effusion is present, given the wide variation in normal joint fluid volume (Table 1).

Nevertheless, MRI has become a useful tool for evaluating and monitoring children with JIA, particularly those with subclinical disease [18]. It is especially valuable for assessment of axial joints such as the cervical spine and sacroiliac joints (SIJ), and is also the modality of choice for assessing temporomandibular (TMJ) involvement [19].

Synovial inflammation, i.e. a thickened, hyperaemic synovium, most often, but not always combined with an effusion, is the key indicator of disease activity in JIA. For most joints, the use of intravenous contrast is needed to differentiate between a pathological synovial membrane and an effusion (Fig. 2). From previous work, taking the influence of timing into consideration, we know that a normal synovium is thin with barely visible enhancement

Table 1 Published reference standards for synovial thickness and joint fluid in different joints.

JOINT references	*n*	Age (years)	Cohort	Study design	Centre	*N*	Scan (sagittal)	Synovium echogenicity	Synovium thickness (bone-capsular distance, exc. knee)	Joint fluid
HIP										
Rohrschneider [47]	166	0.3–17	NA	Prospective	Mono	NA	ant rec, ER	Hypo	Mean 5.5 mm, 95% CI [5.4, 5.6]*,#	Presence 12%, an
Robben [48]	58	1.7–12.5	NA	Prospective	Mono	1	ant rec	Hyper/hypo	Mean 4.7 mm, 95% CI [4.5, 4.9]	Presence 4%
Tien [49]	784	2.5–6.6	(1)	NA	NA	NA	ant rec, NR	Iso	Mean 7.3 mm, 95% CI [7.2, 7.4]#	NA
Trauzeddel [50]	445	1–18	(2) (3)	NA	Multi	11	ant rec, NR	NA	Range 5.1–7.5 mm**,!	NA
Zuber [51]	408	0–18	(2)	NA	Mono	3	ant rec	NA	Med 6.7 mm, (C10-C90 5.9–7.3 mm) (≥16 y)##,!	Absence
Collado [52]	60	2–16	NA	NA	Mono	1	ant rec, ER	NA	Mean 5.2 mm, 95% CI [5.2, 5.2]##	Absence
Wittoek [53]	485	0.2–18	NA	Prospective	Mono	6	ant rec, ER	NA	Med 3.4 mm, Range (0.9–9.1)!	NA
KNEE										
Windshall [54]	435	1–18	NA	NA	Multi	9	suprapat	NA	Mean 3.2 mm, 95% CI [1.3–6.2] (16–18 y)#	Presence 64%, hypo
Collado [52]	60	2–16	NA	NA	Mono	1	suprapat	NA	Mean 1.3 mm, 95% CI [1.2, 1.4]	Presence 60%, an
Dias [55]	127	3–17	(1)	Prospective	Mono	2	suprapat	NA	Med 2.0 mm, Percentile 2.5th–97.5th [1.4–3.3] (14–17 y)**,***,##,!	Presence 76%****
SHOULDER										
Trauzeddel [56]	445	1–18	(2) (3)	NA	Multi	> 3	ant rec	NA	Mean 3.5 mm, 95% CI [2.6, 4.5]**,##	Absence
ELBOW										
Trauzeddel [57]	437	1–18	(2) (3)	NA	Multi	> 2	ant rec	NA	Mean 3.5 mm, 95% CI [3.4, 3.6]**,##	NA
WRIST										
Rosendahl [58]	116	6–16	(1)	Prospective	Mono	1	dorsal rec N/F	Hypo		
RC									Mean 0.4 mm, 95% CI [0.3, 0.5]**	Presence 50%, an
MC									Mean 0.5 mm, 95% CI [0.4, 0.6]**	Presence 10%, an
FINGERS										
Collado[52]	60	2–16	NA	NA	Mono	1	dorsal rec	NA		
MCP									Mean 0.6 mm, 95% CI [0.5, 0.7]*****	Presence (some), an
PIP									Mean 0.6 mm, 95% CI [0.6, 0.7]*****	

Cohort, recruitment method: (1) population-based, (2) patients with disease not involving the joint, and (3) children of investigators/friends
Synovium thickness: the bone-capsular distance is provided with the exception of the knee, for which the thickness of the suprapatellar recess is reported
Joint fluid: percentage of joints with presence of fluid, echogenicity of fluid
an anechoic, *ant rec* anterior recess, *CI* confidence interval, *dorsal rec* dorsal recess, *ER* external rotation, *hyper* hyperechoic, *hypo* hypoechoic, *iso* isoechoic, *MC* midcarpal joint, *MCP* metacarpophalangeal joint, *Med* median, *Mono* monocentric, *Multi* multicentric, *n* number of included cases, *NA* not applicable, *N/F* neutral/flexion, *NR* neutral rotation, *PIP* proximal interphalangeal joint, *RC* radiocarpal joint: suprapat: suprapatellar recess, *N* total number of examiners
* For height > 100 cm; Mean 2.1 mm (< 65 cm), 5.1 mm (65–100 cm)
** Right side
*** Double synovial layer thickness with light transducer compression to squeeze the fluid away
**** In at least one of the knees
***** Second digit
# Increases with age and height
Increases with age
! Results could not be reported as mean and 95% CI

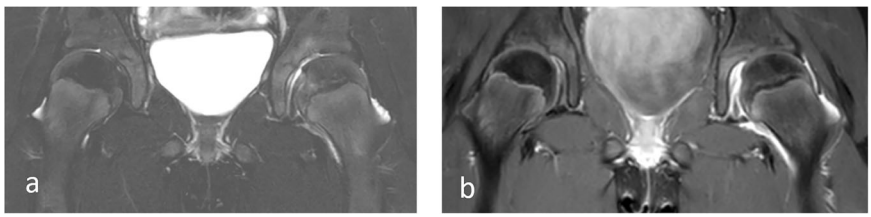


Fig. 2 Nine-year-old girl with psoriasis-related JIA and pain in her left thigh. MRI, with (**a**) a coronal T2-weighted SPAIR sequence, showed a sliver of joint fluid in her left hip, whilst the T1-weighted, fat-saturated post-contrast image (**b**) showed vivid synovial enhancement, consistent with arthritis, underscoring the need for intravenous contrast administration to assess active inflammation

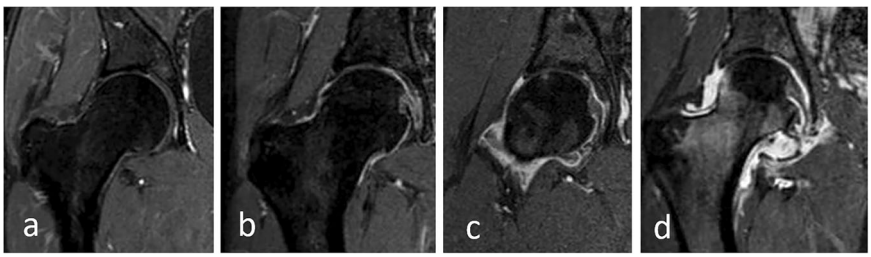


Fig. 3 Hip MRI (T1-weighted, fat-saturated post-contrast images) in four different children aged 12 years, showing different grades of synovial enhancement: (**a**) normal, (**b**) mildly increased synovial enhancement, (**c**) moderately increased, and (**d**) severely increased synovial enhancement

[20, 21], and that there is a continuum towards a thickened, pathologiclal membrane showing vivid enhancement. To monitor disease activity, several grading systems have been established for different joints, of which the more robust ones are listed in Supplementary material A. A grading system for synovial enhancement of the hips, according to Tanturri de Horatio, is shown in Fig. 3.

Regarding the TMJ, there are suggestions for scoring systems [22, 23], but as the authors state, there are challenges regarding repeatability, also shown in a recent Dutch publication [24]. Despite its drawbacks, MRI of the TMJ is a sensitive and specific diagnostic tool in the work-up of the JIA patient.

Technical requirements and suggested protocols

Both 1.5-T and 3-T MR machines are feasible, given the appropriate type and positioning of coils. Applying techniques to reduce the need for sedation are mandatory. However, the literature on child-specific reconstruction methods is sparse [25].

Protocols for assessing the axial joints, such as the cervical spine, sacroiliac and TMJs, and the extremities, based on previous recommendations from the ESPR-ESSR [26], as well as published updates [19, 27], are listed in Table 2. A basic protocol is suggested, together with joint–specific add-ons and potential new sequences to be considered.

The basic protocol should include fluid-sensitive sequences (e.g., short tau inversion recovery (STIR), T2-weighted fat-saturated (T2 FS) or T2 Dixon water only images) for the assessment of joint fluid and oedema, and a T1-weighted sequence for the assessment of growth changes and chronic structural change [19, 26]. Alternatively, a proton density (PD)-weighted FS sequence might replace the fluid-sensitive sequence for visualisation of cartilage, as well as fluid (Fig. 4). If another fluid-sensitive sequence is preferred over the PD FS sequence, an additional cartilage sequence should be considered. Finally, recent studies have shown that the T2 Dixon fat-only images can replace T1-weighted FS images, thus shortening the scan time significantly [28, 29].

As mentioned above, the use of intravenous contrast is needed to differentiate between an effusion and a hyperaemic and thickened synovial membrane. Due to diffusion of contrast into the joint fluid, the timing of post-contrast images, preferably in two planes, should be short and standardised, for instance after a 2–3 min delay [30]. See Table 2 for examples of child- and joint-specific protocols. For MR imaging of the SIJ, the role of intravenous contrast is limited, although it might be helpful in equivocal cases [26, 31].

Because the hips are commonly involved in children with juvenile spondyloarthropathy, a (true) axial acquisition with a larger field of view to visualise the entire pelvis, including the hips, has been advised [26]. This extended view also allows for assessment of pelvic enthesitis (Table 2).

Table 2 Suggested joint-specific MRI protocols

Basic sequences	Joints							Aims
	Knee	Ankle/foot including MTFJ	Hip	ERA − LLS + SI + hips***	Cervical spine	Wrist/hand including MCP	TMJ	
Fluid sensitive sequence*	Axial and sagittal (R), coronal (O)	Sagittal and coronal (R), axial (O)	Coronal and axial (R)	Sagittal LLS (R), coronal and axial—sacrum oriented; include hips (R)	Sagittal and axial (R), coronal (O)	Coronal and axial (R)	Sagittal oblique (R)	JE, BME, BE, cartilage loss (if PD-weighted FS used)
T1-weighted TSE	Coronal (R)	Sagittal (R)	Coronal (R)	Coronal and axial—sacrum oriented; include hips (R)	Sagittal (R)	Coronal (R)	Coronal and sagittal oblique (R)	BME, BE, growth change (TMJ)
T1-weighted FS pre-Gad	Sagittal (R)	Sagittal (R)	Coronal (R)	Coronal—sacrum oriented; includes hips (R)	Sagittal (R)	Coronal and axial (R)	Sagittal oblique (O)	Synovitis
T1-weighted FS or Dixon pos-Gad—1st acquisition 2 min.	1st Sagittal and 2nd axial (R)	1st Sagittal and 2nd coronal (R), axial (O)	1st Coronal and 2nd axial (R)	1st Coronal and 2nd axial—sacrum oriented; include hips (R)	1st Sagittal and 2nd coronal (R), axial (O)	1st Coronal and 2nd Axial (R)	Sagittal oblique for each joint and Coronal of both joints (R)	Synovitis
Additional specific sequences	Gradient echo (3D) coronal (O)	Gradient echo (3D) sagittal (O)	Gradient echo (3D) sagittal (O)	No	No	Gradient echo (3D) Coronal (O)	PD Sagittal Oblique closed & open mouth (O), T1-MPRAGE Sagittal (O)	Gradient echo for Cartilage loss and BE; PD in the TMJ for disk evaluation
New sequences to consider—FLAIR FS/DIR/qDESS	Sagittal or axial	Sagittal	Coronal	Coronal or Axial—sacrum oriented; include hips	Sagittal or axial	Coronal or axial	No	Synovitis
New sequences to consider—diffusion	Axial	Axial	Axial	Axial—sacrum oriented; includes hips	Axial	Axial	No	Synovitis
New sequences to consider—T2 Dixon**	Axial, sagittal and coronal	Sagittal and coronal; axial (O)	Coronal and axial	Sagittal LLS, coronal and axial—sacrum oriented; include hips	Sagittal, axial and coronal	Coronal and axial	Sagittal and coronal oblique	JE, BME, BE

STIR short tau inversion recovery, *TSE* turbo spin echo, *FS* fat suppression, *FLAIR FS* fluid attenuated inversion recovery with fat suppression, *DIR* dual inversion recovery, *qDESS* quantitative double-echo in steady-state, *R* recommended, *O* optional, *MTFJ* metatarsophalangeal joints, *MCFJ* metacarpophalangeal joints, *PD* proton density, *T1-MPRAGE* magnetisation-prepared rapid gradient echo, *JE* joint effusion, *BME* bone marrow oedema, *BE* bone erosions

* T2-weighted FS or Dixon/STIR/PD-weighted FS or Dixon

** Fat only and water only: replacing T1-weighted TS and fluid-sensitive sequences

*** Combined protocol ERA (enthesitis-related arthritis) for LLS (lower lumbar spine) + SI (sacro-iliac joints) + hips

Future perspectives

During the past years, significant efforts have been made to reduce the need for intravenous gadolinium administration, both due to unwanted side effects and examination time [32]. Alternative MR sequences, such as fluid attenuated inversion recovery with fat suppression (FLAIR FS), dual inversion recovery (DIR) and quantitative double-echo in steady-state (qDESS) [33, 34] and diffusion-weighted sequences have been evaluated [35]. Currently, contrast-enhanced MRI is often indispensable in the diagnostic work-up of the JIA patient.

Radiography

Although conventional radiography (CR) has its limitations in detecting inflammatory change, soft tissue involvement and early structural change, it still plays an important role in narrowing the differentials, particularly in children presenting with monoarthritis, and in evaluating severe joint damage and growth disturbances in children with JIA [26, 36].

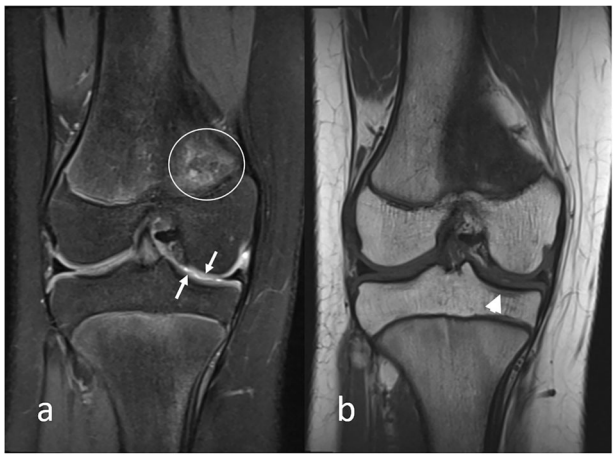


Fig. 4 Knee MRI in an 11-year-old girl with JIA, (**a**) coronal PD-weighted fat-saturated image showing irregular cartilage in the femorotibial medial compartment (arrow) and (**b**) subtle subchondral sclerosis on a coronal T1-weighted image (arrowhead). Note the oedema in the distal medial femoral metaphysis, representing a cortical desmoid (circle)

Except for the sacroiliac joints, the TMJs and the spine [26], CR remains the preferred modality for assessment of chronic change [8], of which knees, ankles, hands and feet are the most frequent sites showing radiographic change [37]. The radiographic findings differ significantly from those in adults and vary according to mode of onset and age. In younger children, the initial findings might be more developmental rather than destructive, i.e. bony overgrowth/architectural distortion, whereas in older children and adolescents destructive changes might supervene [38] (Fig. 5). Similar, in other appendicular joints, accelerated bone maturation might result in architectural distortion and remodelling, and subsequent premature closure of the growth plate with shortening of bones. Children with later-onset JIA sometimes have destruction/erosions and narrowed joint space as the first feature, often followed by malalignment. Evaluation and grading of chronic changes can be performed by comparing serial radiographs or by using one of the scoring systems for hands [18–20] or for hips [21].

Technical requirements and suggested protocols

High-resolution radiographs are advised. Currently, no agreed recommendations or protocols exist; however, a relatively recent systematic review [39] suggests an initial routine CR of the wrist, hands and forefeet in polyarticular JIA with positive rheumatoid factor (RF)/anti-citrullinated protein antibodies (ACPA) and in new-onset RF/ACPA-negative polyarticular JIA with adverse prognostic factors. In other JIA subtypes, routine CR is not recommended, except at the discretion of the paediatric rheumatologist for symptomatic joints. Follow-up of destructive change and/or malalignment should be guided by clinical findings. For the appendicular joints, both sides should be included to identify growth disturbances. In contrast to the adult protocol, one front view often suffices (PA of wrist/hands; AP of ankles/feet, knees, hips, shoulders, and elbows).

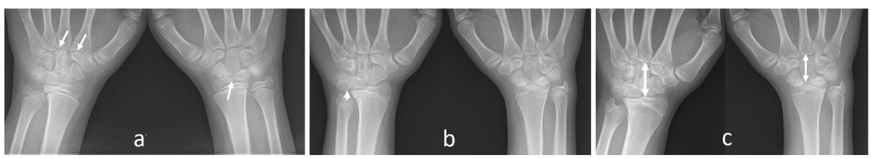


Fig. 5 Serial radiographs of the hands in a boy with polyarticular JIA (initially HLA B 27 negative at presentation age 2 years, but positive at age 17) show the development and progression of chronic degenerative change from 12 years to 18 years of age: (**a**) active inflammation of the carpals, with osteoporosis and growth disturbances (left carpals > right), as well as structural change with joint space narrowing (left carpometacarpal, right radiocarpal (arrows), (**b**) negative left ulnar variance at age 12 years (arrowhead) and progression of right radiocarpal joint space narrowing with crowding of the proximal carpal bones, and (**c**) reduced carpal length at age 15 (double arrows), radial deviation of carpal bones and dorsal subluxation (better seen on a lateral projection)



Fig. 6 Cone-beam CT, sagittal view of the TMJ, (**a**) a 12-year-old boy with a normally shaped fossa-eminence and condyle, (**b**) a 14-year-old girl with a normal fossa, but subtle anterior flattening of the condyle, and (**c**) a 15-year-old with a moderately widened fossa-eminence and a mildly to moderately flattened condyle. This figure has been reproduced from [46] under the Creative Commons Attribution 4.0 International License

Assessment of bone health

For assessment of bone health, dual-energy X-ray absorptiometry (DXA) is the most commonly used method, preferring the total body less head and lumbar spine (LS 1–4) locations [40]. To adjust for skeletal size, volume bone mineral density (or bone mineral apparent density, in g/cm^3) is calculated, or BMD *Z*-scores are adjusted for height [41] or bone age [42]. A recent study indicates that radiogrammetry based on a hand radiograph might provide an adjuvant tool to DXA, given that thorough calibration is performed [43].

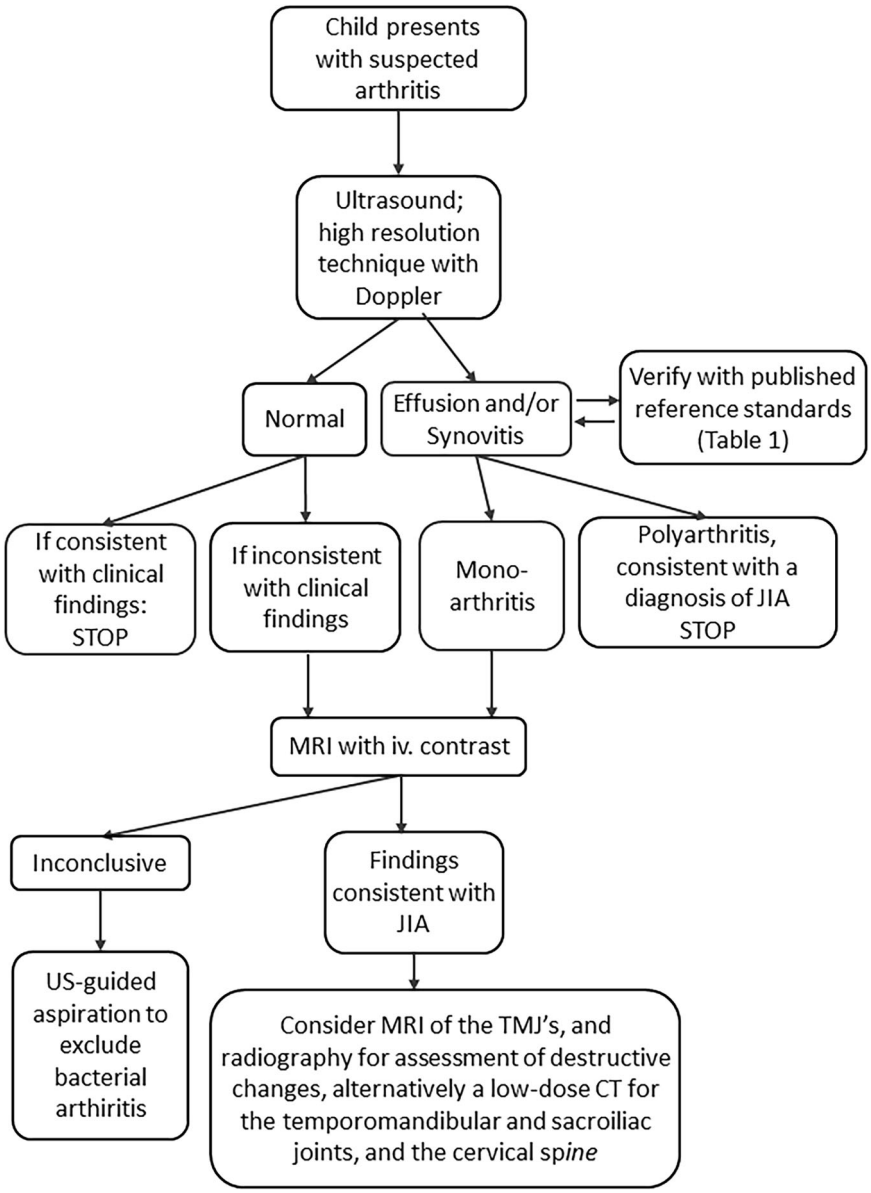


Fig. 7 Suggested investigative imaging pathway for suspected JIA

Computed tomography (CT)

Although CT, and in particular the novel photon counting detector CT technique, provides detailed images of the osteochondral domain, the method plays a limited role in the evaluation of children with JIA. Non-contrast CT can be used to evaluate structural damage, erosions, or ankylosis, with acquisition focused on thin-section axial images and multiplanar reconstructions. Currently, it is used for assessment of joints that are difficult to examine with CR, such as the TMJ, the upper cervical spine and the sacroiliac joint [26] in cases where MRI is contraindicated. In addition, CT is useful for preoperative planning, providing high-resolution imaging that serves as a roadmap for surgical interventions such as joint replacement or arthrodesis.

Technical requirements and suggested protocols

Modern CT scanners incorporate features that minimise radiation dose, such as iterative reconstruction algorithms, automated exposure modulation, and child-specific protocols. Key technical considerations include using multidetector CT with slice thicknesses of 0.5–1 mm for detailed imaging of small joints, employing dose-reduction techniques like low kiloVolt peak (kVp) settings (e.g. 80–100 kVp) and iterative reconstruction. Contrast is not routinely used in CT for patients with JIA due to the limited indications [44].

CBCT of the TMJs

For TMJs, cone beam computed tomography (CBCT) is currently accepted as the imaging modality of choice for visualisation of bony structures [45], especially in cases where MRI is equivocal or contraindicated. It provides multiplanar reconstructions to a relatively low radiation burden as compared to conventional CT, and depicts subtle erosions, flattening of articulating surfaces, subchondral cysts, subchondral sclerosis and osteophyte formation (Fig. 6). Recently, a novel, validated scoring system for monitoring the development of chronic change was published [46].

Differential diagnosis

In a child with acute-onset monoarthritis, the differential diagnosis must include septic arthritis, trauma, malignancy and haematological diseases, of which leukaemia is highly relevant. In addition, chronic non-bacterial osteomyelitis, postinfectious arthritis, acute rheumatic fever, and Lyme disease, among others, should be considered.

Summary statements

JIA is not uncommon in clinical practice. The radiologist has an essential role in the diagnostic pathway towards an early diagnosis, to prevent chronic structural damage. An ultrasound of the involved peripheral joint(s) is a core component of the assessment and should be performed in line with the ESPR MSK task force guidelines. If inconsistency between clinical and ultrasound findings, additional imaging with MRI, including intravenous injection of a gadolinium-based contrast agent, is required. For evaluation of the axial joints, MRI is the primary diagnostic imaging tool. Plain radiographs for the assessment of destructive change, deformity, and malalignment should be considered; alternatively, a low-dose CT for the axial skeleton and the TMJs. We have provided an extensive overview of published ultrasound and MRI-based reference standards for joint fluid and synovial appearances, as well as a flow chart of imaging techniques (Fig. 7) to facilitate differentiation between normality and pathology, as well as available MR-based scoring systems for disease activity. Moreover, we have suggested feasible child- and joint-specific MRI protocols. Communication with involved clinicians is a core component of the radiological assessment.

Patient summary

JIA is the most common rheumatological disease in childhood. This article provides an evidence-based summary of the appropriate imaging tests that children should undergo when there is clinical concern for JIA. A child-specific approach to imaging is crucial for a correct diagnosis.

Abbreviations

ACPA	Anti-citrullinated protein antibodies
CR	Conventional radiography
CT	Computed tomography
DIR	Dual inversion recovery
DXA	Dual-energy X-ray absorptiometry
ESPR	European Society of Pediatric Radiology
FLAIR FS	Fluid attenuated inversion recovery with fat suppression
JIA	Juvenile idiopathic arthritis
kVp	kiloVolt peak
MRI	Magnetic resonance imaging
PD	Proton density
PreS	Pediatric Rheumatology European Society
qDESS	Quantitative double-echo in steady-state
RF	Rheumatoid factor
SIJ	Sacroiliac joints
STIR	Short tau inversion recovery
TMJ	Temporomandibular joint

Supplementary information

The online version contains supplementary material available at https://doi.org/10.1007/s00330-025-11891-9.

Acknowledgements

This paper was endorsed by the Executive Council of the European Society of Radiology (ESR) and the Executive Committee of the European Society of Paediatric Radiology (ESPR) in July 2025.

Funding

Open access funding provided by UiT The Arctic University of Norway (incl University Hospital of North Norway).

Compliance with ethical standards

Guarantor
The scientific guarantor of this publication is Karen Rosendahl.

Conflict of interest
The authors of this manuscript declare no relationships with any companies, whose products or services may be related to the subject matter of the article.

Statistics and biometry
No complex statistical methods were necessary for this paper.

Informed consent
Written informed consent was not required for this study.

Ethical approval
Institutional Review Board approval was not required.

Study subjects or cohorts overlap
Not applicable.

Methodology

- Practice recommendations

Author details
[1]Department of Medicine, Faculty of Medicine of the University of Porto (FMUP), Porto, Portugal. [2]Department of Radiology, University Hospital Center of São João Porto (CHUSJ), Porto, Portugal. [3]Pediatric Radiology Unit, Radiology Division, Diagnostic Department, University Hospitals of Geneva, Geneva, Switzerland. [4]Department of Imaging, IRCCS Bambino Gesù Children's Hospital, Rome, Italy. [5]Department of Clinical Medicine, UiT the Artic University of Norway, Tromsø, Norway. [6]Department of Radiology, University Hospital of North Norway, Tromsø, Norway. [7]Department of Radiology and Nuclear Medicine, St. Olav University Hospital, Trondheim, Norway. [8]Faculty of Medicine and Health Sciences, Institute for Circulation and Medical Imaging, Norwegian University of Science and Technology, Trondheim, Norway. [9]Department of Radiology, University Children's Hospital Ljubljana, Ljubljana, Slovenia. [10]Department of Diagnostic Imaging. Sant Joan de Deu Barcelona Children Hospital, University of Barcelona, Barcelona, Spain.

Received: 24 February 2025 Revised: 19 May 2025 Accepted: 18 June 2025
Published online: 19 August 2025

References
1. Thierry S, Fautrel B, Lemelle I, Guillemin F (2014) Prevalence and incidence of juvenile idiopathic arthritis: a systematic review. Joint Bone Spine 81:112–117
2. Prakken B, Albani S, Martini A (2011) Juvenile idiopathic arthritis. Lancet 377:2138–2149
3. Lionetti G, Kimura Y, Schanberg LE et al (2013) Using registries to identify adverse events in rheumatic diseases. Pediatrics 132:e1384–e1394
4. Davies, HD, Committee On Infectious Diseases (2016) Infectious complications with the use of biologic response modifiers in infants and children. Pediatrics 138:e20161209
5. Arvidsson LZ, Smith HJ, Flatø B, Larheim TA (2010) Temporomandibular joint findings in adults with long-standing juvenile idiopathic arthritis: CT and MR imaging assessment. Radiology 256:191–200
6. Glerup M, Rypdal V, Arnstad ED et al (2020) Long-term outcomes in juvenile idiopathic arthritis: eighteen years of follow-up in the population-based nordic juvenile idiopathic arthritis cohort. Arthritis Care Res 72:507–516
7. Ravelli A, Martini A (2007) Juvenile idiopathic arthritis. Lancet 369:767–778
8. Colebatch-Bourn AN, Edwards CJ, Collado P et al (2015) EULAR-PReS points to consider for the use of imaging in the diagnosis and management of juvenile idiopathic arthritis in clinical practice. Ann Rheum Dis 74:1946–1957
9. Malattia C, Damasio MB, Magnaguagno F et al (2008) Magnetic resonance imaging, ultrasonography, and conventional radiography in the assessment of bone erosions in juvenile idiopathic arthritis. Arthritis Rheum 59:1764–1772
10. Sande NK, Bøyesen P, Aga AB et al (2021) Development and reliability of a novel ultrasonographic joint-specific scoring system for synovitis with reference atlas for patients with juvenile idiopathic arthritis. RMD Open 7:e001581
11. Ting TV, Vega-Fernandez P, Oberle EJ et al (2019) Novel Ultrasound Image Acquisition Protocol and Scoring System for the Pediatric Knee. Arthritis Care Res 71:977–985
12. Windschall D, Trauzeddel R, Gohar F et al (2024) Development and validation of a pediatric internationally agreed ultrasound knee synovitis protocol (PIUS-knee) by the PReS imaging working party. Pediatr Rheumatol Online J 22:94
13. Terslev L, Iagnocco A, Bruyn G et al (2017) The OMERACT ultrasound group: a report from the OMERACT 2016 meeting and perspectives. J Rheumatol 44:1740–1743
14. Saoussen M, Yasmine M, Hiba B, Alia F, Kawther BA, Ahmed L (2023) The role of ultrasonography in assessing remission in juvenile idiopathic arthritis: a systematic review. Eur J Pediatr 182:2989–2997
15. Rossi-Semerano L, Ravagnani V, Collado P et al (2023) Validity of ultrasonography in detecting enthesitis in children: a systematic literature review. Joint Bone Spine 90:105538
16. Avenarius D (2017) The paediatric wrist: normal age related appearances on magnetic resonance imaging and radiographs. A dissertation for the degree of Philosophiae Doctor. UiT the Arctic University of Norway, Faculty of Health Sciences, IKM, Tromsø
17. Haavardsholm EA, Bøyesen P, Østergaard M, Schildvold A, Kvien TK (2008) Magnetic resonance imaging findings in 84 patients with early rheumatoid arthritis: bone marrow oedema predicts erosive progression. Ann Rheum Dis 67:794–800
18. Mazzoni M, Pistorio A, Magnaguagno F et al (2023) Predictive value of magnetic resonance imaging in patients with juvenile idiopathic arthritis in clinical remission. Arthritis Care Res 75:198–205
19. Hemke R, Herregods N, Jaremko JL, Maas M (2024) Imaging of juvenile idiopathic arthritis. Radiol Clin North Am 62:889–902
20. Angenete OW, Augdal TA, Jellestad S, Rygg M, Rosendahl K (2018) Normal magnetic resonance appearances of the temporomandibular joints in children and young adults aged 2–18 years. Pediatr Radiol 48:341–349
21. Clemente EJI, Tolend M, Navallas M, Doria AS, Meyers AB (2023) MRI of the temporomandibular joint in children with juvenile idiopathic arthritis: protocol and findings. Pediatr Radiol 53:1498–1512
22. Tolend MA, Twilt M, Cron RQ et al (2018) Toward establishing a standardized magnetic resonance imaging scoring system for temporomandibular joints in juvenile idiopathic arthritis. Arthritis Care Res 70:758–767
23. Angenete OW, Augdal TA, Rygg M, Rosendahl K (2021) MRI in the assessment of TMJ-arthritis in children with JIA; repeatability of a newly devised scoring system. Acad Radiol 29:1362–1377
24. de Sonnaville WFC, Speksnijder CM, Zuithoff N et al (2024) The reliability and validity of the juvenile idiopathic arthritis magnetic resonance scoring system for temporomandibular joints. J Craniomaxillofac Surg 52:906–913
25. Bedoya MA, Iwasaka-Neder J, Tsai A et al (2025) Deep learning MR reconstruction in knees and ankles in children and young adults. Is it ready for clinical use?. Skeletal Radiol 54:509–529
26. Hemke R, Herregods N, Jaremko JL et al (2020) Imaging assessment of children presenting with suspected or known juvenile idiopathic arthritis: ESSR-ESPR points to consider. Eur Radiol 30:5237–5249
27. Vereecke E, Diekhoff T, Eshed I et al (2024) ESR Essentials: imaging of sacroiliitis-practice recommendations by ESSR. Eur Radiol 34:5773–5782
28. Tanturri de Horatio L, Zadig PK, von Brandis E, Ording Müller LS, Rosendahl K, Avenarius D (2023) Whole-body MRI in children and adolescents: Can T2-weighted Dixon fat-only images replace standard T1-weighted images in the assessment of bone marrow? Eur J Radiol 166:110968
29. Zadig P, von Brandis E, Ording Müller LS, Tanturri de Horatio L, Rosendahl K, Avenarius D (2023) Pediatric whole-body magnetic resonance imaging: comparison of STIR and T2 Dixon sequences in the detection and grading of high signal bone marrow changes. Eur Radiol 33:5045–5053

30. Rieter JF, de Horatio LT, Nusman CM et al (2016) The many shades of enhancement: timing of post-gadolinium images strongly influences the scoring of juvenile idiopathic arthritis wrist involvement on MRI. Pediatr Radiol 46:1562–1567
31. Otobo TM, Herregods N, Jaremko JL et al (2021) Reliability of the preliminary OMERACT juvenile idiopathic arthritis MRI score (OMERACT JAMRIS-SIJ). J Clin Med 10:4564
32. Thoenen J, MacKay JW, Sandford H, Gold GE, Kogan F (2022) Imaging of synovial inflammation in osteoarthritis, from the AJR special series on inflammation. AJR Am J Roentgenol 218:405–417
33. Handa A, Bedoya MA, Iwasaka-Neder J, Johnston PR, Lo MS, Bixby SD (2024) Measuring synovial thickness on knee MRI in pediatric patients with arthritis: Is contrast necessary? Pediatr Radiol 54:988–1000
34. Milks KS, Singh J, Benedict JA, Rees MA (2024) Fluid-attenuated inversion-recovery sequence with fat suppression as an alternative to contrast-enhanced MRI in pediatric synovitis. Pediatr Radiol 54:96–104
35. Barendregt AM, Mazzoli V, van Gulik EC et al (2020) Juvenile idiopathic arthritis: diffusion-weighted MRI in the assessment of arthritis in the knee. Radiology 295:373–380
36. Kljucevsek D, Potocnik Tumpaj V, Gazikalovic A (2024) The role of radiography in diagnosing, monitoring and prognosing juvenile idiopathic arthritis. Pediatr Radiol 54:481–489
37. van Rossum MA, Boers M, Zwinderman AH et al (2005) Development of a standardized method of assessment of radiographs and radiographic change in juvenile idiopathic arthritis: introduction of the Dijkstra composite score. Arthritis Rheum 52:2865–2872
38. Shelmerdine SC, Di Paolo PL, Rieter J, Malattia C, Tanturri de Horatio L, Rosendahl K (2018) A novel radiographic scoring system for growth abnormalities and structural change in children with juvenile idiopathic arthritis of the hip. Pediatr Radiol 48:1086–1095
39. Marteau P, Adamsbaum C, Rossi-Semerano L et al (2018) Conventional radiography in juvenile idiopathic arthritis: joint recommendations from the French societies for rheumatology, radiology and paediatric rheumatology. Eur Radiol 28:3963–3976
40. Ward LM, Weber DR, Munns CF, Högler W, Zemel BS (2020) A contemporary view of the definition and diagnosis of osteoporosis in children and adolescents. J Clin Endocrinol Metab 105:e2088–e2097
41. Crabtree NJ, Arabi A, Bachrach LK et al (2014) Dual-energy X-ray absorptiometry interpretation and reporting in children and adolescents: the revised 2013 ISCD pediatric official positions. J Clin Densitom 17:225–242
42. Annexstad EJ, Bollerslev J, Westvik J et al (2019) The role of delayed bone age in the evaluation of stature and bone health in glucocorticoid treated patients with Duchenne muscular dystrophy. Int J Pediatr Endocrinol 2019:4
43. Augdal T, Angenete O, Zadig P et al (2024) The assessment of bone health in children with juvenile idiopathic arthritis; comparison of different imaging-based methods. Pediatr Rheumatol Online J 22:80
44. Demehri S, Baffour FI, Klein JG et al (2023) Musculoskeletal CT imaging: state-of-the-art advancements and future directions. Radiology 308:e230344
45. Kadesjö N, Benchimol D, Falahat B, Näsström K, Shi XQ (2015) Evaluation of the effective dose of cone beam CT and multislice CT for temporomandibular joint examinations at optimized exposure levels. Dentomaxillofac Radiol 44:20150041
46. Augdal TA, Angenete OW, Shi XQ et al (2023) Cone beam computed tomography in the assessment of TMJ deformity in children with JIA: repeatability of a novel scoring system. BMC Oral Health 23:12
47. Rohrschneider WK, Fuchs G, Troger J (1996) Ultrasonographic evaluation of the anterior recess in the normal hip: a prospective study on 166 asymptomatic children. Pediatr Radiol 26:629–634
48. Robben SG, Lequin MH, Diepstraten AF, Den Hollander JC, Entius CA, Meradji M (1999) Anterior joint capsule of the normal hip and in children with transient synovitis: US study with anatomic and histologic correlation. Radiology 210:499–507
49. Tien YC, Yang CY, Chih HW (2000) The normal width of anterior hip synovial recess in children. J Pediatr Orthop 20:264–266
50. Trauzeddel RF, Lehmann H, Windschall D et al (2017) Age-dependent arthrosonographic reference values of the hip joint in healthy children and adolescents—a cross-sectional multicenter ultrasound study. Pediatr Radiol. https://doi.org/10.1007/s00247-017-3862-5
51. Zuber Z, Owczarek A, Sobczyk M et al (2017) Establishing percentile charts for hip joint capsule and synovial cavity thickness in apparently healthy children. Pediatr Rheumatol Online J 15:8
52. Collado P, Naredo E, Calvo C, Crespo M (2007) Assessment of the joint recesses and tendon sheaths in healthy children by high-resolution B-mode and power Doppler sonography. Clin Exp Rheumatol 25:915–921
53. Wittoek R, Decock C, Dewaele N et al (2023) Structural ultrasound of joints and tendons in healthy children: development of normative data. Pediatr Rheumatol Online J 21:105
54. Windschall D, Trauzeddel R, Haller M et al (2016) Pediatric musculoskeletal ultrasound: age- and sex-related normal B-mode findings of the knee. Rheumatol Int 36:1569–1577
55. Dias SC, Carvalho DC, Castro M et al (2025) Knee-ultrasound: reference values for the amount of joint fluid and synovial appearances in healthy children and adolescents. Pediatr Radiol 55:1127–1137
56. Trauzeddel R, Windschall D, Trauzeddel RF et al (2017) Arthrosonographic reference values of the shoulder joint in healthy children and adolescents: a cross-sectional multicentre ultrasound study. Klin Padiatr 229:293–301
57. Trauzeddel R, Lehman H, Trauzeddel RF et al (2019) Age dependent ultrasound B-mode findings of the elbow joint in healthy children and adolescents. Rheumatol Int 39:1007–1018
58. Rosendahl K, Bruserud IS, Oehme N et al (2018) Normative ultrasound references for the paediatric wrist; dorsal soft tissues. RMD Open 4:e000642

Publisher's Note

Springer Nature remains neutral with regard to jurisdictional claims in published maps and institutional affiliations.

ESR Essentials: juvenile idiopathic arthritis; what every radiologist needs to know - practice recommendations by the European Society of Paediatric Radiology

Electronic Supplementary Material

Supplement A.

Validated, joint specific scoring systems for active inflammation and / or chronic change in JIA by imaging method.

Joint	Radiograph	Ultrasound	MRI	CBCT
Knee	Pettersson et al[1]	PAUSS-knee[2] CARRA JIA US Workgroup[3]	JAMRIS[4]	NA
Ankle	NA	PAUSS-ankle[5]	NA	NA
Hip	Shelmerdine et al [6] Bertarmino et al [7]	NA	Tanturri de Horatio et al[8]	NA
Spine	NA	NA	NA	NA
SIJ	NA	NA	SPARCC SIS: Weiss et al [9] and Panwar et al[10]	NA
Wrist	Ravelli et al - Adapted Sharp/van der Heijde score[11] Poznanski et al [12]	NA	Malattia et al [13] Damasio et al [14]	NA
TMJ	NA	NA	Angenete et al [15]	Augdal et al [16]

References

1. Pettersson H, Rydholm U. Radiologic classification of knee joint destruction in juvenile chronic arthritis. Pediatr Radiol. 1984;14(6):419-21. https://doi.org/10.1007/BF02343432
2. Vega-Fernandez P, Rogers K, Sproles A, Thornton S, Huggins J, Lovell DJ, Cassedy A, Meyers AB, Ting TV. Diagnostic Accuracy Study of the Pediatric-Specific Ultrasound Scoring System for the Knee Joint in Children With Juvenile Idiopathic Arthritis. Arthritis Care Res (Hoboken). 2024;76(2):251-8. https://doi.org/10.1002/acr.25218
3. Ting TV, Vega-Fernandez P, Oberle EJ, De Ranieri D, Bukulmez H, Lin C, Moser D, Barrowman NJ, Zhao Y, Benham HM, Tasan L, Thatayatikom A, Roth J, Childhood A, Rheumatology Research Alliance Juvenile Idiopathic Arthritis Ultrasound W. Novel Ultrasound Image Acquisition Protocol and Scoring System for the Pediatric Knee. Arthritis Care Res (Hoboken). 2019;71(7):977-85. https://doi.org/10.1002/acr.23746
4. Hemke R, van Rossum MA, van Veenendaal M, Terra MP, Deurloo EE, de Jonge MC, van den Berg JM, Dolman KM, Kuijpers TW, Maas M. Reliability and responsiveness of the Juvenile Arthritis MRI Scoring (JAMRIS) system for the knee. Eur Radiol. 2013;23(4):1075-83. https://doi.org/10.1007/s00330-012-2684-y
5. Vega-Fernandez P, Rogers K, Avar-Aydin PO, Quinlan-Waters M, Huggins J, Brunner HI, Lovell DJ, Altaye M, Cassedy A, Meyers AB, Ting TV. Validation of the ankle-specific pediatric arthritis ultrasound scoring system in children with juvenile idiopathic arthritis. Semin Arthritis Rheum. 2024;69:152545. https://doi.org/10.1016/j.semarthrit.2024.152545

6. Shelmerdine SC, Di Paolo PL, Rieter J, Malattia C, Tanturri de Horatio L, Rosendahl K. A novel radiographic scoring system for growth abnormalities and structural change in children with juvenile idiopathic arthritis of the hip. Pediatr Radiol. 2018;48(8):1086-95. https://doi.org/10.1007/s00247-018-4136-6
7. Bertamino M, Rossi F, Pistorio A, Lucigrai G, Valle M, Viola S, Magni-Manzoni S, Malattia C, Martini A, Ravelli A. Development and initial validation of a radiographic scoring system for the hip in juvenile idiopathic arthritis. J Rheumatol. 2010;37(2):432-9. https://doi.org/10.3899/jrheum.090691
8. Tanturri de Horatio L, Shelmerdine SC, d'Angelo P, Di Paolo PL, Magni-Manzoni S, Malattia C, Damasio MB, Toma P, Avenarius D, Rosendahl K. A novel magnetic resonance imaging scoring system for active and chronic changes in children and adolescents with juvenile idiopathic arthritis of the hip. Pediatr Radiol. 2023;53(3):426-37. https://doi.org/10.1007/s00247-022-05502-8
9. Weiss PF, Maksymowych WP, Lambert RG, Jaremko JL, Biko DM, Paschke J, Brandon TG, Xiao R, Chauvin NA. Feasibility and reliability of the Spondyloarthritis Research Consortium of Canada sacroiliac joint inflammation score in children. Arthritis Res Ther. 2018;20(1):56. https://doi.org/10.1186/s13075-018-1543-x
10. Panwar J, Tse SML, Lim L, Tolend MA, Radhakrishnan S, Salman M, Moineddin R, Doria AS, Stimec J. Spondyloarthritis Research Consortium of Canada Scoring System for Sacroiliitis in Juvenile Spondyloarthritis/Enthesitis-related Arthritis: A Reliability, Validity, and Responsiveness Study. J Rheumatol. 2019;46(6):636-44. https://doi.org/10.3899/jrheum.180222
11. Ravelli A, Ioseliani M, Norambuena X, Sato J, Pistorio A, Rossi F, Ruperto N, Magni-Manzoni S, Ullmann N, Martini A. Adapted versions of the Sharp/van der Heijde score are reliable and valid for assessment of radiographic progression in juvenile idiopathic arthritis. Arthritis Rheum. 2007;56(9):3087-95. https://doi.org/10.1002/art.22835
12. Poznanski AK, Hernandez RJ, Guire KE, Bereza UL, Garn SM. Carpal length in children--a useful measurement in the diagnosis of rheumatoid arthritis and some concenital malformation syndromes. Radiology. 1978;129(3):661-8. https://doi.org/10.1148/129.3.661
13. Malattia C, Damasio MB, Pistorio A, Ioseliani M, Vilca I, Valle M, Ruperto N, Viola S, Buoncompagni A, Magnano GM, Ravelli A, Toma P, Martini A. Development and preliminary validation of a paediatric-targeted MRI scoring system for the assessment of disease activity and damage in juvenile idiopathic arthritis. Ann Rheum Dis. 2011;70(3):440-6. https://doi.org/10.1136/ard.2009.126862
14. Damasio MB, Malattia C, Tanturri de Horatio L, Mattiuz C, Pistorio A, Bracaglia C, Barbuti D, Boavida P, Juhan KL, Ording LS, Rosendahl K, Martini A, Magnano G, Toma P. MRI of the wrist in juvenile idiopathic arthritis: proposal of a paediatric synovitis score by a consensus of an international working group. Results of a multicentre reliability study. Pediatr Radiol. 2012;42(9):1047-55. https://doi.org/10.1007/s00247-012-2392-4
15. Angenete OW, Augdal TA, Rygg M, Rosendahl K. MRI in the Assessment of TMJ-Arthritis in Children with JIA; Repeatability of a Newly Devised Scoring System. Acad Radiol. 2022;29(9):1362-77. https://doi.org/10.1016/j.acra.2021.09.024
16. Augdal TA, Angenete OW, Shi XQ, Sall M, Fischer JM, Nordal E, Rosendahl K. Cone beam computed tomography in the assessment of TMJ deformity in children with JIA: repeatability of a novel scoring system. BMC Oral Health. 2023;23(1):12. https://doi.org/10.1186/s12903-022-02701-5

B. Research Line II

Paper 3 - Reliability of CEUS and MRI for grading knee-joint inflammation in juvenile idiopathic arthritis

Dias SC, Ferreira CC, Santos I, Castro M, Rodrigues M, Aguiar F, Dias CC, Nguyen B, Silva V, Ramos I, Ključevšek D, Brito I, Rosendahl K.

Eur Radiol 36, 7379–7390 (2026). https://doi.org/10.1007/s00330-026-12627-z

EUROPEAN SOCIETY OF RADIOLOGY
European Radiology

PAEDIATRIC Open Access

Reliability of CEUS and MRI for grading knee-joint inflammation in juvenile idiopathic arthritis

Sílvia Costa Dias[1,2*], Catarina Costa Ferreira[2], Inês Santos[3], Miguel Castro[2], Mariana Rodrigues[4], Francisca Aguiar[4], Cláudia Camila Dias[5,6], Bac Nguyen[7], Vitor Silva[2], Isabel Ramos[1], Damjana Ključevšek[8], Iva Brito[1,4] and Karen Rosendahl[9,10]

Abstract

Objective To examine the reliability of contrast-enhanced MRI (CEMRI) and contrast-enhanced ultrasound (CEUS) for grading arthritis.

Materials and methods Prospective study on 1–18-year-olds with juvenile idiopathic arthritis (JIA), performed during 2023/2024. All had CEUS and CEMRI of the knee on the same day. Two observers independently scored the US-video-clip for inflammation (0–3 scale), with a second reading after 6 weeks. Using VueBox®, peak enhancement (PE), time to peak (TTP) and wash-in area under the curve (WiAUC) were measured by both observers, separately. The MRIs were scored for inflammation (0–3 scale) twice by two observers. Peak enhancement intensity (PEI), TTP and initial area under the curve (iAUC) (Syngo.via®) were measured.

Results Fifty-two patients (35 females), median age 12.4 years (IQR 8.9–15.6 years), were included. CEUS showed almost perfect intra/interreader agreement for the degree of overall inflammation (intrareader kappa 0.90 [0.83–0.98], interreader kappa 0.85 [0.76–0.93]). Interreader PE and WiAUC agreement was excellent (ICC 0.99 [95% CI 0.99–1.00] and 0.97 [95% CI 0.95–0.98], respectively), while TTP performed moderately (ICC 0.66 [95% CI 0.40–0.80]). On CEMRI, intra/interreader agreement for overall synovial inflammation was almost perfect (intrareader kappa 0.94 [95% CI 0.88–1.00]; interreader kappa 0.92 [95% CI 0.85–1.00]). Interreader PEI and iAUC agreement was excellent (ICC 0.99 [95% CI 0.98–0.99] and 0.98 [95% CI 0.97–0.99], respectively), while TTP had good agreement (ICC 0.76 [95% CI 0.59–0.86]).

Conclusion Subjective grading of synovial inflammation on a 0–3 scale demonstrated high reliability for both CEUS and CEMRI. Both methods have excellent relative reliability (ICC) for quantitative measurements; however, their absolute precision (LoA) is poor.

Key Points

Question *Are CEUS and CEMRI reliable tools to grade the activity of knee-joint arthritis in children with juvenile idiopathic arthritis?*

Findings *Subjective grading of arthritis performed well within and between observers for both CEUS and CEMRI. Both methods provide reliable dynamic measurements; however, their precision is poor.*

Clinical relevance *CEUS offers high-precision, real-time imaging for grading active knee-joint inflammation in children with juvenile idiopathic arthritis, with future potential to replace the current standard of CEMRI.*

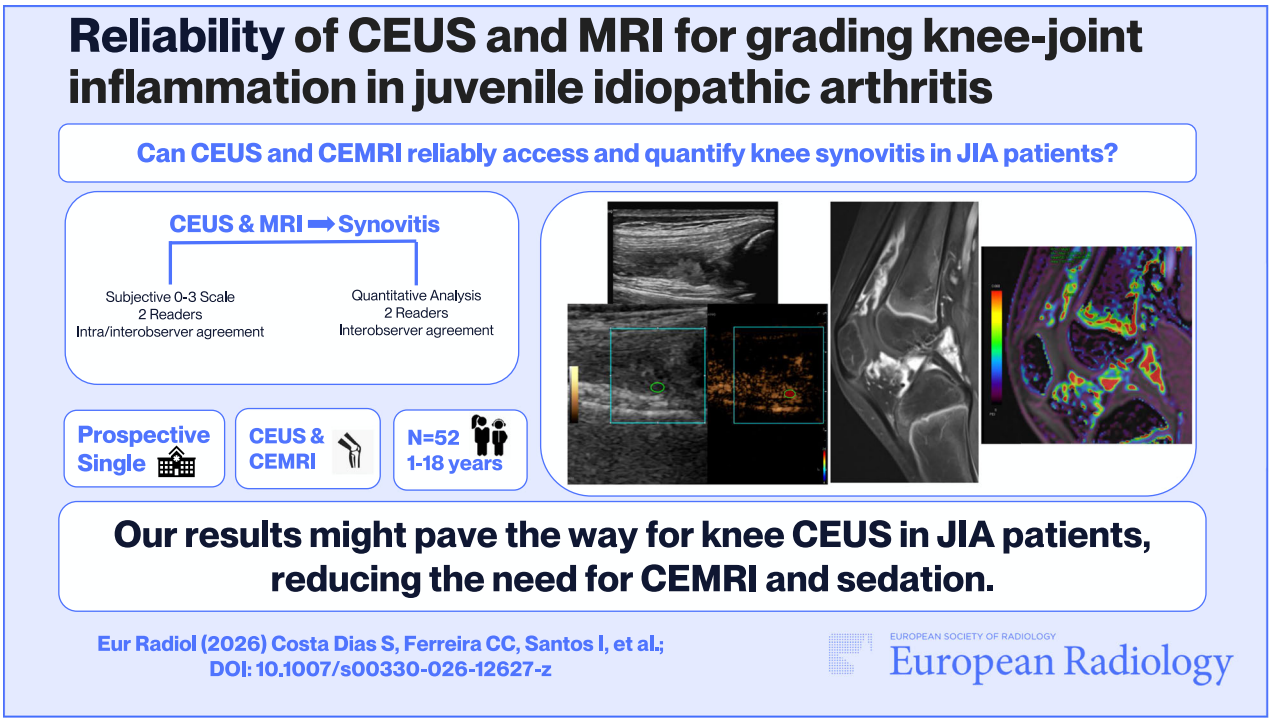
*Correspondence:
Sílvia Costa Dias
silviacostadias@hotmail.com
Full list of author information is available at the end of the article

Springer

© The Author(s) 2026. **Open Access** This article is licensed under a Creative Commons Attribution 4.0 International License, which permits use, sharing, adaptation, distribution and reproduction in any medium or format, as long as you give appropriate credit to the original author(s) and the source, provide a link to the Creative Commons licence, and indicate if changes were made. The images or other third party material in this article are included in the article's Creative Commons licence, unless indicated otherwise in a credit line to the material. If material is not included in the article's Creative Commons licence and your intended use is not permitted by statutory regulation or exceeds the permitted use, you will need to obtain permission directly from the copyright holder. To view a copy of this licence, visit http://creativecommons.org/licenses/by/4.0/.

Keywords Synovitis, Arthritis, Knee, Ultrasonography, Magnetic resonance imaging

Graphical Abstract



Introduction

Juvenile idiopathic arthritis (JIA) is a heterogeneous disease including all forms of chronic arthritis of unknown origin and with onset before 16 years of age [1, 2]. It affects 1–2 in 1000 children (f:m 3:1) and is characterised by chronic synovial inflammation, with risk of developing progressive joint destruction [3]. Although modern treatment has reduced the morbidity, children are still faced with periods of active disease, pain and reduced mobility, often continuing into adulthood [4, 5].

The diagnosis is based on history, clinical and laboratory findings, with imaging emerging as an important tool narrowing differential diagnosis, monitoring disease activity and detecting treatment complications [6]. While radiography still plays a role in joint damage evaluation and secondary growth disturbances, US and MRI are the preferred methods for assessment of disease activity [6]. Several examination techniques, protocols and grading systems for inflammatory change of the knee joint have been suggested for both US and MRI; however, the literature on their reliability is limited, including two papers on MRI with 25 patients each [7, 8] and none on US.

This study aimed to evaluate the reliability of contrast-enhanced ultrasound (CEUS) and contrast-enhanced MRI (CEMRI) for assessing knee synovitis in JIA, both subjectively (0–3 scale) and quantitatively (for CEUS: peak enhancement [PE], time to peak [TTP], wash-in area under the curve [WiAUC]; for CEMRI: peak enhancement intensity [PEI], TTP, initial area under the curve [iAUC]).

Finally, we aimed to assess the reliability of the inflammatory components of the juvenile arthritis MRI scoring (JAMRIS) system for the knee, a system also including assessment of bone marrow oedema [7].

Materials and methods

This is part of a prospective, single-centre study on children with a known diagnosis of JIA, performed during 2023–2024. Participants were consecutively recruited from the Paediatric Rheumatology Clinic at the University Hospital Centre of São João Porto (CHUSJ). Children aged 1–18 years, meeting the ILAR criteria [9] for JIA, with current or previous knee involvement, were included. Excluded were children with a history of intra-articular steroid injection or trauma to the knee within the last 2 months.

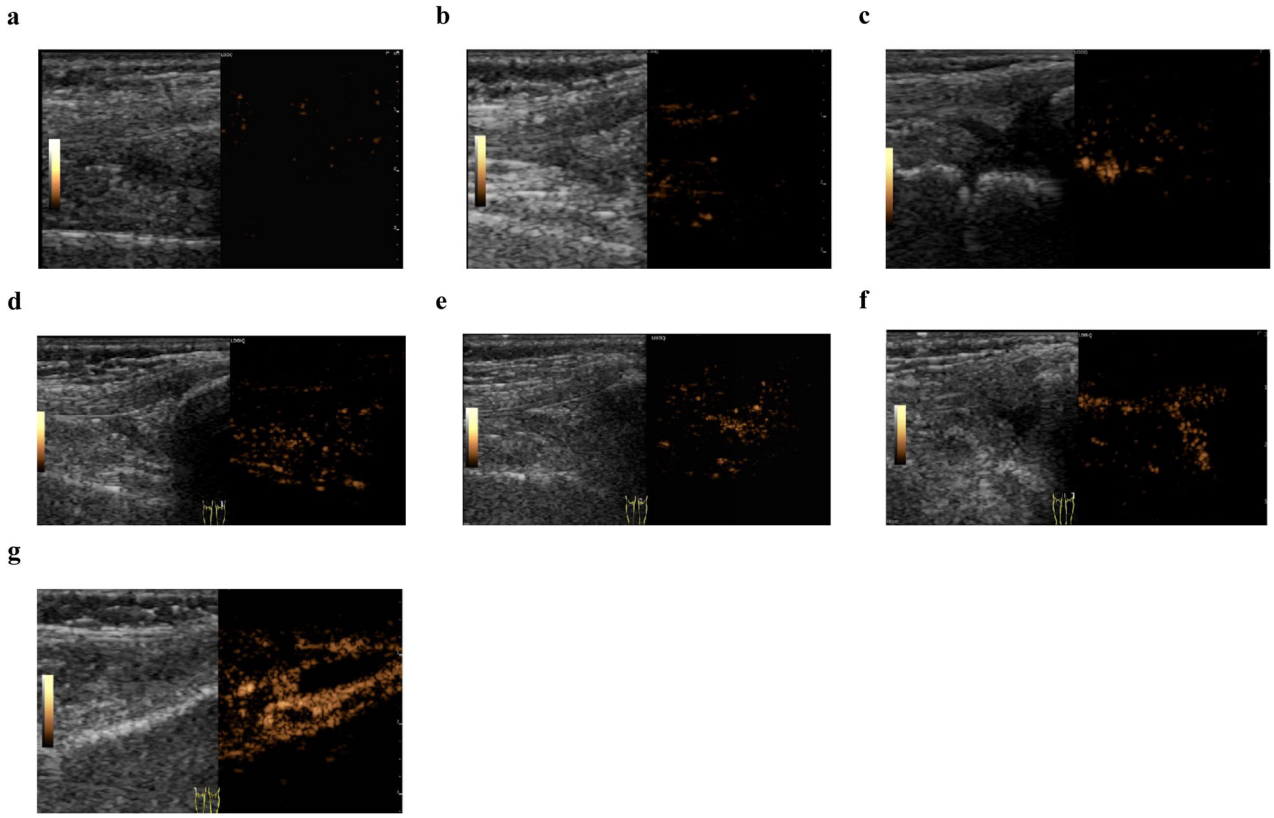


Fig. 1 CEUS atlas, with examples of the suprapatellar recess of the knee, longitudinal view. Sofware of VueBox® with Dual-screen mode with simultaneous display of grey-scale image (left) and contrast-only image (right) in the same view: **a**, **b** Grade 0 (few bubbles allowed); **c**, **d** Grade 1 (mild); **e**, **f** Grade 2 (moderate); **g** Grade 3 (severe)

For this reliability study, we used demographic and CEUS/CEMRI data. The study was approved by the Regional Ethics Committee (number 282-20), and written informed consent was obtained from each participant and/or their caregiver, according to national guidelines.

Imaging techniques

All children had a CEUS examination of the affected knee, with an additional CEMRI performed later on the same day, at an interval of at least 60 min, both with the child supine and 30° knee flexion. Intravenous access using a 20 G catheter was secured via an antecubital vein and used for both examinations. According to the European Medicines Agency [10], almost 100% of the microbubbles in SonoVue are eliminated through the lungs within 15 min. No general anaesthesia was given.

The ultrasound examinations were performed by one examiner with 12 years of experience in paediatric radiology, using a Logiq E10 machine (Version R3, General Electric®) with a linear 6–15 MHz transducer and defined pre-sets, according to a standardised protocol [11]. Sagittal scans through the suprapatellar recess were performed to identify the most prominent and hyperaemic synovium (Colour/Power/Micro Doppler). For the CEUS, a vascular linear 2–10 MHz transducer, with an adjusted musculoskeletal contrast preset, was used. A 3-way intravenous cannula was adapted to the catheter. Next, a bolus of Sulfur Hexafluoride (Sonovue®) contrast was injected; 2.4 mL to patients < 50 kg and 4.8 mL to those > 50 kg, followed by 10 mL saline chaser. Thereafter, a 2-min continuous, sagittal acquisition was performed in the same position.

The MRI examinations were performed on a 3-Tesla scanner (Siemens® Magnetom Vida) by a specially trained MRI radiographer, using an 18-channel phased-array knee transmit/receive (Tx/Rx) coil, according to a predefined protocol (Supplemental Material). A cushion (Multipad, Pearl Technology) was used to immobilise the knee. Gadolinium (Gadobutrol—Gadovist®, Bayer) was injected with a pump (0.1 mmol/Kg) at a rate of 1–3 mL/s, according to the size of the needle.

For this reliability study, we used the T1 vibe Dixon fat-saturated (FS) pre-gadolinium and T1 vibe Dixon FS controlled aliasing in parallel imaging results in higher acceleration (CAIPIRINHA) first 2 min with gadolinium

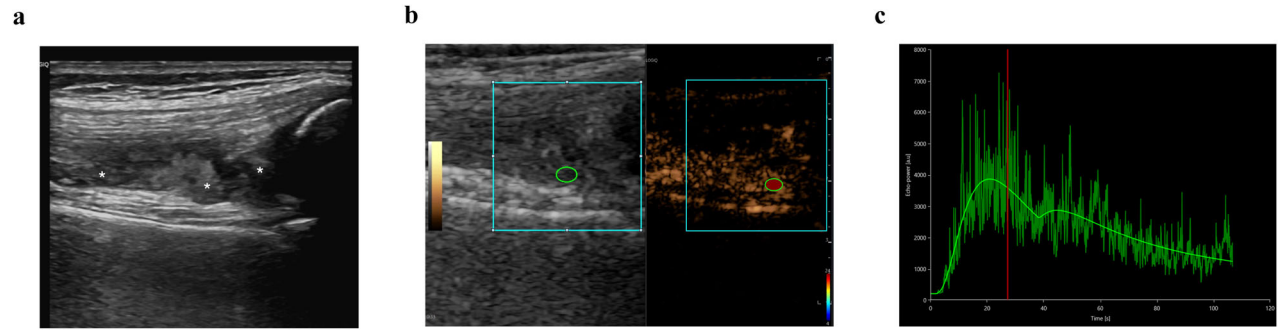


Fig. 2 CEUS of the knee in a 7-year-old girl with JIA: **a** B-mode, sagittal view through the suprapatellar recess, showing severe synovial thickening (*); **b** CEUS, dual-screen mode with simultaneous display of grey-scale image (left) and contrast-only image (right) in the same view, showing the enhancing synovium with a region of interest (ROI) placed within (software VueBox); **c** corresponding time-intensity curve of the synovial enhancement during the first 120 s within the ROI



Fig. 3 CEMRI atlas with sagittal postcontrast examples of the knee: **a** Grade 0 (none/subtle synovial enhancement); **b**, **c** Grade 1 (mild synovial enhancement); **d** Grade 2 (moderate synovial enhancement); **e** Grade 3 (severe synovial enhancement)

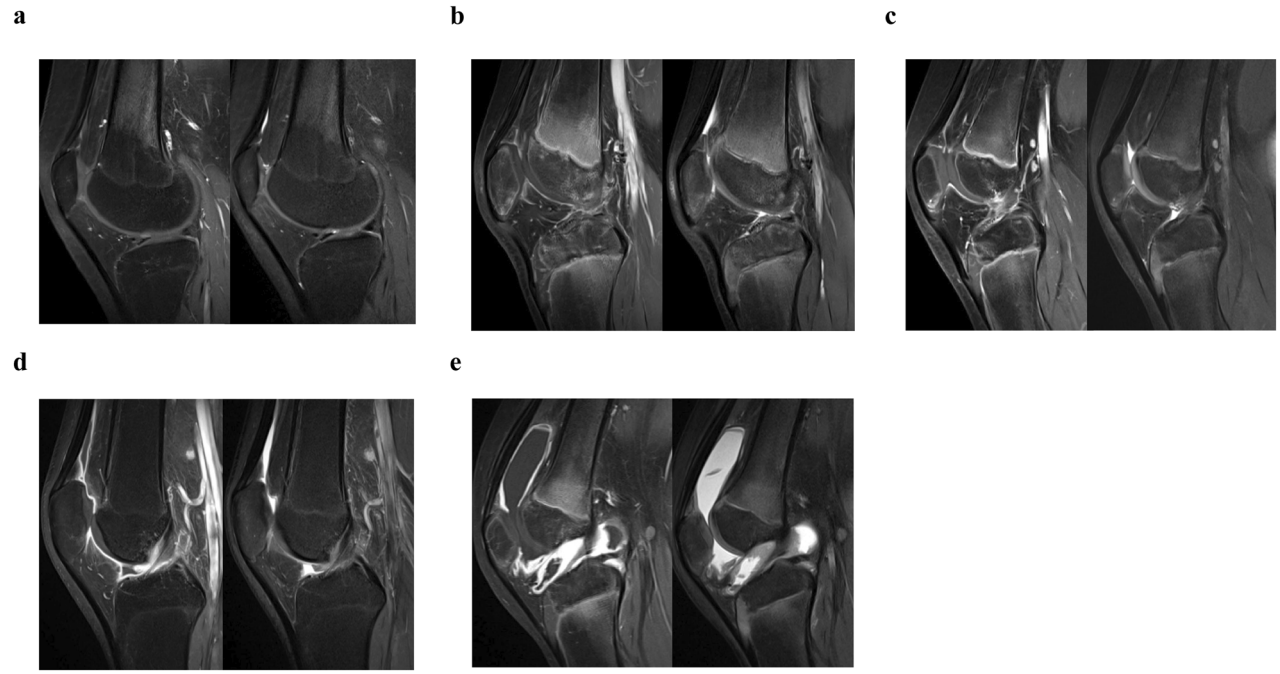


Fig. 4 CEMRI + PDFS atlas with paired examples, sagittal images, postcontrast left side image and PDFS right side image: **a** Grade 0 (none/subtle synovial enhancement or effusion); **b**, **c** Grade 1 (mild synovial enhancement/thickening ± effusion); **d** Grade 2 (moderate synovial enhancement/thickening + effusion); **e** Grade 3 (severe synovial enhancement/thickening + effusion)

(isotropic) and T1-w TSE FS post-gadolinium sagittal and axial series.

Image analysis

CEUS

Subjective assessment of synovial inflammation on a 0–3 scale. All CEUS videoclips (0–120 s) were anonymised, archived and reviewed retrospectively. Two observers independently and blinded to additional information, scored the degree of contrast enhancement on a 0–3 scale, adjusted from Klauser et al [12, 13]: grade 0 (few bubbles in the synovium); grade 1 (mild; patchy, synovial enhancement, intensity lower than surrounding tissue); grade 2 (moderate; more homogenous and diffuse synovial enhancement, intensity equal/slightly > surrounding tissue) or grade 3 (severe; fast/intense, homogenous synovial enhancement, intensity > surrounding tissue). An atlas (one still image from the 2-min videoclips —not later used for quantitative analysis—of seven patients) was devised to illustrate the 0–3 scale used (Fig. 1). A repeat grading (videoclips differently ordered) was performed after 6 weeks by both observers, independently.

Dynamic CEUS—quantitative assessment of synovial inflammation. The DICOM video clip was post-processed with the CEUS quantification software VueBox® (version 7.5; Bracco Imaging). A sagittal frame showing the most prominent synovial membrane was selected in consensus by the two observers. Based on an applied colour intensity map, each observer chose three different regions of interest (ROIs), with a predefined saved standardised ROI (approximately 3.2–4.2 mm^2, depending on the original size of the US image) for measurement of the most enhancing synovium (Fig. 2). PE, TTP and WiAUC were measured by both observers, separately.

MRI

Subjective assessment of synovial inflammation. Based on the T1-w TSE FS pre- and postcontrast images, all MRI examinations were evaluated in a blinded fashion without knowledge of clinical findings, by two radiologists, independently (one paediatric and one musculoskeletal radiologist with 12 and 14 years of experience, respectively). The overall synovial enhancement and degree of inflammation were scored separately, on a 0–3 scale according to a recent study [4]. Overall synovial enhancement was based on the degree of synovial enhancement/synovial thickening and scored as grade 0 (none/subtle); grade 1 (mild); grade 2 (moderate) or grade 3 (severe) (Fig. 3). Overall degree of inflammation was based on a comprehensive evaluation of degree and extent

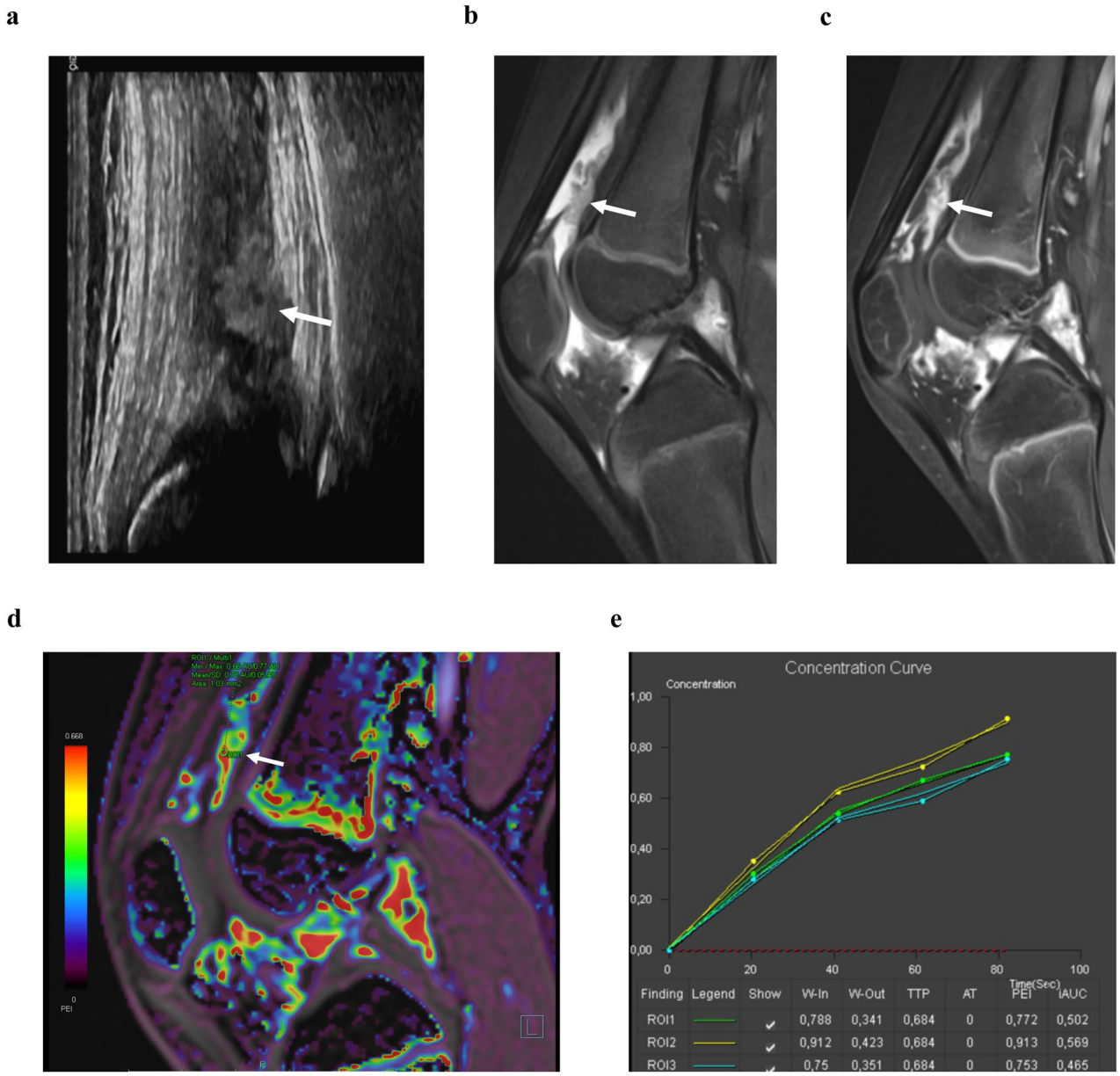


Fig. 5 CEMRI in a 7-year-old girl with JIA (same patient as Fig. 1). **a** B-mode, sagittal view showing thickened synovium (arrow). **b** MRI PD FS image and **c** T1 TSE FS postcontrast image, same sagittal plane, showing thickened and enhancing synovium (arrow). **d** Syngo.via® colour peak enhancement intensity (PEI) map with a region of interest (ROI) placed within the enhancing synovium, in the same areas as for CEUS. **e** Three dynamic enhancement curves (0–100 s), representing perfusion in 3 different ROIs; concentration curves display the concentration of the contrast agent in the *y*-axis along time in the *x*-axis

of synovial enhancement and the presence or not of an effusion (defined as ≥ 2 mm at the maximum), and scored as grade 0 (none/subtle synovial enhancement or effusion); grade 1 (mildly increased synovial enhancement/thickening, ± effusion); grade 2 (moderately increased synovial enhancement/thickening, + effusion) or grade 3 (severely increased synovial enhancement/thickening + effusion). An illustrated atlas, using single, sagittal images from five different JIA patients, was devised to standardise grading (Fig. 4).

The MRIs were also scored using elements of the JAMRIS-system [7]; synovial hypertrophy (scored on postcontrast images at six different locations, as 0 (< 2 mm thick), 1 (≥ 2–4 mm) or 2 (> 4 mm) (minimum score 0, maximum 12)) and bone marrow changes suggestive of oedema (scored as grade 0 (none); grade 1

(< 10% of the whole bone volume); 2 (10–25%) or 3 (≥ 25%) (minimum total score 0, maximum 24)). A repeat grading was performed after 6 weeks by both observers, separately, and blinded to previous results.

Dynamic CEMRI—quantitative assessment of synovial inflammation. From the sagittal T1-w TSE FS post-gadolinium series, a sagittal section, corresponding to the chosen CEUS view, was identified by the two observers in consensus, and used for the dynamic CEMRI measurements. Using the Syngo.via® Tissue 4D application, the two observers, independently, placed three different circular ROIs (approximately 1mm^2 area, with the lowest possible standard deviation [SD]) within a vividly enhancing portion of the synovium, guided by the colour PEI map (Fig. 5). PEI, TTP and iAUC were measured.

Table 1 Demographic data on the study population

Patients	
n (%)	52 (100)
Sex, female, *n* (%)	35 (67.4)
Age, years, Mdn (IQR)	12.4 (8.9–15.6)
Height, cm, Mdn (IQR)	149.0 (129.0 –161.0)
Weight, kg, Mdn (IQR)	39.7 (26.1–56.6)
BMI, Mdn (IQR)	18.3 (16.1–21.8)
JIA subtypes, *n* (%)	52 (100)
Systemic	2 (3.8)
Oligoarthritis persistent	30 (57.7)
Oligoarthritis extended	5 (9.6)
Polyarthritis FR negative	6 (11.5)
Polyarthritis FR positive	1 (1.9)
Psoriatic arthritis	4 (7.7)
Enthesitis-related arthritis	4 (7.7)
Age at JIA diagnosis, years, Mdn (IQR)	5.0 (2.0–8.0)
Duration of JIA's disease, years, Mdn (IQR)	6.0 (3.3–9.0)
Right knee studied, *n* (%)	28 (53.8)

Mdn median, *IQR* interquartile range, *BMI* body mass index

Statistical analysis

Continuous data were presented as medians (with interquartile range [IQR]) or means (with standard deviations [SD]) as appropriate, and dichotomous data as absolute/relative frequencies. For categorical variables, intra- and interobserver agreement was assessed using linear weighted kappa (κ) coefficients (95% confidence interval [CI]) and proportion of absolute agreement. A κ of < 0 was considered poor, 0–0.20 slight, 0.21–0.40 fair, 0.41–0.60 moderate, 0.61–0.80 substantial and 0.81–1.00 almost perfect [14]. For comparison purposes, we also employed the intraclass correlation coefficient (ICC), two-mixed, type consistency [15, 16], with 95% CIs (0–0.39 poor, 0.40–0.59 fair, 0.60–0.74 good; and 0.75–1.00 excellent), reflecting relative agreement [17].

Differences in continuous variables were analysed using Bland–Altman plots and 95% limits of agreement (LoAs), reflecting absolute agreement [18]. The quantitative CEUS and CEMRI data were not normally distributed, remaining skewed after log-transformation; thus, non-parametric LoAs were used (2.5th percentile and the 97.5th percentile of the log-differences), reporting the back-transformed values to acquire exponential/ratios for interpretation of bias and LoA. Differences in continuous variables were also analysed using ICCs (two-way mixed; consistency type) as appropriate.

The JAMRIS Score was considered a continuous variable, adding up the scores of the different locations to a maximum of 12 for synovial hypertrophy and 24 for bone marrow oedema (BMO). ICC (two-way mixed; consistency type) was used to test for intra- and interobserver agreement. The statistical analyses were performed using

Table 2 Subjective CEUS-scoring assessment of synovial inflammation of the knee joint in 52 children with JIA, based on reading of the videoclips taken by observer one

CEUS-feature	Intraobserver		Interobserver		
	Linear kappa value (95% CI)	ICC (95% CI)	Linear kappa value (95% CI)	Proportion absolute agreement (95% CI)	ICC (95% CI)
Degree of synovial contrast enhancement on a 0–3 scale	0.89 (0.81–0.98)—R1 0.90 (0.84–0.98)—R2	0.97 (0.95–0.98)—R1 0.97 (0.96–0.99)—R2	0. 85 (0.76–0.94)	0.83 (0.69–0.91)	0.96 (0.93–0.98)

R1 = reader one, R2 = reader two
Linear weighted kappa values and ICCs for intra- and interobserver agreement and proportion of absolute agreement for interobserver variation are reported

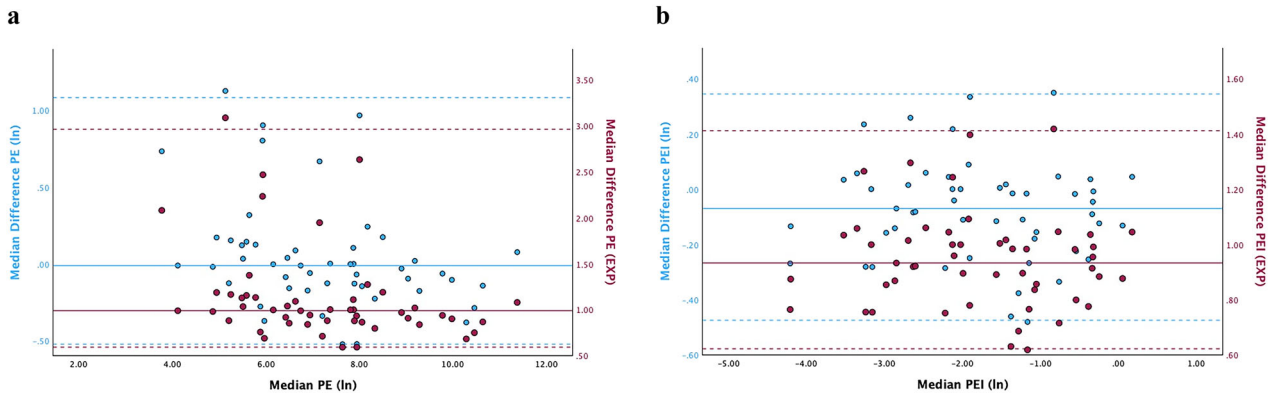


Fig. 6 Non-parametric Bland–Altman plot of interobserver agreement: **a** for peak enhancement (PE) on CEUS, the primary *y*-axis (left) displays the difference between observers on a natural log (ln) scale, whilst the secondary *y*-axis (right) displays the corresponding back-transformed ratios (EXP). The solid horizontal line (blue) indicates the median bias of −0.01 (corresponding back-transformed bias: 0.99, solid red line), the blue stippled lines indicate the 95% LoAs from −0.53 to 1.08 (corresponding back-transformed ratio LoAs: 0.59–2.96, stippled red lines); **b** for peak enhancement intensity (PEI) on CEMRI, the primary *y*-axis (left) displays the difference between observers on a natural log (ln) scale, whilst the secondary *y*-axis (right) displays the corresponding back-transformed ratios (EXP). The solid horizontal line (blue) indicates the median bias of −0.07 (corresponding back-transformed bias: 0.93, solid red line), the blue stippled lines indicate the 95% LoAs from −0.47 to 0.34 (corresponding back-transformed ratio LoAs: 0.62–1.41, stippled red lines)

SPSS software (v.30, IBM) or Jamovi® v.2.6.26. A $p < 0.05$ was considered statistically significant.

Results

Fifty-two patients (35 females) were included, median age 12.4 years (IQR 8.9–15.6). Demographic data and disease characteristics are given in Table 1. The distribution of subjective CEUS and CEMRI-scores for synovial inflammation on a 0–3 scale was balanced, with approximately 8–17 cases in each of the groups.

Contrast-enhanced ultrasound (CEUS)

Subjective grading of synovial inflammation; intra- and interobserver agreement

Based on the videoclips, assessment of the degree of synovial contrast enhancement on a 0–3 scale performed almost perfectly for both observers, with kappa values of 0.89 (95% CI 0.81–0.98) and 0.90 (95% CI 0.83–0.98), for the two readers, respectively (Table 2). Agreement between observers was almost perfect with a kappa value of 0.85 (95% CI 0.76–0.93) and an absolute agreement of 0.83. Using ICC, the interobserver agreement was excellent (0.96; 95% CI 0.93–0.98).

Dynamic CEUS: quantitative measurement of synovial inflammation; interobserver agreement

Measurements of PE and WiAUC performed well, with ICCs of 0.99 (95% CI 0.99–1.00) and 0.97 (95% CI 0.95–0.98), respectively, while TTP had a moderate interobserver agreement, with an ICC of 0.66 (95% CI 0.40–0.80).

For PE, the interobserver median ratio using a non-parametric Bland–Altman analysis with back-transformation, was 0.99, indicating negligible systematic bias between observers, however, the LoAs (0.59–2.96) were wide, demonstrating poor interobserver reproducibility (Fig. 6). Corresponding figures for WiAUC were 0.94 with 95% LoA of 0.39–3.71, and for TTP, 0.96 with 95% LoA of 0.40–1.81.

MRI

Subjective grading of synovial inflammation; intra- and interobserver agreement

Assessment of overall synovial inflammation on a 0–3 scale showed almost perfect agreement for both observers, with kappa values of 0.91 (95% CI 0.83–0.99) and 0.96 (95% CI 0.91–1.00), respectively (Table 3). The interobserver agreement was 0.89 (95% CI 0.81–0.98), with an absolute agreement of 0.88. Based on ICC, the interobserver agreement was excellent (0.97; 95% CI 0.95–0.98).

Grading overall inflammation of the knee joint based on synovial enhancement, thickening and effusion also performed very well, with kappa values of 0.94 (95% CI 0.88–1.00) and 0.90 (95% CI 0.81–0.98) for each observer, respectively. The interobserver agreement was 0.92 (95% CI 0.85–1.00), with 0.92 of absolute agreement (Table 3). The ICC for interobserver agreement was almost perfect (0.98; 95% CI 0.96–0.99).

Subjective grading using components from the JAMRIS score, inflammatory domain

Assessing synovial hypertrophy for each of the six locations, according to the JAMRIS system, performed well both between and for the same observers (Table 4). For

Table 3 Subjective MRI-scoring assessment of the synovial inflammation of the knee joint of 52 children with JIA, based on T1-w TSE FS pre and postcontrast images

MRI-features	Intraobserver		Interobserver		
	Linear kappa value (95% CI)	ICC (95% CI)	Linear kappa value (95% CI)	Proportion absolute agreement (95% CI)	ICC (95% CI)
Overall synovial inflammation on a 0–3 scale	0.91 (0.83–0.99)—R1 0.96 (0.91–1.00)—R2	0.97 (0.96–0.99)—R1 0.99 (0.98 –0.99)—R2	0.89 (0.81–0.98)	0.88 (0.76–0.95)	0.97 (0.95–0.98)
Overall degree of inflammation, including effusion on a 0–3 scale	0.94 (0.88–1.00)—R1 0.90 (0.81–0.98)—R2	0.98 (0.97–0.99)—R1 0.97 (0.94–0.98)—R2	0.92 (0.85–1.00)	0.92 (0.81–1.00)	0.98 (0.96–0.99)

R1 = reader one, R2 = reader two
Linear weighted kappa values and ICCs for intra- and interobserver agreement and proportion of absolute agreement for interobserver variation are reported

the total score synovial hypertrophy on a 0–12 scale, the agreement was almost perfect for intra-observers, with ICCs of 0.97 (95% CI 0.96–0.99) and 0.99 (95% CI 0.99–1.00). The interobserver agreement was 0.97 (95% CI 0.95–0.98).

BMO was identified in 9/52 and 19/52 patients, respectively, by the two readers, yielding almost perfect intraobserver variation of 0.88 (95% CI 0.79–0.99) and 0.92 (95% CI 0.86–0.95) for the two readers, respectively. The interobserver agreement was moderate with ICC of 0.65 (95% CI 0.39–0.80) (Table 4).

Dynamic CEMRI: semi-quantitative measurement of synovial inflammation; interobserver agreement

Measurements of PEI and iAUC had excellent interobserver agreement with ICCs of 0.99 (95% CI 0.98–0.99) and 0.98 (95% CI 0.97–0.99), respectively, while TTP had a good agreement with an ICC of 0.76 (95% CI 0.59–0.86).

For PEI, the interobserver median ratio was 0.93, indicating a small systematic bias between observers of 7%, however, the 95% LoAs were wide (0.62–1.41) (Fig. 6). For the iAUC, differences between readers were normally distributed, thus, standard Bland–Altman analysis was performed, showing a mean difference between readers of −0.01, with fair 95% LoA of −0.10 to 0.07.

The TTP was considered a categorical variable, as only a few fixed values were allowed by the application, yielding a moderate interobserver agreement, kappa values of 0.58 (95% CI 0.39–0.77) and an absolute agreement of 0.69.

Discussion

We have shown that subjective grading of synovial inflammation on a 0–3 scale performed well, both within and between observers, for CEUS and CEMRI. Interobserver analysis for quantitative measurements revealed overall high ICCs, suggesting a very good ability to distinguish between subjects. However, the LoAs, most of which were wide, indicate that the interobserver precision may be insufficient for tracking subtle changes in a single subject over time.

Evaluating the degree of synovial inflammation with ultrasound and/or CEMRI is important for disease management in children with JIA [19–21]. A recent review provides validated scoring systems for both modalities, as well as published reference values for the amount of joint fluid and synovial thickness [6]. The potential of dynamic CEUS and CEMRI for grading arthritis has been evaluated; however, limited studies have assessed their reproducibility and precision in children [22–25]. In particular, no study evaluating both CEUS and CEMRI based on the same cohort and performed on the same day exists. In a study from 2010, including 22 patients with involvement of the wrist or hip, the reproducibility of dynamic MRI-measurements was reportedly excellent when based on ICCs; however, without elaborating on the results using additional statistical tests [26]. Bennett et al [27,28] in another study of 11 patients treated with intra-articular glucocorticoid injections, found that quantitative MR-measurements were reliable in the assessment of synovial inflammation, using a Bland–Altman approach.

Knowledge of a method's reliability is crucial for the correct interpretation of changes in a specific imaging marker over time. We used two complementary statistical methods: an ICC, "two-mixed type" measuring the overall consistency (reliability) of the markers, and 95% LoA indicating the range where 95% of paired differences are expected to fall. LoA, which shows the clinical relevance of measurement differences, shares similarities with the clinical measure "minimal detectable change" (MDC), also known as "smallest detectable change" (SDC), using a 95% confidence interval, which is similar in calculation to LoA but focused on true change rather than method

Table 4 Juvenile arthritis MRI scoring (JAMRIS) system for the knee—inflammatory domain with synovial hypertrophy and bone marrow oedema: median with interquartile range (IQR) and range measures for both readers

JAMRIS	Reader 1 Median (IQR) *Range (Min–Max)*	Reader 2 Median (IQR) *Range (Min–Max)*	*p*-value[a]	ICC intraobserver	ICC interobserver
Total score synovial hypertrophy (0–12)	3.50 (0.00–8.00) *(0–12)*	3.00 (0.00–8.00) *(0–12)*	0.940	0.97 (0.96–0.99)—R1 0.99 (0.99–1.00)—R2	0.97 (0.95–0.98)
Total score bone marrow oedema (0–24)	0.00 (0.00–1.00) *(0–7)*	0.00 (0.00–0.00) *(0–3)*	**0.041**	0.88 (0.79–0.93)—R1 0.92 (0.86–0.95)—R2	0.65 (0.39–0.80)

R1 = reader one, R2 = reader two
Intraclass correlation coefficient (ICC) for intra- and inter-observers was also assessed in the study population (52 patients with JIA; 35 girls)
[a] Mann–Whitney test
Bold = *p*-value < 0.05 (not italic); Italic = range values (min-max)

agreement [15]. For example, a LoA of 0.62–1.41 as found for PEI (CEMRI) indicates that measurements of the same subject could vary from −38% to 41% between observers. While the high ICC of 0.99 suggests excellent discriminative ability across the scale used, the wide LoAs indicate that the precision is poor for clinical monitoring. The conflicting statistical results can in part be explained by the large arbitrary scales used for both CEMRI (signal intensity, SI) and CEUS (Linear Units, a.u.), reflecting the inherent limitations of manual ROI placement on high-intensity linear scales.

The subset of JAMRIS markers examined performed well for synovial hypertrophy total score, supporting previous results [7]. More recently, Handa et al [29], in a study of 35 patients with JIA, reported moderate to high intraobserver agreement for synovial thickness measurements, with concordance correlation coefficients (CCC) from 0.50 to 0.89 for six locations used in the JAMRIS scoring system. Interobserver agreement was low, with a CCC of 0.47, averaged over six locations, particularly for unenhanced images. In contrast, Verkuil et al [30] demonstrated excellent inter- and intraobserver agreement (ICC) for both unenhanced (double inversion recovery (DIR)) and CEMR images for the JAMRIS-compartments (26 children with JIA, of whom 13 had active inflammation). However, a BA-plot showed wide LoAs, from 1.4 to 1.6 mm for the four readers, reflecting low precision.

In our study, assessment of BMO performed well within observers; however, the interobserver agreement was moderate, with significant differences between the two observers. In comparison, Hemke demonstrated a high ICC of 0.86 and no significant differences between readers [7]. These discrepancies reflect challenges of defining and diagnosing BMO. Recent studies have shown that around 50% of healthy children/adolescents have at least one major BMO-like change in the appendicular skeleton, particularly around knee joints, which, in a clinical setting, can be mistaken for pathology [31–34]. According to JAMRIS [7], changes suggestive of BMO are defined as lesions within the trabecular bone, with ill-defined margins and high signal intensity on T2-weighted fat-saturated images and low signal intensity on T1-weighted images, without mention of what is considered normal variation. Although using their definition, our perception of high T2-signal beyond normality might have differed. Moreover, our cohort included a higher number of young children as compared to the JAMRIS cohort [35, 36].

We acknowledge some limitations to our study. First, the cohort was relatively small; however, the distribution of scores along the 0–3 scale was balanced, reducing the risk of bias. Second, differences in the placement of the ROIs might have influenced the results. Third, the atlases devised for subjective scoring included a few images from the studied cohort, images not used for later scoring. Lastly, intraobserver agreement for quantitative MRI data was not performed.

Conclusion

Subjective grading of synovial inflammation on a 0–3 scale in JIA patients with knee involvement performed well, both within and between observers, for CEUS and CEMRI. Both methods have excellent relative reliability (ICC) for quantitative measurements, meaning that they work at a group level; however, their absolute interobserver precision (LoA) is poor.

Abbreviations

BMO	Bone marrow oedema
CEMRI	Contrast-enhanced MRI
CEUS	Contrast-enhanced ultrasound
iAUC	Initial area under the curve
ICC	Intraclass correlation coefficient
JAMRIS	Juvenile arthritis MRI scoring
JIA	Juvenile idiopathic arthritis

LoA	Limits of agreement
PE	Peak enhancement
PEI	Peak enhancement intensity
ROI	Region of interest
TTP	Time to peak
WiAUC	Wash-in area under the curve

Supplementary information

The online version contains supplementary material available at https://doi.org/10.1007/s00330-026-12627-z.

Acknowledgements

We thank the children and parents for their participation in this study.

Funding

The authors state that this work has not received any funding. Open access funding provided by FCT|FCCN (b-on).

Compliance with ethical standards

Guarantor

The scientific guarantor of this publication is Sílvia Costa Dias.

Conflict of interest

The authors of this manuscript declare no relationships with any companies whose products or services may be related to the subject matter of the article.

Statistics and biometry

One of the authors has significant statistical expertise.

Informed consent

Written informed consent was obtained from all subjects (patients) in this study.

Ethical approval

Institutional Review Board approval was obtained.

Study subjects or cohorts overlap

The study subjects have not been previously reported.

Methodology

- Prospective
- Diagnostic study
- Performed at one institution

Author details

[1]Department of Medicine, Faculty of Medicine of the University of Porto (FMUP), Porto, Portugal. [2]Department of Radiology, University Hospital Centre of São João Porto (CHUSJ), Porto, Portugal. [3]Rheumatology Unit, Unidade Local Saúde Viseu Dão-Lafões, Viseu, Portugal. [4]Paediatric and Young Adult Rheumatology Unit, University Hospital Centre of São João (CHUSJ), Porto, Portugal. [5]Knowledge Management Unit, Faculty of Medicine of the University of Porto (FMUP), Porto, Portugal. [6]CINTESIS@RISE, Department of Community Medicine, Information and Health Decision Sciences (MEDCIDS), Faculty of Medicine of the University of Porto (FMUP), Porto, Portugal. [7]Division of Radiology and Nuclear Medicine, Oslo University Hospital, Rikshospitalet, Oslo, Norway. [8]Department of Radiology, University Children's Hospital Ljubljana, Ljubljana, Slovenia. [9]Department of Clinical Medicine, Faculty of Health Sciences, UiT the Arctic University of Norway, Tromsø, Norway. [10]Section of Paediatric Radiology, University Hospital of North Norway, Tromsø, Norway.

Received: 15 December 2025 Revised: 6 April 2026 Accepted: 27 April 2026
Published online: 15 May 2026

References

1. Gabriel SE, Michaud K (2009) Epidemiological studies in incidence, prevalence, mortality, and comorbidity of the rheumatic diseases. Arthritis Res Ther 11:229
2. Thierry S, Fautrel B, Lemelle I, Guillemin F (2014) Prevalence and incidence of juvenile idiopathic arthritis: a systematic review. Joint Bone Spine 81:112–117
3. Prakken B, Albani S, Martini A (2011) Juvenile idiopathic arthritis. Lancet 377:2138–2149
4. Arvidsson LZ, Smith HJ, Flato B, Larheim TA (2010) Temporomandibular joint findings in adults with long-standing juvenile idiopathic arthritis: CT and MR imaging assessment. Radiology 256:191–200
5. Glerup M, Rypdal V, Arnstad ED et al (2020) Long-term outcomes in juvenile idiopathic arthritis: eighteen years of follow-up in the population-based Nordic juvenile idiopathic arthritis cohort. Arthritis Care Res 72:507–516
6. Costa Dias S, Habre C, Di Paolo PL et al (2026) ESR Essentials: juvenile idiopathic arthritis; what every radiologist needs to know—practice recommendations by the European Society of Paediatric Radiology. Eur Radiol 36:1261–1271
7. Hemke R, van Rossum MA, van Veenendaal M et al (2013) Reliability and responsiveness of the juvenile arthritis MRI scoring (JAMRIS) system for the knee. Eur Radiol 23:1075–1083
8. Hemke R, Tzaribachev N, Nusman CM, van Rossum MAJ, Maas M, Doria AS (2017) Magnetic resonance imaging (MRI) of the knee as an outcome measure in juvenile idiopathic arthritis: an OMERACT reliability study on MRI scales. J Rheumatol 44:1224–1230
9. Petty RE, Southwood TR, Manners P et al (2004) International League of Associations for Rheumatology classification of juvenile idiopathic arthritis: second revision, Edmonton, 2001. J Rheumatol 31:390–392
10. European Medicines Agency (2026) Available via https://www.ema.europa.eu/en/homepage. Accessed 28 Jan 2026
11. Dias SC, Carvalho DC, Castro M et al (2025) Knee-ultrasound: reference values for the amount of joint fluid and synovial appearances in healthy children and adolescents. Pediatr Radiol 55:1127–1137
12. Gong Y, Huang Y, Su Y, He J, Chen S (2021) Value of contrast-enhanced ultrasonography in evaluating rheumatoid arthritis: preliminary research based on an animal model. Med Sci Monit 27:e931327
13. Klauser A, Demharter J, De Marchi A et al (2005) Contrast enhanced gray-scale sonography in assessment of joint vascularity in rheumatoid arthritis: results from the IACUS study group. Eur Radiol 15:2404–2410
14. Landis JR, Koch GG (1977) The measurement of observer agreement for categorical data. Biometrics 33:159–174
15. de Vet HC, Terwee CB, Knol DL, Bouter LM (2006) When to use agreement versus reliability measures. J Clin Epidemiol 59:1033–1039
16. Kottner J, Audige L, Brorson S et al (2011) Guidelines for reporting reliability and agreement studies (GRRAS) were proposed. Int J Nurs Stud 48:661–671
17. Hallgren KA (2012) Computing inter-rater reliability for observational data: an overview and tutorial. Tutor Quant Methods Psychol 8:23–34
18. Bland JM, Altman DG (1999) Measuring agreement in method comparison studies. Stat Methods Med Res 8:135–160
19. Malattia C, Tolend M, Mazzoni M et al (2020) Current status of MR imaging of juvenile idiopathic arthritis. Best Pract Res Clin Rheumatol 34:101629
20. Mazzoni M, Pistorio A, Magnaguagno F et al (2023) Predictive value of magnetic resonance imaging in patients with juvenile idiopathic arthritis in clinical remission. Arthritis Care Res 75:198–205
21. De Lucia O, Ravagnani V, Pregnolato F et al (2018) Baseline ultrasound examination as possible predictor of relapse in patients affected by juvenile idiopathic arthritis (JIA). Ann Rheum Dis 77:1426–1431
22. Ntoulia A, Barnewolt CE, Doria AS et al (2021) Contrast-enhanced ultrasound for musculoskeletal indications in children. Pediatr Radiol 51:2303–2323
23. Nusman CM, Hemke R, Lavini C et al (2017) Dynamic contrast-enhanced magnetic resonance imaging can play a role in predicting flare in juvenile idiopathic arthritis. Eur J Radiol 88:77–81

24. Doria AS, Kiss MH, Lotito AP et al (2001) Juvenile rheumatoid arthritis of the knee: evaluation with contrast-enhanced color Doppler ultrasound. Pediatr Radiol 31:524–531
25. Workie DW, Graham TB, Laor T et al (2007) Quantitative MR characterization of disease activity in the knee in children with juvenile idiopathic arthritis: a longitudinal pilot study. Pediatr Radiol 37:535–543
26. Malattia C, Damasio MB, Basso C et al (2010) Dynamic contrast-enhanced magnetic resonance imaging in the assessment of disease activity in patients with juvenile idiopathic arthritis. Rheumatology 49:178–185
27. Bennett JL, Wood A, Smith N et al (2019) Can quantitative MRI be used in the clinical setting to quantify the impact of intra-articular glucocorticoid injection on synovial disease activity in juvenile idiopathic arthritis? Pediatr Rheumatol Online J 17:74
28. Bunce C (2009) Correlation, agreement, and Bland–Altman analysis: statistical analysis of method comparison studies. Am J Ophthalmol 148:4–6
29. Handa A, Bedoya MA, Iwasaka-Neder J, Johnston PR, Lo MS, Bixby SD (2024) Measuring synovial thickness on knee MRI in pediatric patients with arthritis: is contrast necessary? Pediatr Radiol 54:988–1000
30. Verkuil F, Hemke R, van Gulik EC et al (2022) Double inversion recovery MRI versus contrast-enhanced MRI for evaluation of knee synovitis in juvenile idiopathic arthritis. Insights Imaging 13:167
31. Zadig P, von Brandis E, d'Angelo P et al (2022) Whole-body MRI in children aged 6–18 years. Reliability of identifying and grading high signal intensity changes within bone marrow. Pediatr Radiol 52:1272–1282
32. von Brandis E, Jenssen HB, Avenarius DFM et al (2022) Automated segmentation of magnetic resonance bone marrow signal: a feasibility study. Pediatr Radiol 52:1104–1114
33. Zadig PK, von Brandis E, Flato B et al (2022) Whole body magnetic resonance imaging in healthy children and adolescents: bone marrow appearances of the appendicular skeleton. Eur J Radiol 153:110365
34. von Brandis E, Zadig PK, Avenarius DFM et al (2022) Whole body magnetic resonance imaging in healthy children and adolescents. Bone marrow appearances of the axial skeleton. Eur J Radiol 154:110425
35. Person A, Janitz E, Thapa M (2021) Pediatric bone marrow: normal and abnormal MRI appearance. Semin Roentgenol 56:325–337
36. Tanturri de Horatio L, Zadig PK, von Brandis E, Ording Muller LS, Rosendahl K, Avenarius DFM (2023) Whole-body MRI in children and adolescents: can T2-weighted Dixon fat-only images replace standard T1-weighted images in the assessment of bone marrow? Eur J Radiol 166:110968

Publisher's Note

Springer Nature remains neutral with regard to jurisdictional claims in published maps and institutional affiliations.

Reliability of CEUS and MRI for grading knee-joint inflammation in Juvenile Idiopathic Arthritis

ELECTRONIC SUPPLEMENTARY MATERIAL

Eur Radiol (2026) Costa Dias S, Ferreira CC, Santos I, et al.

Electronic Supplemental Material – MRI Protocol, “Siemens Magnetom Vida 3T” with Knee coil. 30º Flexion.

Sequence	Plane	TR (ms)	TE (ms)	TI (ms)	Averages	FOV read (mm)	FOV phase	Number slices	Slice Thickness (mm)	Flip angle	Gap (mm)	Image Matrix	Bandwidth (Hz/Px)	Acquisition time	Turbo factor	Acceleration mode	Acceleration factor	Others
PD TSE FS	Sagittal	3010	33	---	1	160	100%	32	3	180	0.3	269*384	181	1min31 s	9	SMS	2	SPAIR PE: H>>F Oversampling: 70%
	Axial	4160	38	---	1	160	100%	40	3	180	0.3	269*384	148	1min44 s	9	SMS	2	SPAIR PE: R>>L Oversampling: 40%
	Coronal	3010	33	---	1	160	100%	38	3	150	0.3	269*384	181	1min30 s	7	SMS	2	SPAIR PE: R>>L Oversampling: 30%
T1 TSE	Coronal	718	9.9	---	1	160	100%	38	3	150	0.3	314*448	228	1min09 s	3	SMS	2	PE: R>>L Oversampling: 50%
T1 TSE FS pre - Gd	Sagittal	500	9	---	2	160	100%	32	3	150	0.3	280*400	227	2min51 s	3	SMS	2	PE: H>>F Fat suppression Oversampling: 70%
T1 vibe Dixon fatsat pre contrast	Sagittal	3.91	1.23 and 2.46	---	1	160	100%	80	1.3	9	0	128*128	1180	23s each measurement	---	CAIPIRINHA	2	5 measurements Slice oversampling: 100% PE: P>>A DIXON method
T1 vibe Dixon fatsat caipirinha first 2 min (isotropic)	Sagittal	3.91	1.23 and 2.46	---	1	160	100%	80	1.3	9	0	128*128	1180	23s each measurement	---	CAIPIRINHA	2	5 measurements Slice oversampling: 100% PE: P>>A DIXON method
T1 TSE FS post - Gd	Sagittal	500	9	---	2	160	100%	32	3	150	0.3	280*400	227	2min51 s	3	SMS	2	PE: H>>F Fat suppression Oversampling: 70%
T1 TSE FS post - Gd	Axial	752	8.9	---	2	160	100%	40	3	150	0.3	280*400	228	2min35 s	3	SMS	2	PE: R>>L Fat suppression Oversampling: 5%

Paper 4 - Can CEUS or FLAIR-FS MRI replace Contrast-enhanced MRI for the detection and grading of synovitis in juvenile idiopathic arthritis of the knee? A diagnostic accuracy study

Costa Dias S, Ferreira CC, Santos I, Castro M, Rodrigues M, Aguiar F, Dias CC, Silva V, Ramos I, Ključevšek D, Rosendahl K, Brito I.

Submitted Arthritis Research & Therapy.

Can CEUS or FLAIR-FS MRI replace Contrast-enhanced MRI for the detection and grading of synovitis in juvenile idiopathic arthritis of the knee? A diagnostic accuracy study

Running title: CEUS and FLAIR-FS vs CEMRI in knee JIA

Authors

Sílvia Costa Dias[1,2], Catarina Costa Ferreira[2], Inês Santos[3], Miguel Castro[2], Mariana Rodrigues[1,2,4], Francisca Aguiar[4], Cláudia Camila Dias[5,6], Vítor Silva[2], Isabel Ramos[1], Damjana Ključevšek[7], Karen Rosendahl[8,9], Iva Brito[1,4].

Corresponding Author

Sílvia Costa Dias, MD, EDiPR

[1] Medicine Department, Faculty of Medicine of the University of Porto (FMUP), Porto, Portugal

[2] Radiology Department, University Hospital Center of São João Porto (CHUSJ), Portugal

ORCID ID: 0000-0003-0862-6967

Email: silvia.dias@ulssjoao.min-saude.pt/silviacostadias@hotmail.com

Address: Rua Doutor Melo Leote nº 154, 4100-341 Porto, Portugal

Affiliations

[1] Medicine Department, Faculty of Medicine of the University of Porto (FMUP), Porto, Portugal

[2] Radiology Department, University Hospital Center of São João Porto (CHUSJ), Portugal

[3] Rheumatology Unit, Unidade Local Saúde Viseu Dão-Lafões, Portugal

[4] Paediatric and Young Adult Rheumatology Unit, University Hospital Center of São João (CHUSJ), Porto, Portugal

[5] Knowledge Management Unit, Faculty of Medicine of the University of Porto (FMUP), Porto, Portugal

[6] CINTESIS@RISE, Department of Community Medicine, Information and Health Decision Sciences (MEDCIDS), Faculty of Medicine of the University of Porto (FMUP), Porto, Portugal

[7] Radiology Department, University Children's Hospital Ljubljana, Slovenia

[8] Clinical Medicine Department, Faculty of Health Sciences, UiT the Arctic University of Norway, Tromsø, Norway

[9] Section of Paediatric Radiology, University Hospital of North Norway, Tromsø, Norway

Author Emails

Sílvia Costa Dias: silvia.dias@ulssjoao.min-saude.pt/silviacostadias@hotmail.com

Catarina Costa Ferreira: catarinafcferreira21@gmail.com

Inês Santos: inescnsantos@gmail.com

Miguel Castro: miguelhcastro@gmail.com

Mariana Rodrigues: mariana.j.rodrigues@gmail.com

Francisca Aguiar: francisca.aguiar@ulssjoao.min-saude.pt

Cláudia Camila Dias: camila@med.up.pt

Vítor Silva: vitorsoft@gmail.com

Isabel Ramos: radiologia.hsj@gmail.com

Damjana Ključevšek: damjana.kljucevsek@gmail.com

Karen Rosendahl: karen.rosendahl@unn.no

Iva Brito: ivaobrito@hotmail.com

Authors' Contributions

S.C.D.: Conception; Design of the work; Acquisition; Data Collection; General Analysis; Statistical Analysis; Interpretation of Data; Writing and Revision of the Manuscript; approved the submitted version.

C.C.F.: Conception; Design of the work; Acquisition; Data Collection; Interpretation of Data; Revision of the Manuscript; approved the submitted version.

I.S.: Data Collection; Interpretation of data; Revision of the Manuscript; approved the submitted version.

M.C.: Conception; Design of the work; Interpretation of Data; Revision of the Manuscript; approved the submitted version.

M.R.: Data Collection; Interpretation of data; Revision of the Manuscript; approved the submitted version.

F.A.: Data Collection; Interpretation of data; Revision of the Manuscript; approved the submitted version.

C.C.D.: Design of the work; Statistical Analysis; Interpretation of Data; Revision of the Manuscript; approved the submitted version.

V.S.: Design of the work; Data Collection; Revision of the Manuscript; approved the submitted version.

I.R.: Conception; Design of the work; Interpretation of Data; Revision of the Manuscript; approved the submitted version.

D.K.: Conception; Design of the work; General Analysis; Interpretation of Data; Revision of the Manuscript; approved the submitted version.

K.R.: Conception; Design of the work; General Analysis; Statistical Analysis; Interpretation of Data; Writing and Revision of the Manuscript; approved the submitted version.

I.B.: Data Collection; Design of the work; General Analysis; Interpretation of data; Revision of the Manuscript; approved the submitted version.

Competing Interests and Funding

The authors declare no financial support, funding, or other benefits from commercial sources for the work reported in this manuscript, nor any other financial interests or competing interests that could create a potential conflict of interest with regard to this work.

Ethics Approval and Consent to Participate

This study was approved by the Regional Ethics Committee (approval number 282-20). Written informed consent was obtained from all participants and/or their caregivers.

Consent for Publication

Not applicable.

Data Availability Statement

The datasets generated and/or analysed during the current study are not publicly available due to patient confidentiality and ethical restrictions, but could be available from the corresponding author upon request, subject to ethical and institutional approval.

Acknowledgements

The authors express their sincere gratitude to all the patients and their parents/caregivers for their time, trust, and active cooperation, which made this study possible.
We would also like to express our appreciation to the contribution of the Radiographer Bac Nguyen, from the Division of Radiology and Nuclear Medicine, Oslo University Hospital, Rikshospitalet, Oslo, Norway.

Funding Declaration and Competing Interest Declaration:

The authors declare no financial support, funding, or other benefits from commercial sources for the work reported in this manuscript, nor any other financial interests or competing interests that could create a potential conflict of interest with regard to this work.

Ethics Approval and Consent to Participate:

This study was approved by the Regional Ethics Committee (approval number 282-20). Written informed consent was obtained from all participants and/or their caregivers.

Consent for Publication

Not applicable.

Data Availability Declaration:

The datasets generated and/or analysed during the current study are not publicly available due to patient confidentiality and ethical restrictions but could be available from the corresponding author upon request, subject to ethical and institutional approval.

Abstract:

Objectives: To evaluate the diagnostic accuracy of contrast-enhanced ultrasound (CEUS) and a contrast-free MRI sequence (FLAIR-FS) in detecting and grading synovial inflammation in children with juvenile idiopathic arthritis (JIA) compared to the current standard used in routine clinical practice – contrast-enhanced MRI (CEMRI).

Methods: Patients with JIA and knee involvement underwent clinical and imaging (CEUS and CEMRI) assessment on the same day, blinded to each other. Inflammation was scored subjectively on a 0-3 scale and objectively using VueBox® for CEUS and the program Syngo.via® Tissue 4D application for CEMRI. To establish normal standards, healthy volunteers were invited for a contrast-free knee-MRI.

Results: Fifty-two patients, median age 12.5 years (8.9-15.6 years), and 51 healthy volunteers were included. Sensitivity of CEUS for detecting inflammation was almost perfect, at 97.6% (95% CI 87.4-99.9); however, specificity was moderate, 50% (95% CI 18.7-81.3). Corresponding figures for MRI FLAIR-FS were 92.9% (95% CI 80.5-98.5) and 60.0% (95% CI 26.9-87.8), respectively. Doppler and clinical grading performed poorly.

ROC analysis demonstrated that CEUS and FLAIR-FS had good discriminative performance between non-inflamed and inflamed joints, with AUC-values of 0.899 (95% CI 0.809-0.989) and 0.879 (95% CI 0.778-0.980), respectively. Clinical examination and color/power Doppler performed poorly, whilst micro-Doppler performed fairly. Dynamic CEUS and CEMRI-markers helped discriminate between subjective inflammation grades, particularly between mild and no inflammation.

Conclusions: CEUS and FLAIR-FS (contrast-free MRI sequence) provide accurate detection and grading of knee joint inflammation in children with JIA, with the potential to replace the current standard of CEMRI.

Keywords: Synovitis; Juvenile Idiopathic Arthritis; Knee; Contrast-Enhanced Ultrasound; FLAIR-FS; Micro-Doppler; MRI

Introduction

Juvenile idiopathic arthritis (JIA) is a chronic rheumatic disease of unknown origin, with an onset before the age of 16 and a reported incidence from 1.6–23 per 100 000 children across Europe [1]. In patients with JIA, the knee joint is involved in the majority of patients, followed by the ankle, elbow and wrist [2]. On imaging, active JIA is characterized by synovial inflammation, bone marrow and soft tissue edema and joint effusion, subsequently followed by destructive changes of cartilage and bone [3, 4].

The diagnosis of JIA is one of exclusion, currently based on the ILAR-criteria [5], whilst laboratory data and imaging findings are mostly supportive. Ultrasound with Doppler (US-Doppler) is the initial modality of choice for detection of inflammatory change, followed by contrast-enhanced, magnetic resonance imaging (CEMRI) in cases of equivocal findings [6]. Studies have shown that subclinical synovitis as detected on CEMRI, might play a role in predicting disease relapse/flair [7, 8] and that quantitative CEMRI, using descriptive parameters, might help define disease activity [9, 10]. Despite being a validated method for both detection and grading of inflammatory change, MRI is limited by its need for sedation in younger children, the use of gadolinium with its potential side-effects, but also by costs and limited availability [11]. This has fueled a search for alternative methods, such as contrast-free MRI sequences and contrast-enhanced ultrasound (CEUS) [12-17]. We recently demonstrated that CEUS and CEMRI are precise and reproducible methods for subjective grading of synovial inflammation on a 0-3 scale, and that dynamic CEUS as measured by the peak enhancement (PE) in terms of precision performs poorly because of the very wide scale used [18].

The aims of our study were to evaluate the diagnostic accuracy of CEUS and a contrast-free MRI sequence – fluid-attenuated inversion recovery with fat suppression (FLAIR-FS), in detecting and grading synovial inflammation in children with JIA compared to the

current recommended standard used in routine clinical practice (CEMRI). Moreover, to examine the agreement between CEUS / FLAIR-FS and CEMRI, and a potential added value of dynamic acquisitions.

Methods

Study design and participants

Single-center, prospective cross-sectional diagnostic accuracy study, approved by the Regional Ethics Committee (n 282-20) and conducted in accordance with the Declaration of Helsinki. Written informed consent was obtained from all participants and/or their caregivers. All patients with JIA (according to the ILAR criteria [5]) aged 1-18 years followed in the Pediatric and Young Adult Rheumatology Unit, São João University Hospital, Porto (CHUSJ) during February to October 2024 were invited, of whom those with current or previous involvement of a knee joint were included. Children with a history of intra-articular steroid injection or trauma within the last two months, or with known contraindications to MRI and/or the contrast media used, were excluded. All had a clinical examination, laboratory tests and imaging (US, MRI) performed on the same visit.

To establish normal appearances of the knee joint on a FLAIR-FS sequence, volunteers aged 4-18 years, residing in the same area were invited to undergo an MRI without intravenous contrast, including a FLAIR-FS sequence. Recruitment was conducted via e-mails and direct invitations, and an informal stratification technique was employed to ensure an age-and-sex balanced cohort. Excluded were individuals with chronic disease potentially affecting the skeletal system, or knee trauma within the previous two months.

Clinical and laboratory assessment

Age at diagnosis, duration of the disease, JIA subtype, duration of remission (if applicable) and use of medication was registered. All had a clinical examination by one of three pediatric rheumatologists (7 to 30 years of experience), classifying the knee joint into inactive (grade 0), equivocal (grade 1) or active arthritis (grade 2). Disease activity was assessed using the Childhood Health Assessment Questionnaire (CHAQ) [19, 20], patient and Physician Visual Analog Scale (VAS) and Juvenile Arthritis Disease Activity Score (JADAS-27) [21-23]. Erythrocyte sedimentation rate (ESR); c-reactive protein (CRP); anti-citrullinated protein antibodies (ACPA); rheumatoid factor (RF); anti-nuclear antibody (ANA) and human leukocyte antigen B27 (HLA-B27) was noted. The imaging team was blinded to the clinical data.

Ultrasound assessment

The US examinations were performed with the patient supine, knee 30° flexed, by one radiologist with 12 years of experience in pediatric radiology, using a Logiq E10 machine (Version R3, General Electric) and a linear 6-15 MHz transducer, according to a previously published protocol [24]. For the present study, sagittal scans of three different locations (supra-, para- and infrapatellar) were used, and the location showing most pathology was chosen for CEUS (vascular, linear 2-10 MHz transducer). Via a 3-way intravenous cannula adapted to a catheter, a bolus of Sulfur Hexafluoride (Sonovue®) contrast was injected (2.4 mL patients <50 kg and 4.8 mL >50 kg), followed by 10 mL saline chaser. A 2-minute continuous, sagittal acquisition was performed. The same location later was used for CEMRI assessment.

Subjective assessment – Color /Power/ Micro-Doppler and CEUS

Color Doppler (CD), Power Doppler (PD) and Micro-Doppler (MD) activity was assessed in each of three locations (supra, para- and infrapatellar), and graded as no inflammation (grade 0; no signal), mild inflammation (grade 1; up to 3 single Doppler spots or up to 1 confluent spot and 2 single spots or up to 2 confluent spots), moderate inflammation (grade 2; > grade 1 in < 30% of the area of synovial hypertrophy) or severe inflammation (grade 3; confluent signals present in > 30% of the area of synovial hypertrophy) [25]. A score ≥1 in at least one of the three different locations was considered a positive examination. All CEUS video clips (0-120 s) were anonymized (Supplemental Material Movie M1), archived and reviewed retrospectively. A recent reliability study demonstrated high precision and reproducibility for grading contrast enhancement on a 0-3 scale, as 0 (a few contrast bubbles allowed within the synovium); 1 (mild synovial enhancement) (Fig. 1); 2 (moderate synovial enhancement) or 3 (severe synovial enhancement) (Fig. 2) [18].

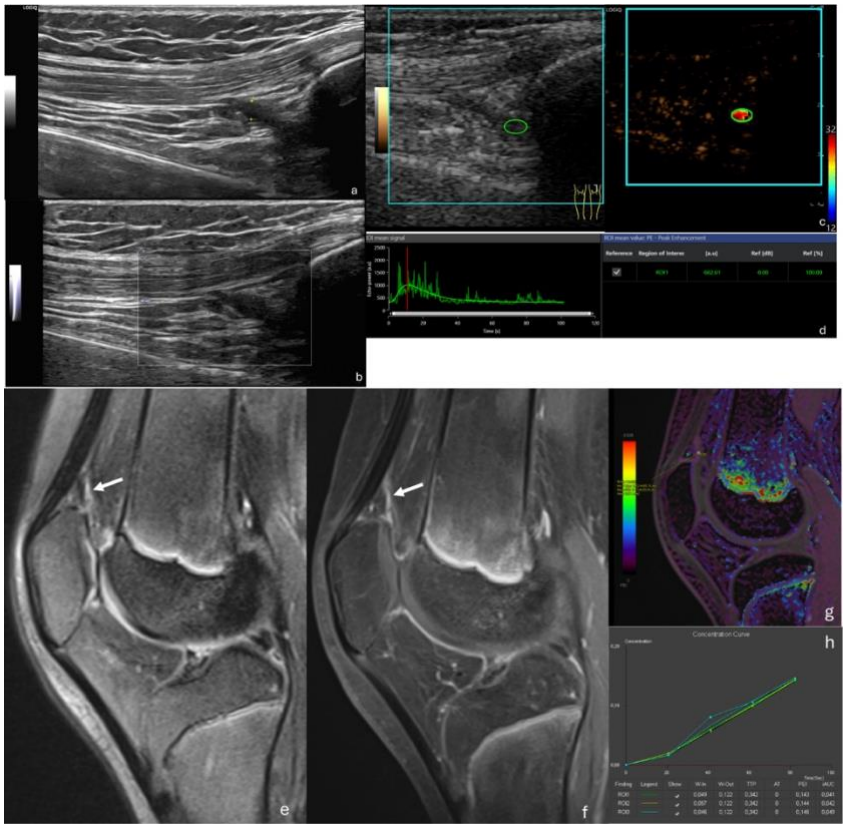


Figure 1. Multimodality imaging of mild knee synovitis (Grade 1) in JIA

Fig. 1. Left knee in a 13-year-old girl with JIA- Mild Case (Grade 1): a. B-mode, sagittal view through the mid suprapatellar recess with synovium between callipers; **b.** Micro-Doppler showing no vascularity within the synovium. **c.** CEUS, dual-screen mode with simultaneous display of gray-scale image (left) and contrast-only image (right) in the same view, showing a mildly enhancing synovium (Grade 1) in the suprapatellar recess with a region of interest (ROI) placed within (software VueBox); **d.** corresponding Time-intensity curve of the synovial enhancement during the first 120 seconds with a Peak Enhancement (PE) of 682.61 (within the interval values for Grade 1). **e.** FLAIR-FS sagittal showing mild synovitis (arrow) in the same plane as CEUS –; **f.** T1-weighted FS sagittal after contrast administration confirming mild synovitis (arrow) in the same plane as FLAIR-FS and CEUS; **g.** Syngo.via® colour Peak Enhancement Intensity (PEI) map with a region of interest (ROI) placed within the enhancing synovium, in the same plane; **h.** Shows three dynamic enhancement curves (0-100 seconds), representing perfusion in 3 different ROIs; Concentration Curves display the concentration of the Contrast Agent in the y-axis along time in the x-axis, and a corresponding Peak Enhancement Intensity of 0.144 (within the interval values for Grade 1).

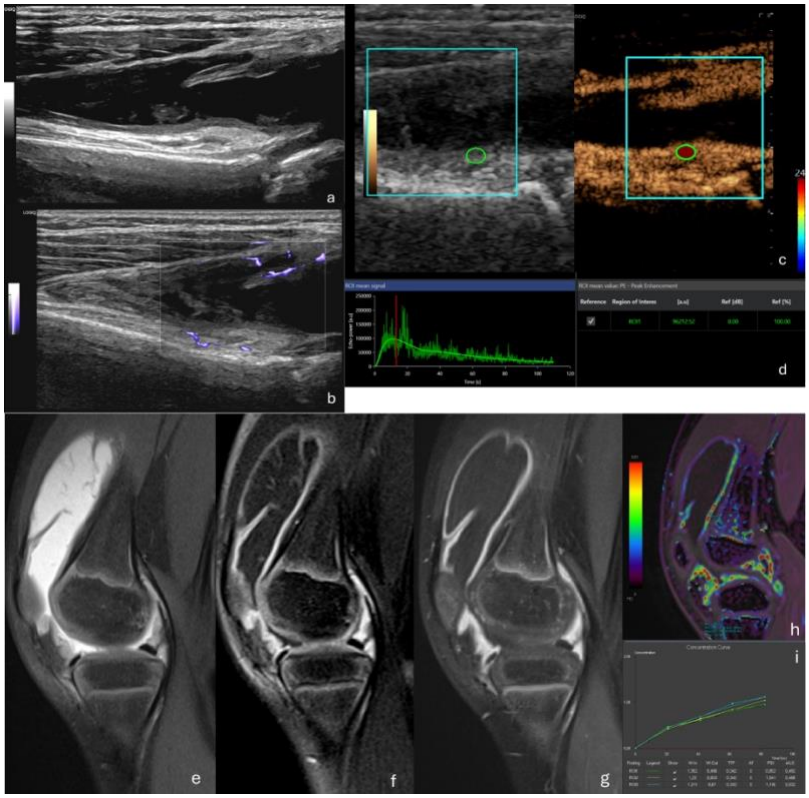


Figure 2. Multimodality imaging of severe knee synovitis (Grade 3) in JIA

Fig. 2. Right knee in a 5-year-old girl with JIA- Severe Case (Grade 3): a. B-mode, sagittal view through the mid suprapatellar recess revealing a large joint effusion and thickened synovium **b.** Micro-Doppler showing increased vascularity within the synovium. **c.** CEUS, dual-screen mode with simultaneous display of gray-scale image (left) and contrast-only image (right) in the same view, showing vividly enhancing synovium, in keeping with synovitis (Grade 3) with a region of interest (ROI) placed within (software VueBox); **d.** corresponding Time-intensity curve of the synovial enhancement during the first 120 seconds with a Peak Enhancement (PE) of 96212.52 (within the interval values for Grade 3). **e.** PD-FS sagittal confirming a severe joint effusion (*) and thickened synovium (arrow); **f.** FLAIR-FS sagittal showing synovitis (arrow) in the same plane as CEUS; **g.** T1-weighted FS sagittal after contrast administration confirming severe synovitis (arrow) in the same plane as FLAIR-FS and CEUS; **h.** Syngo.via® colour Peak Enhancement Intensity (PEI) map with a region of interest (ROI) placed within the enhancing synovium, in the same place; **i.** Shows

three dynamic enhancement curves (0-100 seconds), representing perfusion in 3 different ROIs; Concentration Curves display the concentration of the Contrast Agent in the y axis along time in the x axis, and a corresponding Peak Enhancement Intensity of 1.166 (within the interval values for Grade 3).

Dynamic quantitative assessment - CEUS

The DICOM video clip was post-processed using the software VueBox® (version 7.5; Bracco Imaging, Milan, Italy). From a sagittal frame selected in consensus by two observers, guided by the color intensity map, the most avidly enhancing area of the synovium was located. Peak Enhancement (PE), Time To Peak (TTP) and Wash-in Area Under the Curve (WiAUC) were measured in three different regions of interest (ROI) by two observers, blinded to each other, with a predefined standardized ROI. The mean of three measurements was used for analysis.

MRI acquisition and assessment

All patients and healthy volunteers had a 3T MRI of one knee (Siemens Magnetom Vida Erlangen, Germany), performed by one specially trained radiographer according to standardised protocols for patients (with Gadolinum (Gd) contrast) and for healthy volunteers (without Gd contrast). A cushion (Multipad, Pearl Technology) was used to immobilize the knee in approximatly 30° flexion. The protocols are detailed in Table Supplemental T.S1. In brief, the patient protocol included the following sequences: T1-weighted images (T1-w); T1-w fat-suppressed (fs) pre- and post-intravenous contrast administration (Gd), Proton Density-weighted with fat suppression (Pd-fs), a RESOLVE Diffusion-weighted, T2-weighted FLAIR-FS, and a dynamic 3D T1-w fs. The Gd contrast (Gadobutrol - Gadovist®, Bayer) was administered via infusion pump (0.1 mmol per kilo of body weight), at a rate of 1-3 mL per second, according to the size (gauge) of

the needle. The protocol used for the healthy volunteers was shorter, including T2-weighted FLAIR-FS, Pd-fs and diffusion-weighted sequences Table Supplemental T.S1.

Subjective scoring – CEMRI and FLAIR-FS

The overall degree of inflammation was scored on a 0-3 scale (image atlas; Supplemental Material Fig. 1.S), separately (and blinded to each other), as 0 (no inflammation), 1 (mild inflammation) (Fig. 1), 2 (moderate inflammation) or 3 (severe inflammation) (Fig. 2), with a repeat reading after six weeks, independently, by two observers. FLAIR-FS images from controls were scored in a third session.

Dynamic semi-quantitative assessment – CEMRI

MRI measurements were performed on a Syngo.via® Tissue 4D application, using a sagittal, dynamic 3D T1-w fs post-contrast image, considered a priori by both observers to represent the best fit as compared to the sagittal scan used for CEUS. Three ROIs ($1mm^2$, smallest possible standard deviation (SD)) were selected from the color intensity map, and the mean of three measurements was used for further analysis of Peak Enhancement Intensity (PEI); TTP and initial Area Under the Curve (iAUC).

Statistical analysis

Continuous data are presented as median and interquartile ranges (IQR), whereas categorical data are presented as frequency counts and percentages. The diagnostic performance of CEUS, contrast-free MRI sequence (FLAIR-FS) and clinical examination for diagnosing and grading inflammation was determined using sensitivity, specificity, and accuracy with corresponding 95% confidence intervals (CIs).

Receiver operating characteristic (ROC) analysis (binary) was used to assess the discriminative ability of US-Doppler (CD/PD and MD), CEUS and a contrast-free MRI

sequence (FLAIR-FS), and the discriminative ability of PE/PEI, WiAUC/iAUC and TTP for both techniques, between patients with and without inflammatory change on CEMRI. The area under the ROC curve (AUC) and its 95% CIs were calculated (AUC 0.6-0.7=poor; 0.7-0.8 fair; 0.8-0.9 good; 0.9-1.0 excellent [26]). The optimal cut-off value was determined by the clinical context.

Statistical power was calculated retrospectively for each AUC, considering the sample size (10 negative cases and 42 positive cases) at a significance level of 5%. Statistical power for detecting inflammation was calculated retrospectively, ranging from 0.15 for clinical grade, 0.29 for color/power Doppler, 0.74 for Micro-Doppler, and 0.99 for both CEUS and FLAIR-FS.

Spearman's correlation coefficient was used to examine the strength and direction between PE and PEI (Spearman's rho 0.00–0.10 (negligible), 0.10–0.39 (weak), 0.40–0.69 (moderate), 0.70–0.89 (strong), 0.90–1.0 (very strong)) [27].

Kappa (κ) (linear weighted) coefficients (with 95% CI) and proportion of absolute agreement were applied to test the agreement between CEUS, FLAIR-FS and CEMRI (κ-coefficient < 0=poor; 0-0.20 slight; 0.21–0.40 fair; 0.41–0.60 moderate; 0.61–0.80 substantial; 0.81–1.00 almost perfect [28]).

Independent samples Kruskal-Wallis tests were used to test for differences in PE and PEI according to CEMRI grade (0-3), and for differences in inflammation scores as obtained by CEUS, FLAIR-FS and CEMRI for each of three different locations (suprapatellar/para-patellar/infra-patellar). Post-hoc pairwise comparisons (with Bonferroni corrections) were performed.

The level of statistical significance was set at ≤ 0.05. Statistical analysis was performed using IBM Statistical Package for the Social Sciences (SPSS®) version 30, Jamovi version 2.6.26 (computer software) or Rstudio version 2026.01.1+403.

Results

Fifty-two patients (Fig 3), median age 12.5 years (8.9-15.6 years) and 51 healthy volunteers were included.

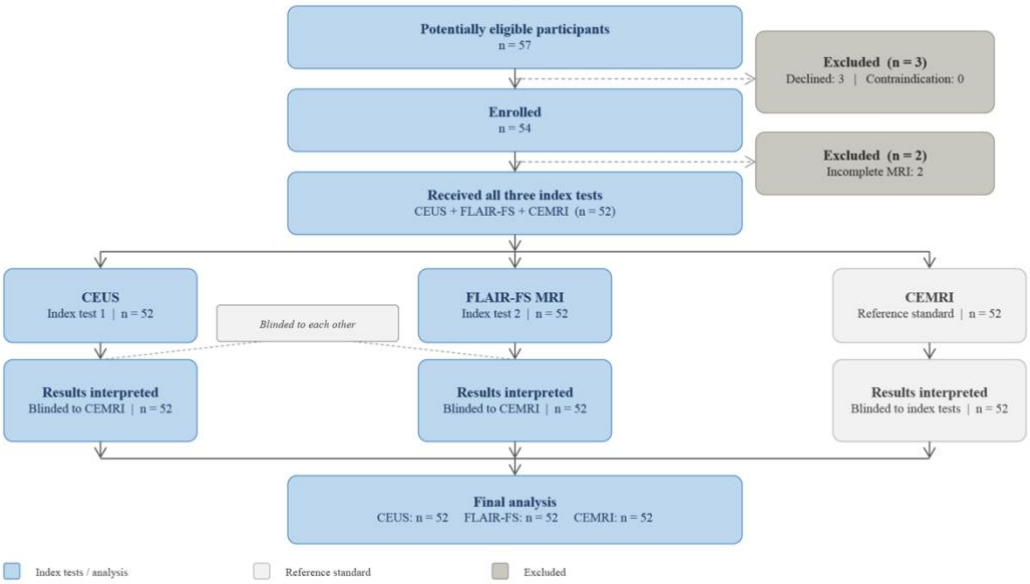


Figure 3. Diagnostic flow diagram

Fig. 3. Flow diagram illustrating participant enrolment, allocation, and analysis.

There were no significant differences in clinical characteristics between patients and healthy volunteers (Table 1).

Table 1. Demographic and clinical characteristics of 52 patients with JIA and 51 healthy volunteers.

		Patients	Healthy volunteers	p-value[a,b]
n (%)		52 (100.0)	51 (100.0)	
Sex Female, n (%)		35 (67.4)	34 (66.7)	0.945[a]
Age years, Mdn (IQR)		12.4 (8.9 – 15.6)	13.3 (9.3 – 15.5)	0.678[b]
Height cm, Mdn (IQR)		149.0 (129.0–161.0)	1.6 (1.3 – 1.6)	0.952 [b]
Weight kg, Mdn (IQR)		39.7 (26.1 – 56.6)	45.5 (3.6 – 57.2)	0.549 [b]
BMI*, Mdn (IQR)		18.3 (16.1 – 21.8)	18.7 (16.6 – 20.3)	0.545 [b]
JIA Subtypes, n (%)		52 (100)		
Systemic		2 (3.8)		
Oligoarthritis	Persistent	30 (57.7)		
Oligoarthritis	Extended	5 (9.6)		
Polyarthritis	RF negative	6 (11.5)		
Polyarthritis	RF positive	1 (1.9)		
Psoriatic	Arthritis	4 (7.7)		
Enthesitis-related arthritis		4 (7.7)		
Age at JIA diagnosis years, Mdn (IQR)		5.0 (2.0 – 8.0)		
Duration JIA's Disease years, Mdn (IQR)		6.0 (3.3 – 9.0)		
Remission at Study Date, n (%)		43 (82.7%)		
Remission JIA's Disease years, Mdn (IQR)		2.9 (0.5 – 4.3)		
Right Knee studied, n (%)		28 (53.8)		
CHAQ**, Mdn (IQR)		0 (0.0 – 0.3)		
JIA Activity Score (JADAS-27), Mdn (IQR)		1 (0.0 – 4.4)		
Erythrocyte Sedimentation Rate, mm/h, Mdn (IQR)		10 (6.0 – 16.0)		
C-Reactive Protein, mg/dL, Mdn (IQR)		0.95 (0.4 – 2.1)		
Anti-citrullinated protein antibodies- n positive/n total		0/50		
Rheumatoid Factor - n positive/n total		1/51		
Anti-nuclear Antibody - n positive/n total		43/51		
Human Leukocyte Antigen B27 - n positive/n total		3/47		

Mdn=Median; IQR=Interquartile Range *=Body Mass Index;**Childhood Health Assessment Questionnaire

[a]Pearson's Chi-square [b]Mann-Whitney Test.

Among patients, based on the reference standard (CEMRI), 10/52 (19.2%) knee joints were considered non-inflamed, 18 (34.6%) were mildly inflamed, 16 (30.8%) were moderately inflamed and 8 (15.4%) were severely inflamed. The diagnostic performance of CEUS, MRI-FLAIR-FS and clinical examination for detecting inflammation compared to the reference standard, is detailed in Table 2. For this analysis, 3 knee joints with equivocal findings on clinical examination were considered pathological.

Table 2. Diagnostic performance of CEUS, MRI FLAIR-FS, Doppler and clinical examination for knee synovitis detection

	TP	**TN**	**FP**	**FN**	**Sensitivity (95% CI)**	**Specificity (95% CI)**	**Accuracy (95% CI)**
Contrast-enhanced US	41	5	5	1	97.6% (87.4-99.9)	50.0% (18.7-81.3)	88.5% (76.6-95.7)
US with CD/PD	12	10	0	30	28.6% (15.7-44.6)	100.0% (69.2-100.0)	42.3% (28.7-56.8)
US with MD	21	10	0	21	50.0% (34.2-65.8)	100.0% (69.2-100.0)	59.6% (45.1-73.0)
MRI FLAIR-FS	39	6	4	3	92.9% (80.5-98.5)	60.0% (26.2-87.8)	86.5% (74.2-94.4)
Clinical Grade	11	9	1	31	26.2% (13.9-42.0)	90.0% (55.5-99.8)	38.5% (25.3-53.0)

52 joints in 52 patients. CEUS and Doppler grades based on worst of three locations (supra-, para-, infrapatellar); FLAIR-FS based on the whole knee, all graded on a 0–3 scale. Reference standard: CEMRI (based on the whole knee). Clinical examination on a 0–1 scale (grades 1 and 2 merged).

TP true-positive, TN true-negative, FP false-positive, FN false-negative, CI confidence interval; *CD/PD Color/Power Doppler; MD Micro-Doppler; FLAIR-FS Fluid attenuated inversion recovery with fat suppression.*

Sensitivity of CEUS for detecting inflammation was almost perfect, at 97.6% (95% CI 87.4-99.9), however, specificity was only moderate, 50% (95% CI 18.7-81.3). The five false positives were all scored as mild inflammation in CEUS and the false negative was a mild case in CEMRI. Adding dynamic CEUS-marker would have correctly re-classified 2 of the false positives and the false negative.

The CEUS-score was based on the suprapatellar view in 46/52 (88.5%) of the knees (29/52 - 55.8% middle view; 10/52 - 19.2% lateral view; 7/52 – 13.5% medial view); parapatellar view in 3/52 (5.8%) knees (2/52 – 3.8% lateral view; 1/52 – 1.9% medial view) and on the infrapatellar view (deep infrapatellar bursitis) in 3/52 (5.8%) of the knees.

There was a significant difference in the severity of inflammation among the three locations (CEUS p=0.010; FLAIR-FS p=0.026 and CEMRI p=0.034). Higher severity scores were seen in the parapatellar and infrapatellar (Fig. 4) locations as compared to the suprapatellar location for all three imaging techniques, post hoc tests reaching statistical significance for CEUS between the supra and infrapatellar locations (p=0.043, with Bonferroni correction).

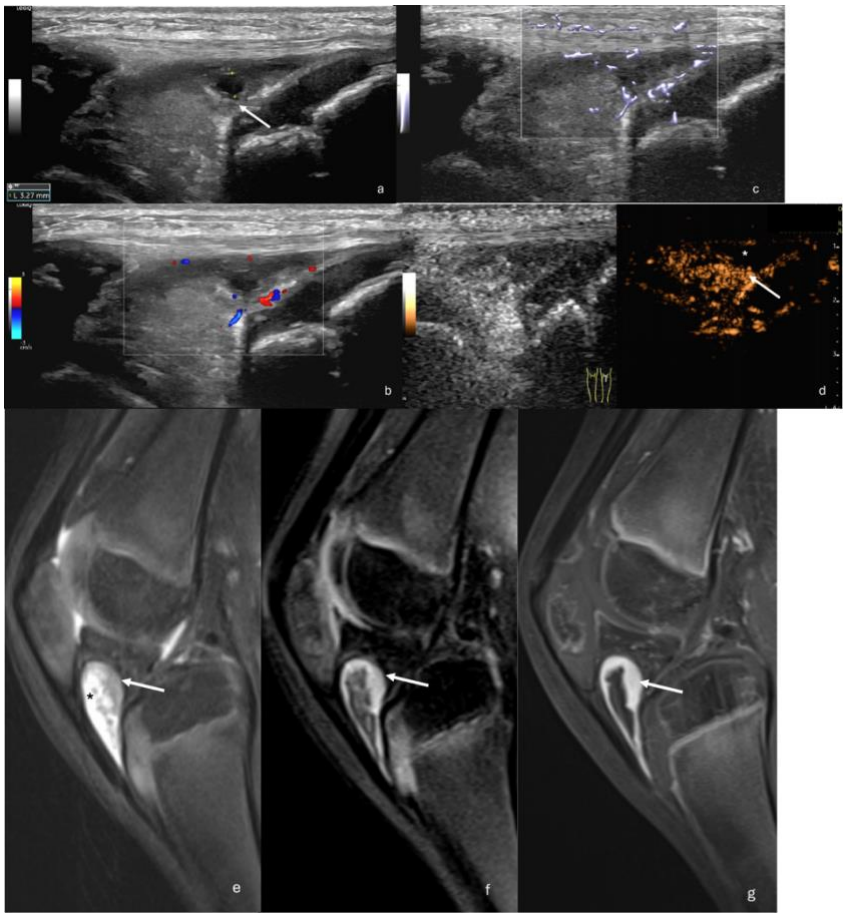


Figure 4. Multimodality imaging of deep infrapatellar bursitis in JIA

Fig. 4. – Left knee in a 6-year-old boy with JIA: a. B-mode, sagittal view through the infrapatellar recess, showing deep infra-patellar bursitis, with fluid between callipers, with severe synovial thickening (arrow) and hyperechogenicity/inflammatory change of the Hoffa fat pad (arrowhead); **b**. Colour Doppler with hyperaemia; more expressive in **c.** with Micro Doppler mode. **d.** CEUS, dual-screen mode with simultaneous display of gray-scale image (left) and contrast-only image (right) in the same view, showing heavily enhancing synovium within the deep infra-patellar bursitis, delineating more clearly the synovitis (arrow) from the non-enhancing fluid (*).**e.** PD-FS sagittal confirming the deep infra-patellar bursitis, with fluid (*) and thickened synovium within the bursa (arrow); **f.** FLAIR-FS sagittal showing the synovitis within the bursa (arrow) in the same plane as CEUS; **g.** T1-weighted FS sagittal after contrast administration confirming the synovitis within the bursa (arrow) in the same plane as FLAIR-FS and CEUS.

The sensitivity of FLAIR-FS for detecting inflammation was 92.9% (95% CI 80.5-98.5) with a specificity of 60.0% (95% CI 26.9-87.8) (Table 2). The four false positives were all scored as mild inflammation in FLAIR-FS and the three false negatives were score as mild in CEMRI. Adding the result of a dynamic CEMRI-marker (PEI) would have re-classified 3 of the false positives and all three false negatives correctly.

Discriminative performance of different markers

ROC analysis indicated strong discriminative ability for both CEUS and FLAIR-FS, with AUC-values of 0.899 (95% CI 0.809-0.989) and 0.879 (95% CI 0.778-0.980), respectively, whilst clinical examination performed poorly (AUC 0.592 (95% CI 0.414-0.769) (Fig. 5). Although Youden's index indicated optimal statistical cut-offs, sensitivity and specificity at clinically meaningful thresholds were 0.976/0.500 for CEUS, and 0.929/0.400, respectively, for FLAIR-FS. For micro and color/power Doppler, ROC analysis indicated fair and poor discriminative ability, respectively, with AUC values of 0.750 for Micro-Doppler (Fig. 6) and 0.643 for color/power Doppler.

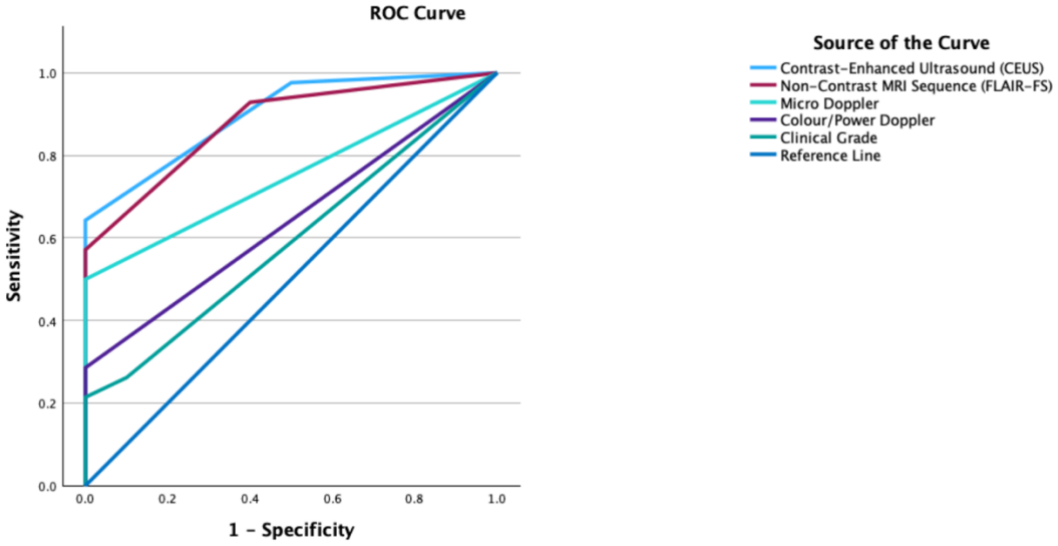


Figure 5. ROC Curves for Imaging Techniques in JIA

Fig. 5. ROC (Receiver Operating Characteristics) curve illustrating discriminative performance for different imaging techniques in a cohort of 52 patients with JIA.

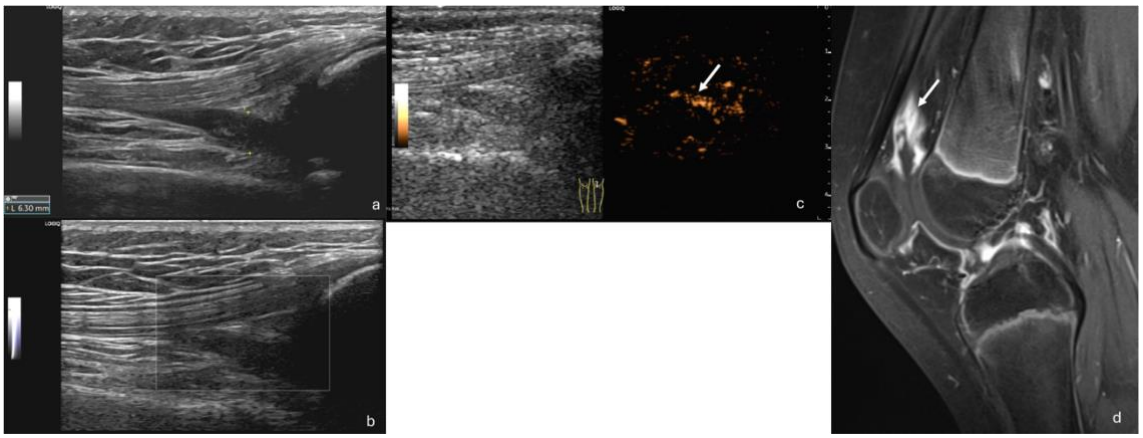


Figure 6. Multimodality imaging of a false negative Micro-Doppler knee case in JIA

Fig. 6. Left knee in a 9-year-old girl with JIA: a. B-mode, sagittal view through the mid suprapatellar recess revealing thickened synovium (between callipers); **b.** Micro Doppler negative, without signal in the synovium. **c.** CEUS, dual-screen mode with simultaneous display of gray-scale image (left) and contrast-only image (right) in the same view, showing the moderate enhancing synovium, in keeping with synovitis; **d.** T1-weighted FS sagittal after contrast administration confirming the synovitis in the suprapatellar recess (arrow).

Intra- and interobserver agreement for scoring synovial inflammation on a 0-3 scale

Results for CEUS and CEMRI has been published elsewhere [18].

FLAIR-FS

Both intra- and interobserver agreement for assessing inflammation on a 0-3 scale was almost perfect with weighted-κ of 0.90 (95% CI 0.82-0.98) and 0.84 (95% CI 0.73 – 0.95), respectively for the two observers, and weighted-κ 0.81 (95% CI 0.70 – 0.93) between observers. Weighted-κ for scoring images from healthy volunteers was 1 (CI 95% 1-1) (50 cases showing score 0 and 1 case score 1).

Agreement between the reference standard (CEMRI) and alternative methods

Agreement between CEMRI and CEUS for grading inflammatory change on a 0-3 scale was good (weighted-κ 0.64 (95% CI 0.51-0.76); absolute agreement 59.6%). Disagreement never exceeded one grade (Supplemental Material Table T.S2).

Agreement between CEMRI and MRI FLAIR-FS for grading inflammatory change on a 0-3 scale was almost perfect (weighted-κ 0.85 (CI 95% 0.76-0.95); absolute agreement 0.85 (Supplemental Material Table T.S3).

Agreement between Clinical Grade (0-2) and CEMRI on a 0-2 scale (merging grades 2 and 3) was only slight (weighted-κ 0.17 (CI 95% 0.04-0.31); absolute agreement 0.33 (Supplemental Material Table T.S4).

Dynamic markers

Peak Enhancement (PE) on CEUS and Peak Enhancement Intensity (PEI) on CEMRI

ROC analysis demonstrated that both PE and PEI discriminated well between non-inflamed and inflamed joints, with AUC-values of 0.812 (95% CI 0.682-0.941) and 0.844 (95% CI 0.734-0.954) respectively (Supplemental Material Fig. 2aS.).

Although Youden's index indicated optimal statistical cut-offs, sensitivity and specificity at clinically meaningful thresholds were set at 81%/60% for both PE and PEI (cutoff value for PE was 406.558 arbitrary units and for PEI 0.075 arbitrary units). There was a strong positive correlation between PE and PEI, with a Spearman's rho of 0.803 with $p < 0.001$ (95% CI 0.674 – 0.884).

Wash-in Area Under the Curve (WiAUC) on CEUS and initial Area Under the Curve (iAUC) on CEMRI

WiAUC and iAUC discriminated well between non-inflamed and inflamed joints, with AUC-values of 0.836 (95% CI 0.715-0.956) and 0.830 (95% CI 0.713-0.947), respectively (Supplemental Material Fig. 2bS).Sensitivity and specificity at clinically meaningful thresholds were set at 91%/60% for WiAUC and 86%/60% for iAUC (cutoff value for for WiAUC 1671.438 arbitrary units and iAUC 0.026 arbitrary units).

Time To Peak (TTP) on CEUS and on CEMRI

The AUC-value for CEUS TTP was 0.56 (95% CI 0.327-0.792), with a sensitivity and specificity at 67%/60%, respectively (cutoff value of 9.572 seconds (s)). For CEMRI, the TTP had an AUC-value under 0.5.

There was a statistically significant difference in median PE for CEUS across four different scores ($p<0.001$) (Supplemental Material Table T.S5). Significant differences were seen between scores, except for score 0 and 1 ($p=0.365$), score 1 and 2 ($p=0.311$) and score 2 and 3 ($p=0.059$) (adjusted with Bonferroni corrections).

Similar, there was a statistically significant difference in median PEI for CEMRI across the four different scores ($p<0.001$) (Supplemental Material Table T.S6). Significant differences were seen between groups, except for group 0 and 1 ($p=1.000$) and group 2 and 3 ($p=0.230$) (adjusted with Bonferroni corrections).

Discussion

This study revealed that, overall, both contrast-enhanced ultrasound and the contrast-free MRI sequence FLAIR-FS, demonstrated high diagnostic accuracy in the detection of inflammatory change of the knee in children with JIA, using CEMRI as the reference standard. Both FLAIR-FS and CEUS had a high sensitivity in identifying inflammation, whilst US with doppler and clinical grade alone performed poorly, with low sensitivity, despite high specificity. Of note is the moderate specificity for both FLAIR-FS and CEUS.

MRI

Limited studies have assessed the role of contrast-free MRI sequences in detecting and grading inflammatory changes in JIA and report that both diffusion-weighted imaging [29], the Double Inversion Recovery (DIR) sequence and PD-weighted images [30] are promising techniques [14]. Moreover, that measurement of the synovial thickness, as a marker of synovitis, is reliable [15]. However, previous studies are small [14, 30, 31] using different MRI scanners [15, 31] without standardization of post-contrast image acquisition [14, 15, 29, 30], the latter being of significant importance for the assessment of synovial contrast enhancement and grading [32]. In the study by Barendregt et al., including 45 patients with a median age of 14 years, of whom 14 had arthritis according to the reference standard (CEMRI), diffusion-weighted imaging had 92% sensitivity and 78% specificity for detection of synovial inflammation [29]. However, although the observers could detect synovitis with relatively high accuracy, distinction between the synovial membrane and surrounding tissues remained challenging. Another study, addressing the FLAIR-FS sequence including 39 children, median age 12.9 years, of whom 48% had synovitis, the authors found sensitivities of 79% - 84% for the detection of synovitis, with specificities of 94% - 83% [31]. To our knowledge this was the first study to explore the FLAIR-FS sequence in children, however, the cohort was heterogenous, with only eight patients having JIA. As such, it should be interpreted with caution.

Two studies have examined the ability of contrast-free sequences for the assessment of synovial thickness, one by using a DIR sequence [14] and one by using a combination of T2-fs and 3D proton density (Pd)-weighted images [15], both with CEMRI as reference. In the study from Verkuil et al., including 26 children with JIA of whom 13 with knee arthritis, the authors concluded that the DIR sequence adequately delineated the synovial lining, and that synovial thickness measurement provided values that strongly correlated

with conventional CEMRI. The study was, however, limited by its small numbers and lack of standardization of post-contrast image acquisition. In the study using 3D PD- and T2-weighted images, including 35 children with JIA, median age 14 years, the authors reported that the unenhanced series was equivalent to CEMRI in assessment of synovial thickness. Although mean differences between two measurements were less than 0.2mm for all measured locations, the absolute agreement, given by 95% limits of agreement (LoA), was not reported. We have previously shown that, despite high correlation between two measurements, the 95% LoA might still be wide with poor precision in the semi-quantitative analysis [18].

In sum, contrast-free MRI sequences tend to overestimate synovial inflammation, rather than underestimate.

Neither over- nor underdiagnosis is ideal, as both carry distinct risks. In our study, the FLAIR-FS sequence demonstrated high diagnostic accuracy for inflammatory changes. The only errors were four mild false positives and three mild false negatives, highlighting the known difficulty in differentiating physiological from mildly increased synovial enhancement [33]. Adding PEI, the most robust dynamic CEMRI marker, corrected three false positives to negative and all three false negatives to positive, leaving only one false positive. Thus, dynamic post-contrast MRI helps resolve equivocal cases, despite its low measurement precision. Additionally, FLAIR-FS underestimated one case, grading it as moderate while CEMRI graded it as severe.

Two previous studies, one on knees and one on wrists, have concluded that DCE-MRI represent a promising method for the assessment of disease activity in JIA [8, 34], later supported by a study on the temporomandibular joints [35]. A recent review from 2025 does not elaborate on the helpfulness of dynamic-CEMRI [36], however in our study,

PEI-values, using a program in SyngoVia®, added to the discrimination of non-inflamed and mildly inflamed joints.

CEUS

The literature on contrast-enhanced ultrasound for the assessment of synovitis in children is even more limited. In 2001, Doria et al. explored the role of color Doppler CEUS in the evaluation of JIA in 22 patients with knee-JIA and five controls [12]. Based on clinical and laboratory data, the knees were classified as asymptomatic, subclinical or in remission. To quantitatively assess the degree of synovial enhancement, a region of interest over the suprapatellar bursa was delineated [12]. Then, the mean pixel intensity values of that particular area were recorded before and after contrast administration. In all three groups, CEUS revealed significant enhancement of knee joints compared to healthy controls. The authors concluded that CEUS was valuable in the early detection of synovial inflammation [12]. In a recent review, the CEUS technique has been thoroughly described [13], however, additional data to support its use in children with JIA is lacking.

Our study showed that CEUS offers high sensitivity and accuracy for grading synovial inflammation, but with a specificity, performing similarly to FLAIR-FS. Mirroring FLAIR-FS, all five false positives were mild, reflecting the continuous spectrum between physiological and mildly pathological synovial enhancement [33]. Applying the estimated PE cutoff re-classified two false positives as negative and the single false negative as positive. This leaves only three false positives, supporting PE use in equivocal cases despite poor quantitative precision [18].

Interestingly, the inflammation-score, on both CEUS, FLAIR-FS and CEMRI, was higher for the para- and infrapatellar recesses as compared to the suprapatellar recess,

underscoring the importance of evaluating all available locations during an ultrasound examination.

In sum, although both CEUS and the FLAIR-FS have high diagnostic accuracy in the detection of inflammatory change, we would argue that CEUS should be considered in children under the age of five, to reduce the use of sedation.

In contrast, US-Doppler performed poorly, though Micro-Doppler slightly outperformed Color and Power Doppler despite adhering to OMERACT Ultrasound Group guidelines [25, 37]. Conversely, the preliminary CARRA MSUS 0-3 scoring systems for pediatric elbow, wrist, and finger arthritis showed excellent reliability among sonographers of varying expertise [38]. However, because this scoring relied solely on static images, it reflects the reliability of the reading process rather than the complete examination; thus, these results should be interpreted with caution.

This study proposes a hypothesis-generating, structured imaging pathway (Fig. 7) that incorporates normative data to minimize gadolinium and sedation use, rather than acting as a validated clinical guideline [24]. This approach requires future prospective validation in larger, longitudinal JIA cohorts.

In our study, clinical grading of arthritis performed poorly, with low sensitivity, but a high specificity, supporting the use of imaging [36].

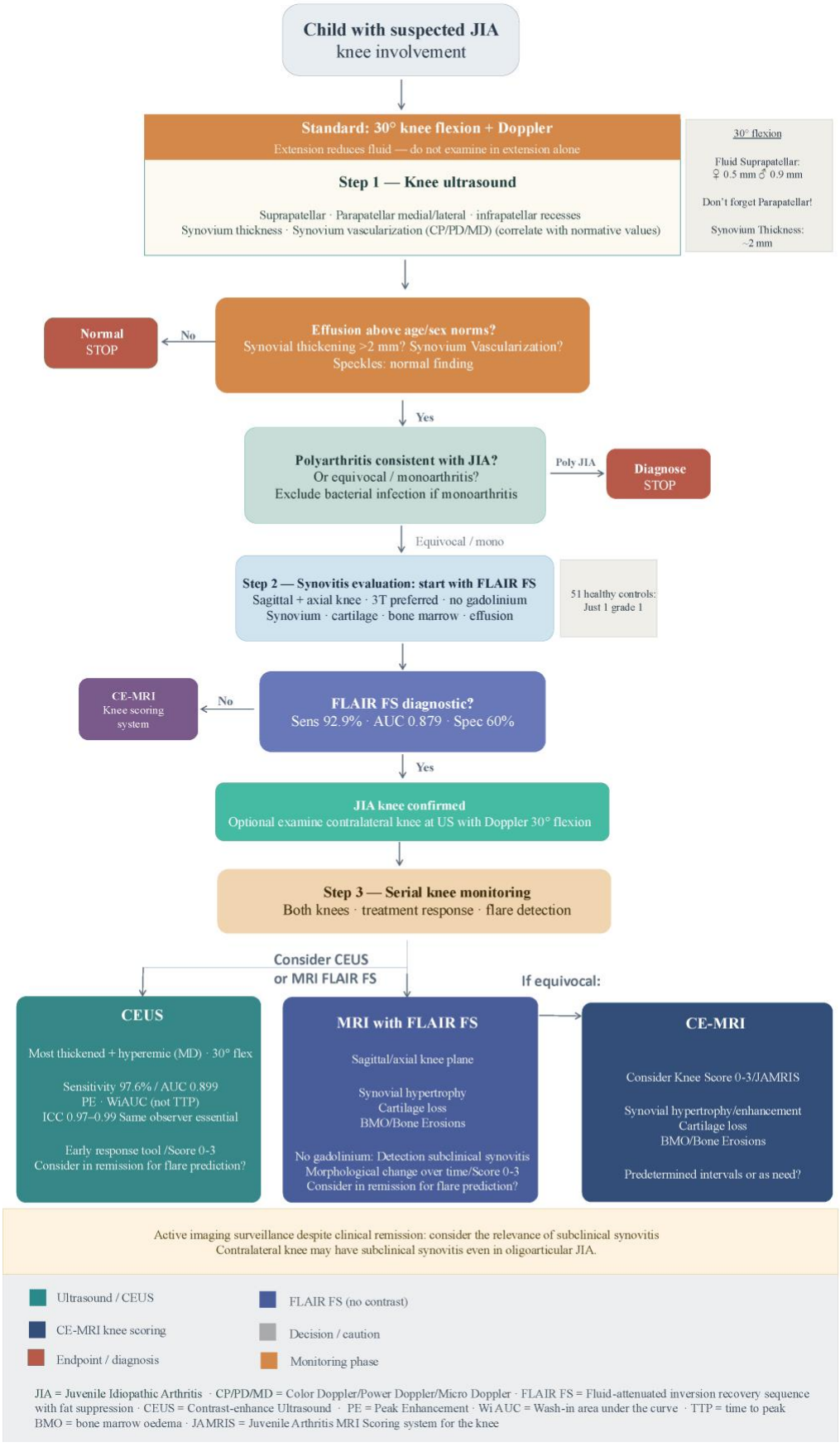


Figure 7. Proposed stratified imaging algorithm for JIA knee involvement

Fig. 7. Proposed stratified imaging algorithm for juvenile idiopathic arthritis knee involvement: clinical decision flowchart.

The study acknowledges limitations due to a small, though balanced, cohort, where a low number of non-inflamed joints (10 cases) resulted in unstable specificity estimates. Additionally, the study was constrained by an inability to perform multivariate regression and subgroup analysis, alongside the potential for differential bias due to the separate evaluation of healthy control images. The strengths were the standardized and validated imaging methods used for both CEUS and CEMRI [18]; all MRIs performed by a single, specially trained radiographer and scored twice by two radiologists, independently; all CEUS performed by one examiner and read twice by two readers, independently. Finally, FLAIR-FS was performed in healthy pediatric volunteers, matched by age and sex as a control group and all examinations were performed on the same day by expert teams.

Conclusion

Contrast-enhanced ultrasound and FLAIR-FS have high diagnostic accuracy in the detection of knee inflammation in children with JIA, using CEMRI as the reference standard, thereby allowing for reduced use of MRI-contrast.

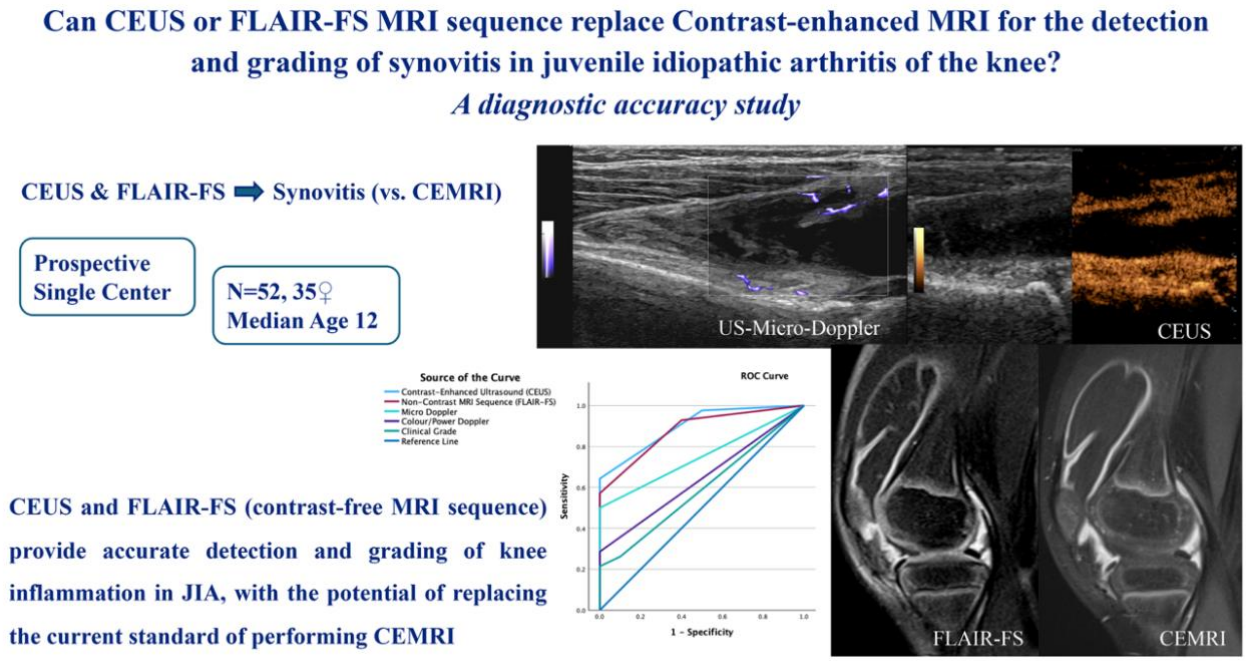
References

1. Thierry S, Fautrel B, Lemelle I, Guillemin F. Prevalence and incidence of juvenile idiopathic arthritis: a systematic review. Joint Bone Spine. 2014;81(2):112-7. doi:10.1016/j.jbspin.2013.09.003
2. Hemke R, Nusman CM, van der Heijde DM, Doria AS, Kuijpers TW, Maas M, et al. Frequency of joint involvement in juvenile idiopathic arthritis during a 5-year follow-up of newly diagnosed patients: implications for MR imaging as outcome measure. Rheumatol Int. 2015;35(2):351-7. doi:10.1007/s00296-014-3108-x
3. Ravelli A, Martini A. Juvenile idiopathic arthritis. Lancet. 2007;369(9563):767-78. doi:10.1016/S0140-6736(07)60363-8
4. Bechtold S, Simon D. Growth abnormalities in children and adolescents with juvenile idiopathic arthritis. Rheumatol Int. 2014;34(11):1483-8. doi:10.1007/s00296-014-3022-2
5. Petty RE, Southwood TR, Manners P, Baum J, Glass DN, Goldenberg J, et al. International League of Associations for Rheumatology classification of juvenile idiopathic arthritis: second revision, Edmonton, 2001. J Rheumatol. 2004;31(2):390-2.
6. Costa Dias S, Habre C, Di Paolo PL, d'Angelo P, Augdal TA, Angenete OW, et al. ESR Essentials: juvenile idiopathic arthritis; what every radiologist needs to know-practice recommendations by the European Society of Paediatric Radiology. Eur Radiol. 2025 doi:10.1007/s00330-025-11891-9

7. Mazzoni M, Pistorio A, Magnaguagno F, Viola S, Urru A, Magnano GM, et al. Predictive Value of Magnetic Resonance Imaging in Patients With Juvenile Idiopathic Arthritis in Clinical Remission. Arthritis Care Res (Hoboken). 2023;75(1):198-205. doi:10.1002/acr.24757
8. Nusman CM, Hemke R, Lavini C, Schonenberg-Meinema D, van Rossum MA, Dolman KM, et al. Dynamic contrast-enhanced magnetic resonance imaging can play a role in predicting flare in juvenile idiopathic arthritis. Eur J Radiol. 2017;88:77-81. doi:10.1016/j.ejrad.2017.01.003
9. Hemke R, Lavini C, Nusman CM, van den Berg JM, Dolman KM, Schonenberg-Meinema D, et al. Pixel-by-pixel analysis of DCE-MRI curve shape patterns in knees of active and inactive juvenile idiopathic arthritis patients. Eur Radiol. 2014;24(7):1686-93. doi:10.1007/s00330-014-3168-z
10. Workie DW, Graham TB, Laor T, Rajagopal A, O'Brien KJ, Bommer WA, et al. Quantitative MR characterization of disease activity in the knee in children with juvenile idiopathic arthritis: a longitudinal pilot study. Pediatr Radiol. 2007;37(6):535-43. doi:10.1007/s00247-007-0449-6
11. Ouyang M, Bao L. Gadolinium Contrast Agent Deposition in Children. J Magn Reson Imaging. 2025;61(1):70-82. doi:10.1002/jmri.29389
12. Doria AS, Kiss MH, Lotito AP, Molnar LJ, de Castro CC, Medeiros CC, et al. Juvenile rheumatoid arthritis of the knee: evaluation with contrast-enhanced color Doppler ultrasound. Pediatr Radiol. 2001;31(7):524-31. doi:10.1007/s002470100474
13. Ntoulia A, Barnewolt CE, Doria AS, Ho-Fung VM, Lorenz N, Mentzel HJ, et al. Contrast-enhanced ultrasound for musculoskeletal indications in children. Pediatr Radiol. 2021;51(12):2303-23. doi:10.1007/s00247-021-04964-6
14. Verkuil F, Hemke R, van Gulik EC, Barendregt AM, Nassar-Sheikh Rashid A, Schonenberg-Meinema D, et al. Double inversion recovery MRI versus contrast-enhanced MRI for evaluation of knee synovitis in juvenile idiopathic arthritis. Insights Imaging. 2022;13(1):167. doi:10.1186/s13244-022-01299-0
15. Handa A, Bedoya MA, Iwasaka-Neder J, Johnston PR, Lo MS, Bixby SD. Measuring synovial thickness on knee MRI in pediatric patients with arthritis: is contrast necessary? Pediatr Radiol. 2024;54(6):988-1000. doi:10.1007/s00247-024-05929-1
16. Thoenen J, MacKay JW, Sandford HJC, Gold GE, Kogan F. Imaging of Synovial Inflammation in Osteoarthritis, From the AJR Special Series on Inflammation. AJR Am J Roentgenol. 2022;218(3):405-17. doi:10.2214/AJR.21.26170
17. Ma W, Cai J, Zhang W, Suo S, Zu J, Yao Q, et al. Diagnostic performance of double inversion recovery MRI sequence for synovitis of the wrist joints in rheumatoid arthritis. Radiol Med. 2023;128(8):978-88. doi:10.1007/s11547-023-01669-8
18. Dias SC, Ferreira CC, Santos I, Castro M, Rodrigues M, Aguiar F, et al. Reliability of CEUS and MRI for grading knee-joint inflammation in juvenile idiopathic arthritis. Eur Radiol. 2026 doi:10.1007/s00330-026-12627-z
19. Singh G, Athreya BH, Fries JF, Goldsmith DP. Measurement of health status in children with juvenile rheumatoid arthritis. Arthritis Rheum. 1994;37(12):1761-9. doi:10.1002/art.1780371209
20. Melo-Gomes JA, Ruperto N, Canhao H, Fonseca JE, Quintal A, Salgado M, et al. The Portuguese version of the Childhood Health Assessment Questionnaire (CHAQ) and the Child Health Questionnaire (CHQ). Clin Exp Rheumatol. 2001;19(4 Suppl 23):S126-30.
21. Consolaro A, Ruperto N, Bazso A, Pistorio A, Magni-Manzoni S, Filocamo G, et al. Development and validation of a composite disease activity score for juvenile idiopathic arthritis. Arthritis Rheum. 2009;61(5):658-66. doi:10.1002/art.24516
22. Consolaro A, Bracciolini G, Ruperto N, Pistorio A, Magni-Manzoni S, Malattia C, et al. Remission, minimal disease activity, and acceptable symptom state in juvenile idiopathic arthritis: defining criteria based on the juvenile arthritis disease activity score. Arthritis Rheum. 2012;64(7):2366-74. doi:10.1002/art.34373
23. Consolaro A, Ruperto N, Bracciolini G, Frisina A, Gallo MC, Pistorio A, et al. Defining criteria for high disease activity in juvenile idiopathic arthritis based on the juvenile arthritis

disease activity score. Ann Rheum Dis. 2014;73(7):1380-3. doi:10.1136/annrheumdis-2013-204186
24. Dias SC, Carvalho DC, Castro M, Dias CC, Ramos I, Brito I, et al. Knee-ultrasound: reference values for the amount of joint fluid and synovial appearances in healthy children and adolescents. Pediatr Radiol. 2025;55(6):1127-37. doi:10.1007/s00247-025-06243-0
25. Terslev L, Iagnocco A, Bruyn GAW, Naredo E, Vojinovic J, Collado P, et al. The OMERACT Ultrasound Group: A Report from the OMERACT 2016 Meeting and Perspectives. J Rheumatol. 2017;44(11):1740-3. doi:10.3899/jrheum.161240
26. Nahm FS. Receiver operating characteristic curve: overview and practical use for clinicians. Korean J Anesthesiol. 2022;75(1):25-36. doi:10.4097/kja.21209
27. Schober P, Boer C, Schwarte LA. Correlation Coefficients: Appropriate Use and Interpretation. Anesth Analg. 2018;126(5):1763-8. doi:10.1213/ANE.0000000000002864
28. Landis JR, Koch GG. The measurement of observer agreement for categorical data. Biometrics. 1977;33(1):159-74.
29. Barendregt AM, Mazzoli V, van Gulik EC, Schonenberg-Meinema D, Nassar-Sheikh Rashid A, Nusman CM, et al. Juvenile Idiopathic Arthritis: Diffusion-weighted MRI in the Assessment of Arthritis in the Knee. Radiology. 2020;295(2):373-80. doi:10.1148/radiol.2020191685
30. Vo Chieu VD, Vo Chieu V, Dressler F, Kornemann N, Pfeil A, Bottcher J, et al. Juvenile idiopathic arthritis of the knee: is contrast needed to score disease activity when using an augmented MRI protocol comprising PD-weighted sequences? Eur Radiol. 2023;33(5):3775-84. doi:10.1007/s00330-022-09292-3
31. Milks KS, Singh J, Benedict JA, Rees MA. Fluid-attenuated inversion-recovery sequence with fat suppression as an alternative to contrast-enhanced MRI in pediatric synovitis. Pediatr Radiol. 2024;54(1):96-104. doi:10.1007/s00247-023-05804-5
32. Rieter JF, de Horatio LT, Nusman CM, Muller LS, Hemke R, Avenarius DF, et al. The many shades of enhancement: timing of post-gadolinium images strongly influences the scoring of juvenile idiopathic arthritis wrist involvement on MRI. Pediatr Radiol. 2016;46(11):1562-7. doi:10.1007/s00247-016-3657-0
33. Tanturri de Horatio L, Shelmerdine SC, d'Angelo P, Di Paolo PL, Magni-Manzoni S, Malattia C, et al. A novel magnetic resonance imaging scoring system for active and chronic changes in children and adolescents with juvenile idiopathic arthritis of the hip. Pediatr Radiol. 2023;53(3):426-37. doi:10.1007/s00247-022-05502-8
34. Malattia C, Damasio MB, Basso C, Verri A, Magnaguagno F, Viola S, et al. Dynamic contrast-enhanced magnetic resonance imaging in the assessment of disease activity in patients with juvenile idiopathic arthritis. Rheumatology (Oxford). 2010;49(1):178-85. doi:10.1093/rheumatology/kep343
35. Buch K, Peacock ZS, Resnick CM, Rothermel H, Kaban LB, Caruso P. Regional differences in temporomandibular joint inflammation in patients with juvenile idiopathic arthritis: a dynamic post-contrast magnetic resonance imaging study. Int J Oral Maxillofac Surg. 2020;49(9):1210-6. doi:10.1016/j.ijom.2020.01.010
36. Roth J, Malattia C. New developments in ultrasound and MRI imaging of pediatric rheumatic diseases. Best Pract Res Clin Rheumatol. 2025;39(3):102069. doi:10.1016/j.berh.2025.102069
37. D'Agostino MA, Terslev L, Aegerter P, Backhaus M, Balint P, Bruyn GA, et al. Scoring ultrasound synovitis in rheumatoid arthritis: a EULAR-OMERACT ultrasound taskforce-Part 1: definition and development of a standardised, consensus-based scoring system. RMD Open. 2017;3(1):e000428. doi:10.1136/rmdopen-2016-000428
38. Vega-Fernandez P, Esteban Y, Oberle E, Proulx-Gauthier JP, Clark M, Shenoi S, et al. Reliability of the Pediatric Specific Musculoskeletal Ultrasound Scoring Systems for the Elbow, Wrist, and Finger Joints. J Rheumatol. 2023;50(2):236-9. doi:10.3899/jrheum.220382

Graphical Abstract



Figures Title and Captions

Figure 1. Multimodality imaging of mild knee synovitis (Grade 1) in JIA

Fig. 1. Left knee in a 13-year-old girl with JIA- Mild Case (Grade 1): a. B-mode, sagittal view through the mid suprapatellar recess with synovium between callipers; **b.** Micro-Doppler showing no vascularity within the synovium. **c.** CEUS, dual-screen mode with simultaneous display of gray-scale image (left) and contrast-only image (right) in the same view, showing a mildly enhancing synovium (Grade 1) in the suprapatellar recess with a region of interest (ROI) placed within (software VueBox); **d.** corresponding Time-intensity curve of the synovial enhancement during the first 120 seconds with a Peak Enhancement (PE) of 682.61 (within the interval values for Grade 1). **e.** FLAIR-FS sagittal showing mild synovitis (arrow) in the same plane as CEUS –; **f.** T1-weighted FS sagittal after contrast administration confirming mild synovitis (arrow) in the same plane as FLAIR-FS and CEUS; **g.** Syngo.via® colour Peak Enhancement Intensity (PEI) map with a region of interest (ROI) placed within the enhancing synovium, in the same plane; **h.** Shows three dynamic enhancement curves (0-100 seconds), representing perfusion in 3 different ROIs; Concentration Curves

display the concentration of the Contrast Agent in the y-axis along time in the x-axis, and a corresponding Peak Enhancement Intensity of 0.144 (within the interval values for Grade 1).

Figure 2. Multimodality imaging of severe knee synovitis (Grade 3) in JIA

Fig. 2. Right knee in a 5-year-old girl with JIA- Severe Case (Grade 3): a. B-mode, sagittal view through the mid suprapatellar recess revealing a large joint effusion and thickened synovium **b.** Micro-Doppler showing increased vascularity within the synovium. **c.** CEUS, dual-screen mode with simultaneous display of gray-scale image (left) and contrast-only image (right) in the same view, showing vividly enhancing synovium, in keeping with synovitis (Grade 3) with a region of interest (ROI) placed within (software VueBox); **d.** corresponding Time-intensity curve of the synovial enhancement during the first 120 seconds with a Peak Enhancement (PE) of 96212.52 (within the interval values for Grade 3). **e.** PD-FS sagittal confirming a severe joint effusion (*) and thickened synovium (arrow); **f.** FLAIR-FS sagittal showing synovitis (arrow) in the same plane as CEUS; **g.** T1-weighted FS sagittal after contrast administration confirming severe synovitis (arrow) in the same plane as FLAIR-FS and CEUS; **h.** Syngo.via® colour Peak Enhancement Intensity (PEI) map with a region of interest (ROI) placed within the enhancing synovium, in the same place; **i.** Shows three dynamic enhancement curves (0-100 seconds), representing perfusion in 3 different ROIs; Concentration Curves display the concentration of the Contrast Agent in the y axis along time in the x axis, and a corresponding Peak Enhancement Intensity of 1.166 (within the interval values for Grade 3).

Figure 3. Diagnostic flow diagram

Fig. 3. Flow diagram illustrating participant enrolment, allocation, and analysis.

Figure 4. Multimodality imaging of deep infrapatellar bursitis in JIA

Fig. 4. – Left knee in a 6-year-old boy with JIA: a. B-mode, sagittal view through the infrapatellar recess, showing deep infra-patellar bursitis, with fluid between callipers, with severe synovial thickening (arrow) and hyperechogenicity/inflammatory change of the Hoffa fat pad (arrowhead); **b**. Colour Doppler with hyperaemia; more expressive in **c.** with Micro Doppler mode. **d.** CEUS, dual-screen mode with simultaneous display of gray-scale image (left) and contrast-only image (right) in the same view, showing heavily enhancing synovium within the deep infra-patellar bursitis, delineating more clearly the synovitis (arrow) from the non-enhancing fluid (*).**e.** PD-FS sagittal confirming the deep infra-patellar bursitis, with fluid (*) and thickened synovium within the bursa (arrow); **f.** FLAIR-FS sagittal showing the synovitis within the bursa (arrow) in the same plane as CEUS; **g.** T1-weighted FS sagittal after contrast administration confirming the synovitis within the bursa (arrow) in the same plane as FLAIR-FS and CEUS.

Figure 5. ROC Curves for Imaging Techniques in JIA

Fig. 5. ROC (Receiver Operating Characteristics) curve illustrating discriminative performance for different imaging techniques in a cohort of 52 patients with JIA.

Figure 6. Multimodality imaging of a false negative Micro-Doppler knee case in JIA

Fig. 6. Left knee in a 9-year-old girl with JIA: a. B-mode, sagittal view through the mid suprapatellar recess revealing thickened synovium (between callipers); **b.** Micro Doppler negative, without signal in the synovium. **c.** CEUS, dual-screen mode with

simultaneous display of gray-scale image (left) and contrast-only image (right) in the same view, showing the moderate enhancing synovium, in keeping with synovitis; **d.** T1-weighted FS sagittal after contrast administration confirming the synovitis in the suprapatellar recess (arrow).

Figure 7. Proposed stratified imaging algorithm for JIA knee involvement

Fig. 7. Proposed stratified imaging algorithm for juvenile idiopathic arthritis knee involvement: clinical decision flowchart.

Movie Supplemental. CEUS video of severe knee synovitis in JIA

Movie Supplemental: 2 min CEUS video of right knee in a 5-year-old girl with JIA the severe grade of synovitis in the suprapatellar recess (longitudinal view) – same case Fig. 2.

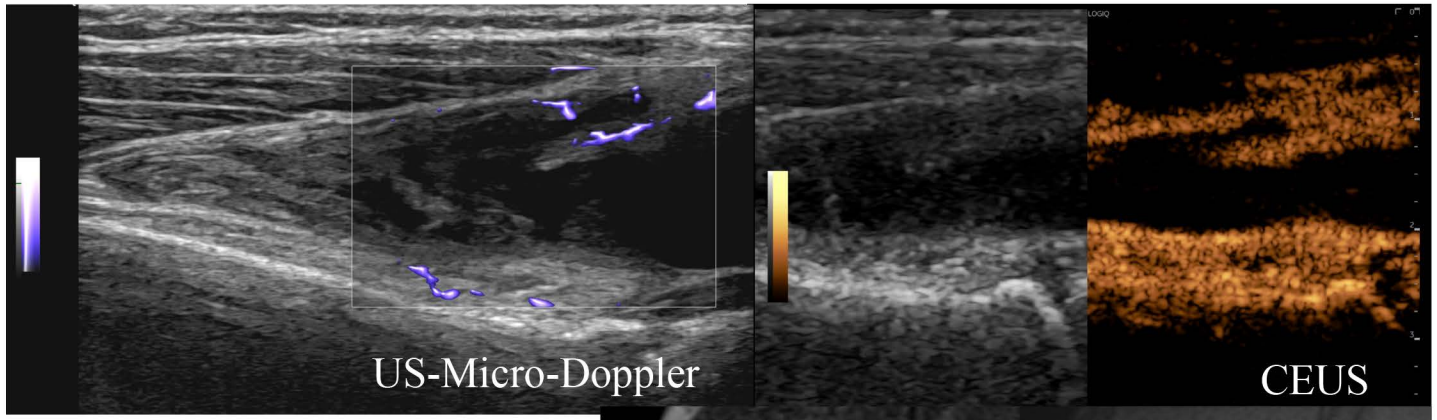
Can CEUS or FLAIR-FS MRI sequence replace Contrast-enhanced MRI for the detection and grading of synovitis in juvenile idiopathic arthritis of the knee?

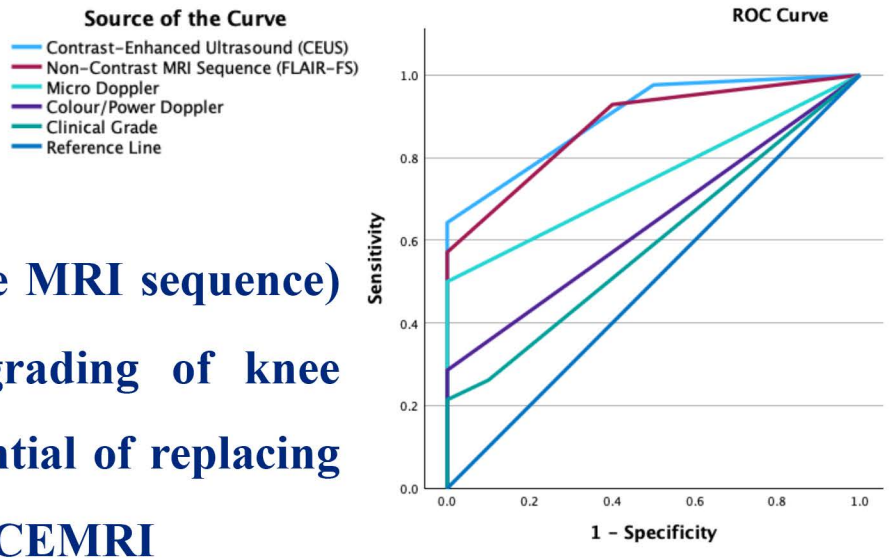
A diagnostic accuracy study

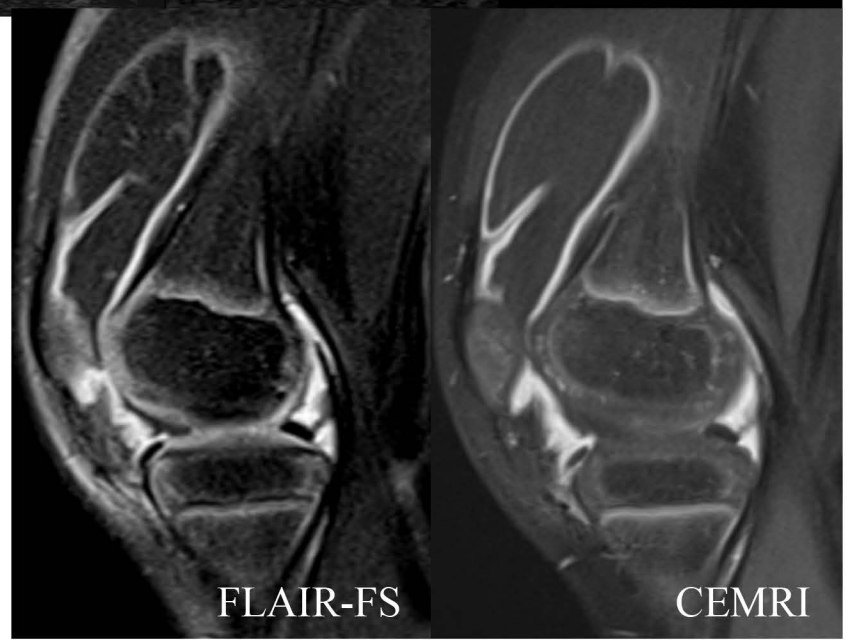
CEUS & FLAIR-FS ➡ Synovitis (vs. CEMRI)

Prospective
Single Center

N=52, 35♀
Median Age 12

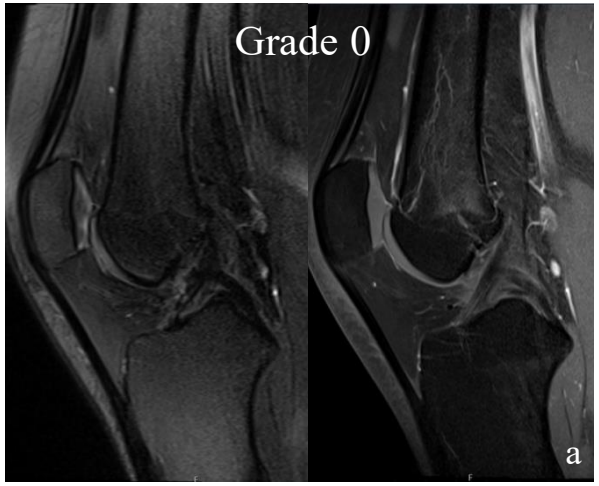




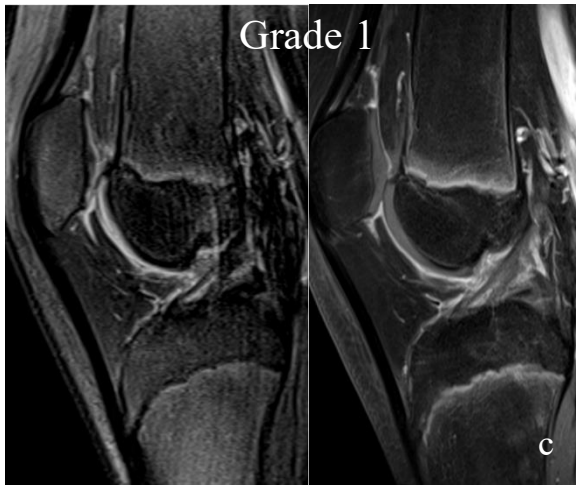


CEUS and FLAIR-FS (contrast-free MRI sequence) provide accurate detection and grading of knee inflammation in JIA, with the potential of replacing the current standard of performing CEMRI

FLAIR-FS Imaging Atlas

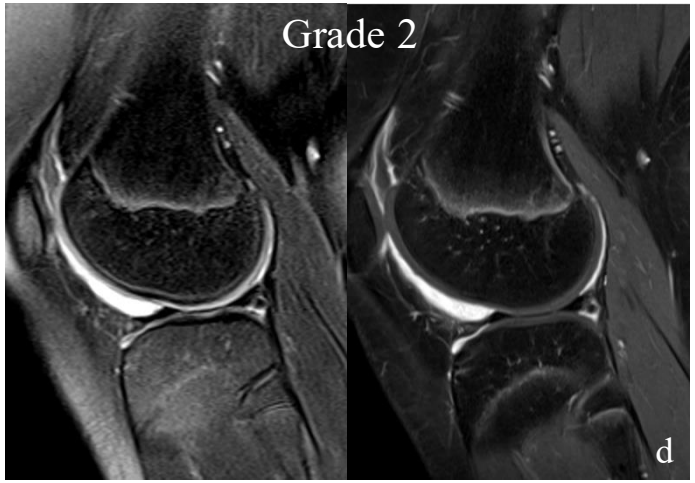


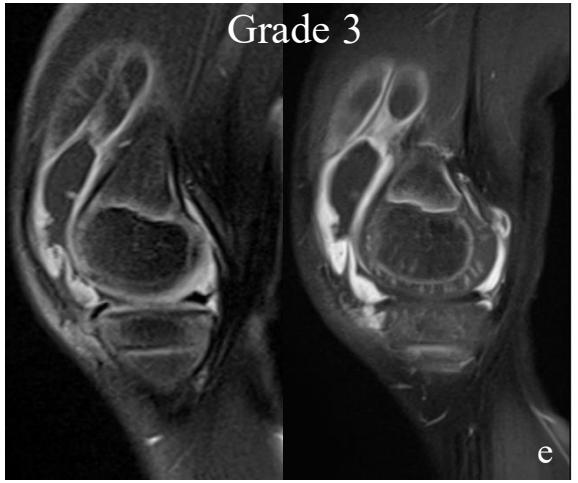


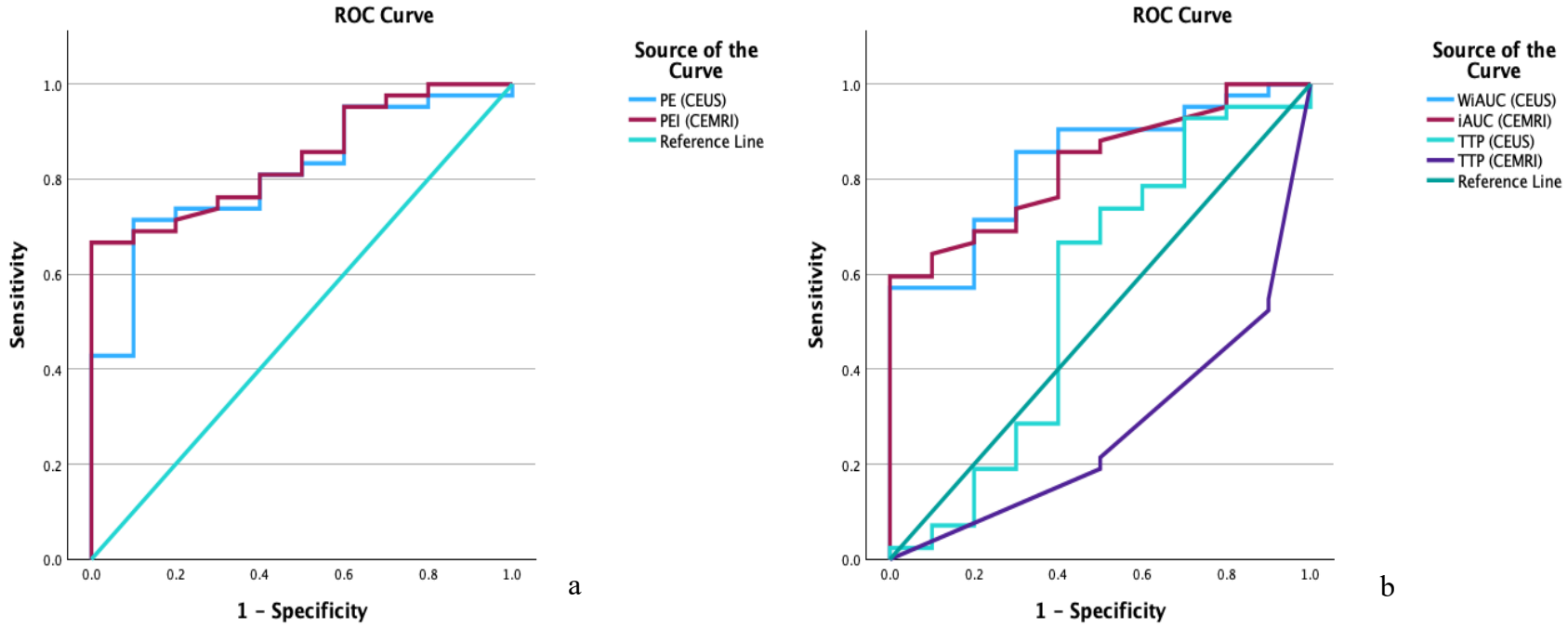


Supplemental Material Fig. S1. **FLAIR-FS + CEMRI Atlas with paired examples of the knee:** sagittal FLAIR-FS on the left side; at same level sagittal post-contrast on right side:

- Grade 0 (none/subtle synovial enhancement CEMRI) – a;
- Grade 1 (Mild synovial enhancement/thickening CEMRI) – b and c;
- Grade 2 (Moderate synovial enhancement/thickening CEMRI) – d;
- Grade 3 (Severe synovial enhancement/thickening CEMRI) – e.







Supplemental Material Fig. S2. ROC curves showing the discriminative performance of different quantitative CEUS and CEMRI markers in 52 patients with JIA, (a) Peak Enhancement (PE) in CEUS and Peak Enhancement Intensity (PEI) in CEMRI. In b. wash-in area under the curve (WiAUC) in CEUS and initial Area Under the Curve (iAUC) in CEMRI and time to peak (TTP) in CEUS and CEMRI.

Sequence	Plane	TR (ms)	TE (ms)	TI (ms)	Averages	FOV read (mm)	FOV phase	Number slices	Slice Thickness (mm)	Flip angle	Gap (mm)	Image Matrix	Bandwidth (Hz/Px)	Acquisition time	Turbo factor	Acceleration mode	Acceleration factor	Others
PD TSE FS*	Sagittal*	3010	33	---	1	160	100%	32	3	180	0.3	269*384	181	1min31s	9	SMS	2	SPAIR PE: H>>F Oversampling: 70%
	Axial*	4160	38	---	1	160	100%	40	3	180	0.3	269*384	148	1min44s	9	SMS	2	SPAIR PE: R>>L Oversampling: 40%
	Coronal	3010	33	---	1	160	100%	38	3	150	0.3	269*384	181	1min30s	7	SMS	2	SPAIR PE: R>>L Oversampling: 30%
T1 TSE	Coronal	718	9.9	---	1	160	100%	38	3	150	0.3	314*448	228	1min09s	3	SMS	2	PE: R>>L Oversampling: 50%
Diffusion b values - 0 and 800*	Axial	8320	61	---	2	220	100%	32	3	180	0.3	160*160	919	3min05s	23	GRAPPA	2	PE: A>>P Concatenations: 2 EPI factor: 80
T2 Flair FS*	Axial*	9000	87	2200	2	160	100%	40	3	150	0.3	224*320	220	3min20s	23	GRAPPA	2	Fat suppression PE: R>>L Concatenations: 2
	Sagittal*	9000	87	2200	2	160	100%	32	3	150	0.3	224*320	220	3min20s	23	GRAPPA	2	Fat suppression PE: A>>P Concatenations: 2
T1 TSE FS pre - Gd	Sagittal	500	9	---	2	160	100%	32	3	150	0.3	280*400	227	2min51s	3	SMS	2	PE: H>>F Fat suppression Oversampling: 70%
T1 vibe Dixon fatsat pre contrast	Sagittal	3.91	1.23 and 2.46	---	1	160	100%	80	1.3	9	0	128*128	1180	23s each measurement	---	CAIPIRINHA	2	5 measurements Slice oversampling: 100% PE: P>>A DIXON method
T1 vibe Dixon fatsat caipirinha first 2 min (isotropic)	Sagittal	3.91	1.23 and 2.46	---	1	160	100%	80	1.3	9	0	128*128	1180	23s each measurement	---	CAIPIRINHA	2	5 measurements Slice oversampling: 100% PE: P>>A DIXON method
T1 TSE FS post - Gd	Sagittal	500	9	---	2	160	100%	32	3	150	0.3	280*400	227	2min51s	3	SMS	2	PE: H>>F Fat suppression Oversampling: 70%
T1 TSE FS post - Gd	Axial	752	8.9	---	2	160	100%	40	3	150	0.3	280*400	228	2min35s	3	SMS	2	PE: R>>L Fat suppression Oversampling: 5%

(“Siemens Magnetom Vida 3T”) Knee coil. 30º Flexion; Knee placed centrally in the magnet field. Cushing description.

* Healthy Volunteers’ Protocol

The dynamic contrast-enhance sequence consisted of five consecutive measurements or stacks with 80 slices, a temporal resolution of 23 seconds, repetition time of 3.91ms, two echo times of 1.23ms and 2.46ms (two point DIXON method), slice thickness of 1.3mm, no gap, field of view of 160*160, and image matrix of 128*128. The acceleration method was the CAIPIRINHA, with an acceleration factor of 2.
The contrast agent (Gadobutrol) was administered immediately at the beginning of the DCE sequence at a dose of 0.1 mmol per kilogram of body weight and directly followed by a 20 ml saline injection. The injection rate depended on the needle gauge, ranging between 1 and 3 ml per second.

The children were supine, with their lower limbs extended. The knee under study was positioned on the 18-channel phased array knee RF coil, with a flexion of approximately 30º. The knee was positioned centrally in the middle of the RF coil and then placed at the magnet's isocenter. An appropriate cushion (Multipad, Pearl Technology) was used to correct knee immobilisation.

DP FAT SAT SAGITAL

TR – 3010 ms
TE – 33 ms
Averages – 1
FOV read – 160mm
FOV phase – 100%
N cortes – 32
Gap – 0.3 mm
Phase encoding direction – H>>F
Oversampling – 70%
Slice Thickness – 3mm
FA – 180º
FAT water contrast – SPAIR
Image matrix – 269*384
Acceleration mode – SMS – acceleration factor PE – 2 and SMS factor – 2
Saturation band – up
Turbo factor – 9
Bandwidth – 181 Hz/Px
Acquisition time – 1min31sec

DP FAT SAT CORONAL

TR – 3010 ms
TE – 33 ms
Averages – 1
FOV read – 160mm
FOV phase – 100%
N cortes – 38
Gap – 0.3 mm
Phase encoding direction – L>>R
Oversampling – 30%

Slice Thickness – 3mm
FA – 150º
FAT water contrast – SPAIR
Image matrix – 269*384
Acceleration mode – SMS – acceleration factor PE – 2 and SMS factor – 2
Saturation band – up
Turbo factor – 7
Bandwidth – 181 Hz/Px
Acquisition time – 1min30sec

DP FAT SAT AXIAL

TR – 4160 ms
TE – 38 ms
Averages – 1
FOV read – 160mm
FOV phase – 100%
N cortes – 40
Gap – 0.3 mm
Phase encoding direction – R>>L
Oversampling – 40%
Slice Thickness – 3mm
FA – 180º
FAT water contrast – SPAIR
Image matrix – 269*384
Acceleration mode – SMS – acceleration factor PE – 2 and SMS factor – 2
Saturation band – between knees
Turbo factor – 9
Bandwidth – 148 Hz/Px
Acquisition time – 1min44sec

T1 CORONAL

TR – 718 ms
TE – 9.9 ms
Averages – 1
FOV read – 160mm
FOV phase – 100%
N cortes – 38
Gap – 0.3 mm
Phase encoding direction – R>>L
Oversampling – 50%
Slice Thickness – 3mm
FA – 150º
Image matrix – 314*448
Acceleration mode – SMS – acceleration factor PE – 2 and SMS factor – 2
Saturation band – none
Turbo factor – 3
Bandwidth – 228 Hz/Px
Acquisition time – 1min09sec

T2 DARK-FLUID (FLAIR) SAGITAL

TR – 9000 ms
TE – 87 ms
TI – 2200 ms
Averages – 2
Concatenations – 2
FOV read – 160mm
FOV phase – 100%
N cortes – 32
Gap – 0.3 mm
Phase encoding direction – A>>P

Oversampling – 0%
Slice Thickness – 3mm
FA – 150º
Image matrix – 224*320
Acceleration mode – GRAPPA – acceleration factor PE – 2
Saturation band – none
Turbo factor – 23
Bandwidth – 220 Hz/Px
Acquisition time – 3min20sec

T2 DARK-FLUID (FLAIR) AXIAL

TR – 9000 ms
TE – 87 ms
TI – 2200 ms
Averages – 2
Concatenations – 2
FOV read – 160mm
FOV phase – 100%
N cortes – 40
Gap – 0.3 mm
Phase encoding direction – R>>L
Oversampling – 0%
Slice Thickness – 3mm
FA – 150º
Image matrix – 224*320
Acceleration mode – GRAPPA – acceleration factor PE – 2
Saturation band – none
Turbo factor – 23
Bandwidth – 220 Hz/Px
Acquisition time – 3min20sec

DWI RESOLVE 3SCAN TRACE

TR – 8320 ms
TE – 61 ms
Averages – 2
Concatenations – 2
FOV read – 220mm
FOV phase – 100%
N cortes – 32
Gap – 0.3 mm
Phase encoding direction – A>>P
Oversampling – 0%
Slice Thickness – 3mm
FA – 180º
Image matrix – 160*160
Acceleration mode – GRAPPA – acceleration factor PE – 2
Saturation band – none
b values – 0 and 800 s/mm^2
Turbo factor – 23
Bandwidth – 919 Hz/Px
EPI factor – 80
Acquisition time – 3min05sec

T1 FAT SAT SAGITAL PRE CONTRAST

TR – 500 ms
TE – 9 ms
Averages – 2
FOV read – 160mm
FOV phase – 100%
N cortes – 32
Gap – 0.3 mm

Phase encoding direction – H>>F
Oversampling – 70%
Slice Thickness – 3mm
FA – 150º
FAT water contrast – fat saturation
Image matrix – 280*400
Acceleration mode – SMS – acceleration factor PE – 2 and SMS factor – 2
Saturation band – none
Turbo factor – 3
Bandwidth – 227 Hz/Px
Acquisition time – 2min51sec

T1 VIBE DIXON CAIPI SAGITAL PRE CONTRAST

TR – 3.91 ms
TE 1 and 2 – 1.23 ms and 2.46 ms
Averages – 1
FOV read – 160mm
FOV phase – 100%
N cortes – 80
Gap – without gap
Phase encoding direction – P>>A
Oversampling – 0% and slice oversampling – 100%
Slice Thickness – 1.3mm
FA – 9º
FAT water contrast – Dixon
Image matrix – 128*128
Acceleration mode – CAIPIRINHA – acceleration factor PE – 2
Saturation band – none
Bandwidth – 1180 Hz/Px
Acquisition time – 23sec

T1 VIBE DIXON CAIPI SAGITAL DYNAMIC – 5 MEASUREMENTS – DCE MRI

TR – 3.91 ms
TE 1 and 2 – 1.23 ms and 2.46 ms
Averages – 1
FOV read – 160mm -- 160*160mm
FOV phase – 100%
N cortes – 80
Gap – without gap
Phase encoding direction – P>>A
Oversampling – 0% and slice oversampling – 100%
Slice Thickness – 1.3mm
FA – 9º
FAT water contrast – Dixon
Image matrix – 128*128
Acceleration mode – CAIPIRINHA – acceleration factor PE – 2
Saturation band – none
Bandwidth – 1180 Hz/Px
Acquisition time – 23sec

5 medidas 23 segundos cada, contrast agent administered immediately at the time of beginning of the DCE-MRI study.

T1 FAT SAT SAGITAL POST CONTRAST

TR – 500 ms
TE – 9 ms
Averages – 2
Concatenations – 2
FOV read – 160mm
FOV phase – 100%
N cortes – 32
Gap – 0.3 mm

Phase encoding direction – H>>F
Oversampling – 70%
Slice Thickness – 3mm
FA – 150º
FAT water contrast – fat saturation
Image matrix – 280*400
Acceleration mode – SMS – acceleration factor PE – 2 and SMS factor – 2
Saturation band – none
Turbo factor – 3
Bandwidth – 227 Hz/Px
Acquisition time – 2min51sec

T1 FAT SAT AXIAL POST CONTRAST

TR – 752 ms
TE – 8.9 ms
Averages – 2
Concatenations – 2
FOV read – 160mm
FOV phase – 100%
N cortes – 32
Gap – 0.3 mm
Phase encoding direction – R>>L
Oversampling – 5%
Slice Thickness – 3mm
FA – 150º
FAT water contrast – fat saturation
Image matrix – 280*400
Acceleration mode – SMS – acceleration factor PE – 2 and SMS factor – 2
Saturation band – none
Turbo factor – 3
Bandwidth – 228 Hz/Px
Acquisition time – 2min35sec

Supplemental Material Tables T.2S – T.6S

T.2S. Agreement between CEMRI and CEUS for subjective grading of inflammatory change on a 0-3 scale.

CEUS	**CEMRI**				Total
	No inflammation (0)	Mild inflammation (1)	Moderate inflammation (2)	Severe inflammation (3)	
No inflammation	5	1	0	0	6
Mild inflammation	5	12	2	0	19
Moderate inflammation	0	5	7	1	13
Severe inflammation	0	0	7	7	14
Total	10	18	16	8	52

T. 3S. Agreement between CEMRI and MRI FLAIR-FS subjective grading of inflammatory change on a 0-3 scale in a cohort of 52 children and adolescents with JIA.

MR FLAIR-FS	**CEMRI**				Total
	No inflammation (0)	Mild inflammation (1)	Moderate inflammation (2)	Severe inflammation (3)	
No inflammation	6	3	0	0	9
Mild inflammation	4	15	0	0	19
Moderate inflammation	0	0	16	1	17
Severe inflammation	0	0	0	7	7
Total	10	18	16	8	52

T.4S. Agreement between the CEMRI (0-2 scale, merging grades 2 and 3) and Clinical Grade for subjective grading of inflammatory change on a 0-2 scale in a cohort of 52 children and adolescents with JIA.

CLINICAL GRADE	**CEMRI**			Total
	No inflammation (0)	Mild inflammation (1)	Moderate and Severe inflammation (2+3)	
Inactive	9	17	14	40
Equivocal Arthrtis	1	0	2	3
Active	0	1	8	9
Total	10	18	24	52

T. 5S. Peak enhancement (PE) values (arbitrary units), median (Mdn) with inter quartile range (IQR) - for 52 patients (35 females), by CEUS grade group (0-3)

Location	CEUS Grades				
	0	1	2	3	p– value[1]
	(n=6)	(n=19)	(n=13)	(n=14)	
Peak Enhancement (PE)					
Mdn	**149.39**	**559.00**	**1770.19**	**9836.16**	**<0.001**
(IQR)	**(62.63 – 204.93)**	**(322.94 – 841.71)**	**(1001.59 – 2625.52)**	**(3690.25 – 24174.80)**	

[1] Kruskal-Wallis test

T. 6S. Peak enhancement intensity (PEI) values (arbitrary units), median (Mdn) with inter quartile range (IQR) - for 52 patients (35 females), by MRI grade group (0-3)

Location	MRI Grades				
	0	1	2	3	p – value[1]
	(n=10)	(n=18)	(n=16)	(n=8)	
Peak Enhancement Intensity (PEI)					
Mdn	**0.06**	**0.12**	**0.29**	**0.71**	**<0.001**
(IQR)	**(0.03 – 0.12)**	**(0.05 – 0.18)**	**(0.20 – 0.46)**	**(0.58 – 0.73)**	

[1] Kruskal-Wallis test

C. Research Line III

Paper 5 - Knee Ultrasound in Juvenile Idiopathic Arthritis: A Comparative Study with Normative Reference Values

Costa Dias S, Ferreira CC, Santos I, Castro M, Rodrigues M, Aguiar F, Dias CC, Ramos I, Ključevšek D, Brito I, Rosendahl K.

Submitted Pediatric Rheumatology.

Knee Ultrasound in Juvenile Idiopathic Arthritis: A Comparative Study with Normative Reference Values.

Authors

Sílvia Costa Dias; Catarina Costa Ferreira; Inês Santos, Miguel Castro; Mariana Rodrigues, Francisca Aguiar, Cláudia Camila Dias, Isabel Ramos, Damjana Ključevšek[7], Iva Brito, Karen Rosendahl

Corresponding Author and Authors Affiliations

Corresponding author:

Sílvia Costa Dias, MD, EDiPR.

ORCID ID: 0000-0003-0862-6967

Universidade do Porto, Porto, Portugal, Medicine Department, Faculty of Medicine.

Hospital de São João, Porto, Portugal, Radiology Department;

silviacostadias@hotmail.com/ silvia.dias@ulssjoao.min-saude.pt

Catarina Costa Ferreira, MD;

Hospital de São João, Porto, Portugal, Radiology Department;

catarinafcferreira21@gmail.com

Inês Santos, MD; Unidade Local de Saúde de Viseu Dão-Lafões, Viseu, Portugal, Rheumatology Unit

inescnsantos@gmail.com

Miguel Castro, MD;

Hospital de São João, Porto, Portugal, Radiology Department;

miguelhcastro@gmail.com

Mariana Rodrigues, MD;

Hospital de São João, Porto, Portugal, Paediatric and Young Adult Rheumatology Unit.

Universidade do Porto, Porto, Portugal, Medicine Department, Faculty of Medicine.

mariana.j.rodrigues@gmail.com

Francisca Aguiar, MD;

Hospital de São João, Porto, Portugal, Paediatric and Young Adult Rheumatology Unit;

francisca.aguiar@ulssjoao.min-saude.pt

Cláudia Camila Dias, PhD;

Universidade do Porto, Porto, Portugal, Medicine Department, Faculty of Medicine.

Centre for Health Technology and Services Research, Porto, Portugal, Department of Community Medicine, Information and Health Decision Sciences (MEDCIDS);

camila@med.up.pt

Isabel Ramos, PhD;

Universidade do Porto, Porto, Portugal, Medicine Department, Faculty of Medicine;

radiologia.hsj@gmail.com

Damjana Ključevšek, PhD;

University Children's Hospital, Ljubljana, Slovenia, Radiology Department;

damjana.kljucevsek@gmail.com

Iva Brito, PhD;

Universidade do Porto, Porto, Portugal, Medicine Department, Faculty of Medicine;

Hospital de São João, Porto, Portugal, Paediatric and Young Adult Rheumatology Unit;

ivaobrito@hotmail.com

Karen Rosendahl, PhD; UiT The Arctic University of Norway, Tromsø, Norway, Department of Clinical Medicine, Faculty of Health Sciences.

University Hospital of North Norway, Tromsø, Norway, Section of Paediatric Radiology;

karen.rosendahl@unn.no

Funding Declaration and Competing Interest Declaration:

The authors declare no financial support, funding, or other benefits from commercial sources for the work reported in this manuscript, nor any other financial interests or competing interests that could create a potential conflict of interest with regard to this work.

Data Availability Declaration:

The datasets generated and/or analysed during the current study are not publicly available due to patient confidentiality and ethical restrictions but could be available from the corresponding author upon request, subject to ethical and institutional approval.

Author Contribution Declaration

S.C.D.: Conception; Design of the work; Acquisition; Data Collection; General Analysis; Statistical Analysis; Interpretation of Data; Writing and Revision of the Manuscript; approved the submitted version.

C.C.F.: Conception; Design of the work; Acquisition; Data Collection; Interpretation of Data; Revision of the Manuscript; approved the submitted version.

I.S.: Data Collection; Interpretation of data; Revision of the Manuscript; approved the submitted version.

M.C.: Conception; Design of the work; Interpretation of Data; Revision of the Manuscript; approved the submitted version.

M.R.: Data Collection; Interpretation of data; Revision of the Manuscript; approved the submitted version.

F.A.: Data Collection; Interpretation of data; Revision of the Manuscript; approved the submitted version.

C.C.D.: Design of the work; Statistical Analysis; Interpretation of Data; Revision of the Manuscript; approved the submitted version.

I.R.: Conception; Design of the work; Interpretation of Data; Revision of the Manuscript; approved the submitted version.

D.K.: Conception; Design of the work; General Analysis; Interpretation of Data; Revision of the Manuscript; approved the submitted version.

I.B.: Data Collection; Design of the work; General Analysis; Interpretation of data; Revision of the Manuscript; approved the submitted version.

K.R.: Conception; Design of the work; General Analysis; Statistical Analysis; Interpretation of Data; Writing and Revision of the Manuscript; approved the submitted version.

Abstract

Introduction: Differentiating physiological findings from pathological synovitis in Juvenile Idiopathic Arthritis (JIA) remains a diagnostic challenge.

Methods: A prospective comparative study evaluated 127 healthy volunteers (aged 3–17) and 52 consecutive JIA patients (aged 1–18). All underwent bilateral knee examinations using identical high-end ultrasound machines and a standardized protocol. Beyond tracking traditional recesses, novel measurements for intercondylar cartilage thickness and ossified patellar length were recorded.

Results: Healthy controls displayed an asymmetric fluid topology, with fluid pooling predominantly in the suprapatellar recess ($p < 0.001$); this compartmentalization was entirely eradicated in JIA patients ($p = 0.474$). The clinically "unaffected" knees of unilateral JIA patients exhibited significantly thicker synovium than healthy controls ($p < 0.001$), uncovering subclinical synovitis. Colour Doppler showed an absolute diagnostic separation, tracking strictly negative bilaterally (Grade 0) across all 127 healthy controls ($p < 0.001$). Cartilage thickness naturally decreased with age in both groups, but JIA girls displayed accelerated, pathological thinning compared to healthy peers ($p < 0.001$). Conversely, JIA patients exhibited longer patellar lengths bilaterally, indicating inflammatory periarticular overgrowth (p 0.030 and p 0.011).

Discussion: Standardized regional fluid mapping might help prevent false-positive overdiagnosis from innocent physiological fluid. Uncovering subclinical synovial proliferation in asymptomatic contralateral joints points to a systemic disease dimension that escapes clinical examination.

Conclusion: Our findings demonstrate that active JIA eradicates the asymmetric fluid topology naturally seen in healthy children, instead causing a uniform, homogeneous fluid expansion across all three knee recesses. The discovery of significant synovial thickening within the clinically "unaffected" knees, of patients with a history of unilateral JIA, confirms the presence of subclinical multiple joint involvement that remains elusive to conventional physical examination. Age-stratified biomarkers of cartilage matrix degradation and hyperaemic bone overgrowth, as well as the high Doppler specificity for JIA, validate international guidelines positioning ultrasound as the definitive first-line diagnostic modality.

Keywords: Juvenile Idiopathic Arthritis; Synovitis; Ultrasound; Knee.

List of Abbreviations:

CHUSJ: University Hospital Centre of São João Porto

CI: confidence intervals

ESPR: European Society of Paediatric Radiology

FMUP: Faculty of Medicine of the University of Porto

ILAR: International League of Associations for Rheumatology

IQR: interquartile ranges

JIA: Juvenile Idiopathic Arthritis

Mdn: median

MRI: Magnetic resonance imaging

MSUS: Musculoskeletal Ultrasound

OR: odds ratios

PIUS-Knee: Paediatric Internationally agreed Ultrasound Knee Protocol

RF: Rheumatoid Factor

ROC: receiver operating characteristic

Background

Juvenile Idiopathic Arthritis (JIA) is the most common chronic inflammatory musculoskeletal disease in childhood, with a reported incidence ranging from 1.6–23.0 per 100,000 children under 16 years of age, across Europe [1]. In a recent recommendation by the European Society of Paediatric Radiology (ESPR), ultrasound with Doppler was formally designated as the first-line imaging examination when JIA is suspected. Magnetic resonance imaging (MRI) remains valuable primarily when ultrasound findings are inconclusive or inconsistent with the clinical data [2].

The knee is the most frequently involved joint in JIA and is consequently the most extensively studied joint by musculoskeletal ultrasound (MSUS). Synovitis of the knee, manifesting as synovial hypertrophy, joint effusion, and synovial hypervascularity, represents the hallmark of ultrasound assessment. However, chronic inflammation in JIA also inflicts damage on deeper articular structures, most notably the cartilage. Cartilage thinning serves as an early marker of joint damage, often preceding irreversible radiographic changes. Ultrasound evaluation of cartilage thickness at the intercondylar notch of the distal femur has been rigorously validated in comparison to MRI [3-5]. Similarly, ultrasound assessment of the ossified patella provides a complementary window into skeletal maturation, capturing the potential impact of chronic hyperaemic inflammation on periarticular bone development.

In order to correctly interpret ultrasound findings in a child with suspected JIA, a comprehensive knowledge of age- and sex-stratified reference values in healthy children is crucial [6-8]. To address this clinical need, this study aims to compare quantitative knee ultrasound findings in a cohort of healthy children and adolescents, with physiological variants, with those in patients diagnosed with JIA.

Methods

This study was designed to evaluate and compare MSUS metrics between two distinct paediatric populations. First, a cross-sectional study was conducted within a school setting in Porto, Portugal to establish the healthy control cohort. The protocol was approved by the Institutional Ethics Committee of University Hospital Centre of São João Porto (CHUSJ) / Faculty of Medicine of the University of Porto (FMUP) (registration number 191/22) and by the school's administrative board. Written informed consent was obtained from the caretakers of all participants, and assent was secured from the children/volunteers where applicable. Children and adolescents aged 3-17 years were invited to participate via invitations sent to parents' representatives. Exclusion criteria were chronic medicated disease that might affect the skeletal system or having experienced a knee trauma within the last two months [8].

The second cohort comprised a prospective, single-centre study of paediatric patients with a verified diagnosis of JIA, conducted between 2023 and 2024. This arm of the study was formally approved by the same Ethics Committee (registration number 282-20), and written informed consent was obtained from each participant and/or their caregiver, according to national guidelines. Participants were consecutively recruited from the Paediatric Rheumatology Clinic at the CHUSJ. Patients aged 1-18 years, meeting the International League of Associations for Rheumatology (ILAR) criteria [9] for JIA, and presented with either current or documented historical knee involvement, were eligible for inclusion. Children with a history of intra-articular steroid injection or a trauma to the knee within the last two months were excluded [10].

Clinical assessment

For the JIA patient cohort, comprehensive clinical and demographic data were systematically collected, including age at diagnosis, overall disease duration, and duration

of clinical remission (when applicable). Additionally, the specific JIA subtype, any history of bilateral knee involvement and regular engagement in sports activities (quantified as total hours per week) were recorded. The imaging team was blinded to the clinical data.

To ensure standardized scoring and avoid statistical unit errors from analysing interdependent joints, a single index knee was selected for each patient. Clinicians designated the most severely affected knee side for primary analysis; in cases presenting with a history of bilateral disease, the joint that was either more recently affected or exhibited greater clinical severity was selected ("index knee").

Ultrasound protocol

The healthy volunteer cohort was examined by one of two experienced examiners (a paediatric radiologist and a musculoskeletal radiologist, with 10 and 12 years of experience in MSUS, respectively), whilst the patient cohort was examined by the paediatric radiologist. To ensure technical consistency, all examinations across both cohorts were performed using an identical imaging protocol on two identical-model high-end ultrasound systems (Logiq E10, Version R3; GE HealthCare). Both systems utilized a high-frequency linear transducer (6–15 MHz) operating under identical, optimized musculoskeletal pre-set definitions, matching the methodology validated in a previous healthy reference sample of 127 children and adolescents [8].

Bilateral knee examinations were performed with the child supine. With the knee positioned in 30° of flexion, structures were systematically evaluated via a mid-longitudinal suprapatellar view and transverse views across both the lateral and medial parapatellar recesses (Figure 1). Additionally, the suprapatellar recess was dynamically evaluated in full extension and during a standardised manual provocation manoeuvre, as previously described [8]. The presence and amount of fluid, and whether or not the fluid

contained echogenic speckles, were documented across all scanning positions (Figure 1). To quantify synovial thickness, the mid/central suprapatellar recess was evaluated in the longitudinal plane. Light transducer compression was applied to displace any fluid away, allowing assessment of the double synovial layer.

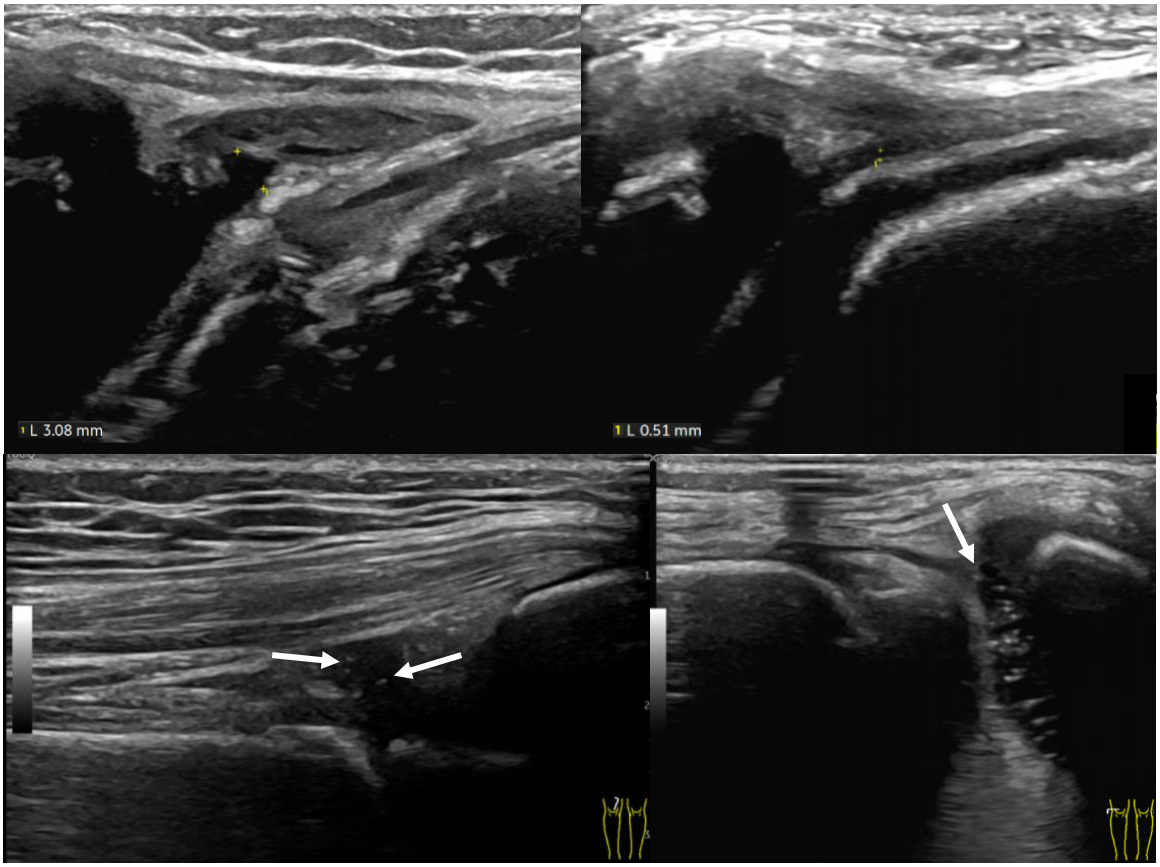


Fig 1. **(a,b)** Transverse ultrasound images of the medial parapatellar recess demonstrating fluid measurements. **(a)** An 8-year-old female with JIA showing increased fluid depth of 3.1mm (between callipers) with coexisting synovitis (asterisk). **(b)** An 8-year-old female healthy volunteer demonstrating a physiological fluid depth of 0.5 mm (between callipers). **(c)** An 8-year-old male healthy volunteer with some speckles (arrows) within the suprapatellar recess in longitudinal view. **(d)** An 11-year-old male healthy volunteer with multiple speckles (arrow) within the lateral joint space in transverse view.

Beyond conventional assessments of joint effusion and synovial thickness, the scanning protocol introduced two novel structural measurements not reported in the baseline

reference sample; thickness of the intercondylar cartilage (knee flexed) and the ossified patellar length (knee extended) – Figure 2.



Fig 2. (a,b) Transverse view obtained in 90º flexion demonstrating the measurement technique of intercondylar cartilage thickness. (c,d) Longitudinal view obtained in full extension demonstrating the measurement technique for ossified patella length.

Synovial vascularity assessment via colour Doppler

Colour Doppler settings were optimized for low-velocity flow. Synovial vascularity was graded using a semi-quantitative scale adapted from Ting et al [11] and further modified to optimize sensitivity for the paediatric population [12], as: no inflammation (grade 0; no signal), mild inflammation (grade 1; up to 3 single Doppler spots or up to 1 confluent spot and 2 single spots or up to 2 confluent spots), moderate inflammation (grade 2; > grade 1 in < 30% of the area of synovial hypertrophy) or severe inflammation (grade 3; confluent signals present in > 30% of the area of synovial hypertrophy).

Colour Doppler activity was mapped across three standard anatomical scanning views: the mid-longitudinal suprapatellar view and the transverse views through both the lateral and medial parapatellar recesses.

Statistical analysis

Data normality testing indicated a non-normal distribution; thus, continuous variables are expressed as medians (Mdn) with interquartile ranges (IQR) and were stratified into four age groups (1–6, 7–9, 10–13, and 14–18 years).

Two-group, multi-group, and bilateral paired continuous comparisons were performed using Mann-Whitney U, Kruskal-Wallis, and Wilcoxon signed-rank tests, respectively. Comparisons of fluid depth across the three recesses of the same knee (suprapatellar, medial and lateral parapatellar) were performed using Friedman's test, with Bonferroni-adjusted pairwise comparisons, given the related, within-subject nature of these measurements.

Categorical variables (effusion presence and colour Doppler grades) were analysed using Chi-Square or Fisher's exact tests.

A multivariable logistic regression model with backward stepwise selection identified independent predictors of the outcome. Initial candidates included sex, age category, colour Doppler positivity, longitudinal suprapatellar double synovial layer/fluid, and transverse parapatellar lateral/medial fluid. Model predictive performance was evaluated via receiver operating characteristic (ROC) curve analysis. The optimal diagnostic cut-off was determined using Youden's Index, prioritizing a clinically relevant sensitivity threshold of $\geq 80\%$. Significance was set at $p \leq 0.05$. Analyses were performed using IBM SPSS Statistics version 30 (IBM Corp., Armonk, NY, USA).

Results

The study enrolled 179 participants: 127 healthy volunteers (52.8% female; median age 10.9 years, IQR: 8.4–13.4) and 52 JIA patients (67.3% female; median age 12.4 years, IQR: 8.9–15.6). No statistically significant differences existed between cohorts regarding age, sex, height, or weight ($p > 0.05$). Detailed baseline demographics are summarized in Table 1.

Table 1. Demographic and clinical characteristics for a total of 179 participants; 127 healthy volunteers and 52 patients with JIA. Median (Mdn); interquartile range (IQR); range - minimum and maximum (Min, Max); centimetres (cm); kilograms (kg)

Location	Volunteers (n=127)	Patients (n=52)	p – value[1,2]
Sex Female, n (%)	67 (52.8%)	35 (67.3%)	0.074[1]
Age in years			
Mdn	10.9	12.4	0.600[2]
(IQR)	(8.4 – 13.4)	(8.9 – 15.6)	
(Minimum-Maximum)	(3.1 – 17.4)	(1.9 – 18.3)	
Height in cm			
Mdn	143.3	149.0	0.538[2]
(IQR)	(130.0 – 159.0)	(129.0 – 161.0)	
(Minimum-Maximum)	(94.0 – 187.0)	(86.1 – 175.0)	
Weight in kg			
Mdn	37.4	39.7	0.395[2]
(IQR)	(27.0 – 51.2)	(26.1 – 56.6)	
(Minimum-Maximum)	(14.3 – 74.5)	(12 – 96.1)	
Sport activities total hours per week			
Mdn	**3.0**	**1.0**	**<0.001**[2]
(IQR)	**(2.0 – 5.0)**	**(0.0 – 1.5)**	
(Minimum-Maximum)	**(0.0 – 17.0)**	**(0.0 – 3.3)**	

[1]Pearson's Chi-square, [2]Mann-Whitney test

To evaluate recess fluid dynamics, echogenic speckles and synovial/cartilage thickness, metrics from the clinically designated index knee of JIA patients (right: n = 28, left: n =

24) were utilized. For comparative analysis against the healthy control cohort, baseline measurements from both the right and left knees of the volunteers were initially cross tested. Side-to-side comparisons within the healthy control cohort revealed no statistically significant differences between right and left knees ($p>0.05$). Consequently, the right knees of healthy volunteers were systematically selected as the normative reference.

JIA phenotypes classified by ILAR criteria included persistent oligoarthritis (n=30; 57.7%), extended oligoarthritis (n=5; 9.6%), rheumatoid-factor (RF)-negative polyarthritis (n=6; 11.5%), RF-positive polyarthritis (n=1; 1.9%), psoriatic arthritis (n=4; 7.7%), enthesitis-related arthritis (n=4; 7.7%) and systemic JIA (n=2; 3.8%).

Contralateral knee subgroup analysis

A secondary analysis within the JIA cohort evaluated the impact of contralateral knee history, stratifying patients by prior disease activity (n=27, 51.9%) versus strictly unaffected status (n=25, 48.1%). This sub-analysis revealed no statistically significant differences between the two subgroups regarding sex ($p=0.061$), age ($p=0.610$), or weekly sports engagement ($p=0.937$).

Joint fluid distribution and recess dynamics

JIA patients demonstrated consistently greater fluid accumulation across nearly all evaluated recesses and positions compared to healthy controls ($p < 0.05$, Table 2), except during the dynamic provocation manoeuvre. Within the JIA cohort, fluid metrics showed no statistically significant variations based on biological sex ($p = 0.259–0.792$), stratified age groups ($p = 0.216–0.906$), or weekly sports engagement ($p = 0.280–0.883$).

Fluid distribution remained highly consistent between right and left JIA index knees, except for a marginally higher volume in the lateral parapatellar recess when the right

knee was included (p=0.046). Dynamic imaging revealed a highly significant reduction in maximum suprapatellar fluid depth when moving from 30° flexion to full extension (p<0.001).

Table 2. Fluid in the recesses and synovial thickness in the suprapatellar recess (double layer) in mm by location, in 127 healthy volunteers and 52 patients with JIA. Median (Mdn); interquartile range (IQR); range - minimum and maximum (Min, Max).

Location	Volunteers (n=127; 67 Females)	Patients (n=52; 35 Females)	p – value[1]
Fluid Longitudinal Suprapatellar			
Mdn	**0.7**	**0.9**	**0.024**
(IQR)	**(0.0 – 1.3)**	**(0.6 – 1.2)**	
(Minimum-Maximum)	**(0.0 – 3.0)**	**(0.0 – 10.9)**	
Fluid Longitudinal Suprapatellar Extension			
Mdn	**0.0**	**0.0**	**0.001**
(IQR)	**(0.0 – 0.0)**	**(0.0 – 0.8)**	
(Minimum-Maximum)	**(0.0 – 1.7)**	**(0.0 – 9.8)**	
Fluid Longitudinal Provocation			
Mdn	2.2	2.2	0.188
(IQR)	(1.3 – 3.1)	(1.5 – 3.7)	
(Minimum-Maximum)	(0.0 – 6.6)	(0.6 – 19.6)	
Fluid Transverse Parapatellar			
Lateral, Mdn	**0.0**	**0.8**	**0.002**
(IQR)	**(0.0 – 0.9)**	**(0.0 – 1.3)**	
(Minimum-Maximum)	**(0.0 – 2.4)**	**(0.0 – 6.7)**	
Medial, Mdn	**0.0**	**0.9**	**<0.001**
(IQR)	**(0.0 – 0.8)**	**(0.6 – 1.5**	
(Minimum-Maximum)	**(0.0 – 1.8)**	**(0.0 – 6.0)**	
Synovial Thickness Longitudinal Suprapatellar			
Mdn	**2.0**	**3.3**	**<0.001**
(IQR)	**(1.6 – 2.3)**	**(2.6 – 4.5)**	
(Minimum-Maximum)	**(1.1 – 4.2)**	**(1.0 – 10.8)**	

[1]Mann-Whitney test

Spatial Distribution and Fluid Topology

Intra-group analysis across the suprapatellar, medial parapatellar, and lateral parapatellar recesses revealed distinct topological profiles. In healthy volunteers, fluid depth varied significantly by compartment ($p < 0.001$), remaining significantly higher in the suprapatellar recess than in both the medial ($p = 0.005$; Figure 1) and lateral recesses ($p = 0.021$), with no difference between parapatellar recesses ($p = 1.000$).

Conversely, this physiological fluid compartmentalization was lost in the JIA cohort, which demonstrated uniform fluid expansion and no statistically significant differences in fluid depth among the three recesses ($p = 0.474$; pairwise post-hoc $p = 0.718–1.000$).

Intra-patient side-to-side comparisons within the JIA cohort showed that clinically selected index knees contained significantly higher fluid volumes than their contralateral counterparts across nearly all landmarks and positions, including the suprapatellar recess at 30° flexion, under provocation, and the medial parapatellar recess (all $p<0.001$), except the lateral parapatellar recess ($p=0.185$). This asymmetry remained highly significant when stratifying patients by contralateral history (previous involvement, n=27/52; unaffected, n=25/52), with the volumetric gap widening in the strictly unilateral subgroup.

Cross-cohort analysis comparing healthy controls to the unaffected contralateral knees of the unilateral JIA subgroup revealed no statistically significant differences in fluid depth across any compartment ($p=0.193–0.538$). Conversely, compared to healthy controls, the currently contralateral knees of patients (non-index knee) with a history of bilateral disease demonstrated persistent, significant fluid elevations exclusively within the parapatellar compartments (lateral: $p=0.018$; medial: $p=0.035$).

Speckles within the joint fluid

No statistically significant difference in the presence of echogenic speckles within the joint recesses was observed between the two cohorts, with speckles detected in at least one recess in 20% of healthy volunteers compared to 31% of JIA patients (p=0.109) (Figure 1). Stratifying JIA patients by sex (p=0.622) or weekly sports engagement (p=0.853) revealed no significant variations.

Synovial thickness/subclinical synovial proliferation and Doppler assessment

Synovial thickness was significantly higher in JIA patients than in healthy volunteers, with medians of 3.3 mm (IQR 2.6–4.5) versus 2.0 mm (IQR 1.6–2.3) (p<0.001; Table 2). Within the JIA cohort, synovial thickness remained statistically uniform when stratified by sex (p=0.325) or age cohorts (p=0.236).

Intra-patient side-to-side analysis revealed distinct thickness profiles based on historical involvement (Figure 3). In patients with a history of bilateral disease (n=27), despite only two having active bilateral arthritis at examination, index knees demonstrated significantly thicker synovial layers than contralateral joints (median 3.5 mm [IQR: 2.6–4.5] vs 3.3 mm [IQR: 2.3–3.8]; p=0.031). This inter-limb asymmetry was even more pronounced in strictly unilateral patients (n=25; p<0.001), with index knees showing marked thickening (median 3.3 mm [IQR: 2.5–4.3] vs 2.3 mm [IQR: 2.1–3.0]). Notably, these clinically unaffected contralateral knees also demonstrated a significantly thicker synovial membrane than healthy volunteer reference joints (median 2.3 mm [IQR: 2.1–3.0] vs. 2.0 mm [IQR: 1.6–2.3]; p<0.001; Figures 3 and 4).

Synovial colour Doppler hypervascularity (Grade ≥ 1) differed significantly between cohorts (p<0.001), detected in 11.5% (6/52) of JIA patients but none of the 127 healthy volunteers.

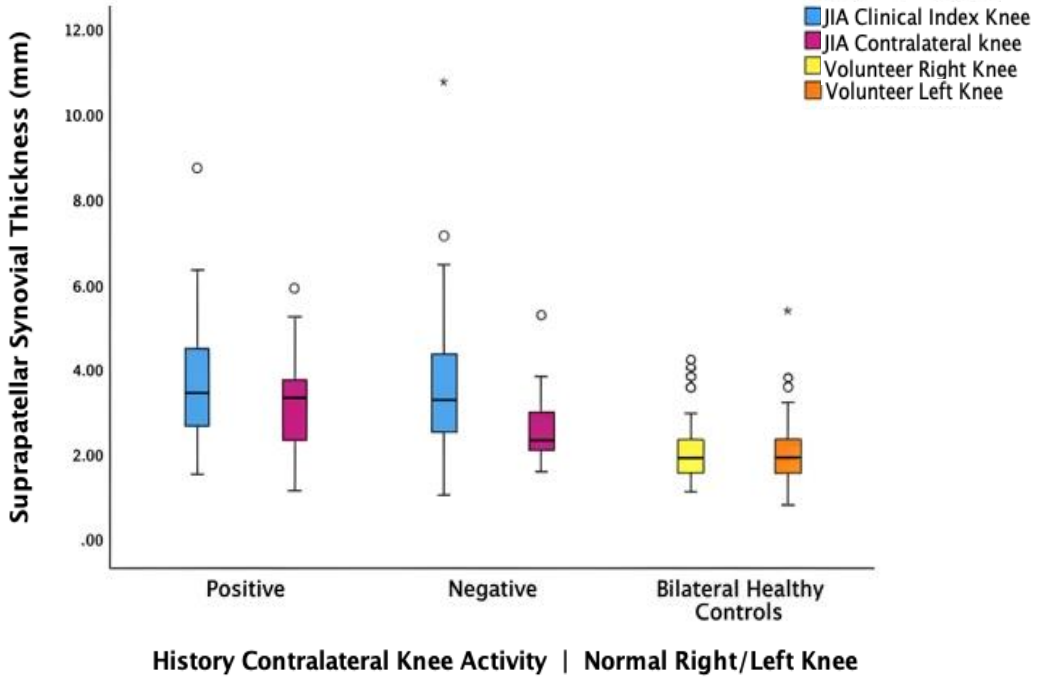


Fig 3. Boxplots, showing thickness of the double-layered synovium (in mm) in suprapatellar recess by history of the contralateral knee (disease or no disease): Positive (index knee vs. a diseased contralateral knee) and Negative (index knee vs. a non-diseased contralateral knee); Bilateral Healthy Controls thickness of double layered synovium (right vs. the left knee of healthy volunteers).

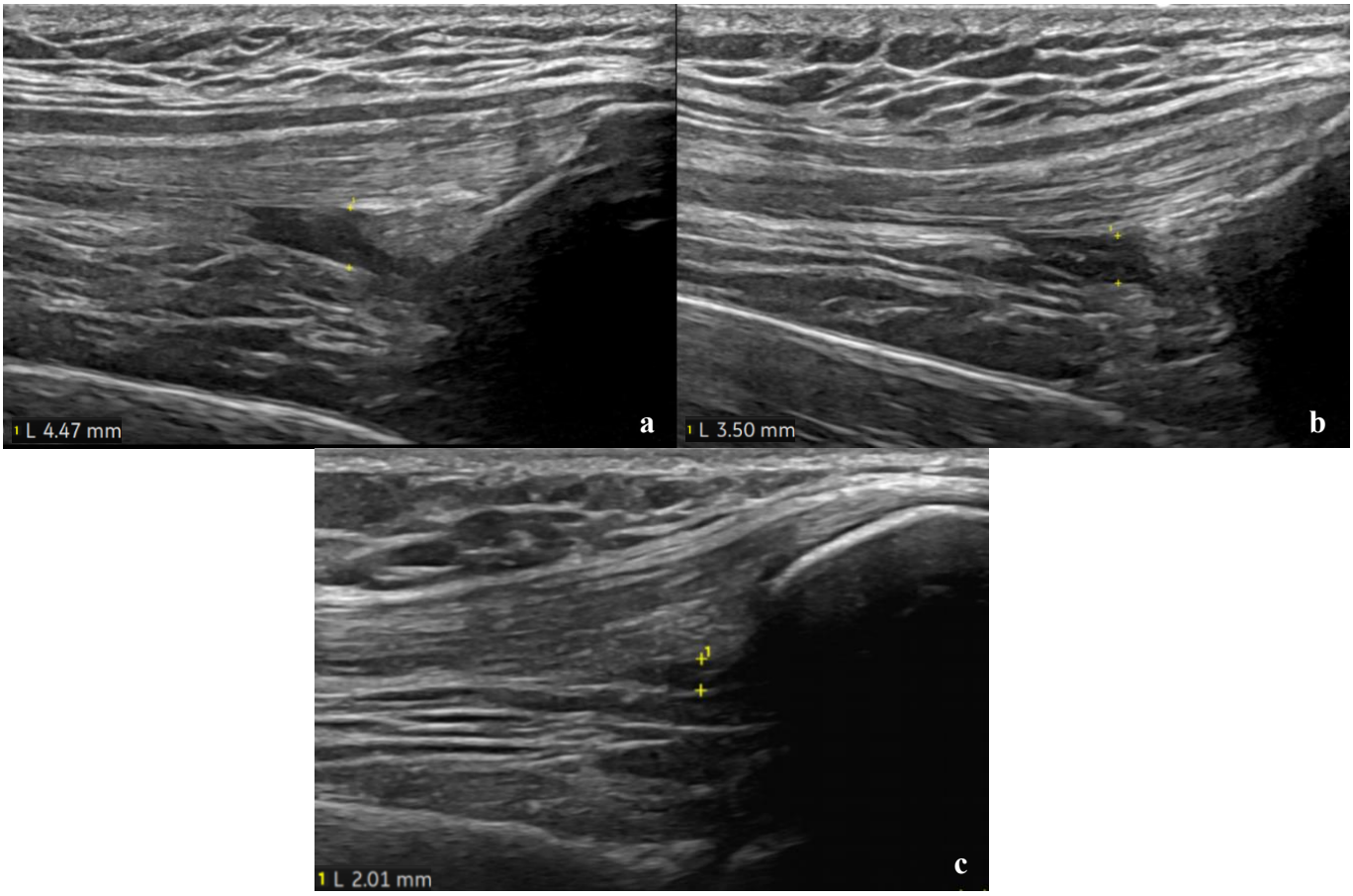


Fig 4. Longitudinal ultrasound images of the suprapatellar recess demonstrating the measurement of the mid-central synovial double-layer thickness. **(a)** A 16-year-old female patient with JIA showing marked synovial thickening of 4.5 mm (between callipers) in the clinically affected index knee, compared to **(b)** a thickness of 3.5 mm in the contralateral, historically unaffected knee. **(c)** A 16-year-old female healthy volunteer demonstrating a normal, physiological synovial double-layer thickness of 2.0 mm.

Intercondylar Cartilage thickness

In female JIA patients, the femoral intercondylar cartilage was significantly thinner than in healthy volunteers (median 2.9 mm vs. 3.1 mm; p=0.037; Table 3). Cartilage thickness showed no side-to-side differences in either volunteers (p=0.207) or patients (p=0.583) but decreased significantly across age groups in both cohorts (volunteers: p<0.001; patients: p=0.009).

Table 3. Femoral intercondylar cartilage thickness (in mm) for 52 JIA patients and 127 healthy volunteers by sex. Median (Mdn); interquartile range (IQR); range - minimum and maximum (Min, Max).

Location	Females (n=102)		p – value[1]	Males (n=77)		p – value[1]
Transverse Intercondylar Cartilage	Volunteers (n=67)	Patients (n=35)	**0.037**	Volunteers (n=60)	Patients (n=17)	0.432
Mdn	**3.1**	**2.9**		3.4	3.6	
(IQR)	**(2.7 – 3.5)**	**(2.6 – 3.2)**		(3.1 – 3.8)	(3.1 – 4.1)	
(Minimum-Maximum)	**(1.9 – 4.3)**	**(1.5 – 3.6)**		(2.3 – 4.7)	(1.6 – 4.6)	

[1]Mann-Whitney test

Patellar bone length

Bilaterally, the ossified patella was significantly longer in JIA patients than in healthy volunteers (right: 35.7 vs. 33.6 mm, p=0.030; left: 35.4 vs. 32.4 mm, p=0.011; Table 4). For both cohorts, right ossified patellar length was significantly greater than the left (p<0.001).

Table 4. Length of the ossified patella (in mm) by side for 52 JIA patients and 127 healthy volunteers. Median (Mdn); interquartile range (IQR); range - minimum and maximum (Min, Max).

Location	Right (n=179)		p – value[1]	Left (n=179)		p – value[1]
Length of the ossified patella	**Volunteers (n=127)**	**Patients (n=52)**	**0.030**	**Volunteers (n=127)**	**Patients (n=52)**	**0.011**
Mdn	**33.6**	**35.7**		**32.4**	**35.4**	
(IQR)	**(26.8 – 37.0)**	**(28.9 – 39.4)**		**(25.6 – 36.0)**	**(29.2– 38.8)**	
(Minimum-Maximum)	**(0.0 – 45.9)**	**(1.8 – 43.4)**		**(0.0 – 44.1)**	**(2.1 – 42.2)**	

[1]Mann-Whitney test

Disease prediction model

A multivariable logistic regression model was developed using backward selection to predict JIA presence. The final model incorporates longitudinal suprapatellar double synovial thickness (mm) and transverse medial parapatellar fluid depth (mm), demonstrating strong discriminative power with an area under the ROC curve (AUC) of 0.892 (95% CI: 0.832–0.951; Figure 5). The log-odds (Y) of having the disease are expressed as: Y= -6.149+1.743*suprapatellar synovium thickness+1.236*medial parapatellar fluid.

Individual disease probability (P) is calculated via logistic transformation: $P=1/(1+exp^{-y})$. At an optimal probability threshold of 0.206, the model achieved 86.5% sensitivity and 79.5% specificity.

For example, for a child presenting with a 4.5 mm longitudinal suprapatellar double synovial thickness and a 1.5 mm transverse medial parapatellar fluid depth, the log odds (Y) are calculated as: Y = -6.149+1.743*4.5+1.236*1.5 = 3.5485. Applying the logistic transformation yields a predictive disease probability (P) of: $P= 1/1+exp^{-3.5485} = 0.972$. Because this probability (0.972 - 97.2%) vastly exceed the established diagnostic threshold of 0.206, the model classified the child as having a very high probability of active disease.

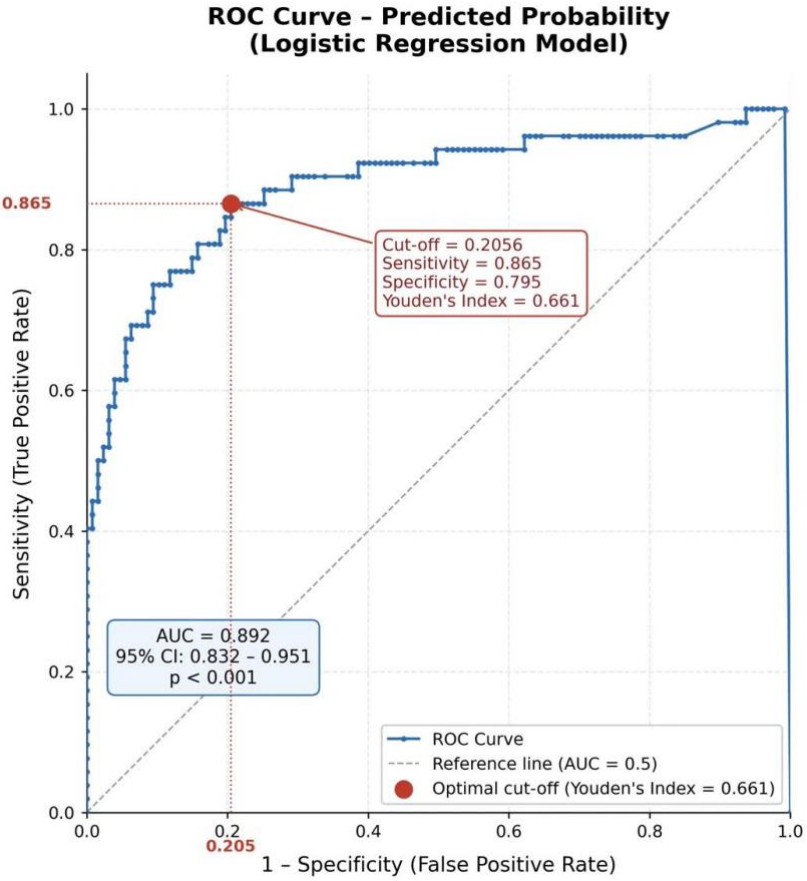


Fig 5. Receiver Operating Characteristic (ROC) curve of the multivariable disease prediction model. The model demonstrated strong discriminative performance with an area under the curve (AUC) of 0.892 (95% CI: 0.832–0.951). At the optimal probability threshold of 0.206, the model achieves 86.5% sensitivity and 79.5% specificity.

Discussion

We have shown that, in healthy volunteers, fluid within the knee joint predominantly accumulates in the suprapatellar recess, leaving the medial and lateral parapatellar recesses virtually dry. Conversely, JIA patients demonstrated a homogeneous, uniform fluid expansion across all three compartments, resulting in nearly identical median fluid depths across both the suprapatellar and parapatellar recesses. Another highly impactful observation is the finding of subclinical synovial thickening in the clinically "unaffected" knees of patients presenting with a strictly unilateral JIA history.

Interestingly, during provocation, no differences in the amount of fluid were seen in the suprapatellar recess between the two groups. We speculate that this may be due to difficulties in relocating fluid from the inflamed medial and lateral recesses amongst patients.

Our findings demonstrate that relying solely on a suprapatellar view risks a high false-positive rate, as innocent physiological fluid is common in healthy children in this region. Crucially, the presence of matching fluid expansion in the parapatellar recesses serves as a far more specific diagnostic marker for true inflammatory pathology. These findings strongly validate the 5-view imaging methodology advocated by the Paediatric Internationally agreed Ultrasound Knee Protocol (PIUS-Knee) [13] and highlight that parapatellar views must be treated as mandatory components rather than optional additions to the standard paediatric knee exam.

When analysing the 25 patients with an asymmetrical disease profile, the contralateral knee (which had never demonstrated clinical signs of swelling, pain, or limited mobility) exhibited a significantly thicker synovial membrane than the reference joints of the

healthy volunteer cohort ($p < 0.001$). These finding challenges traditional clinical diagnostic paradigms and underscores the superior sensitivity of MSUS over physical examination. The observed synovial thickening in clinically silent joints strongly supports the biological concept of a "subclinical systemic background" in JIA.

The inter-observer agreement and measurement reproducibility for the healthy volunteer cohort were rigorously evaluated and established in our previous publication [8]. In short, the inter-rater reliability analysis demonstrated excellent reproducibility across all standardized ultrasound metrics. Consequently, these validated imaging standards were strictly maintained throughout the current comparative study.

Even when active, hyperaemic inflammation seems isolated to a single knee joint, JIA operates as a systemic disease. Soluble pro-inflammatory cytokines (such IL-6 and TNF-alpha) circulate through the vasculature [14], potentially triggering low-grade, generalized synovial proliferation in anatomically distant joints [15, 16]. This systemic spillover is further evidenced by elevated serum levels of monocyte-derived alarmin proteins — MRP8/14 (S100A8/A9) and S100A12 — which persist even during apparent clinical remission, interacting with TLR4 on distant synovial endothelium to perpetuate subclinical inflammation [17-19].

Parallel cellular and neural pathways further prime remote sites. Activated memory T cells traffic from the index joint to distant synovium via chemokine gradients [20, 21], while tissue-resident memory T cells permanently established in previously inflamed synovium maintain joint-specific inflammatory memory even during clinical remission [22]. Furthermore, neuro-immune crosstalk through afferent cytokine receptor-bearing sensory neurons and efferent neuropeptide release further primes contralateral and distant joint synoviocytes [23, 24].

Because physical examination misses these early subclinical low-grade structural changes, MSUS is indispensable. It consistently identifies subclinical synovitis and tenosynovitis beyond clinical reach, frequently prompting reclassification from oligoarticular to polyarticular disease pathways [16, 25]. Early detection of this subclinical tissue proliferation potentially offers paediatric rheumatologists a window of opportunity to intercept phenotypic transition before irreversible structural damage occurs.

In a previous study establishing normative references of joint fluid and synovial thickness across sex and age groups, we demonstrated that girls had less joint fluid as compared to boys, and that the amount of fluid increased by age group [8]. Remarkably, these physiological sex- and age-dependent discrepancies were absent within the JIA cohort in the present study. This lack of demographic variation is probably likely due to higher volume inflammatory exudate and synovial hypersecretion associated with active arthritis, which effectively overwhelmed and masked the subtle underlying physiological baseline variations.

A similar pattern was observed regarding the qualitative presence of echogenic speckles within the fluid-filled recesses. While our healthy reference sample established that boys displayed a significantly higher baseline prevalence of intra-articular speckles [8], no such gender difference could be confirmed among the JIA patients. However, this interpretation must be approached with caution; the JIA cohort contained a substantially lower proportion of male participants (32.7%), a demographic skew typical of JIA epidemiology that may have underpowered the sub-analysis and hampered our ability to detect a true underlying difference.

In line with inflammatory pathology, absolute synovial thickness was significantly greater in the JIA patient cohort than in the healthy volunteer group. Interestingly, within

the JIA cohort, synovial thickness demonstrated no statistical relationship with advancing age categories. This contradicts the physiological baseline trends established in our healthy reference sample, where normal growth was characterized by a progressive, age-dependent thickening of the double-layer synovium [8]. This loss of physiological correlation indicates that the localized molecular drives of inflammatory tissue hypertrophy entirely supersede and obscure the normal structural trajectories of paediatric skeletal maturation.

While B-mode features can occasionally overlap between healthy growth and low-grade inflammation, colour Doppler signal within the synovial provided absolute diagnostic specificity, with a strictly negative signal observed across all healthy controls. This robustly supports international consensus guidelines positioning ultrasound as the definitive first-line diagnostic method [2]. However, we should highlight that physiological Doppler signal outside the synovial can be found in certain areas like in the cartilage, physis and fat pads, and should not be confused as an active inflammatory process (Figure 6) [8, 26].

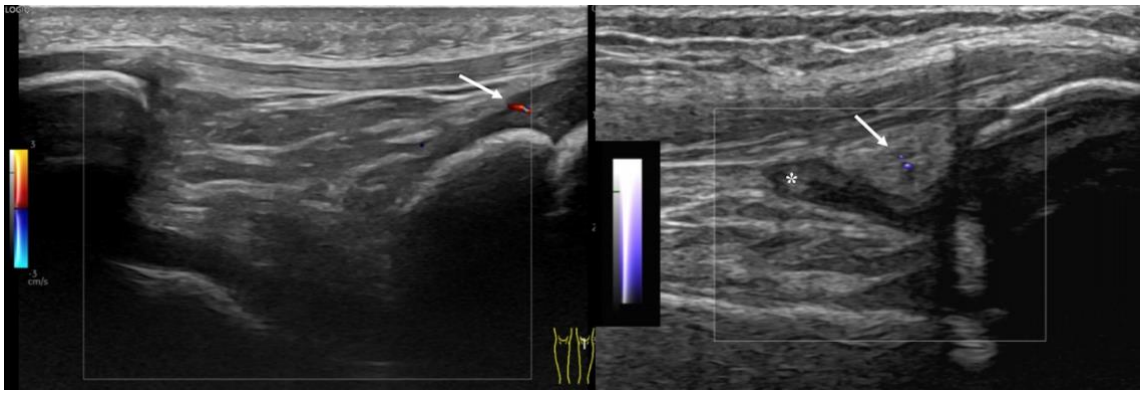


Fig 6. (a) An 8-year-old female healthy volunteer showing normal vessel within the anterior tuberosity cartilage (arrow) in the infrapatellar longitudinal view. (b) A 9-year-old male patient with JIA showing small physiological vascularity in the quadricipital fat pad (arrow) and also in synovial thickening without Micro-Doppler signal (asterisk) in the suprapatellar recess in longitudinal view.

Quantitative structural analysis of the distal femoral hyaline cartilage in our healthy cohort aligned robustly with the normative baselines established by Windschall et al.[6], Spannow et al. [27], and Gau et al.[28], confirming a physiological trajectory characterized by a progressive age-dependent thinning and a baseline dimorphism wherein girls exhibit thinner cartilage than boys. Crucially, when cross-examining the pathological sample, JIA female patients demonstrated a significantly thinner intercondylar cartilage layer compared directly to their age-matched healthy female peers. This accelerated thinning represents an objective imaging biomarker of early proteoglycan matrix degradation and chondrocyte depletion driven by chronic, low-grade intra-articular inflammation. While Sahin et al. [29] documented a cartilage profile comparable to our female cohort, their data did not adjust for biological sex, leaving their results potentially confounded by a heavy demographic skew toward female participants (77%).

Furthermore, our evaluation of the ossified patellar length uncovered striking biological contrasts to previous literature. While Windschall et al. [6] reported strict left-to-right symmetry in patellar dimensions among healthy children, our data revealed an asymmetric overgrowth pattern, with longer right patellar lengths documented across both cohorts. Most notably, the JIA patient cohort displayed significantly larger bilateral patellar dimensions than the healthy volunteers. This somatic acceleration is highly indicative of inflammatory-driven periarticular bone overgrowth, wherein active synovial hyperaemia stimulates the adjacent epiphyseal growth plates and accelerates ossification centres. The patella is considered an epiphyseal equivalent, being for this reason more susceptible to inflammatory conditions. This hypothesis is further reinforced by our maturational data; despite the JIA cohort skewing chronologically younger than the volunteer cohort, every JIA patient had already initiated bilateral patellar ossified nucleus

development, completely contrasting the incomplete ossification patterns expected and observed within the age-matched healthy reference sample.

A major methodological strength of this study lies in the strict standardization of the imaging workflow. Both the healthy volunteer and the JIA patient cohorts were evaluated using an identical scanning protocol, utilizing the exact same anatomical views, patient positioning, and optimized musculoskeletal pre-sets across two identical models of a high-end ultrasound system. Furthermore, inter-observer and machine-driven bias were minimised by having a single, highly experienced paediatric radiologist conduct all pathological examinations. This rigorous comparative framework ensures that the observed structural variations reflect true biological and pathological differences rather than bias and/or technical artifacts.

The two-variable predictive model demonstrated excellent discriminative capacity (AUC = 0.892) with a balanced, clinically meaningful sensitivity and specificity, underscoring its practical utility. Although generalizability across all disease subtypes requires caution, more than half of our cohort had persistent oligoarthritis, the subtype where knee involvement is most prevalent. This lends targeted relevance to our model. However, its clinical application must always be contextualized within the individual child's clinical presentation, ensuring other forms of arthritis are excluded during the diagnostic process.

Other limitations must be acknowledged. First, both arms of this investigation were designed as single-centre studies conducted within a single geographical region in Porto, Portugal. Second, the study population consisted entirely of Caucasian individuals, which may limit the direct generalizability of these normative and pathological metrics to ethnically diverse paediatric populations worldwide. Future multi-centre, international validation studies across heterogeneous demographic groups are warranted to confirm the universal applicability of these age- and sex-stratified thresholds.

Conclusion

Our findings demonstrate that JIA eradicates the asymmetric fluid topology naturally seen in healthy children, instead causing a uniform, homogeneous fluid expansion across all three knee recesses. The discovery of significant synovial thickening within the clinically "unaffected" knees of patients with a history of unilateral JIA confirms the presence of subclinical systemic joint involvement that remains elusive to conventional physical examination. Finally, the observed accelerated patellar ossification and significant cartilage thinning in JIA patients—stratified against the novel, sex- and age-specific normative reference limits provided herein—deliver powerful, objective imaging biomarkers to track early matrix degradation and periarticular bone overgrowth.

References

1. Thierry S, Fautrel B, Lemelle I, Guillemin F. Prevalence and incidence of juvenile idiopathic arthritis: a systematic review. Joint Bone Spine. 2014;81(2):112-710.1016/j.jbspin.2013.09.003.
2. Costa Dias S, Habre C, Di Paolo PL, d'Angelo P, Augdal TA, Angenete OW, et al. ESR Essentials: juvenile idiopathic arthritis; what every radiologist needs to know-practice recommendations by the European Society of Paediatric Radiology. Eur Radiol. 202510.1007/s00330-025-11891-9.
3. Pradsgaard DO, Fiirgaard B, Spannow AH, Heuck C, Herlin T. Cartilage thickness of the knee joint in juvenile idiopathic arthritis: comparative assessment by ultrasonography and magnetic resonance imaging. J Rheumatol. 2015;42(3):534-4010.3899/jrheum.140162.
4. Pradsgaard DO, Horlyck A, Spannow AH, Heuck C, Herlin T. A Comparison of Radiographic Joint Space Width Measurements Versus Ultrasonographic Assessment of Cartilage Thickness in Children with Juvenile Idiopathic Arthritis. J Rheumatol. 2019;46(3):301-810.3899/jrheum.170571.
5. Spannow AH, Stenboeg E, Pfeiffer-Jensen M, Fiirgaard B, Haislund M, Ostergaard M, et al. Ultrasound and MRI measurements of joint cartilage in healthy children: a validation study. Ultraschall Med. 2011;32 Suppl 1:S110-610.1055/s-0029-1245374.
6. Windschall D, Trauzeddel R, Haller M, Krumrey-Langkammerer M, Nimtz-Talaska A, Berendes R, et al. Pediatric musculoskeletal ultrasound: age- and sex-related normal B-mode findings of the knee. Rheumatol Int. 2016;36(11):1569-7710.1007/s00296-016-3528-x.
7. Collado P, Vojinovic J, Nieto JC, Windschall D, Magni-Manzoni S, Bruyn GA, et al. Toward Standardized Musculoskeletal Ultrasound in Pediatric Rheumatology: Normal Age-Related Ultrasound Findings. Arthritis Care Res (Hoboken). 2016;68(3):348-5610.1002/acr.22670.
8. Dias SC, Carvalho DC, Castro M, Dias CC, Ramos I, Brito I, et al. Knee-ultrasound: reference values for the amount of joint fluid and synovial appearances in healthy children and adolescents. Pediatr Radiol. 2025;55(6):1127-3710.1007/s00247-025-06243-0.
9. Petty RE, Southwood TR, Manners P, Baum J, Glass DN, Goldenberg J, et al. International League of Associations for Rheumatology classification of juvenile idiopathic arthritis: second revision, Edmonton, 2001. J Rheumatol. 2004;31(2):390-2
10. Dias SC, Ferreira CC, Santos I, Castro M, Rodrigues M, Aguiar F, et al. Reliability of CEUS and MRI for grading knee-joint inflammation in juvenile idiopathic arthritis. Eur Radiol. 202610.1007/s00330-026-12627-z.
11. Ting TV, Vega-Fernandez P, Oberle EJ, De Ranieri D, Bukulmez H, Lin C, et al. Novel Ultrasound Image Acquisition Protocol and Scoring System for the Pediatric Knee. Arthritis Care Res (Hoboken). 2019;71(7):977-8510.1002/acr.23746.
12. Terslev L, Iagnocco A, Bruyn GAW, Naredo E, Vojinovic J, Collado P, et al. The OMERACT Ultrasound Group: A Report from the OMERACT 2016 Meeting and Perspectives. J Rheumatol. 2017;44(11):1740-310.3899/jrheum.161240.
13. Windschall D, Trauzeddel R, Gohar F, Adiguzel-Dundar H, Hardt S, Krumrey-Langkammerer M, et al. Development and validation of a pediatric internationally agreed ultrasound knee synovitis protocol (PIUS-knee) by the PReS imaging working party. Pediatr Rheumatol Online J. 2024;22(1):9410.1186/s12969-024-01029-4.
14. de Jager W, Hoppenreijs EP, Wulffraat NM, Wedderburn LR, Kuis W, Prakken BJ. Blood and synovial fluid cytokine signatures in patients with juvenile idiopathic arthritis: a cross-sectional study. Ann Rheum Dis. 2007;66(5):589-9810.1136/ard.2006.061853.
15. Haslam KE, McCann LJ, Wyatt S, Wakefield RJ. The detection of subclinical synovitis by ultrasound in oligoarticular juvenile idiopathic arthritis: a pilot study. Rheumatology (Oxford). 2010;49(1):123-710.1093/rheumatology/kep339.

16. Magni-Manzoni S. Ultrasound in juvenile idiopathic arthritis. Pediatr Rheumatol Online J. 2016;14(1):3310.1186/s12969-016-0096-2.
17. Gerss J, Roth J, Holzinger D, Ruperto N, Wittkowski H, Frosch M, et al. Phagocyte-specific S100 proteins and high-sensitivity C reactive protein as biomarkers for a risk-adapted treatment to maintain remission in juvenile idiopathic arthritis: a comparative study. Ann Rheum Dis. 2012;71(12):1991-710.1136/annrheumdis-2012-201329.
18. Foell D, Wulffraat N, Wedderburn LR, Wittkowski H, Frosch M, Gerss J, et al. Methotrexate withdrawal at 6 vs 12 months in juvenile idiopathic arthritis in remission: a randomized clinical trial. JAMA. 2010;303(13):1266-7310.1001/jama.2010.375.
19. Vogl T, Tenbrock K, Ludwig S, Leukert N, Ehrhardt C, van Zoelen MA, et al. Mrp8 and Mrp14 are endogenous activators of Toll-like receptor 4, promoting lethal, endotoxin-induced shock. Nat Med. 2007;13(9):1042-910.1038/nm1638.
20. Buckley CD. Michael Mason prize essay 2003. Why do leucocytes accumulate within chronically inflamed joints? Rheumatology (Oxford). 2003;42(12):1433-4410.1093/rheumatology/keg413.
21. Hwang SH, Jung SH, Lee S, Choi S, Yoo SA, Park JH, et al. Leukocyte-specific protein 1 regulates T-cell migration in rheumatoid arthritis. Proc Natl Acad Sci U S A. 2015;112(47):E6535-4310.1073/pnas.1514152112.
22. Chang MH, Levescot A, Nelson-Maney N, Blaustein RB, Winden KD, Morris A, et al. Arthritis flares mediated by tissue-resident memory T cells in the joint. Cell Rep. 2021;37(4):10990210.1016/j.celrep.2021.109902.
23. Andersson U, Tracey KJ. Neural reflexes in inflammation and immunity. J Exp Med. 2012;209(6):1057-6810.1084/jem.20120571.
24. Chavan SS, Pavlov VA, Tracey KJ. Mechanisms and Therapeutic Relevance of Neuro-immune Communication. Immunity. 2017;46(6):927-4210.1016/j.immuni.2017.06.008.
25. Quesada-Masachs E, Lopez-Corbeto M, Moreno-Ruzafa E. Ultrasound in pediatric rheumatology: Highlighting the differences with adults. Eur J Rheumatol. 2022;11(3):S348-S5710.5152/eujrheum.2022.21119.
26. Collado P, Windschall D, Vojinovic J, Magni-Manzoni S, Balint P, Bruyn GAW, et al. Amendment of the OMERACT ultrasound definitions of joints' features in healthy children when using the DOPPLER technique. Pediatr Rheumatol Online J. 2018;16(1):2310.1186/s12969-018-0240-2.
27. Spannow AH, Pfeiffer-Jensen M, Andersen NT, Herlin T, Stenbog E. Ultrasonographic measurements of joint cartilage thickness in healthy children: age- and sex-related standard reference values. J Rheumatol. 2010;37(12):2595-60110.3899/jrheum.100101.
28. Gau CC, Yao TC, Gan ST, Lin SJ, Yeh KW, Chen LC, et al. Age, gender, height and weight in relation to joint cartilage thickness among school-aged children from ultrasonographic measurement. Pediatr Rheumatol Online J. 2021;19(1):7110.1186/s12969-021-00554-w.
29. Sahin N, Ozdemir Cicek S, Pac Kisaarslan A, Dursun I, Poyrazoglu MH, Dusunsel R. The effect of intra-articular steroid injection on the cartilage and tendon thicknesses in juvenile idiopathic arthritis. Mod Rheumatol. 2024;34(4):791-710.1093/mr/road093.

Acknowledgements:

The authors express their sincere gratitude to all the patients, volunteers and their parents/caregivers for their time, trust, and active cooperation, which made this study possible.

DISCUSSION

DISCUSSION

As a critical first step toward a meaningful interpretation of imaging findings in pathologic knee joints, we sought to establish normative ultrasound reference values in healthy children. This initiative aligns with the European Society of Paediatric Radiology (ESPR) Musculoskeletal Taskforce's ongoing open research project to update normative ultrasound references across all paediatric joints.

Specifically, regarding the knee, a review of the literature revealed a lack of studies differentiating joint fluid measurements from synovial thickness, as well as limited data on how knee positioning and dynamic manoeuvre influence fluid distribution. To address these gaps, we developed a comprehensive, Doppler ultrasound protocol. This protocol was designed to clarify these physiological variables in healthy subjects, providing a robust baseline for later application in patient cohorts.

Subsequently, we collaborate in the development of practice recommendations endorsed by the European Society of Paediatric Radiology and the European Society of Radiology (ESR) on the appropriate use of imaging modalities, including ultrasound, MRI, radiography, and CT, for the diagnosis and monitoring of JIA. Within these recommendations, the critical role of normative reference standards was emphasised, and existing joint-specific scoring systems across different imaging techniques for JIA patients were comprehensively reviewed. This work culminated in the proposal of a multimodality diagnostic imaging algorithm designed for clinical application in children with suspected JIA.

The remaining three papers constitute the core results of this thesis (Papers 3, 4, and 5). To rigorously evaluate these advanced imaging techniques for synovitis assessment, it was critically important to first establish their reproducibility and consistency (Paper 3). Building upon this framework of reliability, the cornerstone of this thesis evaluates their diagnostic accuracy and clinical feasibility (Paper 4). To synthesise these findings, Paper 5 compares ultrasound characteristics between healthy volunteers and JIA patients using an identical protocol. These comparative data enabled the development of a predictive model that estimates the probability of JIA based on specific ultrasound features. Consequently, this thesis follows a sequential chain of methodological and clinical

inquiries: Are these measurement tools reliable? Are they diagnostically accurate? And what incremental value do they offer beyond clinical and conventional Doppler ultrasound assessment? This progression mirrors the hierarchical framework for evaluating clinical imaging efficacy described by Thornbury [87]. This model dictates that technical validity and reproducibility must be established before diagnostic accuracy claims can be assessed, and accuracy verified before clinical utility can be asserted. Together, the foundational normative work (Paper 1) and the ESPR practice recommendations (Paper 2) provide the indispensable framework encompassing these questions.

Research Line I

The Normative Ultrasound values and Imaging Recommendations in JIA; (Papers 1&2)

In the first prospective study [88], a normative ultrasound reference standard for the paediatric knee was established using a school population cohort of 127 healthy volunteers (254 knees) aged 3–17 years. This work represents the first in the literature to distinctly quantify joint fluid separate from synovial thickness, considering the influence of age, sex, and physical activity levels.

A central finding of this study was the presence of measurable joint fluid in 75.6% of healthy children in at least one of the suprapatellar recesses, when examined at 30° of knee flexion. Crucially, a significant reduction in fluid volume was observed during knee extension. This emphasises the critical importance of standardised joint positioning during ultrasound examinations; specifically, maintaining approximately 30° of flexion is essential to avoid underestimating fluid volume, a risk that increases in full extension. In comparison, Windschall et al. [89] performed supra- and parapatellar scans in a "neutral" position, which likely yielded smaller fluid measurements. Furthermore, their approach measured total recess depth, thereby merging joint fluid with double-layer synovial thickness into a single measurement. While Collado et al. [90] did utilise 30° of flexion, they applied firm transducer compression during measurement. This manoeuvre inevitably displaces joint fluid, meaning their lower values likely reflected synovial thickness alone rather than a true fluid measurement.

Another interesting finding was that significantly more joint fluid was detected in males and in children with a higher number of weekly sports hours. While this relationship between joint fluid and athletic activity has been previously documented in adults using post-exercise MRI [91, 92], our study is the first to demonstrate this association in a paediatric population. This increase in fluid volume may be interpreted as an adaptive physiological response designed to protect the joint against the mechanical stress imposed by physical exercise.

The presence of echogenic speckles within the joint fluid as a normal phenomenon, observed in 25% of healthy children and predominantly in physically active males,

represents a novel finding in the literature. While the clinical significance of these speckles remains to be fully elucidated, we hypothesise that they may be related to joint fluid viscosity or specific biochemical components. In an adult population with knee osteoarthritis, Miyaguchi et al. [93] demonstrated through fluid analysis that 12 weeks of exercise significantly increased both synovial fluid viscosity and the molecular weight of hyaluronan. Given that normal joint fluid contains a high concentration of hyaluronan, synthesised by synovial cells, which influences joint lubrication and cartilage metabolism, the visible speckles in active children might reflect a physiological alteration in fluid composition or viscosity induced by repetitive mechanical loading [94-96].

Our study was the first to distinctly separate joint fluid from synovial tissue measurements within the suprapatellar recess. This differentiation helps understand the nature of synovitis in children with JIA. By applying gentle transducer compression to displace the fluid, we quantified the synovium as a double-layer thickness. Although we also tested single-layer ultrasound measurements, the results lacked consistency, likely due to the narrower range of values and the technical challenges in isolating a single layer in the absence of fluid. Interestingly, the median double-layer synovial thickness in our healthy cohort was around 2 mm for the older age group. This is the exact cut-off used in the JAMRIS knee MRI scoring system for synovitis [19]. Similarly, an MRI study of healthy children reported that synovial thickness did not exceed 1.8 mm [97]. While a direct comparison between ultrasound and MRI requires caution due to inherent technical differences, our findings strongly raise awareness regarding the clinical application of such a rigid cut-off. Our results demonstrate that the synovium is thicker in older children, exhibiting a relatively wide 2.5^{th} – 97.5^{th} percentile interval (e.g. 1.3-3.9 mm in the 10-13 years group).

Another relevant finding from our study was the complete absence of colour Doppler signals within the synovium across all 127 healthy volunteers (254 knees), despite the easy identification of vessels in adjacent structures, such as those within the epiphyseal cartilage. This lack of vascular flow in healthy synovium suggests that detectable Doppler signal within the synovial tissue is unlikely to reflect normal physiological signal. A limitation of this initial phase was the lack of microvascular Doppler imaging technology;

however, we subsequently addressed this by integrating advanced micro-Doppler techniques into the ultrasound protocol for our clinical patient cohort.

A.1. Statistical considerations

We acknowledge that stratifying a cohort of 127 participants into four age groups and further by sex produces relatively small sub-groups for isolated non-parametric reference interval calculations. However, several factors mitigate this limitation. First, our bilateral scanning protocol provided 254 knee US to evaluate intra-subject symmetry. Apart from the lateral parapatellar recess, where fluid volume was slightly greater on the right side ($p=0.004$), the amount of joint fluid did not differ significantly between the left and right knees. Regarding synovial thickness, significant differences were found according to age groups, whereas no significant side-to-side variation was observed. Consequently, to maintain statistical integrity and avoid the artificial inflation of sample size through highly correlated bilateral data, the primary reference metrics for both joint fluid and double-layer synovial thickness are reported for the right knee only.

Second, our primary clinical objective was not to establish rigid, micro-stratified sub-group thresholds, but rather to map the broader physiological continuum of the paediatric knee. Finding a 97.5th percentile of 3.9 mm in healthy 10–13-year-olds provides crucial, biologically driven evidence that healthy children routinely exceed current 2.0 mm diagnostic cut-offs, a conclusion that remains clinically robust despite sub-group sample size limitations.

A.2. From Normative Data to Imaging Recommendations

Paper 2 contextualises all available joint-specific normative data as essential, *a priori* information required to evaluate a child with suspected JIA. Furthermore, all specific validated JIA joint scoring systems across different imaging modalities are compiled, serving as a practical guide for radiologists on what pathological features to evaluate in each particular joint.

For the MRI protocol, we deliver a concise, one-page reference table covering all major joints; this matrix outlines current standard sequences alongside innovative sequences. Non-contrast sequences, such as FLAIR-FS, are highlighted as viable additions for the assessment of synovitis, encouraging their clinical adoption to generate more robust scientific data in the paediatric field. Finally, this paper provides a practical clinical imaging pathway for the workup of JIA patients, which aligns seamlessly with the overarching objective of this thesis.

B. Research Line II

Reliability of CEUS, FLAIR-FS and CEMRI and the Diagnostic Accuracy of the new methods (CEUS and FLAIR-FS) compared to the Gold Standard (CEMRI); (Papers 3&4)

Following the establishment of normative reference boundaries and clinical imaging guidelines, this phase of the thesis evaluates the clinical performance of advanced imaging modalities in JIA patients. Specifically, Paper 3 assesses the inter-observer reliability and reproducibility of CEUS, and CEMRI.

The reliability of FLAIR-FS is addressed in Paper 4. Building upon this framework of reliability, the core aim of Paper 4 is to determine the diagnostic accuracy and clinical feasibility of these two innovative gadolinium-free alternatives (FLAIR-FS and sedation-free CEUS), compared directly against the current gold standard (CEMRI) for detecting and grading knee synovitis

B.1. Methodological reliability and spatial perfusion limits (Paper 3)

The results of Paper 3 provide the mandatory methodological validation required before considering shifting clinical paradigms toward gadolinium-free or bedside imaging in juvenile idiopathic arthritis [87]. Our findings demonstrate that the semi-quantitative 0–3 visual grading system is robust, yielding almost perfect inter-observer agreement across both CEUS (kappa = 0.85) and CEMRI (kappa = 0.92). This high reproducibility confirms that visual grading is a stable imaging biomarker, independent of individual reader subjectivity. In comparison with the initial multi-centre validation of the JAMRIS system, where only ICCs were available, our results revealed an interobserver ICC of 0.97 (95% CI 0.95–0.98) with two readers, whereas the JAMRIS inter-observer ICC value for knee synovitis was 0.95 (95 % CI 0.91–0.97) across 5 readers [19].

Our CEUS visual agreement surpassed the PDUS live score reported by Sande et al. [98] (interobserver kappa = 0.60). This high level of reproducibility is a direct consequence of the methodological work established in paper 1; by mandating a strict 30° knee flexion protocol and utilizing dynamic loop reviews rather than static images, we successfully

minimised reader subjectivity and eliminated the spatial confounding of joint fluid and synovium. Ultimately, these robust findings support the reliable translation of both modalities into clinical practice for longitudinal paediatric monitoring.

When evaluated against the existing literature, the performance of the CEMRI protocol and its quantitative perfusion tracking in this thesis demonstrates important methodological nuances. Historically, the integration of quantitative perfusion or Dynamic Contrast-Enhanced MRI (DCEMRI) in JIA has been restricted by the small, irregular morphology of paediatric joints and a lack of standardised post-processing workflows. Previous paediatric DCEMRI studies, such as those by Hemke et al. [99] and Nusman et al. [100], have shown that while quantitative parameters can correlate well with macroscopic disease activity, reproducibility can be compromised due to variations in protocols and how software algorithms define synovial boundaries.

Our findings contribute to further discussion in this topic. While software-derived metrics like WiAUC (CEUS) and PEI/iAUC (CEMRI) demonstrated near-perfect ICCs (> 0.97), their wide Bland-Altman 95% limits of agreement dictate clinical caution. This discrepancy underscores that while these parameters are highly capable of ranking disease severity relative to a cohort, their absolute numerical values fluctuate between observers. Consequently, for longitudinal treatment monitoring, relying on absolute perfusion values may introduce artificial variability. This volatility is likely driven by the technical difficulty of drawing manual Regions of Interest (ROIs) along the microscopic, irregular borders of the paediatric synovium, proving that even automated tools are vulnerable to boundary definition errors.

In the broader context of musculoskeletal MRI, authors who rely only on relative reliability metrics like the ICC frequently overestimate the readiness of software tools (such as Syngo.via®) for routine multi-centre clinical trials. By explicitly identifying the wide Bland-Altman limits of agreement for CEMRI iAUC and PEI, this study highlights that while a single software platform can reliably separate severe synovitis from mild changes across a patient population, the absolute numbers are too observer-dependent to track subtle, millimetre scale changes in an individual child over time.

Peak Enhancement (PE) on CEUS demonstrated excellent ICCs (0.99); however, even wider limits of agreement were obtained, demonstrating poor interobserver reproducibility.

Conversely, Time to Peak (TTP) performed poorly across both modalities, likely due to its dependency on patient-specific haemodynamic and injection velocity, suggesting it should be excluded from routine JIA monitoring protocols. This systematic failure across entirely different imaging platforms aligns with broader paediatric perfusion literature, proving that TTP is deeply confounded by extrinsic factors such as patient-specific cardiac output, variable heart rates, manual contrast bolus injection velocities and even the catheter calibre. Therefore, this thesis delivers a clear recommendation to the paediatric radiology community to transition away from TTP-driven kinetics. This critique of TTP is highly consistent with previous perfusion literature [101-103], yet its confirmation in our paediatric cohort reinforces that rapid, automated temporal parameters are fundamentally unsuitable for a population with highly dynamic resting heart rates and variable peripheral venous access.

Ultimately, the fact that CEUS mirrored the reproducibility of the current reference standard (CEMRI) provides compelling justification for its integration into serial imaging algorithms, matching diagnostic stability while eliminating paediatric sedation and gadolinium accumulation risks. By matching the exact reliability profile of a 3T CEMRI reference standard, we effectively dismantle the historical bias that ultrasound is too operator-dependent to serve as a primary imaging tool. This identical reliability satisfies the primary prerequisite for clinical paradigm replacement, validating our standardised CEUS protocol as a highly dependable surrogate for serial disease tracking.

B.2. Clinical Validation and Diagnostic Accuracy of CEUS and FLAIR-FS (Paper 4)

While Paper 3 established the stability and reproducibility of these advanced imaging tools, Paper 4 evaluates their true diagnostic capability and accuracy when compared directly against the reference standard (CEMRI). A major methodological advantage of this validation phase, which directly resolves a profound gap in the existing literature, is the integration of our sex- and age-matched healthy volunteer group (n = 51). By mapping

the appearance of the unenhanced knee synovium under strict physiological conditions using our optimised 3 Tesla FLAIR-FS parameters (TE = 87 ms; TI = 2200 ms; flip angle = 150°), we were uniquely positioned to determine whether this non-contrast sequence could maintain high specificity and safely prevent false-positive overdiagnosis in healthy children.

CEUS achieved a sensitivity of 97.6% (95% CI: 87.4–99.9%) and an area under the receiver operating characteristic curve (AUC) of 0.899 (95% CI: 0.809–0.989), representing the highest sensitivity among all evaluated modalities. However, its specificity was only moderate at 50.0% (95% CI: 18.7–81.3%).

For fluid-attenuated inversion recovery fat-suppressed (FLAIR FS) MRI, the sensitivity for detecting inflammation was 92.9% (95% CI: 80.5–98.5%), with a specificity of 60.0% (95% CI: 26.9–87.8%) and an AUC of 0.879 (95% CI: 0.778–0.980). These results align with previous literature. The original study by Yoo et al. [35] demonstrated that FLAIR-FS provides good diagnostic performance for synovitis of any severity, reporting site-level and patient-level accuracies of 92.1–93.9% and 90.9%, respectively. Conversely, evaluating Hoffa synovitis on unenhanced MRI yielded only moderate sensitivity (78.9–87.5%) and low specificity (47.1–64.3%). Across previous global assessments, sensitivity ranged from 78.9% to 92.3%, specificity from 47.1% to 95.0% [35, 38, 39].
The accuracy for FLAIR-FS in our study was 86.5% (95% CI 74.2-94.4) when compared to CEMRI, with a similar result obtained by the paediatric JIA study. Milks et al. [39] revealed an accuracy for the 2 readers of 83% (95% CI 0.69-0.93) and 86% (95% CI 0.71-0.95). Our obtained AUC value of 0.879 reveals a good-to-excellent discriminative range of the model.

The low specificity observed in both techniques can be partially attributed to the small number of negative CEMRI cases in our sample (10 cases with a score of 0, compared to 18 cases with a score of 1). Because the specificity formula (Specificity = True Negatives / (True Negatives + False Positives)) depends entirely on the number of true negative cases, a small denominator ensures that each misclassified negative case exerts a disproportionately large impact on the final estimate. Furthermore, rather than relying strictly on the Youden index (J), we selected an optimal cut-off value based on the clinical context to favour higher sensitivity. This addresses a critical clinical need, as clinicians

generally require high sensitivity to avoid missing active inflammation, even at the expense of lower specificity.

As anticipated, inter-technique agreement with CEMRI was higher for FLAIR-FS than for CEUS, likely due to the shared methodological nature of evaluating the same imaging modality (MRI). Nevertheless, the agreement between CEMRI and CEUS for grading inflammatory changes on a 0–3 scale remained good, with a weighted kappa of 0.64 (95% CI: 0.51–0.76) and an absolute agreement of 59.6% (where disagreement never exceeded a single grade). Agreement between CEMRI and FLAIR-FS was almost perfect, yielding a weighted kappa of 0.85 (95% CI: 0.76–0.95) and an absolute agreement of 85.0%. Crucially, no prior studies investigating non-contrast sequences for synovitis assessment, in either adult or paediatric populations, have included healthy volunteers as a comparator group. Consequently, our study is the first capable of confirming that these sequences remain negative in truly healthy paediatric knees.

B.2.1. Visual scoring system on a 0-3 scale

The use of a 0–3 subjective grading scale was a deliberate methodological choice with important clinical implications. This scale aligns directly with grading systems used in daily practice for both ultrasound and MRI synovitis assessments. Consequently, it is clinically intuitive, rapidly applicable, and requires no dedicated software or post-processing.

In contrast, multi-domain instruments like the JAMRIS scoring system for the knee [19], which encompasses synovial hypertrophy, bone marrow oedema, cartilage loss, and erosions, require systematic scoring across multiple anatomical sites. This process is often too time-consuming for routine clinical practice.

B.2.2. Challenges related to imaging Bone Marrow Oedema

More critically, the BMO domain requires particular caution in paediatric populations. Studies from the Norwegian whole-body MRI working group have documented that BMO-like changes are frequent normal findings in healthy growing bones, affecting the metaphyses and epiphyses of both the appendicular and axial skeleton [104-106]. Without age-appropriate reference standards, these normal maturational changes can be indistinguishable from pathological oedema. This challenge is directly corroborated by the moderate interobserver agreement for BMO in our Paper 3 data (ICC 0.65; 95% CI

0.39–0.80), which contrasts sharply with the almost perfect agreement for overall synovial inflammation scoring. This discrepancy reflects the difficulty of defining BMO beyond normal variation in the growing skeleton. By focusing on overall synovial inflammation rather than individual structural domains, our 0–3 scale avoids these pitfalls and provides highly reliable, clinically practical grading.

B.2.3. Misclassifications on FLAIR-FS and CEUS vs CEMRI

The previously reported FLAIR-FS tendency to underestimate synovitis was not clearly observed in our study; we identified three false negatives, graded as 0 and in CEMRI they were graded as mild (rather than moderate or severe synovial inflammation). We had one additional case of underestimation, being classified as moderate inflammation on FLAIR-FS and as severe in CEMRI. And we had four false positives in FLAIR-FS classified as mild when they were 0 in CEMRI.

For CEUS, there was a clear tendency to over diagnose synovitis compared to CEMRI, yielding five false positives (all scored as mild inflammation on CEUS) and only one false negative, which was classified as a mild case on CEMRI.

Altogether, this mainly reflects the known difficulties, in both techniques, in the differentiation between physiological and mildly increased synovial enhancement.

B.2.4. MRI FLAIR-FS; limitations and pitfalls

FLAIR-FS has several inherent limitations, such as the inability to reliably distinguish proteinaceous or haemorrhagic fluid from synovial tissue, residual signal in large effusions when TI calibration is imperfect, and signal alterations following intra-articular corticosteroid injections. Radiologists must be aware of these limitations when incorporating FLAIR-FS into clinical protocols.

In our FLAIR-FS studies, we observed a cartilage-related pitfall previously reported by Yoo et al. [35]. These authors noted that the most superficial layer of patellar articular cartilage appeared hyperintense on FLAIR-FS images, creating the false impression that the synovial lining was continuous over the articular cartilage. While they described this artefact at that specific anatomical site in adults, our evaluation of paediatric examinations revealed this pitfall in additional locations, such as the tuberosity cartilage. Because FLAIR-FS nulls free fluid and fat signals, tissues with intermediate T1 signals remain

visible. This includes not only the synovium but also, and most notably, the superficial zone of articular cartilage, which possesses a higher water content and a different collagen fibre orientation than deeper zones.

Furthermore, in paediatric populations, we must account for thicker overall cartilage with higher water content across all zones compared to adults. Consequently, the T1 contrast between the superficial and deep zones is less distinct, and the overall cartilage signal is globally elevated on fluid-sensitive sequences. Compounding this challenge, the epiphyseal cartilage exhibits an even higher water content, appearing hyperintense on FLAIR-FS. This represents a highly specific paediatric pitfall that radiologists must recognise, as it poses an interpretive challenge that increases the risk of overestimating synovitis.

B.3. Performance of Doppler, Microvascular Doppler Imaging

Conventional colour and power Doppler performed poorly (Paper 4). Although the complete absence of a Doppler signal in all 127 healthy volunteers bilaterally confirms near-perfect specificity, sensitivity can be sacrificed in patients, in cases of early/mild inflammation. This reflects the well-established limitation of conventional Doppler in detecting slow microvascular flow. Microvascular Doppler (MD) Imaging represents a promising intermediate modality. Alis et al. [15] demonstrated that Superb Microvascular Imaging (SMI) (a vendor specific Microvascular Doppler Imaging) was superior to PDUS in depicting synovial vascularity in JIA knees. Similarly, Diao et al. [107] found no significant differences in sensitivity between SMI and CEUS for detecting synovial vascularity in a cohort of 63 patients with active RA and 48 patients in clinical remission.

A multicentre prospective repeatability study of SMI [16] in 76 children with JIA reported excellent intraobserver reliability (ICC 0.972) and strong interobserver reliability (ICC 0.828–0.928), independent of examiner experience, further supporting its potential as a contrast-free monitoring tool. The investigators utilised a clinical grading system similar to ours: 0 (clinically normal), 1 (mild/equivocal), 2 (active), and 3 (highly active), defining a score of ≥ 2 as clinically active arthritis. In contrast, our clinical scale comprised only three grades: 0 (normal), 1 (equivocal), and 2 (active), and for our ROC analysis, we considered scores ≥ 1 as positive.

When comparing populations, they evaluated synovial vascularity and clinical scores in 75 participants, finding that 35 cases (47%) met the criteria for active disease, while 40 cases scored ≤ 1. In our cohort of 52 cases, we observed only three clinically equivocal cases and nine active cases (17%). There is a substantial difference in the clinical proportions of active/inactive patients. In their study, discordant cases included three clinically normal joints (score 0) that exhibited synovial vascularity grades 2–3 (suggesting subclinical arthritis), 10 participants with a clinical score of 1 but elevated vascularity grades (grades 2–3), and six clinically active cases (score ≥ 2) showing no hypervascularity. In our study population, colour and power Doppler performed poorly, with MD yielding only slight improvements; this finding diverges from the established Doppler literature.

MD employs advanced clutter-filter algorithms to suppress motion artefact, while preserving slow microvascular flow signals, detecting a layer of synovial vascularity that colour and power Doppler routinely miss [16]. SMI has repeatedly graded synovial vascularity higher than power Doppler in the same joints, with one direct comparison reporting a mean SMI score of 1.1 against a mean power Doppler score of 0.3 in patients with confirmed synovitis ($p < 0.01$) [108]. Alis et al. [15] formalised this advantage specifically in the JIA knee, demonstrating measurable incremental diagnostic yield over power Doppler. Quantitative SMI vascular indexes have been shown to correlate with circulating inflammatory markers including ESR, CRP, and serum amyloid A, and to predict disease relapse in patients otherwise classified as clinically inactive [109]. A systematic review in adults of SMI across rheumatic disease further consolidated these findings, identifying consistent superiority over conventional Doppler in detecting low-grade and subclinical synovial vascularity [110]. This supports a tiered strategy: using conventional Doppler first, followed by MD imaging if subclinical inflammation is still suspected. However, our patient cohort did not replicate this high sensitivity with MD imaging, suggesting that its clinical performance may vary outside controlled research settings.

We collect the available data comparing the different Doppler modalities and CEUS (Table 2) in synovitis (including RA and JIA). Published studies in JIA compare SMI vs power Doppler only, being the key papers: Alis et al. [15], Kandemirli et al. [111], Sun et al. [109] and Windschall et al. [108]. Every one of these studies compares SMI against

power Doppler ultrasound; with superiority of MD. None includes colour Doppler as a third comparator arm. To our knowledge, Paper 4 of this thesis represents the first direct head-to-head comparison of colour Doppler, power Doppler, and MD Imaging within the same JIA cohort, revealing equivalent performance between the two conventional modalities and superior sensitivity of MD for synovial inflammation

Parameter	CD	PD	MD	CEUS
Min. detectable flow	**≥~3 cm/s** [112, 113] wall filter limit	**~1–3 cm/s** [112, 113] wall filter limit	**<~0.1 cm/s** [112] SVD adaptive filter	**<<0.1 cm/s** [107, 112] microbubble signal
Inter-rater reliability (ICC/κ) synovitis	JIA: used previously	**RA:** MCP live — Inter κ 0.79 **RA:** Non-MCP still — Inter κ 0.86 (mean) **RA:** Non-MCP live — Inter κ 0.61 (mean) [114] **JIA:** still — κ: Intra 0.91 / Inter 0.80 **JIA:** still — ICC: Intra 0.96 / Inter 0.97 **JIA:** live — Inter only: κ 0.60 / ICC 0.91 [98]	**JIA:** Intra ICC 0.97 Inter ICC 0.83–0.93 [16]	**RA:** Inter κ 0.62-0.82 [115] **JIA**: Intra κ 0.89–0.90 / Inter κ 0.85 ICC: Intra 0.97 / Inter 0.96 [86]
Vascularity detection (synovitis) ***Diao:*** *CEUS vs MDI* ***Polido:*** *CEUS vs CDI/PDI*	Classically: lower than PDI in small vessels	Reference standard in use	**MDI vs PDI — RA:** 60.4% vs 25.6% [116] **JIA:** SMI > PDI across all studies [15, 108, 109, 111]	**Klauser:** CEUS 97.3% vs 60.1% (US+PDUS) [RA, n=113] [49] **Diao:** CEUS = MDI [RA, n=111] [107] **Polido:** CEUS 83.8% vs 49.2% DUS (CDI+PDI combined) [RA, 23 studies] [50]
Contrast agent required	No	No	No	**Yes** — SonoVue IV injection [86, 107]

Table 2. Comparative Modality Performance. CD (colour Doppler); PD (power Doppler); MD (micro-Doppler); CEUS (contrast-enhanced ultrasound); ICC (intraclass correlation coefficient); RA (rheumatoid arthritis); JIA (juvenile idiopathic arthritis)

B.4. Performance of Clinical examination

The finding that clinical assessment demonstrated limited discriminative performance relative to CEMRI (Paper 4) reflects a recognised limitation of physical examination in detecting low-grade or subclinical synovitis, rather than a failure of clinical assessment as a whole. Multiple studies have demonstrated the superiority of imaging over clinical examination for detecting synovitis, particularly at the mild end of the inflammatory spectrum. Magni-Manzoni et al. [117] confirmed that ultrasound outperforms clinical examination; in their study, 104 joints (6.3%) exhibited clinical synovitis, whereas 167 joints (10%) demonstrated ultrasound-detected synovitis. Of the 1,560 clinically normal joints, 86 (5.5%) had subclinical synovitis. Consequently, ultrasound findings led to the reclassification of five patients as having polyarthritis who had originally been classified as having oligoarthritis or no synovitis on clinical evaluation.

Similarly, Malattia et al. [118] showed that clinical criteria are insensitive to low-level inflammation in JIA patients evaluated for treatment efficacy. Nonetheless, clinical examination remains the cornerstone of JIA disease activity scoring. It is highly sensitive to moderate-to-severe synovitis and provides essential contextual information, such as pain, range of motion, and global assessment, that imaging cannot capture. Imaging thus provides complementary data at the lower end of the inflammatory spectrum, extending rather than replacing clinical assessment.

B.5. Statistical considerations

A major critical contribution of this thesis is the elucidation of the fundamental methodological distinction between relative and absolute reliability metrics when evaluating quantitative software analysis. In adult RA literature, investigators frequently propose software-driven quantification as the objective future of imaging based solely on excellent ICCs, which routinely fall between 0.85 and 0.95. However, our study introduces a mandatory methodological warning to the field by demonstrating how a high ICC can mask substantial absolute variance.

While software-derived metrics like PE/WiAUC (CEUS) and PEI/iAUC (MRI) demonstrated near-perfect ICCs (> 0.97), their wide Bland-Altman 95% limits of agreement dictate clinical prudence. This discrepancy underscores that while these

parameters are highly capable of ranking disease severity relative to a cohort, their absolute numerical values fluctuate between observers. Consequently, for longitudinal treatment monitoring, relying on absolute perfusion values may introduce artificial variability.

Statistically, this divergence occurs because the ICC reflects relative reliability, confirming that both readers successfully rank patients from least to most inflamed in an identical sequence, whereas the Bland-Altman limits of agreement quantify the absolute difference between individual measurements. In clinical practice, this absolute consistency is paramount. The volatility in absolute values observed in our study is likely driven by the technical difficulty of drawing manual ROIs along the microscopic, irregular borders of the paediatric synovium, proving that even automated tools remain vulnerable to subtle inter-observer variations in boundary definition.

C. Research Line III

Ultrasound Comparison: Healthy Volunteers Versus JIA Patients; (Paper 5)

C.1. How different are our patients from the healthy volunteers?

Placing JIA patients and healthy volunteers side by side within a rigorously standardised imaging framework exposed a series of differences that collectively redefine what a normal paediatric knee looks like under ultrasound and, crucially, what it does not.

One of the most compelling divergences concerned the distribution of intra-articular fluid. Healthy knees at 30 degrees of flexion follow a predictable anatomical hierarchy: fluid gravitates toward the suprapatellar recess, leaving the medial and lateral parapatellar recesses virtually voided ($p < 0.001$). This pattern was not observed in JIA, where no statistically significant differences in the amount of fluid were found across the examined recesses, in contrast with the topographic asymmetry that defines physiological joint distribution. The clinical consequence of this finding is immediate and practical. A radiologist relying only on the suprapatellar view could misclassify normal children as pathological, since a modest suprapatellar fluid collection is an entirely innocent finding in the healthy paediatric knee. This observation is consistent with the five-view methodology of the PIUS-Knee protocol [119] supporting parapatellar imaging as a standard component of the paediatric knee examination.

Also relevant was the behaviour of the synovial membrane in joints that had never attracted clinical attention. Among the 25 patients with a strictly unilateral disease history, the contralateral non-affected knee had a significantly thicker synovium compared to the healthy group ($p < 0.001$). This silent synovial thickening could plausibly reflect systemic pro-inflammatory mediators, principally IL-6 and TNF-alpha, which do not respect clinical boundaries and circulate freely, potentially sustaining low-grade proliferative activity in anatomically remote synovium. What makes this finding clinically interesting is its prognostic potential. Identifying this increased synovial thickness involvement in a supposedly unaffected joint may flag patients on a trajectory toward extended

polyarticular disease and possibly offer a window for earlier therapeutic escalation before structural damage becomes established.

The effects of an inflammatory disease extended beyond solely fluid and synovium measurements. The healthy cohort exhibited the expected demographic architecture, sex- and age-related gradients in fluid volume and echogenic speckle presence (Paper 1), none of which was observed in the JIA group. Inflammatory hypersecretion appears to overwhelm these subtle physiological signals entirely, rendering demographic stratification diagnostically non-relevant in the context of disease. The same pattern held for synovial thickness, with progressive age-dependent thickening documented in healthy volunteers, which was absent in JIA patients, whose synovial hypertrophy followed the molecular logic of inflammation rather than the biological clock of skeletal maturation.

Structural cartilage and bone metrics added further differences for the pathological picture. Femoral intercondylar cartilage in healthy children followed the established normative trajectory described by Windschall et al. [89], Spannow et al. [120], and Gau et al. [121], thinning progressively with age and measuring consistently thinner in girls than in boys. In our study, JIA girls showed intercondylar cartilage significantly thinner than that of age-matched healthy peers, a finding that may relate to proteoglycan matrix depletion and chondrocyte loss under sustained inflammatory load. The earlier work of Sahin et al. [122] identified a broadly similar cartilage profile but was limited by the absence of sex-stratified analysis, a methodological gap that our data explicitly address. At the other end of the structural spectrum, JIA patients demonstrated enlarged patellar dimensions bilaterally, potentially reflecting the influence of synovial hyperaemia on adjacent epiphyseal growth plates, as the patella is an epiphyseal equivalent. Notably, despite the JIA cohort presenting a younger minimum age than the volunteer cohort (1.9 vs 3.1 years), every JIA patient had already started bilateral patellar ossification, a maturational milestone that remained incomplete in a proportion of the healthy group. This ossification overstep constitutes a distinctive inflammatory skeletal fingerprint.

On Doppler performance, colour Doppler delivered high specificity in the healthy cohort, returning a Grade 0 signal bilaterally in all 127 volunteers ($p < 0.001$). This suggests that detectable synovial vascularity in a child is unlikely to reflect normal physiology within the comparator population studied here, reinforcing international guideline recommendations for ultrasound as the first-line diagnostic technique in suspected

paediatric joint inflammation (Paper 2). A particular point is the equivalence of colour and power Doppler in this context. Contrary to the widespread clinical assumption that power Doppler is the more sensitive modality, both techniques yielded identical results within our JIA cohort. This observation is consistent with evidence from other inflammatory arthritis literature demonstrating that colour and power Doppler share some fundamental detection physics. No substantial difference in slow-flow detection between the two modalities has been identified on lasted-generation ultrasound equipment [12, 123]. Across different machines, sensitivity has been shown to depend more on device optimisation than on modality choice, with power Doppler outperforming colour Doppler on only half of platforms tested and colour Doppler outperforming power Doppler on the other half [124]. The modality that does consistently outperform power Doppler is MD.

C.2. How the ultrasound findings can predict the diagnostic probability of JIA in the knee joint

The multiparametric differences documented between cohorts naturally raised the question of whether a small number of ultrasound variables could be combined into a clinically usable predictive instrument. A multivariable logistic regression model was therefore constructed from the variables showing the greatest between-group discrimination, arriving at a two-parameter solution: longitudinal suprapatellar recess double synovial thickness and transverse medial parapatellar recess fluid depth, both measured in millimetres and both routinely obtainable within a standard five-view multiparametric musculoskeletal ultrasound (MSUS) examination. The resulting model achieved an AUC of 0.892 (95% CI: 0.832–0.951), reflecting strong and clinically meaningful discriminative capacity.

We hypothesise that the variable selection is conceptually coherent. Suprapatellar synovial thickness indexes the structural hallmark of JIA (membrane hypertrophy), whilst medial parapatellar fluid depth captures the functional hallmark, the pathological redistribution of fluid from its physiological suprapatellar reservoir into the parapatellar compartments. These two measurements therefore address two important dimensions of the disease process, which likely explains why a model of only two variables achieves discrimination approaching 0.9. Importantly, neither variable requires contrast

administration, advanced post-processing, or extended scanning time, making the model directly implementable within existing clinical workflows.

Appropriate caution is nonetheless warranted in interpreting and applying these types of models. The cohort was drawn predominantly from patients with persistent oligoarthritis, the subtype most characteristically associated with knee involvement, which both strengthens the model's relevance to this clinical context, but limits its direct extrapolation to systemic, enthesitis-related, or psoriatic JIA subtypes where disease expression and joint biology may differ. More fundamentally, the model provides a probability estimate, not a diagnosis. Its application must always be contextualised within the individual child's full clinical presentation, and other causes of paediatric knee synovitis (including reactive arthritis, septic arthritis, and mechanical, etc) must be excluded before imaging findings are acted upon. Probability estimates are a supplement to clinical reasoning, not a substitute for it.

The methodological integrity supporting the model is a further source of confidence. The identical scanning protocol, equipment, anatomical views, and operator applied across both cohorts means that the variables entering the regression reflected genuine biological signal rather than inter-operator or inter-machine noise. Extending this rigour to multicentre, internationally diverse validation cohorts is the natural and necessary next step, both to test the generalisability of the model's discriminative thresholds across ethnic and demographic groups and to establish the external validity that would be required before clinical implementation could be responsibly recommended.

D. The Pinnacle of Subclinical Synovitis

Evidence, Uncertainty, and the Remission Criteria Question

Subclinical synovitis, defined as imaging-detected inflammation in clinically inactive joints, emerges from two independent papers of this thesis using different modalities. In Paper 4, CEUS and FLAIR-FS detected synovitis in patients with low or absent clinical scores, whilst clinical assessment demonstrated limited discriminative performance, especially at the lower end of the inflammation spectrum (17 CEMRI Mild cases and 14 CEMRI Moderate+Severe cases clinically classified as inactive). In Paper 5, clinically unaffected knees in oligoarticular JIA patients showed synovial thickening significantly exceeding the healthy group from Paper 1. Both findings are consistent with the literature, although we need to reassess our patient group clinically to analyse the flare rate.

The largest and most methodologically developed JIA study to date is from Mazzoni et al. [125], who evaluated 90 clinically inactive JIA patients using CEMRI across multiple joint sites. Despite satisfying Wallace remission criteria [126-128], subclinical synovitis was detected in 65.5% of patients. Synovitis detected with CEMRI emerged as the strongest independent predictor of subsequent flare, occurring in 74.6% of patients with residual synovitis compared with 41.9% of those without ($p = 0.002$). These findings suggest that CEMRI may represent a more sensitive tool for defining true disease remission in JIA. Nusman et al. [100] investigated whether dynamic CEMRI parameters could predict flare in clinically quiescent JIA in a cohort of 32 patients with inactive disease. Thirteen patients (39.4%) had synovial hypertrophy, and twelve patients experienced a flare within the two-year follow-up period; however, the authors did not provide a direct cross-tabulation of synovial hypertrophy and flare status at the individual patient level. Mean synovial hypertrophy score did not differ significantly between persistently inactive and flaring patients. The only significant difference between groups was maximum synovial enhancement on dynamic CEMRI ($p = 0.05$), a difference that did not survive correction for multiple testing.

Beyond single-joint CEMRI, whole-body MRI has extended this evidence base to multi-joint monitoring, detecting subclinical inflammation across the skeleton, though its methodology remains complex [129]. De Lucia et al. [130] found baseline ultrasound

positivity, particularly in combination with power Doppler, predicted relapse in JIA. Miotto e Silva et al. [131] demonstrated in a prospective 30-month follow-up study that positive power Doppler signal in joints of JIA patients in clinical remission conferred a five times higher risk of flare, and joints with active subclinical synovitis flared significantly more frequently at both 6 and 12 months of follow-up. Notably, the risk was 14 times higher in patients who were in remission while still on medication, reflecting the less stable nature of medication-dependent remission.

In contrast, Nieto-Gonzalez et al. [132] found that ultrasound-detected subclinical synovitis did not predict flare recurrence in 56 JIA patients in stable remission undergoing tumour necrosis factor inhibitor (TNFi) tapering, suggesting that the predictive value of subclinical synovitis may be context-dependent. An important counterpoint was provided by Magni-Manzoni et al. [133], who found that ultrasound-detected synovial abnormalities were common in 39 children with JIA in clinical remission (affecting 76.9%) but did not predict an early flare of synovitis over a two-year follow-up. Although this study dates from 2013, it may reflect that not all imaging-detected subclinical synovitis carries equivalent prognostic weight, and that the predictive value may depend on the imaging modality, the feature assessed (B-mode vs Doppler vs CEUS), the specific joint, and the treatment context.

In comparison, Han et al. [134] in a meta-analysis of 13 articles on RA, found that power Doppler positivity predicted flare (pooled OR 4.52, 95% CI 2.61–7.84) and progressive bone erosion (OR 11.85, 95% CI 5.01–28.03 at joint level) in patients with RA in clinical remission. Subclinical tenosynovitis was also identified as a risk factor for flare by Zacariaz Hereter et al. [135] in RA in clinical remission. Despite converging cross-sectional and short-term longitudinal evidence for subclinical synovitis in JIA, the field remains at an early stage. The systematic review by Saoussen et al. [136] identified conflicting results in JIA patients regarding the predictive value of MSUS for flare. This heterogeneity was attributed to the absence of standardised protocols, validated paediatric-specific scoring systems, and normative comparators as key limiting factors in existing studies. These limitations were directly addressed by the design of Papers 1, 4, and 5. However, no study has followed a JIA cohort sufficiently long with structured serial imaging, validated tools, and radiological endpoints to determine whether subclinical synovitis drives progressive structural damage at a clinically meaningful rate

in the current treatment era. The honest clinical message is that imaging reveals more than clinical examination; what to do with all of it requires prospective, longitudinal, outcomes-anchored studies.

The ARCTIC trial [137] is a randomised controlled trial to evaluate whether escalating treatment to reach an imaging remission target (defined by power doppler signal alone) improves outcomes in adult RA. Although the results did not demonstrate a benefit of treatment escalation guided by imaging over clinical remission alone, no equivalent trial exists in JIA, representing the most important evidence gap in the field.

The current JIA Wallace remission criteria [126] are exclusively defined by clinical and laboratory parameters without imaging components. Treating to this target has been formalised in international treat-to-target recommendations [138], yet achievement of remission remains inconsistent: a systematic review found remission frequencies ranging from 7% at 18 months to approximately 40% after 10 years from diagnosis, with wide variation by disease subtype [139].

The data of this thesis provide three enabling contributions towards potential future imaging integration: Paper 1 provides the normative reference standards without which imaging-defined remission criteria cannot be operationally defined. Paper 3 reliability results for CEUS and CEMRI 0–3 grading support their potential use as future clinical trial endpoints. Paper 4 validates CEUS and FLAIR-FS as accurate tools showing near-absence of FLAIR-FS signal in healthy knees. The prospective, longitudinal, treat-to-target trials needed to determine whether imaging-defined remission improves outcomes for children with JIA can now be designed with the validated tools, reliability data, and normative framework this thesis provides.

E. A Proposed Stratified Imaging Algorithm for the Suspicion of JIA in the Knee

The findings of this thesis suggest a possible stratified imaging algorithm, incorporating new techniques, for the evaluation of suspected JIA with knee involvement (Figure 5), addressing a gap not yet covered by current literature [8, 20, 140]. Drawing on the normative ultrasound reference values from Paper 1, the reliability data from Paper 3, and the diagnostic performance of CEUS and FLAIR-FS from Paper 4, the proposed pathway follows three sequential steps: initial ultrasound assessment using age- and sex-adjusted normative thresholds; non-contrast FLAIR-FS MRI for synovitis confirmation in equivocal or monoarticular presentations; and a possibility of serial monitoring incorporating CEUS, FLAIR-FS, and CEMRI according to imaging and clinical need. CEMRI with formal knee scoring remains available when FLAIR-FS findings are non-diagnostic. This algorithm is not intended as a validated clinical guideline but rather as a hypothesis-generating framework, illustrating how the tools and normative data developed in this thesis could be integrated into a gadolinium and sedation sparing (with CEUS), structured imaging pathway, pending prospective validation in larger, longitudinal JIA cohorts.

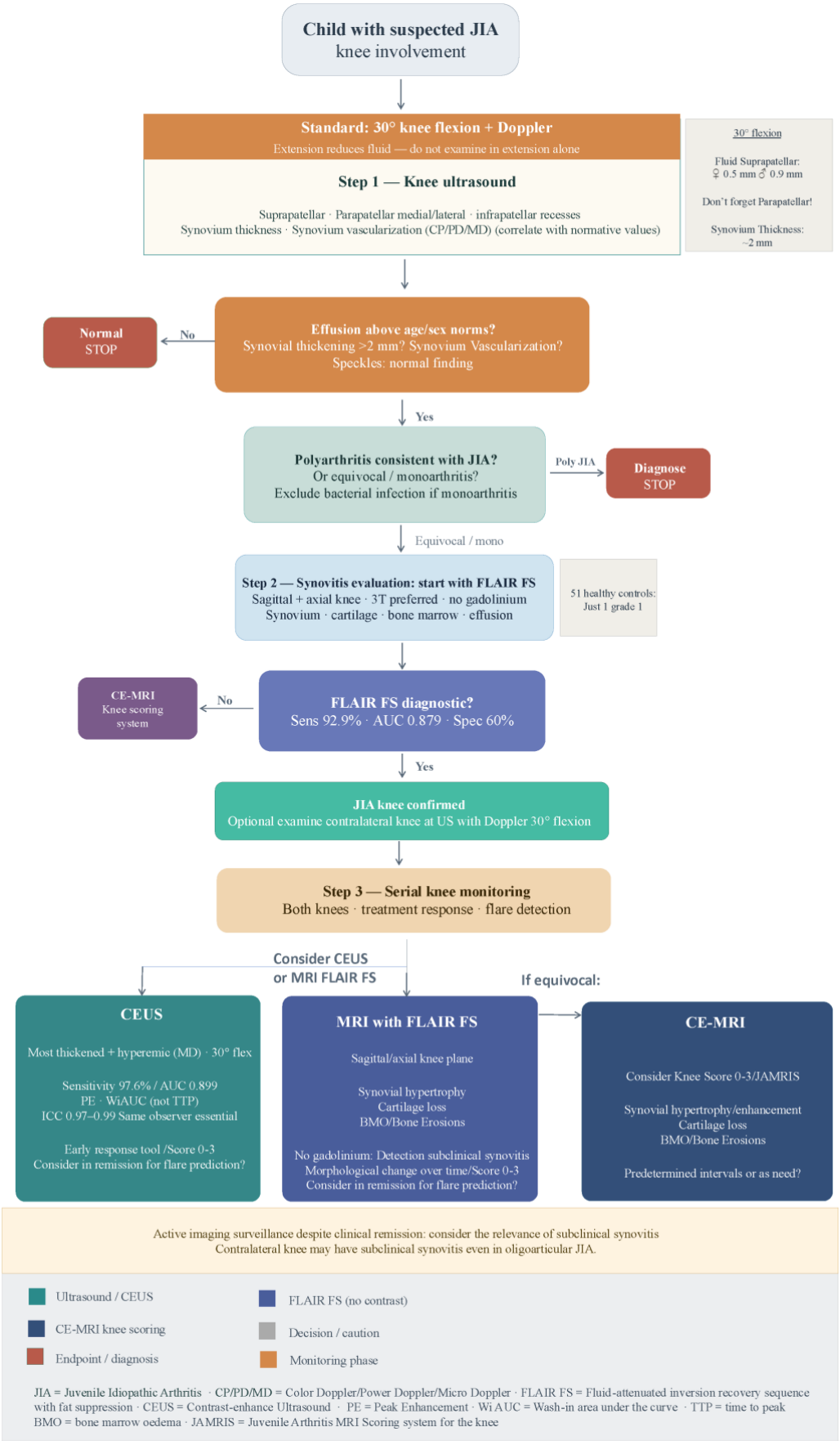


Figure 5. Proposed stratified imaging algorithm for juvenile idiopathic arthritis knee involvement: clinical decision flowchart.

F. Strengths and Limitations of Our Work

This thesis has several significant strengths. It addresses a clinically important and insufficiently studied area, the non-invasive, gadolinium-sparing assessment of knee synovitis in children with JIA, through a coherent, multi-paper programme built on a common patient cohort and shared methodology. The establishment of age- and sex-specific normative ultrasound reference values in Paper 1 provides a foundational contribution that anchors the diagnostic validity of Papers 4 and 5 and addresses a recognised gap in the paediatric imaging literature. The reliability study in Paper 3 used a robust multi-reader, multi-method design with appropriate statistical methodology, supporting its potential use in future clinical trial context. The diagnostic performance of CEUS and FLAIR-FS was evaluated against CEMRI as the accepted reference standard, with standardised acquisition protocols applied consistently across studies. The timing of post-gadolinium acquisition significantly influences synovial scoring, as demonstrated by Rieter et al. [24] who showed that late post-contrast images yielded significantly higher synovial enhancement and inflammation scores than early images. This underscores the importance of acquisition standardisation, which was directly addressed in this thesis through the evidence-based 2–3-minute delay established in Paper 2 and applied in the subsequent study. The inclusion of a healthy group in MRI with a FLAIR-FS sequence in Paper 4, demonstrating near-absence of knee synovitis, further strengthens the specificity of the diagnostic findings. A further strength emerging from the integration of Papers 1 and 5 is the ability to directly compare JIA patients against a structured normative framework. This revealed new data: it not only quantified how much synovial thickness in JIA patients significantly exceeds normative values, but also that patients demonstrate differences in both the amount and distribution of joint fluid compared to the healthy group, objectifying subclinical articular change in a way that would not have been possible without the normative dataset established in Paper 1. Notably, Paper 4 of this thesis represents the first study to directly compare modern CEUS against CEMRI as the formal reference standard for synovitis assessment in children with JIA, filling a previously unexplored field in paediatric musculoskeletal imaging.

Several limitations must be acknowledged. All studies were conducted at a single tertiary centre, limiting generalisability and requiring multicentre validation. The normative cohorts were predominantly Caucasian, limiting ethnic representativeness. Synovial

biopsy was not available as the true histological reference standard, meaning CEMRI, whilst the accepted imaging reference, remains an imperfect surrogate. The patient cohort (n=52) limits subgroup analyses by JIA subtype and treatment. The predominantly oligoarticular composition of our group (57.7%) may limit the generalisability of the ultrasound predictor model, especially to polyarticular and systemic subtypes. However, it should be noted that the knee joint is the most clinically relevant joint in oligoarticular JIA [141]. The subtype-specific adjustment would have compromised the statistical power of the analyses given the sample size. The cross-sectional design of Papers 4 and 5 precludes longitudinal conclusions about whether detected subclinical synovitis carries prognostic significance. CEUS remains off label in children for musculoskeletal indications, requiring ethics committee oversight and continued pharmacovigilance. Intraobserver agreement for quantitative CEMRI data was not performed in Paper 3, limiting the complete characterisation of within-observer variability. Regarding FLAIR-FS, the broader paediatric validation landscape remains limited, prior to Milks et al. [39] in 2024, no dedicated paediatric study of FLAIR-FS for synovitis existed. That study involved only 42 knees from a heterogeneous group of 39 patients, at a single centre, in a retrospective design. As of 2025, there remains only one dedicated paediatric FLAIR-FS study in the literature, with no prospective paediatric validation, no multicentre paediatric study, no data in joints other than the knee in children, and no longitudinal data demonstrating that FLAIR-FS can track disease activity over time in JIA. The findings of Paper 4 of this thesis therefore represent an important but early contribution to a field that requires substantially larger, prospective, multicentre studies before FLAIR-FS can be recommended for routine multi-articular clinical use in paediatric inflammatory arthritis.

FUTURE DIRECTIONS/PERSPECTIVES & CONCLUSIONS

A. FUTURE DIRECTIONS/PERSPECTIVES

At least four priority points emerge from this thesis. First, multicentre prospective validation of FLAIR-FS and CEUS across ethnically and geographically diverse populations is needed, addressing the single-centre limitation of this work and providing the ICC and limits of agreement data required to define robust multicentre monitoring protocols. Second, automated segmentation of FLAIR-FS synovial volume and CEUS perfusion ROIs would standardise placement and directly address the limits of agreement limitation attributable to manual ROI variability identified in Paper 3. Third, a prospective longitudinal outcomes study is needed to examine whether subclinical synovitis detected by CEUS, FLAIR-FS, or ultrasound in Papers 4 and 5 predicts disease progression, flare frequency, or functional outcome over two to three years. This study type would transform the contributions of this thesis from enabling to conclusive. As part of this longitudinal follow-up, correlating the ultrasound synovial findings of our patient cohort with inflammatory grades and flare rates will allow assessment of whether the imaging-detected subclinical synovitis identified in this thesis carries clinically meaningful prognostic weight and even therapeutic decisions. It could also inform the development of a predictive model for synovial inflammation in JIA, maybe possible to adjust for predicting activity scores among patients. Fourth, a health economic analysis comparing monitoring strategies for CEUS, FLAIR-FS and clinical assessment, would provide the evidence base needed to support guideline development and inform resource allocation decisions in paediatric rheumatology services.

Beyond these four priorities, further research directions are proposed. A multicentre project in collaboration with the Amsterdam and Norwegian groups is being designed to evaluate FLAIR-FS and DIR in JIA patients across other joints (including the wrist, hip, and ankle), which would address the current limitation of single-joint validation and extend the non-contrast MRI evidence base to the full spectrum of JIA joint involvement.

Tools to optimise the quantification of Doppler signal have been developed, whereby the operator manually delineates the ROI within the thickest part of the synovium and the machine automatically calculates the ratio of colour pixels versus grey pixels, expressed as a percentage, producing a vascular index [15]. Also, volumetric measurements could be of interest, however types of automatic quantifications need to be confronted with the

actual scoring system of synovitis recommended by the OMERACT Ultrasound Group consensus [85].

Finally, applications of deep learning reconstruction to improve image quality and accelerate FLAIR-FS acquisition represent promising technical developments. Feuerriegel et al. [38] demonstrated that a deep learning-accelerated FLAIR-FS sequence with an acquisition time of under two minutes showed comparable diagnostic performance to standard contrast-enhanced imaging for inflammatory knee synovitis, suggesting that scan time, often a barrier to clinical implementation, may be substantially reduced without loss of diagnostic accuracy.

B. CONCLUSIONS

The findings of this doctoral thesis provide critical diagnostic and methodological advancements in the imaging assessment of synovial inflammation in paediatric patients with JIA. By systematically evaluating gadolinium-free and advanced imaging modalities against the reference standard of CEMRI, this work addresses a pressing clinical imperative to minimise GD contrast agent exposure while maintaining diagnostic excellence.

The major conclusions drawn from this thesis are as follows:

- CEUS offers high-precision, real-time imaging for grading active knee inflammation in children with JIA. By demonstrating the highest sensitivity among the evaluated modalities alongside a sedation-free advantage, CEUS shows substantial potential to serve as a reliable alternative to the current gold standard of CEMRI.
- Unenhanced FLAIR-FS MRI serves as a highly robust, contrast-free alternative for detecting synovitis in the knee, yielding almost perfect inter-technique agreement with CEMRI.
- Subjective 0–3 grading scales offer a highly reliable and reproducible framework for routine clinical use. By targeting global synovial inflammation, this approach bypasses extensive scoring requirements.
- Conventional Doppler modalities exhibit near-perfect specificity when normal healthy volunteers are utilised as a comparator group, but they suffer from an unacceptable loss of sensitivity in the presence of low-grade or subclinical inflammation. This underscores the necessity of adopting advanced microvascular techniques like MD to reliably resolve slow microvascular blood flow.
- Methodological rigour in Perfusion Software is paramount; high ICCs can mathematically mask substantial absolute interobserver variance. For longitudinal therapeutic monitoring, clinical decisions must be guided by absolute metrics (such as Bland-Altman limits of agreement) rather than relative rankings, as manual boundary definitions of the microscopic paediatric synovium remain inherently volatile.

In summary, while clinical examination remains the cornerstone of global JIA management, advanced imaging provides an indispensable, complementary mapping of low-grade disease. The transition toward high-sensitivity, non-GD-contrast, or lower-risk modalities investigated in this thesis represents a major step forward in establishing safer, more practical, and highly reliable monitoring pipelines for children with chronic arthritis.

REFERENCES

REFERENCES

1. Petty RE, Southwood TR, Manners P, Baum J, Glass DN, Goldenberg J, et al. International League of Associations for Rheumatology classification of juvenile idiopathic arthritis: second revision, Edmonton, 2001. J Rheumatol. 2004;31(2):390-2
2. Ravelli A, Martini A. Juvenile idiopathic arthritis. Lancet. 2007;369(9563):767-78. doi:10.1016/S0140-6736(07)60363-8
3. Martini A, Lovell DJ, Albani S, Brunner HI, Hyrich KL, Thompson SD, et al. Juvenile idiopathic arthritis. Nat Rev Dis Primers. 2022;8(1):5. doi:10.1038/s41572-021-00332-8
4. Prakken B, Albani S, Martini A. Juvenile idiopathic arthritis. Lancet. 2011;377(9783):2138-49. doi:10.1016/S0140-6736(11)60244-4
5. Giancane G, Consolaro A, Lanni S, Davi S, Schiappapietra B, Ravelli A. Juvenile Idiopathic Arthritis: Diagnosis and Treatment. Rheumatol Ther. 2016;3(2):187-207. doi:10.1007/s40744-016-0040-4
6. Ringold S, Angeles-Han ST, Beukelman T, Lovell D, Cuello CA, Becker ML, et al. 2019 American College of Rheumatology/Arthritis Foundation Guideline for the Treatment of Juvenile Idiopathic Arthritis: Therapeutic Approaches for Non-Systemic Polyarthritis, Sacroiliitis, and Enthesitis. Arthritis Care Res (Hoboken). 2019;71(6):717-34. doi:10.1002/acr.23870
7. Consolaro A, Giancane G, Schiappapietra B, Davi S, Calandra S, Lanni S, et al. Clinical outcome measures in juvenile idiopathic arthritis. Pediatr Rheumatol Online J. 2016;14(1):23. doi:10.1186/s12969-016-0085-5
8. Costa Dias S, Habre C, Di Paolo PL, d'Angelo P, Augdal TA, Angenete OW, et al. ESR Essentials: juvenile idiopathic arthritis; what every radiologist needs to know—practice recommendations by the European Society of Paediatric Radiology. European Radiology. 2026;36(2):1261-71. doi:10.1007/s00330-025-11891-9
9. Sheybani EF, Khanna G, White AJ, Demertzis JL. Imaging of juvenile idiopathic arthritis: a multimodality approach. Radiographics. 2013;33(5):1253-73. doi:10.1148/rg.335125178
10. Brunner E, Ting T, Vega-Fernandez P. Musculoskeletal ultrasound in children: Current state and future directions. Eur J Rheumatol. 2020;7(Suppl1):S28-S37. doi:10.5152/eurjrheum.2019.19170
11. Magni-Manzoni S. Ultrasound in juvenile idiopathic arthritis. Pediatr Rheumatol Online J. 2016;14(1):33. doi:10.1186/s12969-016-0096-2
12. Torp-Pedersen ST, Terslev L. Settings and artefacts relevant in colour/power Doppler ultrasound in rheumatology. Ann Rheum Dis. 2008;67(2):143-9. doi:10.1136/ard.2007.078451

13. Porta F, Radunovic G, Vlad V, Micu MC, Nestorova R, Petranova T, et al. The role of Doppler ultrasound in rheumatic diseases. Rheumatology (Oxford). 2012;51(6):976-82. doi:10.1093/rheumatology/ker433

14. Seskute G, Montvydaite M, Butrimiene I. Power Doppler artifacts in evaluating inflammatory arthritis of small joints: comparison with a superb microvascular imaging technique. J Ultrasound. 2022;25(3):765-71. doi:10.1007/s40477-021-00643-2

15. Alis D, Erol BC, Akbas S, Barut K, Kasapcopur O, Adaletli I. Superb Microvascular Imaging Compared With Power Doppler Ultrasound in Assessing Synovitis of the Knee in Juvenile Idiopathic Arthritis: A Preliminary Study. J Ultrasound Med. 2020;39(1):99-106. doi:10.1002/jum.15079

16. Dohna M, Gohar F, Neuhauser M, Franke D, Memaran N, Raab A, et al. Superb microvascular imaging ultrasound of the knee in patients with juvenile idiopathic arthritis-a repeatability study. Front Pediatr. 2025;13:1759370. doi:10.3389/fped.2025.1759370

17. Malattia C, Damasio MB, Pistorio A, Ioseliani M, Vilca I, Valle M, et al. Development and preliminary validation of a paediatric-targeted MRI scoring system for the assessment of disease activity and damage in juvenile idiopathic arthritis. Ann Rheum Dis. 2011;70(3):440-6. doi:10.1136/ard.2009.126862

18. Malattia C, Tolend M, Mazzoni M, Panwar J, Zlotnik M, Otobo T, et al. Current status of MR imaging of juvenile idiopathic arthritis. Best Pract Res Clin Rheumatol. 2020;34(6):101629. doi:10.1016/j.berh.2020.101629

19. Hemke R, van Rossum MA, van Veenendaal M, Terra MP, Deurloo EE, de Jonge MC, et al. Reliability and responsiveness of the Juvenile Arthritis MRI Scoring (JAMRIS) system for the knee. Eur Radiol. 2013;23(4):1075-83. doi:10.1007/s00330-012-2684-y

20. Hemke R, Herregods N, Jaremko JL, Astrom G, Avenarius D, Becce F, et al. Imaging assessment of children presenting with suspected or known juvenile idiopathic arthritis: ESSR-ESPR points to consider. Eur Radiol. 2020;30(10):5237-49. doi:10.1007/s00330-020-06807-8

21. Avenarius DFM, Nusman C, Malattia C, de Horatio LT, Rosendahl K, Maas M, et al. Current status of wrist imaging in juvenile idiopathic arthritis. Pediatr Radiol. 2018;48(6):801-10. doi:10.1007/s00247-017-4063-y

22. Vo Chieu VD, Vo Chieu V, Dressler F, Kornemann N, Pfeil A, Bottcher J, et al. Juvenile idiopathic arthritis of the knee: is contrast needed to score disease activity when using an augmented MRI protocol comprising PD-weighted sequences? Eur Radiol. 2023;33(5):3775-84. doi:10.1007/s00330-022-09292-3

23. Barendregt AM, Mazzoli V, van Gulik EC, Schonenberg-Meinema D, Nassar-Sheikh Rashid A, Nusman CM, et al. Juvenile Idiopathic Arthritis: Diffusion-weighted MRI in the Assessment of Arthritis in the Knee. Radiology. 2020;295(2):373-80. doi:10.1148/radiol.2020191685

24. Rieter JF, de Horatio LT, Nusman CM, Muller LS, Hemke R, Avenarius DF, et al. The many shades of enhancement: timing of post-gadolinium images strongly influences the scoring of juvenile idiopathic arthritis wrist involvement on MRI. Pediatr Radiol. 2016;46(11):1562-7. doi:10.1007/s00247-016-3657-0

25. Verkuil F, van den Berg JM, van Gulik EC, Barendregt AM, Rashid AN, Schonenberg-Meinema D, et al. Synovial signal intensity on static contrast-enhanced MRI for evaluation of disease activity in juvenile idiopathic arthritis - A look at the bright side of the knee. Clin Imaging. 2022;86:53-60. doi:10.1016/j.clinimag.2022.03.016

26. Ouyang M, Bao L. Gadolinium Contrast Agent Deposition in Children. J Magn Reson Imaging. 2025;61(1):70-82. doi:10.1002/jmri.29389

27. Yu OJ, Kim PH, Yoon HM, Jung AY, Cho YA, Lee JS, et al. Safety of Gadolinium-based Contrast Agents in Children: A Systematic Review and Meta-Analysis. Radiology. 2025;316(1):e241224. doi:10.1148/radiol.241224

28. Cheeney SHE, Maloney E, Iyer RS. Safety considerations related to intravenous contrast agents in pediatric imaging. Pediatr Radiol. 2023;53(7):1352-63. doi:10.1007/s00247-022-05470-z

29. Agency EM. EMA's final opinion confirms restrictions on use of linear gadolinium agents in body scans. Amsterdam: European Medicines Agency; 2017 July 21. Report No.: EMA/457616/2017.

30. Neubauer H, Evangelista L, Morbach H, Girschick H, Prelog M, Kostler H, et al. Diffusion-weighted MRI of bone marrow oedema, soft tissue oedema and synovitis in paediatric patients: feasibility and initial experience. Pediatr Rheumatol Online J. 2012;10(1):20. doi:10.1186/1546-0096-10-20

31. Barendregt AM, Nusman CM, Hemke R, Lavini C, Amiras D, Kuijpers TW, et al. Feasibility of diffusion-weighted magnetic resonance imaging in patients with juvenile idiopathic arthritis on 1.0-T open-bore MRI. Skeletal Radiol. 2015;44(12):1805-11. doi:10.1007/s00256-015-2208-3

32. Sauer A, Li M, Holl-Wieden A, Pabst T, Neubauer H. Readout-segmented multi-shot diffusion-weighted MRI of the knee joint in patients with juvenile idiopathic arthritis. Pediatr Rheumatol Online J. 2017;15(1):73. doi:10.1186/s12969-017-0203-z

33. Barendregt AM, van Gulik EC, Lavini C, Nusman CM, van den Berg JM, Schonenberg-Meinema D, et al. Diffusion-weighted imaging for assessment of synovial inflammation in juvenile idiopathic arthritis: a promising imaging biomarker as an alternative to gadolinium-based contrast agents. Eur Radiol. 2017;27(11):4889-99. doi:10.1007/s00330-017-4876-y

34. Li M, Sauer A, Holl-Wieden A, Pabst T, Neubauer H. Diagnostic value of diffusion-weighted MRI for imaging synovitis in pediatric patients with inflammatory conditions of the knee joint. World J Pediatr. 2020;16(1):60-7. doi:10.1007/s12519-019-00232-8

35. Yoo HJ, Hong SH, Oh HY, Choi JY, Chae HD, Ahn JM, et al. Diagnostic Accuracy of a Fluid-attenuated Inversion-Recovery Sequence with Fat Suppression for Assessment of Peripatellar Synovitis: Preliminary Results and Comparison with Contrast-enhanced MR Imaging. Radiology. 2017;283(3):769-78. doi:10.1148/radiol.2016160155

36. Saranathan M, Worters PW, Rettmann DW, Winegar B, Becker J. Physics for clinicians: Fluid-attenuated inversion recovery (FLAIR) and double inversion recovery (DIR) Imaging. J Magn Reson Imaging. 2017;46(6):1590-600. doi:10.1002/jmri.25737

37. Jahng GH, Jin W, Yang DM, Ryu KN. Optimization of a double inversion recovery sequence for noninvasive synovium imaging of joint effusion in the knee. Med Phys. 2011;38(5):2579-85. doi:10.1118/1.3581060

38. Feuerriegel GC, Goller SS, von Deuster C, Sutter R. Inflammatory Knee Synovitis: Evaluation of an Accelerated FLAIR Sequence Compared With Standard Contrast-Enhanced Imaging. Invest Radiol. 2024;59(8):599-604. doi:10.1097/RLI.0000000000001065

39. Milks KS, Singh J, Benedict JA, Rees MA. Fluid-attenuated inversion-recovery sequence with fat suppression as an alternative to contrast-enhanced MRI in pediatric synovitis. Pediatr Radiol. 2024;54(1):96-104. doi:10.1007/s00247-023-05804-5

40. Handa A, Bedoya MA, Iwasaka-Neder J, Johnston PR, Lo MS, Bixby SD. Measuring synovial thickness on knee MRI in pediatric patients with arthritis: is contrast necessary? Pediatr Radiol. 2024;54(6):988-1000. doi:10.1007/s00247-024-05929-1

41. Verkuil F, Hemke R, van Gulik EC, Barendregt AM, Nassar-Sheikh Rashid A, Schonenberg-Meinema D, et al. Double inversion recovery MRI versus contrast-enhanced MRI for evaluation of knee synovitis in juvenile idiopathic arthritis. Insights Imaging. 2022;13(1):167. doi:10.1186/s13244-022-01299-0

42. de Vries BA, Breda SJ, Sveinsson B, McWalter EJ, Meuffels DE, Krestin GP, et al. Detection of knee synovitis using non-contrast-enhanced qDESS compared with contrast-enhanced MRI. Arthritis Research & Therapy. 2021;23(1):55. doi:10.1186/s13075-021-02436-8

43. Thoenen J, MacKay JW, Sandford HJC, Gold GE, Kogan F. Imaging of Synovial Inflammation in Osteoarthritis, From the AJR Special Series on Inflammation. AJR Am J Roentgenol. 2022;218(3):405-17. doi:10.2214/AJR.21.26170

44. Sidhu PS, Cantisani V, Deganello A, Dietrich CF, Duran C, Franke D, et al. Role of Contrast-Enhanced Ultrasound (CEUS) in Paediatric Practice: An EFSUMB Position Statement. Ultraschall Med. 2017;38(1):33-43. doi:10.1055/s-0042-110394

45. Damasio MB, Ording Muller LS, Augdal TA, Avni FE, Basso L, Bruno C, et al. European Society of Paediatric Radiology abdominal imaging task force: recommendations for contrast-enhanced ultrasound and diffusion-weighted imaging in focal renal lesions in children. Pediatr Radiol. 2020;50(2):297-304. doi:10.1007/s00247-019-04552-9

46. Squires JH, McCarville MB. Contrast-Enhanced Ultrasound in Children: Implementation and Key Diagnostic Applications. AJR Am J Roentgenol. 2021;217(5):1217-31. doi:10.2214/AJR.21.25713

47. Ntoulia A, Barnewolt CE, Doria AS, Ho-Fung VM, Lorenz N, Mentzel HJ, et al. Contrast-enhanced ultrasound for musculoskeletal indications in children. Pediatr Radiol. 2021;51(12):2303-23. doi:10.1007/s00247-021-04964-6

48. Doria AS, Kiss MH, Lotito AP, Molnar LJ, de Castro CC, Medeiros CC, et al. Juvenile rheumatoid arthritis of the knee: evaluation with contrast-enhanced color Doppler ultrasound. Pediatr Radiol. 2001;31(7):524-31. doi:10.1007/s002470100474

49. Klauser A, Demharter J, De Marchi A, Sureda D, Barile A, Masciocchi C, et al. Contrast enhanced gray-scale sonography in assessment of joint vascularity in rheumatoid arthritis: results from the IACUS study group. Eur Radiol. 2005;15(12):2404-10. doi:10.1007/s00330-005-2884-9

50. Polido-Pereira J, Antonio MS, Henriques SO, Sabido J, Fernandes RM, Vieira-Sousa E, et al. How useful is contrast-enhanced ultrasound in rheumatoid arthritis? A systematic review with meta-analysis on the comparison between contrast-enhanced ultrasound and colour or power Doppler ultrasound. Radiol Med. 2025;130(8):1243-53. doi:10.1007/s11547-025-02055-2

51. Song IH, Althoff CE, Hermann KG, Scheel AK, Knetsch T, Schoenharting M, et al. Knee osteoarthritis. Efficacy of a new method of contrast-enhanced musculoskeletal ultrasonography in detection of synovitis in patients with knee osteoarthritis in comparison with magnetic resonance imaging. Ann Rheum Dis. 2008;67(1):19-25. doi:10.1136/ard.2006.067462

52. Dillman JR, Strouse PJ, Ellis JH, Cohan RH, Jan SC. Incidence and severity of acute allergic-like reactions to i.v. nonionic iodinated contrast material in children. AJR Am J Roentgenol. 2007;188(6):1643-7. doi:10.2214/AJR.06.1328

53. Ntoulia A, Anupindi SA, Back SJ, Didier RA, Hwang M, Johnson AM, et al. Contrast-enhanced ultrasound: a comprehensive review of safety in children. Pediatr Radiol. 2021;51(12):2161-80. doi:10.1007/s00247-021-05223-4

54. American College of Radiology. ACR Manual on Contrast Media, Version 2026. 2026

55. Wei K, Mulvagh SL, Carson L, Davidoff R, Gabriel R, Grimm RA, et al. The safety of deFinity and Optison for ultrasound image enhancement: a retrospective analysis of 78,383 administered contrast doses. J Am Soc Echocardiogr. 2008;21(11):1202-6. doi:10.1016/j.echo.2008.07.019

56. Wever-Pinzon O, Suma V, Ahuja A, Romero J, Sareen N, Henry SA, et al. Safety of echocardiographic contrast in hospitalized patients with pulmonary hypertension: a multi-center study. Eur Heart J Cardiovasc Imaging. 2012;13(10):857-62. doi:10.1093/ehjci/jes057

57. Gokli A, Acord MR, Hwang M, Medellin-Kowalewski A, Rubesova E, Anupindi SA. Contrast-enhanced US in Pediatric Patients: Overview of Bowel Applications. Radiographics. 2020;40(6):1743-62. doi:10.1148/rg.2020200019

58. Chung YE, Kim KW. Contrast-enhanced ultrasonography: advance and current status in abdominal imaging. Ultrasonography. 2015;34(1):3-18. doi:10.14366/usg.14034

59. Dietrich CF, Augustiniene R, Batko T, Cantisani V, Cekuolis A, Deganello A, et al. European Federation of Societies for Ultrasound in Medicine and Biology (EFSUMB): An Update on the Pediatric CEUS Registry on Behalf of the "EFSUMB Pediatric CEUS Registry Working Group". Ultraschall Med. 2021;42(3):270-7. doi:10.1055/a-1345-3626

60. Gulani V, Calamante F, Shellock FG, Kanal E, Reeder SB, International Society for Magnetic Resonance in Medicine. Gadolinium deposition in the brain: summary of evidence and recommendations. Lancet Neurol. 2017;16(7):564-70. doi:10.1016/S1474-4422(17)30158-8

61. Le Fur M, Caravan P. The biological fate of gadolinium-based MRI contrast agents: a call to action for bioinorganic chemists. Metallomics. 2019;11(2):240-54. doi:10.1039/c8mt00302e

62. European Medicines Agency. SonoVue (sulfur hexafluoride microbubbles): Summary of Product Characteristics: EMA; 2021 [Available from: https://www.ema.europa.eu/en/documents/product-information/sonovue-epar-product-information_en.pdf.

63. McDonald RJ, McDonald JS, Kallmes DF, Jentoft ME, Murray DL, Thielen KR, et al. Intracranial Gadolinium Deposition after Contrast-enhanced MR Imaging. Radiology. 2015;275(3):772-82. doi:10.1148/radiol.15150025

64. Weller A, Barber JL, Olsen OE. Gadolinium and nephrogenic systemic fibrosis: an update. Pediatr Nephrol. 2014;29(10):1927-37. doi:10.1007/s00467-013-2636-z

65. Li D, Zhang R, Lan H, Chen M, Huang Z, Zhao H, et al. A retrospective study on adverse events of intravenous administration of sulfur hexafluoride microbubbles in abdominal and superficial applications in 83,778 patients. Insights Imaging. 2024;15(1):65. doi:10.1186/s13244-024-01632-9

66. Marckmann P, Skov L, Rossen K, Dupont A, Damholt MB, Heaf JG, et al. Nephrogenic systemic fibrosis: suspected causative role of gadodiamide used for contrast-enhanced magnetic resonance imaging. J Am Soc Nephrol. 2006;17(9):2359-62. doi:10.1681/ASN.2006060601

67. Elbanna KY, Krishna S, Finelli A, Atri M. Contrast-Enhanced Ultrasound of the Indeterminate Renal Mass, From the AJR "How We Do It" Special Series. AJR Am J Roentgenol. 2024;223(6):e2430817. doi:10.2214/AJR.24.30817

68. McDonald JS, Larson NB, Kolbe AB, Hunt CH, Schmitz JJ, Kallmes DF, et al. Acute Reactions to Gadolinium-Based Contrast Agents in a Pediatric Cohort: A Retrospective Study of 16,237 Injections. AJR Am J Roentgenol. 2021;216(5):1363-9. doi:10.2214/AJR.20.23602

69. Tang C, Fang K, Guo Y, Li R, Fan X, Chen P, et al. Safety of Sulfur Hexafluoride Microbubbles in Sonography of Abdominal and Superficial Organs: Retrospective Analysis of 30,222 Cases. J Ultrasound Med. 2017;36(3):531-8. doi:10.7863/ultra.15.11075

70. Piscaglia F, Bolondi L, Medicine ISfUi, Biology Study Group on Ultrasound Contrast Agents. The safety of Sonovue in abdominal applications: retrospective analysis of 23188 investigations. Ultrasound Med Biol. 2006;32(9):1369-75. doi:10.1016/j.ultrasmedbio.2006.05.031

71. Behzadi AH, Zhao Y, Farooq Z, Prince MR. Immediate Allergic Reactions to Gadolinium-based Contrast Agents: A Systematic Review and Meta-Analysis. Radiology. 2018;286(2):731. doi:10.1148/radiol.2017174037

72. Radbruch A, Weberling LD, Kieslich PJ, Eidel O, Burth S, Kickingereder P, et al. Gadolinium retention in the dentate nucleus and globus pallidus is dependent on the class of contrast agent. Radiology. 2015;275(3):783-91. doi:10.1148/radiol.2015150337

73. FDA US Food and Drug Administration. Lumason (Sulfur Hexafluoride Lipid-Type A Microspheres) for Injectable Suspension: Prescribing Information: Bracco Diagnostics Inc.; 2021 [Available from: https://www.accessdata.fda.gov/drugsatfda_docs/label/2021/203684s009lbl.pdf.

74. Malviya S, Voepel-Lewis T, Eldevik OP, Rockwell DT, Wong JH, Tait AR. Sedation and general anaesthesia in children undergoing MRI and CT: adverse events and outcomes. Br J Anaesth. 2000;84(6):743-8. doi:10.1093/oxfordjournals.bja.a013586

75. Malviya S, Voepel-Lewis T, Tait AR. Adverse events and risk factors associated with the sedation of children by nonanesthesiologists. Anesth Analg. 1997;85(6):1207-13. doi:10.1097/00000539-199712000-00005

76. Habre W, Disma N, Virag K, Becke K, Hansen TG, Johr M, et al. Incidence of severe critical events in paediatric anaesthesia (APRICOT): a prospective multicentre observational study in 261 hospitals in Europe. Lancet Respir Med. 2017;5(5):412-25. doi:10.1016/S2213-2600(17)30116-9

77. AIUM Practice Parameter for the Performance of Contrast-Enhanced Ultrasound. J Ultrasound Med. 2024;43(3):E8-E19. doi:10.1002/jum.16360

78. Mao M, Xia B, Chen W, Gao X, Yang J, Li S, et al. The Safety and Effectiveness of Intravenous Contrast-Enhanced Sonography in Chinese Children-A Single Center and Prospective Study in China. Front Pharmacol. 2019;10:1447. doi:10.3389/fphar.2019.01447

79. Torres A, Koskinen SK, Gjertsen H, Fischler B. Contrast-enhanced ultrasound is useful for the evaluation of focal liver lesions in children. Australas J Ultrasound Med. 2021;24(3):143-50. doi:10.1002/ajum.12279

80. U.S. Food and Drug Administration. FDA Approves Lumason for Pediatric Liver Lesion Characterisation and Vesicoureteral Reflux 2016 [Available from: https://www.fda.gov/media/103021/download.

81. Claudon M, Dietrich CF, Choi BI, Cosgrove DO, Kudo M, Nolsoe CP, et al. Guidelines and good clinical practice recommendations for Contrast Enhanced Ultrasound (CEUS) in the liver - update 2012: A WFUMB-EFSUMB initiative in cooperation with representatives of AFSUMB, AIUM, ASUM, FLAUS and ICUS. Ultrasound Med Biol. 2013;39(2):187-210. doi:10.1016/j.ultrasmedbio.2012.09.002

82. Olson MC, Atwell TD, Knudsen JM. Anaphylactic reaction to an ultrasound contrast agent (Lumason) in a patient with systemic mastocytosis. J Clin Ultrasound. 2018;46(8):533-5. doi:10.1002/jcu.22585

83. Kacar M, Rijavec M, Selb J, Korosec P. Clonal mast cell disorders and hereditary alpha-tryptasemia as risk factors for anaphylaxis. Clin Exp Allergy. 2023;53(4):392-404. doi:10.1111/cea.14264

84. Darge K, Papadopoulou F, Ntoulia A, Bulas DI, Coley BD, Fordham LA, et al. Safety of contrast-enhanced ultrasound in children for non-cardiac applications: a review by the Society for Pediatric Radiology (SPR) and the International Contrast Ultrasound Society (ICUS). Pediatr Radiol. 2013;43(9):1063-73. doi:10.1007/s00247-013-2746-6

85. Terslev L, Iagnocco A, Bruyn GAW, Naredo E, Vojinovic J, Collado P, et al. The OMERACT Ultrasound Group: A Report from the OMERACT 2016 Meeting and Perspectives. J Rheumatol. 2017;44(11):1740-3. doi:10.3899/jrheum.161240

86. Dias SC, Ferreira CC, Santos I, Castro M, Rodrigues M, Aguiar F, et al. Reliability of CEUS and MRI for grading knee-joint inflammation in juvenile idiopathic arthritis. Eur Radiol. 2026;36(10):7379-90. doi:10.1007/s00330-026-12627-z

87. Thornbury JR. Eugene W. Caldwell Lecture. Clinical efficacy of diagnostic imaging: love it or leave it. AJR Am J Roentgenol. 1994;162(1):1-8. doi:10.2214/ajr.162.1.8273645

88. Dias SC, Carvalho DC, Castro M, Dias CC, Ramos I, Brito I, et al. Knee-ultrasound: reference values for the amount of joint fluid and synovial appearances in healthy children and adolescents. Pediatr Radiol. 2025;55(6):1127-37. doi:10.1007/s00247-025-06243-0

89. Windschall D, Trauzeddel R, Haller M, Krumrey-Langkammerer M, Nimtz-Talaska A, Berendes R, et al. Pediatric musculoskeletal ultrasound: age- and sex-related normal B-mode findings of the knee. Rheumatol Int. 2016;36(11):1569-77. doi:10.1007/s00296-016-3528-x

90. Collado P, Naredo E, Calvo C, Crespo M. Assessment of the joint recesses and tendon sheaths in healthy children by high-resolution B-mode and power Doppler sonography. Clin Exp Rheumatol. 2007;25(6):915-21.

91. Lohman M, Kivisaari A, Vehmas T, Kallio P, Malmivaara A, Kivisaari L. MRI abnormalities of foot and ankle in asymptomatic, physically active individuals. Skeletal Radiol. 2001;30(2):61-6. doi:10.1007/s002560000316

92. Kursunoglu-Brahme S, Schwaighofer B, Gundry C, Ho C, Resnick D. Jogging causes acute changes in the knee joint: an MR study in normal volunteers. AJR Am J Roentgenol. 1990;154(6):1233-5. doi:10.2214/ajr.154.6.2110734

93. Miyaguchi M, Kobayashi A, Kadoya Y, Ohashi H, Yamano Y, Takaoka K. Biochemical change in joint fluid after isometric quadriceps exercise for patients with osteoarthritis of the knee. Osteoarthritis Cartilage. 2003;11(4):252-9. doi:10.1016/s1063-4584(02)00372-2

94. Dintenfass L. Lubrication in Synovial Joints: A Theoretical Analysis. J Bone Joint Surg Am. 1963;45:1241-56.

95. Ogston AG, Stanier JE. The physiological function of hyaluronic acid in synovial fluid; viscous, elastic and lubricant properties. J Physiol. 1953;119(2-3):244-52. doi:10.1113/jphysiol.1953.sp004842

96. Shimazu A, Jikko A, Iwamoto M, Koike T, Yan W, Okada Y, et al. Effects of hyaluronic acid on the release of proteoglycan from the cell matrix in rabbit chondrocyte cultures in the presence and absence of cytokines. Arthritis Rheum. 1993;36(2):247-53. doi:10.1002/art.1780360217

97. Hemke R, van den Berg JM, Nusman CM, van Gulik EC, Barendregt AM, Schonenberg-Meinema D, et al. Contrast-enhanced MRI findings of the knee in healthy children; establishing normal values. Eur Radiol. 2018;28(3):1167-74. doi:10.1007/s00330-017-5067-6

98. Sande NK, Boyesen P, Aga AB, Hammer HB, Flato B, Roth J, et al. Development and reliability of a novel ultrasonographic joint-specific scoring system for synovitis with reference atlas for patients with juvenile idiopathic arthritis. RMD Open. 2021;7(2) doi:10.1136/rmdopen-2021-001581

99. Hemke R, Lavini C, Nusman CM, van den Berg JM, Dolman KM, Schonenberg-Meinema D, et al. Pixel-by-pixel analysis of DCE-MRI curve shape patterns in knees of active and inactive juvenile idiopathic arthritis patients. Eur Radiol. 2014;24(7):1686-93. doi:10.1007/s00330-014-3168-z

100. Nusman CM, Hemke R, Lavini C, Schonenberg-Meinema D, van Rossum MA, Dolman KM, et al. Dynamic contrast-enhanced magnetic resonance imaging can play a role in predicting flare in juvenile idiopathic arthritis. Eur J Radiol. 2017;88:77-81. doi:10.1016/j.ejrad.2017.01.003

101. Tang MX, Mulvana H, Gauthier T, Lim AK, Cosgrove DO, Eckersley RJ, et al. Quantitative contrast-enhanced ultrasound imaging: a review of sources of variability. Interface Focus. 2011;1(4):520-39. doi:10.1098/rsfs.2011.0026

102. Zhang JL, Rusinek H, Bokacheva L, Chen Q, Storey P, Lee VS. Use of cardiac output to improve measurement of input function in quantitative dynamic contrast-enhanced MRI. J Magn Reson Imaging. 2009;30(3):656-65. doi:10.1002/jmri.21891

103. Ludemann L, Wust P, Gellermann J. Perfusion measurement using DCE-MRI: implications for hyperthermia. Int J Hyperthermia. 2008;24(1):91-6. doi:10.1080/02656730701836954

104. Zadig PK, von Brandis E, Flato B, Ording Muller LS, Nordal EB, de Horatio LT, et al. Whole body magnetic resonance imaging in healthy children and adolescents: Bone marrow appearances of the appendicular skeleton. Eur J Radiol. 2022;153:110365. doi:10.1016/j.ejrad.2022.110365

105. von Brandis E, Zadig PK, Avenarius DFM, Flato B, Kristian Knudsen P, Lilleby V, et al. Whole body magnetic resonance imaging in healthy children and adolescents. Bone marrow appearances of the axial skeleton. Eur J Radiol. 2022;154:110425. doi:10.1016/j.ejrad.2022.110425

106. Zadig P, von Brandis E, d'Angelo P, de Horatio LT, Ording-Muller LS, Rosendahl K, et al. Whole-body MRI in children aged 6-18 years. Reliability of identifying and grading high signal intensity changes within bone marrow. Pediatr Radiol. 2022;52(7):1272-82. doi:10.1007/s00247-022-05312-y

107. Diao XH, Shen Y, Chen L, Zhan J, Fang L, Liu YC, et al. Superb microvascular imaging is as sensitive as contrast-enhanced ultrasound for detecting synovial vascularity in rheumatoid arthritis. Quant Imaging Med Surg. 2022;12(5):2866-76. doi:10.21037/qims-21-859

108. Windschall DG, F. AB1714 Comparison of Superb Microvascular Imaging with Power Doppler Ultrasound in Scoring Knee Synovitis in Juvenile Idiopathic Arthritis: Preliminary Data. Annals of the Rheumatic Diseases. 2024;83:2233–4. doi:10.1136/annrheumdis-2024-eular.183641

109. Sun P, Tong Y, Xu X, Gao M, Shi J. Evaluation of synovial inflammation in juvenile idiopathic arthritis using superb microvascular imaging compared with power Doppler ultrasound. Clin Exp Rheumatol. 2024;42(5):1127-34. doi:10.55563/clinexprheumatol/ksl2uy

110. Seskute G, Jasionyte G, Rugiene R, Butrimiene I. The Use of Superb Microvascular Imaging in Evaluating Rheumatic Diseases: A Systematic Review. Medicina (Kaunas). 2023;59(9) doi:10.3390/medicina59091641

111. Kandemirli SG, Cicek F, Erdemli Gursel B, Bilgin C, Kilic SS, Yazici Z. Superb Microvascular Imaging in Assessment of Synovitis and Tenosynovitis in Juvenile Idiopathic Arthritis. Ultrasound Q. 2021;37(1):56-62. doi:10.1097/RUQ.0000000000000516

112. Aziz MU, Eisenbrey JR, Deganello A, Zahid M, Sharbidre K, Sidhu P, et al. Microvascular Flow Imaging: A State-of-the-Art Review of Clinical Use and Promise. Radiology. 2022;305(2):250-64. doi:10.1148/radiol.213303

113. Rubin JM, Bude RO, Carson PL, Bree RL, Adler RS. Power Doppler US: a potentially useful alternative to mean frequency-based color Doppler US. Radiology. 1994;190(3):853-6. doi:10.1148/radiology.190.3.8115639

114. Terslev L, Naredo E, Aegerter P, Wakefield RJ, Backhaus M, Balint P, et al. Scoring ultrasound synovitis in rheumatoid arthritis: a EULAR-OMERACT ultrasound taskforce-Part 2: reliability and application to multiple joints of a standardised consensus-based scoring system. RMD Open. 2017;3(1):e000427. doi:10.1136/rmdopen-2016-000427

115. Wang T, Wang Z, Yu Y, Huang L, Wang Y, Li Y, et al. The value of contrast-enhanced ultrasound in synovial pathotypes of rheumatoid arthritis: an exploratory study. Eur Radiol. 2026;36(2):1306-18. doi:10.1007/s00330-025-11921-6

116. Madruga Dias J, Cerqueira M, Esperanca Almeida D, Canhao H, Pimentel-Santos F, Iagnocco A. Microvascular imaging is superior to power doppler in synovitis vascular flow detection in rheumatoid arthritis using the OMERACT-EULAR scoring system. Arthritis Res Ther. 2026;28(1):15. doi:10.1186/s13075-025-03706-5

117. Magni-Manzoni S, Epis O, Ravelli A, Klersy C, Veisconti C, Lanni S, et al. Comparison of clinical versus ultrasound-determined synovitis in juvenile idiopathic arthritis. Arthritis Rheum. 2009;61(11):1497-504. doi:10.1002/art.24823

118. Malattia C, Consolaro A, Pederzoli S, Madeo A, Pistorio A, Mazzoni M, et al. MRI versus conventional measures of disease activity and structural damage in evaluating treatment efficacy in juvenile idiopathic arthritis. Ann Rheum Dis. 2013;72(3):363-8. doi:10.1136/annrheumdis-2011-201049

119. Windschall D, Trauzeddel R, Gohar F, Adiguzel-Dundar H, Hardt S, Krumrey-Langkammerer M, et al. Development and validation of a pediatric internationally agreed ultrasound knee synovitis protocol (PIUS-knee) by the PReS imaging working party. Pediatr Rheumatol Online J. 2024;22(1):94. doi:10.1186/s12969-024-01029-4

120. Spannow AH, Stenboeg E, Pfeiffer-Jensen M, Fiirgaard B, Haislund M, Ostergaard M, et al. Ultrasound and MRI measurements of joint cartilage in healthy children: a validation study. Ultraschall Med. 2011;32 Suppl 1:S110-6. doi:10.1055/s-0029-1245374

121. Gau CC, Yao TC, Gan ST, Lin SJ, Yeh KW, Chen LC, et al. Age, gender, height and weight in relation to joint cartilage thickness among school-aged children from ultrasonographic measurement. Pediatr Rheumatol Online J. 2021;19(1):71. doi:10.1186/s12969-021-00554-w

122. Sahin N, Ozdemir Cicek S, Pac Kisaarslan A, Dursun I, Poyrazoglu MH, Dusunsel R. The effect of intra-articular steroid injection on the cartilage and tendon thicknesses in juvenile idiopathic arthritis. Mod Rheumatol. 2024;34(4):791-7. doi:10.1093/mr/road093

123. Carotti M, Galeazzi V, Catucci F, Zappia M, Arrigoni F, Barile A, et al. Clinical utility of eco-color-power Doppler ultrasonography and contrast enhanced magnetic resonance imaging

for interpretation and quantification of joint synovitis: a review. Acta Biomed. 2018;89(1-S):48-77. doi:10.23750/abm.v89i1-S.7010

124. Torp-Pedersen S, Christensen R, Szkudlarek M, Ellegaard K, D'Agostino MA, Iagnocco A, et al. Power and color Doppler ultrasound settings for inflammatory flow: impact on scoring of disease activity in patients with rheumatoid arthritis. Arthritis Rheumatol. 2015;67(2):386-95. doi:10.1002/art.38940

125. Mazzoni M, Pistorio A, Magnaguagno F, Viola S, Urru A, Magnano GM, et al. Predictive Value of Magnetic Resonance Imaging in Patients With Juvenile Idiopathic Arthritis in Clinical Remission. Arthritis Care Res (Hoboken). 2023;75(1):198-205. doi:10.1002/acr.24757

126. Wallace CA, Ruperto N, Giannini E, Arthritis C, Rheumatology Research Alliance, Pediatric Rheumatology International Trials Organization, et al. Preliminary criteria for clinical remission for select categories of juvenile idiopathic arthritis. J Rheumatol. 2004;31(11):2290-4.

127. Wallace CA, Ravelli A, Huang B, Giannini EH. Preliminary validation of clinical remission criteria using the OMERACT filter for select categories of juvenile idiopathic arthritis. J Rheumatol. 2006;33(4):789-95.

128. Wallace CA, Giannini EH, Huang B, Itert L, Ruperto N, Childhood Arthritis Rheumatology Research Alliance, et al. American College of Rheumatology provisional criteria for defining clinical inactive disease in select categories of juvenile idiopathic arthritis. Arthritis Care Res (Hoboken). 2011;63(7):929-36. doi:10.1002/acr.20497

129. Choida V, Bray TJP, van Vucht N, Abbasi MA, Bainbridge A, Parry T, et al. Detection of inflammation by whole-body MRI in young people with juvenile idiopathic arthritis. Rheumatology (Oxford). 2024;63(SI2):SI207-SI14. doi:10.1093/rheumatology/keae039

130. De Lucia O, Ravagnani V, Pregnolato F, Hila A, Pontikaki I, Gattinara M, et al. Baseline ultrasound examination as possible predictor of relapse in patients affected by juvenile idiopathic arthritis (JIA). Ann Rheum Dis. 2018;77(10):1426-31. doi:10.1136/annrheumdis-2017-211696

131. Miotto ESVB, Mitraud SAV, Furtado RNV, Natour J, Len CA, Terreri M. Patients with juvenile idiopathic arthritis in clinical remission with positive power Doppler signal in joint ultrasonography have an increased rate of clinical flare: a prospective study. Pediatr Rheumatol Online J. 2017;15(1):80. doi:10.1186/s12969-017-0208-7

132. Nieto-Gonzalez JC, Rodriguez A, Gamir-Gamir ML, Boteanu A, Lopez-Robledillo JC, Garulo DC, et al. Can ultrasound-detected subclinical synovitis be an indicator of flare recurrence in juvenile idiopathic arthritis remission patients on tapered TNFi? Clin Exp Rheumatol. 2019;37(4):705-12.

133. Magni-Manzoni S, Scire CA, Ravelli A, Klersy C, Rossi S, Muratore V, et al. Ultrasound-detected synovial abnormalities are frequent in clinically inactive juvenile idiopathic arthritis, but do not predict a flare of synovitis. Ann Rheum Dis. 2013;72(2):223-8. doi:10.1136/annrheumdis-2011-201264

134. Han J, Geng Y, Deng X, Zhang Z. Subclinical Synovitis Assessed by Ultrasound Predicts Flare and Progressive Bone Erosion in Rheumatoid Arthritis Patients with Clinical Remission: A Systematic Review and Metaanalysis. J Rheumatol. 2016;43(11):2010-8. doi:10.3899/jrheum.160193

135. Zacariaz Hereter J, Rosa JE, Mollerach FB, Marin J, Ferreyra Garrott LG, Brom M, et al. Ultrasound-detected tenosynovitis as a risk factor for flares in rheumatoid arthritis patients in clinical remission. Clin Rheumatol. 2022;41(6):1843-9. doi:10.1007/s10067-022-06079-1

136. Saoussen M, Yasmine M, Hiba B, Alia F, Kawther BA, Ahmed L. The role of ultrasonography in assessing remission in juvenile idiopathic arthritis: a systematic review. Eur J Pediatr. 2023;182(7):2989-97. doi:10.1007/s00431-023-04956-8

137. Haavardsholm EA, Aga AB, Olsen IC, Lillegraven S, Hammer HB, Uhlig T, et al. Ultrasound in management of rheumatoid arthritis: ARCTIC randomised controlled strategy trial. BMJ. 2016;354:i4205. doi:10.1136/bmj.i4205

138. Ravelli A, Consolaro A, Horneff G, Laxer RM, Lovell DJ, Wulffraat NM, et al. Treating juvenile idiopathic arthritis to target: recommendations of an international task force. Ann Rheum Dis. 2018;77(6):819-28. doi:10.1136/annrheumdis-2018-213030

139. Shoop-Worrall SJW, Kearsley-Fleet L, Thomson W, Verstappen SMM, Hyrich KL. How common is remission in juvenile idiopathic arthritis: A systematic review. Semin Arthritis Rheum. 2017;47(3):331-7. doi:10.1016/j.semarthrit.2017.05.007

140. Chandola S, Bagri N, Jana M. Imaging in Juvenile Idiopathic Arthritis: A Comprehensive Review. Indian J Radiol Imaging. 2026;36(3):426-39. doi:10.1055/s-0045-1811196

141. Zhu L, Wang J, Yin C, Yang C, Qiu M, Tang X, et al. Development and validation of subtype-specific simplified ultrasound assessment systems for juvenile idiopathic arthritis: a prospective observational study. Front Pediatr. 2026;14:1876983. doi:10.3389/fped.2026.1876983